Sumo-Directed Control of the Resolvase Yen1 in Mitotic Cells

Hugo Dorison

▶ **To cite this version:**

Hugo Dorison. Sumo-Directed Control of the Resolvase Yen1 in Mitotic Cells. Genomics [q-bio.GN]. Université Paris-Saclay, 2021. English. NNT : 2021UPASL003 . tel-03539739

HAL Id: tel-03539739
https://theses.hal.science/tel-03539739

Submitted on 22 Jan 2022

HAL is a multi-disciplinary open access archive for the deposit and dissemination of scientific research documents, whether they are published or not. The documents may come from teaching and research institutions in France or abroad, or from public or private research centers.

L'archive ouverte pluridisciplinaire **HAL**, est destinée au dépôt et à la diffusion de documents scientifiques de niveau recherche, publiés ou non, émanant des établissements d'enseignement et de recherche français ou étrangers, des laboratoires publics ou privés.

université PARIS-SACLAY

Sumo-directed control of the resolvase Yen1 in mitotic cells

Thèse de doctorat de l'université Paris-Saclay

École doctorale n°582 Cancérologie : biologie-médecine-santé (CBMS)
Spécialité de doctorat : Aspects moléculaires et cellulaires de la biologie
Unité de recherche : Université Paris-Saclay, Institut Gustave Roussy, CNRS, Intégrité du génome et cancers, 94805, Villejuif, France.
Référent : Faculté de médecine

Thèse présentée et soutenue à Villejuif le 21 Janvier 2020, par

Hugo DORISON

Composition du Jury

Karine DUBRANA Directrice de Recherche, HDR INSERM UMR1274 CEA – Paris Saclay	Présidente
Guy-Franck RICHARD Directeur de Recherche, HDR CNRS UMR3525 Institut Pasteur – PSL	Rapporteur
Teresa TEIXEIRA Directrice de Recherche, HDR CNRS 8226 IBPC – UPMC	Rapporteure
Valérie BORDE Directrice de Recherche, HDR CNRS UMR3244 Institut Curie – UPMC	Examinatrice
Bertrand LLORENTE Directeur de Recherche, HDR UMR7258 INSERM U1068 CRCM	Examinateur
Valeria NAIM Chargée de Recherche, HDR CNRS U9019 IGR – Paris Saclay	Examinatrice
Gérard MAZÓN Chargé de Recherche, HDR CNRS U9019 IGR – Paris Saclay	Directeur de thèse

Thèse de doctorat

NNT : 2021UPASL003

Acknowledgements

I would like first and foremost to thank Dr Gerard Mazón for integrating me in his research group even though we did not share experience prior to the beginning of the thesis. I am further grateful for his sharing of knowledge and techniques all along the PhD project. I must extend my thanks to the whole lab team composed of Dr Ibtissam Talhaoui and formerly Dr Manuel Bernal who provided me with priceless technical insight as well as moral support throughout most of the thesis.

I am equally grateful for the now extended team our lab is a part of and I would like to thank Dr Eric Le Cam, Dr Pauline Dupaigne, Dr Sonia Baconnais, Ali Muhammad and Dr Yann Benureau for a friendly environment and discussions along with manuscript writing guidelines.

I would like to sincerely thank Dr Guy-Franck Richard and Dr Teresa Teixeira for the considerable investment and time they afford me by accepting to be reporters of this thesis. I would like to thank Dr Bertrand Llorente, Dr Valerie Borde, Dr Karine Dubrana and Dr Valeria Naim just as much for agreeing to be examiners of my work.

The friendly exchange of information and technical knowledge with Dr Stephane Marcand and his team at the CEA is a memorable event to me and I would like to thank them all for welcoming me for a few days and the continued exchange of strains and information that followed. Similarly, I would like to thank the Microscopy platform team in the PR at the Gustave Roussy Institute and especially Tudor Manoliu for his dedication and constant tips.

Finally, I would like to thank my family and friends for their substantial support all along the thesis, be it encouragement or knowledgeable advice from Doctors themselves. Last but not least I extend my gratitude to Dr Yidan Wang for manuscript guideline along with year-long moral support.

Index

Main abreviations

HR: Homologous Recombination

DSB: Double Strand Break

SSB: Single Strand Break

ssDNA: Single Strand DNA

dsDNA: Double Strand DNA

DSBR: Double Strand Break Repair

NHEJ: Non-Homologous End Joining

D-loop: Displacement-loop

JM: Joint Molecule

HJ: Holliday Junction

dHJ: Double Holliday Junction

CO: Crossover

NCO: Non-Crossover

SUMO: Small Ubiquitin-like MOdifier

List of Figures

in addition either PNKP (P), APTX (A), or APLF (F). **Left**, in BER, SSB are intermediates. They do not require PARP1 for detection unless they become 'uncoupled' from the BER pathway (dotted line "a"). **Right**, SSBs are intermediates of RER (created by RNaseH2) or products of abortive Top1 cleavage activity. It is unclear whether or not any of these SSBs are detected by PARP1 (dotted line "b"). **[B]** DNA End processing. **Left**, In BER, APE1 remains bound to the SSB, enabling recruitment of Polβ (and associated XRCC1 complexes) via direct interaction with Polβ. **Middle**, at SSBs detected by PARP1, PAR synthesis results in rapid recruitment of XRCC1 protein complexes containing the enzymes necessary for repair of the damaged termini. **Right**, SSBs arising during RER contain 5'-ribonucleotide termini (rNT) and may be channeled directly into long-patch gap filling, avoiding the need for specialized end processing. However, SSBs arising at ribonucleotides via abortive Top1 cleavage activity harbor cyclic 3'-phosphate termini and are likely detected by PARP1 (dotted line "b"). **[C]** Gap filling. Pol β replaces the single missing nucleotide at most SSBs (left, short-patch repair), but under some circumstances gap filling may involve incorporation of more than one nucleotide (typically 2–12 nt) by Pol β and/or Pol δ/ε (right, long-patch repair), resulting in displacement of a single-strand flap, which is then removed by flap endonuclease-1 (FEN1) in a reaction stimulated by PCNA (and possibly PARP1). No need for processing of the 5' end on the removed flap. This may take place if Polβ in BER struggles with 5' processing (dotted line "c"). **[D]** DNA ligation. Short-patch and long-patch repair patches are primarily ligated by the XRCC1/Lig3α and PCNA/Lig1 complexes, interchangeably (dotted line "d").

Page 37. **Figure 9.** Schematic representation of the branching sub-paths in DSB repair. The main separation occurs at the very start when DNA binding complexes compete between direct joining of the broken ends and initiation of resection.

Page 38. **Figure 10.** Non Homologous End Joining adapted from Helleday et al. in 2007 [31].

Page 39. **Figure 11.** Snapshot on homologous recombination by Mazón et al. in 2010 [103]. With minor modifications (top part) Schematic representation of the main steps described in the corpus.

Page 40. **Figure 12.** Resection in yeast by Gobbini et al. in 2016 [20].

Page 42. **Figure 13.** Nucleation of human RAD51 on ssDNA by Subramanyam et al. in 2018 [128] The ATP bound RAD51 nucleoprotein filament is stably nucleated such that each RAD51 monomer binds three nucleotides which facilitates further polymerization of the nucleoprotein filament forming the active pairing unit in strand exchange reactions. Hydrolysis of ATP lowers the affinity of RAD51 for ssDNA and leads to turnover or disassembly of the nucleoprotein filament.

Page 43. **Figure 14.** Rad52-mediated replacement of RPA by Rad51. Figure altered from the original source by San Filippo et al. in 2008 [118] In its recombination mediator role, Rad52 forms a complex with Rad51 and delivers it to RPA-coated ssDNA to seed the assembly of the presynaptic filament. The polymerization of additional Rad51 molecules results in the further displacement of RPA from the DNA.

Page 44. **Figure 15.** model for homology search and D-loop formation by Tavares et al. in 2019 [143]. (i) During homology search, Rad54 promotes DNA probing. The invading DNA (light red) uses Rad54 to bridge the Rad51 filament to dsDNA during the homology search. Rad54 ATPase activity is not required but may enhance probing. (ii) Persistent associations with heterologous DNA (blue, right arrow) may be prevented or dissociated by Rad54 in an ATPase-dependent fashion. Rad54 ATPase exerts quality control to promote homologous pairing. (iii) Rad54 is required for synaptic complex formation without strict requirement for ATPase activity, and (iv) converts such complexes into D-loops dependent on ATP hydrolysis. Rad51 left on the ssDNA outside of the heteroduplex region after removal during heteroduplex formation may able to repolymerize back into the synaptic region. Note that this is a

cartoon representation not meant to model the true scale and structure of the Rad51 filament or Rad54 protein arrangement in the depicted intermediates.

Page 45. **Figure 16.** Schematic representation of the branching paths following homology search and D-loop formation. The D-loop may be displaced allowing annealing to the break end with a non-crossing over outcome. The displaced strand of the D-loop may as well anneal to the opposite break end effectively forming a DNA quadruplex called a Double Holliday Junction. Representation mustered with data from [31, 161].Page 46. **Figure 17.** dHJ dissolution schematic representation by Bizard et al. in 2014 [169]. Migration of the HJs toward one another. The fusion of the two HJs results in a hemicatenated intermediate. Decatenation of this intermediate regenerates the original DNA species present before the initiation of HR. Each strand engaged in the dHJ is reassociated with its original complementary strand, preventing exchange of genetic material between the two homologous sequences.

Page 47. **Figure 18.** dHJ nucleolytic processing representation by Bizard et al. in 2014 [169]. Each HJ of a dHJ is cleaved by a resolvase. Cleavage can be asymmetric or symmetric. This process can generate both CO and NCO products.

Page 49. **Figure 19.** Schematic representation of BIR from Symington et al. in 2014 [28].

Page 49. **Figure 20.** Schematic representation of homology mediated SSA adapted from Helleday et al. 2007 [31]; Symington et al. 2014 [28]; Sallmyr et al. 2018 [198] Following long range resection, Rad52 (green semi-circles) interacts with RPA-bound ssDNA overhangs and aligns and anneals the repeated sequences. Superflous non-homologous 3' single strands overhang as flaps. They are cleaved by structure specific nuclease Rad1-Rad10 (yellow triangles). After that, gap fill and ligation are handled by unknown polymerases and ligases.

Page 51. **Figure 21.** Interstrand Crosslink Repair in humans, simplified. Adapted from Hashimoto et al. 2016 [208] with data and insight from Gourzones et al. 2019 [211] Left panel: In TC-NER repair, CSA and CSB help introduce the incision complex (XPA, XPG, RPA, TFIIH and XPF-ERCC1). TLS polymerases can be as κ, ζ, or REV1. Right panel: FA complex = FANCA, B, C, D2, E, F, G, I, L, FAAP20, FAN1; BTR = BLM-TOP3α-RMI1.

Page 52. **Figure 22.** Recruitment of DNA damage signaling kinases and adaptor proteins to DNA lesions: conserved features between budding yeast and humans. Figure by Lanz et al. in 2019 [215]. Phosphorylation and adaptor proteins play a key role in the recruitment of downstream checkpoint kinases. The colored ovals indicate phosphorylation events mediated by DNA damage signaling kinases (see kinase key). The orange lines indicate protein–protein interactions promoted by the indicated phosphorylation events (also methylation (me) or ubiquitination (Ub)). Activation of the downstream checkpoint kinases by the apical PIKK kinases requires adaptor proteins (outlined in green). In most cases, these adaptor proteins act as scaffolds to directly bind to and recruit the downstream checkpoint kinase. The model, mostly based on extensive work in yeast, posits that the recruitment of the downstream checkpoint kinase to the proximity of the apical PIKK kinase enables the phosphorylation and activation of the downstream checkpoint kinase. In addition to activating the downstream checkpoint kinase, phosphorylation events mediated by the apical PIKK kinases are critical for scaffold assembly, often promoting protein–protein interactions. Accordingly, a conserved feature of several adaptor proteins in budding yeast and humans is the presence of protein domains responsible for binding phosphorylated proteins (FHA and BRCT domains). Notably, other kinases such as CDK and CK2 also catalyze phosphorylation events involved in adaptor recruitment, although these events are often not induced by DNA damage. For DNA-PKcs, while this kinase has been implicated in the phosphorylation of H2AX and 53BP1, it does not seem to be involved in CHK2 phosphorylation.

Page 74. **Figure 31.** Schematic representation of Yen1 protein and its CDK/Cdc14 sites by Talhaoui et al. in 2016 [185]. The conserved functional domains of Yen1 are depicted in solid dark blue, while other conserved domains are shown in solid turquoise. The three clusters of Cdk1 phosphorylation sites are indicated. Cluster 2 sites in the central part of the protein play a role in the inactivation of Yen1 during S-phase and G2 by decreasing its affinity to the substrate when they are phosphorylated. Cluster 3 sites are present embedded into the nuclear localization signal (NLS).

Page 82. **Figure 32.** Yen1 is sumoylated *in vivo* and *in vitro*. a A wild-type chromosomally tagged YEN1-HA strain was synchronized with alpha factor and released into fresh medium to observe phosphorylation of Yen1 by immunoblot (upper) and progression through the cell cycle by FACS (lower). b Wild-type strains expressing Yen1-HA, with (+) or without (−) pCUP-6xHIS-Smt3, were subjected to MMS challenge followed by denaturing Ni-NTA pull-down and immunoblot analysis. Yen1 was detected by anti-HA (top and middle) and a prominent sumoylated doublet is indicated (black rhombus). Membranes were also probed with anti-Smt3 (bottom). Note that un-sumoylated Yen1 binds to Ni due to a histine-rich region. c Yen1-HA was overexpressed in wild-type asynchronous cells, immunoprecipitated with anti-HA, eluted by HA peptide competition and mixed with Aos1-Uba2, Ubc9, and Smt3-3KR in the presence or absence of ATP. After immunoblotting with anti-HA sumoylated forms were detected in the presence of ATP that migrate at similar sizes to those detected in the PD experiments shown in b (far right duplicate for comparison). A control reaction was made with HA-immunoprecipitation of a yen1Δ strain eluted with the same amount of HA peptide. d yen1Δ cells expressing Yen1-HA from a Gal-inducible plasmid or harboring a control plasmid were subjected to MMS treatment (0.03%), and extracts were immunoprecipitated using anti-HA prior to immunoblotting with anti-Smt3 (left) or anti-HA (right). e Indicated strains (WT, siz1Δ, siz2Δ, or siz1Δ siz2Δ) with (+) or without (−) pCUP-6xHIS-Smt3 were subjected to pull-down analysis of Smt3 as in b in conditions of MMS damage and eluates were analysed by immunoblot. The input used for PD was immunoblotted to allow normalization and comparison between strains (bottom). f Purified recombinant 6His-HA-Yen1 protein was incubated under sumoylation conditions with the indicated concentrations of Siz2 followed by immunoblotting with anti-HA. Asterisk indicates breakdown products of Yen1 carried from purification. g Sumoylation reactions were performed as in f but with increasing amounts of synthetic Holliday junction DNA, 458 nM Yen1 and in the absence of Siz2. All experiments were independently replicated at least three times and images are representative of the reproducible results obtained.

Page 84. **Figure 33.** Yen1 interacts with Slx5–Slx8 in the nucleus. a Diploid strains carrying one allele of galactose inducible VC-Slx5 and VN-Yen1 with wild-type copies of YEN1 and SLX5 in the homologous chromosomes were observed by live microscopy. BiFC (white arrows) signal denotes an interaction between the two BiFC (Venus) epitopes. Control diploids lacking one or both of the epitope-tagged proteins (φ) were used to substract background signal. A plasmid carrying Nup49-mCherry was transformed on the diploid strain harboring VC-Slx5/VN-Yen1 to visualize the nuclear perimeter. BiFC interactions were only detected in the nuclear compartment. b Cells carrying either an empty vector or a pYES2 plasmid expressing GST-Slx5 under galactose control were grown in selective media and induced with galactose for 3 h. Lysates were then applied to a glutathione-sepharose column. After washing, the bound proteins were eluted and immunoblotted with α-HA (upper) or α-GST (lower). c Two-hybrid assays were performed with strains carrying the indicated activating domain (AD) or DNA binding domain (BD) fusions. Strains were grown in selective media lacking leucine (L) and tryptophan (W) prior to spotting on media lacking histidine (H) to detect a positive interaction. Experiments were independently replicated three times and images are representative of the reproducible results obtained.

Page 85. **Figure 34.** Yen1 is a direct substrate of the Slx5–Slx8 ubiquitin ligase. a H6-HA-Yen1 (916 nM) was ubiquitinated *in vitro* in the presence of the indicated concentrations of either Slx5/Slx8 or the RING mutant Slx5–6/Slx8 and 0.2 μM DNA. Control lanes with H6-HA-Yen1 in the absence of E3 and Slx5/8 in the absence of Yen1 are shown. Breakdown products of Yen1 are marked with an asterisk. b The ubiquitination reaction was performed as above but with 50 nM Slx5–Slx8 and increasing amounts of DNA. c Strains expressing 6xHis-Ub were subjected to different growth conditions and lysed to pull-down ubiquitinated proteins under denaturing conditions, input Yen1-HA levels were controlled to allow comparisons. d Smt3 denaturing pull-downs were performed in wild type, slx5Δ, or slx8Δ cells (all in a pdr5Δ background) after growth in the presence of MMS. The fold increase in the sumoylated fraction indicated at the bottom of the gel is an average of three trials. Inputs were controlled in each trial to allow comparison of the eluted sumoylated proteins.

Page 87. **Figure 35.** Deletion of SLX8 alters the nuclear distribution and turnover of a fraction of Yen1. a Wild type and slx8Δ cells were synchronized in G1 and released to observe the phosphorylation of Yen1 as a function of cell-cycle progression. b Serial dilutions of the indicated strains were spotted onto YPAD media containing different genotoxins. c Cells with an endogenous HTA1-mCherry carrying plasmids expressing wild-type GFP-Yen1 were observed microscopically after a short induction of the fusion protein. Shown are cells presenting normal nuclear localization (lower) or presenting foci (white arrows, upper). d G1 and G2/M cells of the indicated genetic backgrounds were microscopically examined as in c and classified according to the number of foci they displayed. The graphs show the percentage of cells in each category. The total number of cells individually scored from three video recordings are indicated as (n). Categories were subjected to the Fischer's exact test, asterisks denote significant levels at $P < 0.001$(***) or $P < 0.005$(**). e The duration of foci in the indicated genetic backgrounds was measured by video-microscopy analysis. The mean ± s.d. of the duration time and n are indicated, error bars denote s.d. Asterisks refer to significance at the $P < 0.05$ (**) and $P < 0.001$ (***) levels in unpaired two-tailed Student's t-test. f Cells expressing GFP-Yen1 and Hta1-mCherry were observed by video-microscopy in 2' time-lapse frames. GFP total intensity of the whole cell, the nucleus and the cytoplasm was determined for 5 z-planes and used to calculate the total GFP intensity in each compartment. The graph displays the time course of GFP intensity in a single cell g The indicated pdr5Δ strains, that are permeable to MG132, were synchronized in G1 and subjected to cycloheximide (CHX) treatment during their release from G1 arrest. Where indicated, cells were pre-treated with MG132 for 30 min before, and during release in the presence of CHX. PGK1 was used to normalize the amount of Yen1. h Quantitation of the fraction of Yen1, compared to G1, remaining at the indicated times after release into CHX. The mean ± s.d. of triplicate assays is shown; statistically significant difference in unpaired two-tailed Student's t-test is indicated (**$P < 0.05$)**.** **i FACS** analysis of cells at the beginning and at the end of the CHX treatment.

Page 89. **Figure 36.** Yen1 foci are dynamic and localize preferentially to nucleolar sites in the absence of DNA damage. a slx8**Δ** cells carrying a SIK1-mCherry endogenous marker and an inducible GFP-Yen1 expressing plasmid were observed after short induction of the fusion protein. The white arrow denotes co-localizing signal of GFP-Yen1 with Sik1-mCherry. b Wild-type cells carrying a TetO-TetR array tag on chromosome XII and an inducible GFP-Yen1 expressing plasmid were observed after short induction of the fusion protein. c Cells were subjected to acute challenge with Zeocin (0.01 mg/ml) and observed during their recovery as in Fig. 4. Cells displaying the designated categories of GFP-Yen1 foci were scored at the indicated time points. The total number of cells analysed (n) from two independent recordings were as follows: WT 0 h ($nG1 = 81$, $nG2_{/M} = 267$), WT 1.5 h ($nG1 = 78$, $nG2_{/M} = 124$), WT 3.5 h ($nG1 = 110$, $nG2_{/M} = 118$), slx8Δ 0 h ($nG1 = 107$, $nG2_{/M} = 79$), slx8Δ 1.5 h ($nG1 = 40$, $nG2_{/M} = 73$), slx8Δ 3.5 h ($nG1 = 52$, $nG2_{/M} = 62$). d Cells were subjected to an acute challenge with 0.1% MMS and for foci were observed as in c. The total number of cells analysed (n) from two independent recordings were

as follows: WT 0 h (nG1 = 81, $nG2_{/M}$ = 267), WT 1.5 h (nG1 = 95, $nG2_{/M}$ = 98), WT 3.5 h (nG1 = 139, $nG2_{/M}$ = 137), slx8Δ 0 h (nG1 = 107, $nG2_{/M}$ = 79), slx8Δ 1.5 h (nG1 = 53, $nG2_{/M}$ = 55), slx8Δ 3.5 h (nG1 = 40, $nG2_{/M}$ = 67). e slx8Δ cells carrying SIK1-mCherry were observed after Zeocin challenge to determine GFP-Yen1 co-localization. White arrows indicate GFP-Yen1 foci. f slx8Δ cells were observed as in e, but were subjected to MMS treatment. White arrows indicate GFP-Yen1 foci. Images are representative of the reproducible results obtained after three independent trials. Statistical significance at $P < 0.0001$ in Fischer's exact test at 3.5 h recovery points is indicated by asterisks in c and d.

Page 91. **Figure 37.** K714 is ubiquitinated by Slx5–Slx8. a Recombinant 6xHIS-HA-Yen1 and the mutant 6xHIS-HA-Yen1-K714R (916 nM) were subjected to *in vitro* ubiquitination as in Fig. 3a. b 6xHis-Ubiquitin pull-downs were performed on cells expressing 6His-Ub and carrying endogenous Yen1-HA or its variant Yen1-K714R-HA following treatment with the indicated genotoxics. c Strains carrying endogenous Yen1-HA or its K714R variant were synchronized with alpha factor in G1 and proteins extracted at indicated time points after G1 release and immunoblotted with anti-HA. At time points where Yen1 is modified by CDK1, extracts were subjected to phosphatase treatment (CIP+) and also subjected to phos-tag gel separation. d Strains carrying HTA1-mCherry and the indicated GFP-Yen1 expression plasmids were examined microscopically as in Fig. 4c to assess the presence of the proteins. Foci were quantified as a function of cell-cycle phase, which was determined by cell morphology. The total number of analysed cells (n) and independent video recordings (VR) were as follows: WT (nG1 = 105, nG2/M = 153, VR = 3), yen1-K714R (nG1 = 106, nG2/M = 64, VR = 3), mus81Δ (nG1 = 294, nG2/M = 337, VR = 3), mus81Δ yen1-K714R (nG1 = 203, nG2/M = 306, VR = 3), slx8Δ (nG1 = 166, nG2/M = 172, VR = 3). Statistical differences were estimated by the Fischer's exact test and significance is indicated by asterisks $P < 0.05$(*), $P < 0.005$(**), $P < 0.001$(***). e Sensitivity to the indicated genotoxics was determined by spotting serial dilutions of different strains on the indicated media. f Cycloheximide chase experiment showing persistence of Yen1 after a G1 release in the presence of CHX. g Immunoprecipitated Yen1-K714R-HA was eluted and the protein was sumoylated with Aos1-Uba2, Ubc9, and Smt3-3KR in the presence or absence of ATP. Samples were de-phosphorylated with CIP before loading. h 6xHIS-Smt3 pull-downs were performed on cells expressing 6HIS-Smt3 and carrying YEN1-HA or its variant yen1-K714R-HA under conditions of MMS treatment as indicated. The average fold enrichment is indicated at the bottom of the blot.

Page 93. **Figure 38.** Yen1-K714R increases COs and suppresses spontaneous chromosome segregation defects in mus81Δ cells. a Diagram explaining the Chr. XV DSB-induced crossover reporters. Recombination outcomes were scored in white/red sectored colonies of the indicated strains and normalized to its plating efficiency (PE). The number of independent experiment trials (T) and the total number of recombination events scored (n) were as follows: WT (T = 6, n = 158), yen1Δ (T = 9, n = 538), mus81Δ (T = 5, n = 168), mus81Δ yen1Δ (T = 9, n = 160), yen1-K714R (T = 5, n = 230), and mus81Δ yen1-K714R (T = 5, n = 230). b A strain harboring a lacO/GFP-LacI array tag on chromosome IV was followed by video-microscopy to discriminate chromosome segregation in timely manner from aberrant segregation. Images display a typical normal and aberrant segregation and its respective kymograph. c GFP foci of the indicated strains were observed by video-microscopy and chromosomal segregation was scored as to whether it displayed a proper phenotype (normal) or one of three types of defective phenotypes (non-disjunction, delay, and aberrant chromosome number (acn)). The total number of cells analysed (n) and independent video-recordings (VR) were as follows: WT (n = 606, VR = 3), yen1Δ (n = 133, VR = 3), yen1-K714R (n = 131, VR = 3), mus81Δ (n = 259, VR = 5), yen1-K714R mus81Δ (n = 448, VR = 3) and yen1Δ mus81Δ (n = 289, VR = 3). d Segregation events scored as in c were determined for mus81Δ and mus81Δ yen1Δ strains containing a pYES2 plasmid expressing Yen1-HA under Galactose-inducible control or an empty pYES2 and subjected to

acute over-expression of Yen1-HA or the equivalent mock induction prior to the recording of the video-microscopy. The total number of cells analysed from three VRs were as follows: mus81Δ (+pYES2) n = 245, mus81Δ (+pYES2-Yen1) n = 391, mus81Δ yen1Δ (+pYES2) n = 117, mus81Δ yen1Δ (+pYES2-Yen1) n = 218. Statistically significant differences in a between CO and other outcomes and in c and d between normal and abnormal categories were determined by the Fischer's exact test, asterisks refer to significance at the P < 0.001(***), P < 0.005(**) or P < 0.05(*).

Page 101. **Figure 39. Supplementary Figure 1**. **A**) Strains carrying either a wild-type YEN1 locus or an endogenous replacement with the epitope tagged YEN1-HA or YEN1-3xFLAG were combined to mus81Δ and sensitivity to MMS was monitored with growth of serial dilutions in plates with the indicated doses of MMS. **B)** Smt3 denaturing pull-down under MMS treatment (0.3%) was performed from either a yen1Δ or wild-type strain expressing either empty, 6xHis-Smt3 (His) or His-Flag-Smt3 (HisFlag), small amont of PD was loaded to allow detection of the different bands of Yen1 sumoylation without saturation (dark marks for his-Smt3 or red marks for his-flag-Smt3) **C)** Yen1-HA was overexpressed in wild-type asynchronous cells and equivalent growth was made in an empty yen1Δ strain, extracts were immuno-precipitated with anti-HA, eluted by HA peptide competition and mixed with Aos1-Uba2, Ubc9 and Smt3-3KR in the presence or absence of ATP. When indicated, reactions were subjected to Factor Xa (FXa) treatment to remove the –HA tag. **D)** Smt3 denaturing pull-down under MMS treatment (0.3%) was performed from a wild-type strain and strains containing the Alanine or Aspartic substitution of four Serines of the CDK1 sites of cluster 2 [191]. Second gel compares wild-type with dna2Δ pif1 strain that results in an average (N=2) fold increase of 3.3 ±0.5 (SD) in the sumoylated fraction for the mutant strain.

Page 102. **Figure 40. Supplementary Figure 2**. **A**) Representative fields of strains expressing GFP-Yen1 on a short burst and its co-localizing signal with chromatin (Hta1) **B)** slx8Δ cells showing intra-nuclear foci that were categorized as 1-2 foci, >2 foci, normal or rare events (not included in the other categories) **C**) Strains used in microscopy were monitored for sensitivity to MMS under chronic low expression.

Page 103. **Figure 41. Supplementary Figure 3**. **(a)** Sequential images taken every 2 min of a cell expresing GFP-Yen1 during the re-location of GFP-Yen1 to the nucleus and associated graph showing the total intensity (normalized to 100%) of whole cell and both nuclear and cytoplasmic compartments for each time point. **(b**) 2' time-lapse of a cell containing one focus during its GFP-Yen1 nuclear to cytoplasm re-distribution and associated graph (as in A). Graphs display the average intensity and SD (N=3).

Page 103. **Figure 42. Supplementary Figure 4**. **(a)** Co-Localization of GFP-Yen1 and the Nop1-RFP nucleolar marker in normal and Zeocin challenge conditions. Co-localizing signal of Nop1 can also be detected with BiFC signal between Yen1 and Slx5. **(b**) Co-localization of BiFC signal of the Slx5-Yen1 interaction with the Nop1 nucleolar marker. **(c)** Representative image of a GFP-Yen1 focus localized to chromatin still not completely segregated in a slx8Δ cell (white arrow).

Page 104. **Figure 43. Supplementary Figure 5. (a**) PAGE phos-tag gel comparing phosphorylation status of a wild-type and a yen1-K714R strain during a time course after G1 release. **(b**) cdc14-1 or cdc15-3 cells were arrested at restrictive temperature and protein extracts were either mock treated or treated with CIP phosphatase to reveal the extent of Cdc14- sensitive phosphorylation in both wild-type and yen1-K714R strains. **(c**) Indicated strains (carrying a nuclease-dead ND allele of Yen1 combined or not with the K714R mutation) were subjected to a spot-test sensitivity assay by dropping serial dilutions in plates with the indicated genotoxics. **(d**) Cells arrested in G1 were released in MMS (0.1%) containing

media for 10' and washed out of drug and let recover in fresh YPD, samples at indicated points were analyzed by western-blot and flow-cytometry to monitor the MMS recovery.

Page 105. **Figure 44. Supplementary Figure 6**. Images of representative cells from the 4 different categories used to analyzed proper segregation by video-microscopy (using the LacI-GFP-LacO array). Note the time lapses are not equivalent and delayed and non-disjunction events have significant increases on the time between frames that illustrate its phenotype (acn, aberrant chromosome number).

Page 105. **Figure 45. Supplementary Figure 7**. **(a**) Strains carrying either a pYES2 empty vector or a pYES2-Yen1-HA expression vector were spotted in selective media with or without 0.0025% MMS in conditions allowing basal expression (Glucose repression) or chronic over-expression of YEN1 (Induction with Galactose). **(b**) Analysis by western blot of the expression level of strains used in the segregation assay with acute O/E of Yen1-HA in Figure 7.

Page 106. **Figure 46. Supplementary Figure 8**. **Model explaining the role of Slx5-Slx8 in targeting the active fraction of Yen1 for degradation**. At Anaphase transition (1), the cytoplasmic pool of Yen1 (pink circles) is still phosphorylated by Cdk1 and remains excluded from the nucleus. The action of Cdc14 enables active forms of Yen1 (green circles) to enter the nucleus and be recruited at its active sites with a putative role for sumoylation (2). Slx5-Slx8 removes Yen1 from active sites reducing the time of its association in competition with other HR factors (Sgs1, Mph1, Srs2) (2). After mitosis the Yen1 pool remains nuclear until Cdk1 gradually phosphorylates Yen1 at the entry of S-phase (3). During the G1-S transition the Yen1 pool is targeted to degradation in parallel to its nuclear exclusion (3) and the newly synthesized pool remains cytoplasmic after Cdk1 phosphorylation (4). Any Yen1 that remains in the nucleus is targeted by Slx5-Slx8 to allow its degradation and prevents its persistent accumulation in the nuceus at the S-phase (4).

Page 107. **Figure 47. Supplementary Figure 9. a)** Uncropped immunoblot images from Figure 32 panel b. Squares show the cropping limits used to generate the images in display in panel b. **b)** Uncropped blot used in Figure 32 panel e input control.

Page 115. **Figure 48.** Yen1 contains two Sumo Interacting Motifs (SIMs) in its C-terminal domain **(A)** Diagram showing the conserved domains of Yen1 and the positions of the regulatory Cdk1-phosphorylation sites bundled in three clusters (two last clusters merged) [191]; Amino acid 354 shows the cut-off point for truncated forms of Yen1 in Two-Hybrid assays; the two identified candidate SIMs are shown near the nuclear localization sequence (NLS). **(B)** A Two-hybrid assay was performed with strains carrying the indicated Activator Domain (AD) and DNA Binding Domain (BD) plasmids to test interaction of Yen1 to Smt3 (SUMO) and the Yen1 critical domains for such interaction. Mutations D635A D636A D637A for SIM1 and V675A E677A for SIM2 were introduced to test the putative SIMs. Strains were grown on selective media lacking Leucine and Tryptophan and spotted in selective media also lacking Histidine to reveal interaction of the proteins fused to the AD and BD domains. Non-specific interactions were minimized by the addition of 3-aminotriazole (AT) [534]. **(C)** A SUMO-retention assay was performed where poly-Smt3 chains of multiple sizes generated *in vitro* were immobilized to a Cobalt Ni-NTA matrix and mixed with equal amounts of either Yen1 or the Yen1 mutated in its putative SIMs. After letting Yen1 interact with the poly-Smt3 coated matrix, the matrix was eluted in denaturing conditions and the eluates inspected by western blot for the presence of Yen1 (anti-HA, left panel) and the pre-bound Smt3 chains (right panel).

Page 117. **Figure 49.** Mutation in Yen1 SIMs has no impact to its CDK1 regulation and nuclear shuttling but sensitizes cells to DNA damage **(A)** Strains with a chromosomally inserted copy of –HA tagged wild-type Yen1 or its double SIM mutant (Yen1SIM$^{\Delta\Delta}$) were synchronized with alpha factor and released into

fresh medium to monitor the modification of the protein through the cell cycle by immunoblot (left). Both unmodified and phosphorylated Yen1 are indicated. Average levels of endogenous Yen1 were normalized with PGK1 in triplicate experiments (right). **(B)** Cells carrying an endogenous histone Hta2-mCherry marker and chromosomally –HA tagged versions of Yen1 wild type and Yen1SIM$^{\Delta\Delta}$ were transformed with a plasmid carrying an equivalent version of Yen1 fused with GFP at its C-terminal region. Cells were grown on selective media and observed using a spinning-disk microscope after a brief induction with galactose. Shuttling of the protein from cytoplasm to the nucleus can be observed in representative fields displaying cells with nuclear excluded Yen1 (S-phase and early G2-M) and nuclear localized Yen1 (anaphase to G1). **(C)** Sensitivity to different DNA damaging agents and drugs was determined by spotting serial dilutions of strains carrying different Yen1 mutants in its SIM in a MUS81 deleted background for the indicated media. **(D)** Survival curves to the agents tested in (C) were established by counting colony forming units of the different strains after plating in YPD containing the indicated doses of drugs in replicate trials. Survival was normalized per trial with its respective control YPD counts and the average % survival is plotted in the graphs (+/- SEM). Statistical significance was estimated by the student T-test at $P<0.05$.

Page 118. **Figure 50.** Nuclease activity of Yen1 is not affected by mutation in its SIMs. Activity of Immuno-precipitated Yen1 was tested in a re-constituted cleavage reaction using synthetic Holliday Junctions (HJ) made with oligonucleotides and labeled with Cy5. The DNA products were run in non-denaturing PAGE and revealed by the fluorescence of the Cy5 labeled oligonucleotide. Controls were run to determine the size and apparent size of linear and four-way HJ substrates, respectively.

Page 119. **Figure 51.** The mutation of Yen1's SIMs prevents Yen1 sumoylation *in vivo*. **(A)** Strains carrying endogenous copies of -HA tagged wild type Yen1, Yen1SIM1Δ ^{and} Yen1SIMΔ$^{\Delta}$ mutants, with (+) or without (Ø) the plasmid pCUP-6xHIS-Smt3, were grown in the presence of MMS. Cells were lysed and lysates subjected to a denaturing Ni-NTA pull-down followed by immunoblot analysis. Yen1 was detected by anti-HA (top-left). Membranes were subsequently probed with anti-Smt3 (Bottom-left). Prior to Ni-NTA pull-down, input samples were taken from the lysates and were analyzed by immunoblotting for the levels of Smt3 induction (Right) and relative protein amounts (Anti-PGK1) of each lysate (Bottom-left). (B) **Purified Yen1-HA** and Yen1SIMΔΔ ^{mutant} variant were subjected to an in *vitro sumoylation* reaction containing Aos1-Uba2, Ubc9 and Smt3-3KR and subjected to Tris-Acetate PAGE for comparison of their sumoylation patterns after immunoblotting with anti-HA.

Page 120. **Figure 52.** Mutation in the SIMs of Yen1 prevent foci accumulation in G2/M. **(A)** Cells with an endogenous Hta2-mCherry and YEN1-HA expressing Yen1-GFP observed under a spinning-disk microscope after a brief induction with galactose. The white triangles denote the presence of Yen1-GFP foci. **(B)** Chromosomally tagged Yen1-HA wild type and SIM mutants in the indicated genetic backgrounds and carrying the corresponding Yen1-GFP expressing plasmid were observed under the microscope after a brief induction. Pictures of several fields were taken for each trial and cells were classified according to their cell cycle phase and the presence or absence of Yen1 foci. Violin Plots display the distribution of G2/M cells showing: no foci, 1-2 foci or more than 2 foci for each strain. Counting was performed for over 400 distinct G2/M cells for each strain over several independent trials. **(C)** Cells from the indicated genotypes were treated with MMS (0.1% for 15min) and observed 1h30 and 3h30 after release into fresh media without MMS. Violin plots display the distribution of cells presenting Yen1-GFP foci as in (B), the untreated mus81Δ cells plot is shown as reference. (D) **Cells containing** a deletion on SLX8 were observed for their distribution of foci of the different variants of Yen1-GFP. Violin plots display the distribution of cells as in (B). (E) **Cells** from the indicated genotypes were arrested in G1 and released in the presence of cycloheximide with samples being taken at the indicated time points. Total protein extracts were inspected by immunoblot for the presence of Yen1-

HA and their intensity quantified relative to the loading control obtain by stain-free imaging (BioRad), relative amounts of Yen1 are plotted in the graph to facilitate comparison. Statistical significance for foci distribution difference was estimated by the Fischer exact test and asterisks denote p<0.05 compared to wild-type.

Page 121. **Figure 53.** Mutation of the SIMs of Yen1 impacts the chromosome segregation in mus81Δ cells. **(A)** Diagram showing representative drawings of chromosome segregation in cells harboring a lacO/GFP-LacI array tag on chromosome VII. To discriminate cells with a timely chromosome segregation from those presenting different types of aberrant segregation (delayed segregation, non-disjunction and aberrant chromosomal numbers) a 2h limit of observation was implemented, the time intervals to achieve full GFP-dot separation into daughter cells was determined for each individual cell observed, and cells un-segregated at 2hrs were classified as non-disjunctions. Two sets of representative actual images of a normal segregation pattern and a non-disjunction pattern are shown below the diagram. **(B)** Over 400 cells per strain were individually counted and are represented in violin plots according the time spent to segregate the lacO/lacI array. Statistical relevance of the differences observed was determined by the Fischer exact test at P<0.05.

Page 122. **Figure 54.** Crossover formation is impaired in cells containing the SIM mutant version of Yen1. **(A)** Diagram showing the ch XV based DSB-induced recombination reporter. (B) Graphs summarize recombination outcomes in either red-sectored colonies or all types of colonies (C) combined with the indicated strains and normalized to their Plating Efficiency (PE). Statistical significance was determined by the Fischer exact test at **P<**0.05. (D) Diagram showing the ch II-V based ectopic DSB-induced recombination reporter and its expected outcomes during physical analysis by southern blotting (E) with a probe at the URA3 locus. (F) Quantification of three independent southern blot analyses is plotted relative to PE (Galactose vs Glucose). Statistical significance was determined by the Student T-test at P<0.05.

Page 127. **Figure 55 – Supplementary figure 1.** (A) Alignment of Yen1's SIM1 (Aa 635-646) to already characterized SIMs in Slx5, Elg1 and Rad18 presenting an aliphatic core flanked by acidic (D/E), phosphorylatable (S/T) or polar residues (R/K). (B) Alignment of putative SIM motifs found in different yeast species' Yen1 sequences and matching the architecture of Yen1's SIM1 in S.cerevisiae (C) Disposition of SIM1 in S.cerevisiae and other yeast species relative to the SIM2 and the conserved domains of the bi-partite NLS (containing a regulatory CDK1 site).

Page 128. **Figure 56 – Supplementary figure 2.** Comparison of foci counting between Cter and Nter GFP fusions of Yen1. Strains all bear chromosomally tagged Yen1-HA wild type and SIM mutants in the indicated genetic backgrounds and carrying its corresponding Yen1-GFP expressing plasmid. Left: Results lifted from figure 51 B, the plasmid containing Yen1 and mutants codes a C-terminal GFP fusion. Right: Corresponding backgrounds and plasmids but with an N-terminal GFP fusion to Yen1 and mutants. These data correspond to preliminary results before a definitive switch to Cter GFP. Though the foci distribution turns out to be very similar. Violin Plots display the distribution of G2/M cells showing no foci, 1-2 foci or more than 2 foci for each strain Only between 100 and 400 unique G2/M cells were counted over 2-3 independent trials depending on strains.

Page 134. **Figure 57.** An investigation of the putative interaction between the condensins and Yen1. (A1) Co-immunoprecipitation assays were performed by pulling down cell extracts with a myc-trap magnetic matrix. Inputs were taken from whole cell extracts. Immunoprecipitates were thoroughly washed and blotted for HA with high sensitivity ECL. (A2) Whole cell extracts were confronted to an HA-tagged sepharose matrix at 4°C. After thorough washing they were blotted for myc with high sensitivity ECL (top). Anti-HA blots (middle and bottom) allowed detection of the immunoprecipitates

themselves along with Input levels verification (bottom). (B) Strains are chromosomally tagged with the Auxin inducible Smc2 degron system along with an endogenous Gal promoter and GFP or RFP Yen1 fusion. Cells were synchronized using alpha factor and Yen1 expression induced with a short pulse of galactose. During culture, auxin was added for the middle and right panels. After release cells were plated an followed with time-lapse spinning-disk microscopy with 3 minutes intervals. (C) Cells chromosomally tagged with a Gal promoter fused to Yen1-RFP and a Ycs4 GFP fusion were cultured in asynchronous populations. They were plated following a short burst of galactose induction and a release in glucose. Pictures were taken choosing cells at random only looking at the white light field. White bar: 5 µm.

Page 135. **Figure 58.** Co-localization assays for Yen1 and Ipl1, Sli15 or Rap1. Chromosomally tagged cells with a Gal promoter Yen1-RFP fusion and the auxin inducible Smc2 degron system along with a GFP-fusion of the candidate protein (Ipl1, Sli15 or Rap1) were cultivated and synchronized using alpha factor. Auxin was added to the media following Yen1 induction. (A) Pictures of G2 cells in a situation of de-condensation of chromosomes for cells containing Ipl1-GFP. (B) Similar pictures were taken with Sli15-GFP containing cells. (C) Time-lapse of G2/M phase for the Rap1-GFP containing strain.

Page 136. **Figure 59.** An attempt at BioID. Whole cell extracts are immunoprecipitated on a streptavidin matrix, pulling down all the biotinylated proteins. Cells are chromosomally tagged with the BirA enzyme allowing biotinylation of nearby proteins (noted BioID) with a 3 myc tag. In this experiment, Yen1 is fused with the BioID machinery. In the rightmost well, Ycs4 is tagged with it. Allowing for a positive control with Smc4 bearing a HA tag. The strain with “Yen1-13myc” has only a myc tag on Yen1 so as to represent a negative control with no BioID biotinylation. The BioID enzyme fusion creates a shift in molecular weight as evidenced by the Yen1-BioID and Yen1-13myc weight difference.

Abstract

The repair of double-stranded DNA breaks (DSBs) by homologous recombination involves the formation of branched intermediates that can lead to crossovers following nucleolytic resolution. Ubiquitin and SUMO modification is commonplace amongst the DNA damage repair proteins. What is more, a number of DSB repair factors interact with each other when sumoylated, making use of SUMO interaction motifs (SIMs). The nuclease Yen1 is tightly controlled during the cell cycle to limit the extent of crossover formation and preserve genome integrity. In this manuscript we describe further regulation of Yen1 by ubiquitination, sumoylation and non-covalent interaction with SUMO through its newly characterized SIMs. Yen1 is sumoylated by Siz1 and Siz2 SUMO ligases, especially in conditions of DNA damage. Furthermore, Yen1 is a substrate of the Slx5-Slx8 ubiquitin ligase. Loss of Slx5-Slx8 stabilizes the sumoylated fraction of Yen1, and results in persistent localization of Yen1 in nuclear foci. Slx5-Slx8-dependent ubiquitination of Yen1 occurs mainly at K714 and mutation of this lysine increases crossover formation during DSB repair and suppresses chromosome segregation defects when other nucleases are unavailable. In addition, proper and timely nucleolytic processing from Yen1 is dependent on interactions mediated by non-covalent binding to sumoylated partners. Mutations in the motifs that allow SUMO-mediated recruitment of Yen1 leads to its mis-localization, decreasing Yen1's ability to resolve DNA joint-molecule intermediates and resulting in increased genome instability and chromosome mis-segregation.

Abstract in French

La réparation de cassures d'ADN double brins par recombinaison homologue nécessite la formation d'intermédiaires multibrins qui peuvent être le lieu de formation de crossovers après résolution par des nucléases. La modification de protéines par ubiquitine et SUMO est un mode de contrôle répandu parmi les protéines de la réparation de l'ADN. De plus, certaines protéines de la réparation de cassures double brins interagissent entre elles, lorsqu'elles sont sumoylées, par le biais de motifs d'interaction avec SUMO (SIMs). La nucléase Yen1 subit un contrôle rigoureux lors du cycle cellulaire dans le but de limiter la formation de crossover et ainsi de préserver l'intégrité du génome. Dans ce manuscrit, il sera mis en évidence que Yen1 est régulé de surcroit par l'ubiquitination, la sumoylation et enfin l'interaction non covalente avec le modificateur SUMO via ses SIMs désormais découverts. Yen1 est sumoylé par les SUMO ligases Siz1 et Siz2, d'autant plus en conditions de dommages à l'ADN. En plus de quoi, Yen1 est un substrat de l'ubiquitine ligase Slx5-Slx8. En absence de cette dernière, la fraction sumoylée de Yen1 persiste, ce qui mène à la localisation durable de Yen1 en accumulation ponctuelle dans le noyau. L'ubiquitination de Yen1 par Slx5-Slx8 a surtout lieu à la lysine 714. Une mutation de cette lysine augmente la formation de crossovers, et annule également les défauts de ségrégation des chromosomes qui peuvent avoir lieu en l'absence d'autres nucléases. D'autre part, l'action nucléolytique de Yen1 ne s'effectue correctement que lorsque celui-ci peut interagir de façon non covalente avec des partenaires sumoylés. Des mutations dans les SIMs de Yen1 réduisent sa capacité à découper et résoudre les intermédiaires de la recombinaison, ce qui donne lieu à une augmentation de l'instabilité génomique et de la mauvaise ségrégation des chromosomes.

Outline of the Thesis

The first three chapters of this PhD thesis set the context of the study. The first chapter puts the protein of interest in its context. By broadly describing the sources and types of DNA damage, along with the repair processes to counter them, the position of the target protein and its use in the cell is made clearer. Most DNA repair pathways are quickly described as an overview in the second part of chapter one, with a clear emphasis given to Homologous Recombination (HR) which is described in detail, culminating in a brief description of the use of nucleases such as Yen1.

Chapter two consists of a description of ubiquitination and sumoylation, especially in the context of proteins involved in DNA repair. Finally, the third and last chapter of the introduction focuses on the current knowledge of the yeast Yen1's properties, activity, and control. Chapters 4 and 5 of the thesis cover the results obtained and the main conclusions of our work aimed at understanding the control of Yen1 by SUMO and ubiquitin modifications. Chapter 4 outlines an endeavor to characterize Yen1 ubiquitination and sumoylation, along with the discovery of its specific targeting by the SUMO-targeted-ubiquitin-ligase Slx5-Slx8. Chapter 5 further pursues Yen1's control by sumo-targeted recruitment via newly discovered Sumo Interaction Motifs (SIMs) on its C-terminus and the effects of deregulation of this recruitment when the motifs are mutated. Finally, a brief section describing the work still in progress and future research directions concludes this section.

1 The stability of the DNA molecule : types of damage and specialized DNA repair pathways

1.1 Types and sources of DNA damage

When Watson, Crick and Franklin first described DNA as a double helix macromolecule, it was seen as a very stable structure. After many years of studies, we now know that the DNA is very dynamic. Fully replicated each division, DNA is reworked and recombined by a variety of biological processes. The dynamic properties of DNA are in contrast to its importance for the cell and its self-perpetuation, highlighting the obvious need for protection and proofreading mechanisms [1]. Indeed, DNA is subjected to daily aggressions from within the cell and from the environment. Thus, cells have devised and retained multiple mechanisms for tolerating and repairing the damage [2]. Failures in these mechanisms can lead to serious diseases and malfunctions, as we will discuss further down. Even so, mutations can still happen and be acquired despite the normal function of DNA repair pathways allowing the necessary genetic variability that enables all living beings to adapt to a changing environment and evolve from generation to generation.

Aggressions to DNA come in a myriad of forms, all of them pose a threat to survival in their own way. For a human cell, in a day, over 70 000 events of DNA damage and lesions are estimated to occur. 75% of those are effectively cuts in one of the two strands of the DNA double helix [3]. Also known as Single-Strand Breaks (SSB). Damage can come in the form of lesions in the DNA backbone, modified bases, breaks, but also anomalous or misshapen structures arising from a string of mismatches [4]. The multiple repair mechanism will share the load of repairing the different types of damage. Some mechanisms are specialized for a lesion, while others can deal with a wider range of substrates. Some key proteins overlap different mechanisms and there may be some interplay to broaden the range of substrates while allowing for backup pathways. Indeed, the average number of lesions given above is an estimate for a normal functioning cell. Environmental stresses can increase this number. Any living being must be able to sustain the daily occurrence of DNA damage but also the occasional spikes in lesions from common sources like Ultraviolet (UV) light or radiation.

Even with the tens of thousands of aggressions to the DNA we know about, cells manage to replicate and divide while keeping the mutational load low. Additional details for repair mechanisms, new repair pathways and sub-pathways are still being described to this day. With the growing understanding of the specifics of DNA repair mechanisms it becomes more and more obvious that the cross-utilization and coordination between pathways afford cells an incredible flexibility and adaptability to situations threatening the DNA molecule integrity and the transmission of the genetic information.

This section aims to summarize the major types of DNA damage as well as their potential mutagenic and cytotoxic effects, classified by type of alteration as follows:

1. DNA base damage
2. DNA backbone damage
3. Mismatches and covalent strand links

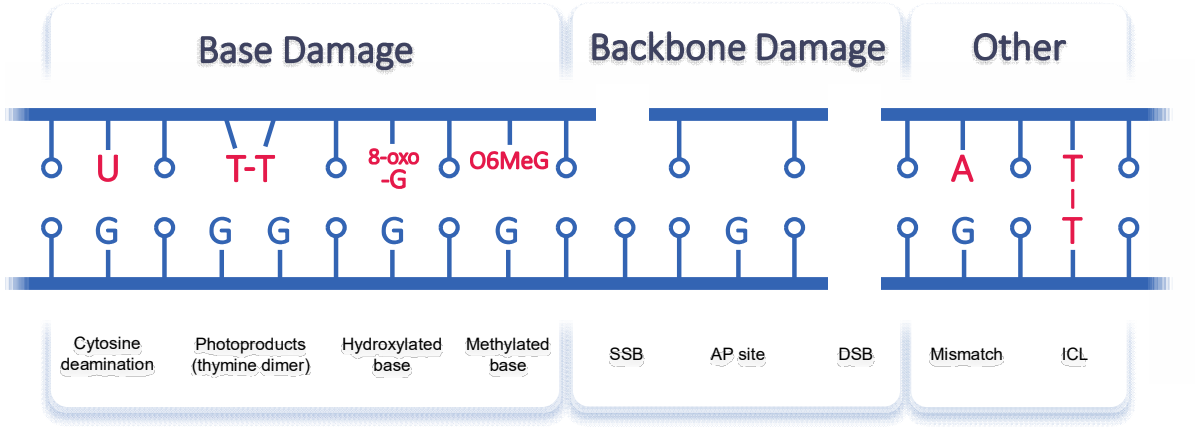

Figure 1. *Schematic representation of the main types of DNA injuries. The three classes are represented by light blue boxes containing some of the main examples of specific DNA lesions. The base in red is the modified one. G = Guanine; T = Thymine; A = Adenine ; U = Uracil. Adapted from multiple sources: Yi et al, 2013 [5]; Abbotts et al, 2017 [6] ; Tubbs et al, 2017 [3].*

1.1.1 Types of DNA damage

1.1.1.1 Base damage: Alkylation, hydroxylation, deamination and photoproducts

Bases can receive an alkyl group through a reaction with a donor, called **alkylation**. This covalent bond modifies the double helix and alters the DNA geometry. Amongst the most common products of these reactions is the methylated base: O^6-methylguanine (O6MeG) [7]. It forms by transfer from a methyl donor such as S-adenosylmethionine (SAM). The latter can spontaneously generate 10-30 O6MeG per mammalian cell per day, 600 partly cytotoxic N3-methyladenine and around 4000 mostly harmless N7-methylguanine [8]. O6MeG is highly mutagenic because of base mispairing which can produce G:C→A:T and T:A→C:G transition mutations. Other base damages generated by SAM, such as 3-methyladenine, 3-methylthymine and 3-methylcytosine, are also potent blocks of DNA replication [6].

Addition of an Oxygen to a base or **hydroxylation** can occur spontaneously as a result of normal metabolism in a cell. This common reaction on the carbon 8 residue of Guanine forms 8-oxo-Guanine (8-oxo-G) which incorrectly pairs with Adenine equally as well as it normally pairs with Cytosine. It can thus cause G:C→A:T transversions [1]. 8-oxo-G appears at a rate of 2800 per human cell per day [3].

Through a spontaneous reaction of **deamination**, DNA bases can loose their exocyclic amine to transition into different bases: Cytosine can become Uracil, Adenine transitions to Hypoxanthine, Guanine converts into xanthine and 5-methyl Cytosine may transform into Thymine. These are more likely to occur on single stranded DNA, during replication for instance. Similarly, exogenous factors such as UV or intercalating agents may enhance the rate of deamination for a given base. This is not a rare occurrence, Deamination of cytosine to uracil and 5-methylcytosine to thymine takes place between 100 and 200 times per cell per day [3, 9]. Based on recent analysis methods, Uracil and Thymine from deaminated bases seem to promote mutagenic events associated with cancer [6].

Cyclobutane pyrimidine dimers (CPDs) and the pyrimidine pyrimidones (6-4) photoproducts (6-4PPs) are two common **photoproducts**. Two Cytosine or Thymine located in close proximity become covalently bonded due to direct absorption of UV light photons (Figure 2) [5]. The link occurs between particular carbons on each base. Around 75% of photoproducts are CPDs and 25% are 6-4PPs [10]. Upon further exposure to UV light the already modified bases can be further altered into their more toxic, Dewar isomers [11]. These photoproducts cause C→T transitions at dipyrimidine target sites including some tandem CC→TT events [12].

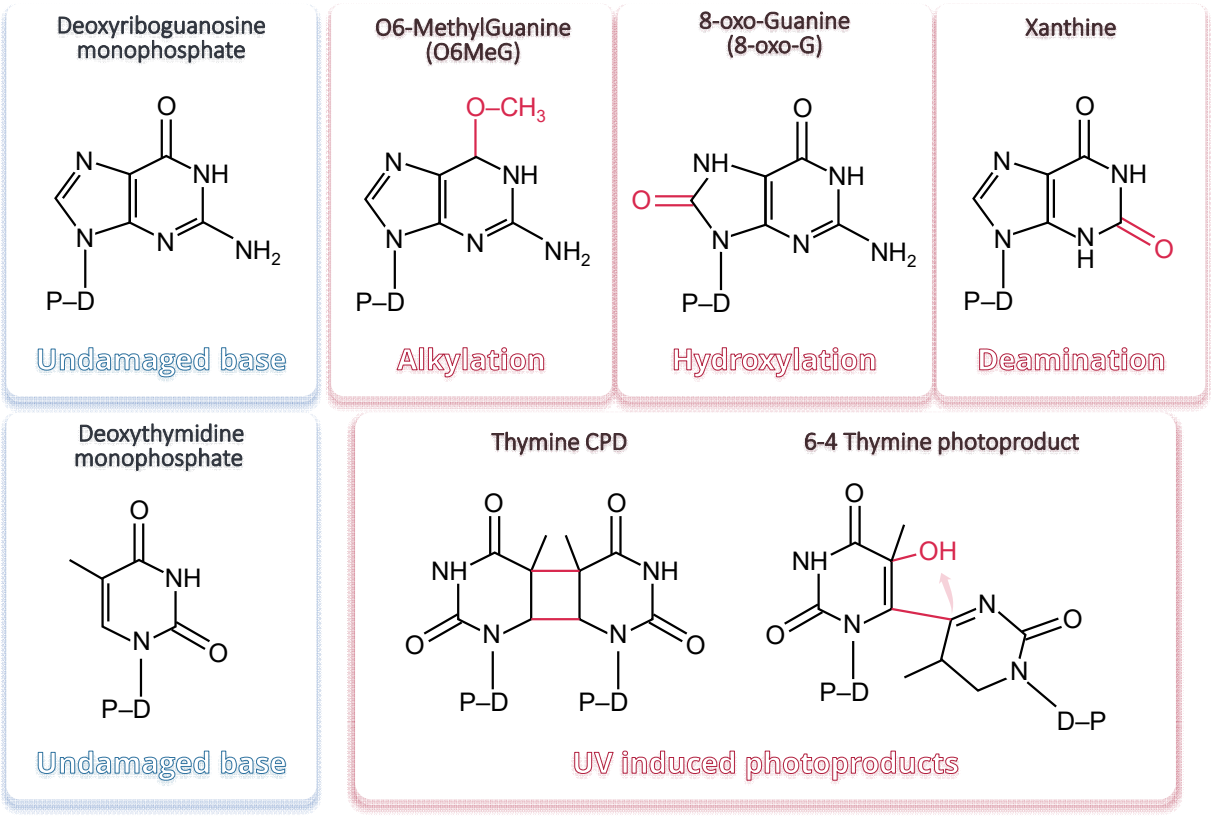

Figure 2. *Examples of altered bases. Top row: Guanine modified with either alkylation, hydroxylation or deamination reactions. Bottom row : Basic thymine photoproducts. Figure devised with data from [5, 13, 14].*

1.1.1.2 DNA backbone damage: Abasic sites and DNA breaks

Hydrolysis of the glycosidic bond separating a purine or pyrimidine and its desoxyribose is called **depurination or depyrimidination** respectively. Such a reaction severs the nitrogenous base from the sugar backbone [7]. This reaction can be spontaneous or the result of cleavage by a DNA glycosylase. The resulting gap is called an **Abasic site** or AP site for both apurinic or apyrimidic sites [6]. AP sites are the most frequent type of endogenous damage [10] with around 10000-12000 occurences per cell per day [3, 9]. They are strong DNA replication and transcription block. They can also be converted in SSBs and bear a high mutagenic potential as they lack coding information [6, 7].

One of the most common modifications of the DNA is the presence of a single-strand discontinuity or **Single-strand Break** (**SSB**) where the DNA backbone is locally severed at one of the two strand of the duplex DNA molecule. While the helical integrity of DNA can be conserved in the presence of these discontinuities, its presence weakens the helical integrity and DNA synthesis is impaired, as helicases will run off the double helix at the break point and polymerases will not be able to further extend synthesis across the break [15, 16]. A cell accounts for around 55000 SSBs per day, although their transitory nature may make their detection difficult [3]. As hinted at before, SSBs can arise from previously modified bases and AP sites. They are also a common intermediary of normal cell cycle processes such as DNA repair or Topoisomerase I activity.

When the backbone of both DNA strands of a duplex are severed in close proximity, there is an actual gap, a **Double-strand Break** (**DSB**) in the normally contiguous double stranded DNA (dsDNA) molecule. Out of all the lesions discussed thus far, DSBs are amongst the most lethal and can lead to a loss of

large stretches of the genome [17]. 25 DSBs are accounted for in any human cell on a daily basis [3] and a single unrepaired DSB can lead to cell death [18]. Even ensuring the viability of the cells, the repair of DSB can be often associated to loss of genetic information or rearrangements. DSBs can occur spontaneously even in ideal environmental conditions with an estimated spontaneous DSB per 10^8 base pair replicated [19]. On top of the spontaneous DBSs, an additional load of DSBs are induced upon exposure to ionizing radiation or DNA-damaging agents such as those used in cancer therapies. Much like SSBs, they can also appear as intermediates of normal cell function [20]. Even though they occur in a controlled environment, programed DSBs need to be taken care of to avoid their deleterious potential if left unrepaired and can be a source of un-targeted DSBs if the nucleases that originate them act off-program.

1.1.1.3 Mismatches and covalent DNA strand links

Rounds of replication are generally considered error-free with the involvement of high fidelity polymerases accompanied with proofreading mechanism [21, 22]. Yet, some bases escape proofreading during DNA replication and end up substituted by a wrong base at a frequency of about 10^{-6} to 10^{-8} bases per cell per generation [7, 21] in what is known as a **Mismatch** base-pair. These bases will not correctly pair with the complementary strand-opposing base, and will be subject to repair by the so-called mismatch repair machinery. Unrepaired mismatched base-pairs will ultimately lead to point mutations and depending on the substituted pair and the genetic code, these may end up altering the coding message of a given gene.

Exposure to bifunctional agents like cisplatin, nitrogen mustards, MMC, psoralens and alkylating agents can create covalent bonds between two bases of an opposing strand of a duplex DNA [23]. That bond is termed an **Interstrand CrossLink** (ICL) and it is a potent blockade of the replication and transcription machinery. It is also possible to find intrastrand crosslinks which will jeopardize the double helix structure and DNA-protein crosslinks which aren't strictly covalent bonds but nevertheless can be a roadblock to replication and transcription [4].

1.1.2 Sources of DNA damage

While the possibilities of spontaneous reactions and DNA lesions due to normal cell processes were presented before, cells also suffer exogenous stresses from their environment. Going through the most prevalent sources of DNA damage and their weight relative to one another should enable us to expect which pathways cell must have in order to survive their environment. The origin of damage is also of paramount importance for accurate repair. Different sources introduce lesions in different ways, with unique signatures, even if the type of damage seems to be ultimately the same. Not all breaks are clean and readily repairable. Sometimes the source of damage dictates the pathway or sub-pathway dedicated to fix the specific issue it created.

1.1.2.1 Endogenous DNA damage

Even in an environment devoid of external stresses, DNA is still subjected to aggressions arising from necessary housekeeping processes within all organisms and single cell beings. Metabolites and products of these reactions may also diffuse through the media to nearby cells. The DNA molecule is thus exposed to unwanted modifications that can alter its code by the modification of its bases, its pairing potential in a double-helix and its length and continuity. While not extensive, this section will cover the most frequent types of DNA damage that can originate in cells from endogenous sources.

Oxidative DNA damage: Reactive oxygen species

Reactive oxygen species (ROS) are generated from the metabolism of cells [24]. While Respiration is the more obvious source of ROS they can also be derived from anabolic processes. ROS are normal constituents of the cell, they participate in biochemical reactions, albeit at very low levels. ROS can also function as cellular messengers and can be used as a defense system against other cells and organisms. The most common ROS are superoxide anion radicals (O_2•−), hydrogen peroxide (H_2O_2) and hydroxyl radicals (•OH). Mitochondrial respiration releases around 1-2% of its daily oxygen consumption as superoxide radicals. H_2O_2 is formed by the superoxide dismutase enzyme from superoxide O_2•− in order to reduce the extent of its toxicity. There are direct sources of H_2O_2 as well in metabolism. Also, spontaneous reduction of H_2O_2 yields •OH.

These unstable radicals are extremely reactive [6]. When present at high enough levels, ROS lead to various modifications of nucleic acids. Around 100 different oxidative base lesions have been described so far [25]. For example: 8-oxo-G is the result of hydroxylation of a Guanine carbon, changing its structure. ROS can directly create Thymine glycols, AP sites and single strand breaks as well [26]. Finally, ROS may also attack DNA via the intermediary effect of lipid peroxidation. Hydroxyl radicals can oxidize lipid molecules, generating various aldehydes that in turn can damage all four DNA bases [7].

Replication as a source of DNA damage

Every enzymatic reaction has an error rate [1], the replication process is no exception. Three billion bases are copied each replication round by High-Fidelity polymerases δ and ε. Lower fidelity DNA synthesis can happen with α, β, σ, γ, λ, REV1, ζ, η, ι, κ, θ, ν, μ, Tdt and PrimPol polymerases during replication or repair [27]. As discussed before, mismatches happen and escape proofreading, albeit at a low rate. Replication will also expose lesions on the coding strands that escaped repair, these lesions will be either tolerated at the expense of increased mutagenesis risk or will lead to fork stalling to attempt repair in the context of on-going replication, increasing the chances of secondary damages, especially DSBs. On top of that, exposure of single-stranded DNA (ssDNA) at the forks by the replicative helicase increases the possibility of spontaneous cytosine deamination, especially if replication forks are stalled or undergo replication at a sub-optimal rate [3].

As stated above, replication fork stalling at a bulky lesion may lead to highly toxic DSBs through fork collapse. Fork collapse can also occur when a replication fork encounters a nick or a SSB, often as a result of Topoisomerase-related release of topological constraints, replication is slowed down and eventually stalls while DNA integrity is being restored. After the transient stalling, the replication must resume. If that fails to happen, fork collapse may occur by run-off at the SSB sites or by active cleavage through specialized endonucleases, allowing the possibility to restart fork replication through homologous recombination [28].

Some DNA sequences are more difficult to replicate because of their content: trinucleotide repeats capable of forming hairpins, AT rich sequences, inverted repeats, and sequences with the potential to form G quadruplexes [28]. These sequences are referred to as Fragile Sites. They correlate with motifs that slow down or pause the DNA replication fork, promoting strand slippage [28]. These sequences are considered to be a source of DSB in mammals and in *Saccharomyces cerevisiae* [9]. Upon replicative stress, they can present gaps and breaks. Moreover, inverted repeats and hairpin structures can be seen as substrates of certain repair mechanisms, leading to chromosome translocations [29].

Transcription as a source of DNA damage

Highly transcribed areas of the genome are more prone to DNA damage. In a similar fashion to replication, ssDNA is exposed during the transcription of the coding DNA strand. Even transiently, the exposed DNA strand becomes a substrate for cytosine deamination [3], and that sensitivity to deamination increases when transcription is lead to a pause or stalls for different reasons ranging from topological constraints to DNA base lesions encountered by the RNApol. In general, most of the transcription stress comes after the generation of persistent R-loops where the nascent RNA strand hybridizes with the template DNA causing spatial rearrangements. These R-loops are associated with increased DNA damage and genomic instability in humans and *S. cerevisiae* [30].

Topoisomerase-induced and programmed strand-breaks

In normal DNA metabolism, the winding of the DNA gets to a point where some relief is needed. For example, unwinding of DNA at a locus for transcription or replication may lead to a more tightly wound region further down the duplex. Topoisomerase enzymes alleviate this tension by performing a nick on supercoiled DNA [31]. The tension is relieved as the non-cut strand can freely rotate until the relaxed DNA is ligated back to its double helix state. There are a variety of ways to get the same result. Topoisomerase I performs a nick on a single strand while Topoisomerase II cuts both strands to allow a free rotation [7]. Thus, double and single strand breaks are transient intermediates expected of Topoisomerase function. While remarkably efficient in releasing topological stresses, Topoisomerases can be impaired by exposure to poisons and chemicals that can make them collapse and lead to actual SSBs or DSBs. Topoisomerases are also sensitive to damaged bases present in the vicinity of their cut site, where a previous DNA base lesion may throw them off and also lead to a break [32].

Moreover, certain cell programs use DSBs as a deliberate way to initiate chromosome rearrangements. All cells that undergo meiosis use a specialized nuclease (Spo11 in *S. cerevisiae*) to induce DSBs and allow chromosome re-arrangements and the necessary covalent-links to undergo the reductional divisions of meiosis [31]. Breaks are also induced during V(D)J recombination to introduce variability in the repertoire of antigen binding proteins [20].

Nucleotide excision repair as source of DSBs

The normal repair of damaged nucleotide can be handled through excision of the damaged bases. Even without malfunction of this process, if several damaged bases are located less than 10 base pairs (bp) apart from each other, and on opposite strands, the simultaneous excision can lead to a DSB [9]. While this may seem unlikely given the length of most living being's genome, acute exposure to DNA damaging drugs creates a strong temporary load of damage that increases the possibility of damaged base being close together. Similarly, tumors and cancerous phenotypes create a local environment that is rich in DNA damage with higher oxidative stress and replicative stress [2].

Erroneous ribonucleotide insertion

Every so often, ribonucleotides may be inserted in DNA instead of the expected desoxyribonucleotides. For instance, each round of cell division in mammals, over a thousand ribonucleotides are incorporated into the genome. The normal process of repair of these nucleotides via excision leads to the formation of an SSB intermediate. If Topoisomerase I encounters a ribonucleotide, it may also form an SSB that it won't be able to religate [33].

1.1.2.2 Exogenous DNA damage

Dealing with damage occurring spontaneously and through cellular processes is already no small feat. As stated earlier more than 50000 occurrences of DNA damage can be accounted for in normal conditions. An additional DNA damage burden comes from the environment on top of the endogenous damage. It can easily double the amount of daily DNA aggressions a cell must deal with. For example, a single day of sunlight exposure can induce up to 10^5 DNA lesions for each exposed keratinocyte [34]. In order to appreciate the importance of the robust and wide-ranging DNA repair processes in cells, the contribution of exogenous agents to the DNA damage load must be further considered. This section below provides a brief description of the most common sources of exogenous DNA damage from environmental exposure.

Ionizing radiation (IR)

Composed of alpha, beta, gamma, neutrons and X-rays, ionizing radiation (IR) is found everywhere in our environment [7]. Unlike chemical agents, which diffuse through the media, IR is highly penetrating. Rays deposit their energy in random events, going through matter easily [9]. They emit from various sources ranging from the man-made medical devices to rocks, soil, radon and cosmic radiations [7].

IR can damage DNA in different ways to produce several types of lesions. The DNA damage can be indirectly induced by exciting nearby water molecules, increasing the local amount of (•OH) ROS, that in turn will cause oxidative lesions such as 8-oxoG and thymine glycols. This indirect action roughly represents two thirds of the IR induced DNA damage load [35, 36]. IR rays may also directly radiolyse DNA producing SSBs and DSB [36]. These IR-induced breaks will bear unconventional signatures on their ends, such as 3'-phosphate or 3'-phosphoglycolate ends, that will need to be processed before repair [9].

Ultraviolet radiation (UV)

Much like IR, UV light can damage DNA either directly or by exciting adjacent molecules [7]. UV light, especially from the UV-C spectra, can induce the formation of photoproducts, single base lesions caused by absorption of photons. The most common UV-C induced photoproducts are the aforementioned CPDs and 6-4PP [5]. Thankfully the most hazardous parts of the radiations from the sun are mostly blocked by the ozone layer. For metazoans, different layers of tissue provide some protection from UV-rays [37, 38].

Alkylating agents

A variety of cytotoxic and mutagenic adducts are formed due to alkylation. Alkylating agents are chemical molecules able to transfer a variety of alkyl moieties to the DNA as is the case for Methyl methanesulfonate (MMS) that produces alkylated species such as O6MeG [5]. Alkylating agents are found in tobacco smoke, food, pollution, coal, pesticides, industrial dyes and also sulfur and nitrogen mustards used in World War I [7].

Polycyclic aromatic hydrocarbons

Benzo[a]pyrene is one of the major Polycyclic aromatic hydrocarbons. They are carcinogens found in tobacco smoke, automobile exhaust and grilled foods. These molecules are DNA intercalants that form direct bulky adducts with DNA bases and specifically Guanine in the case of Benzo[a]pyrene [7]. The resulting DNA adducts have been associated with a higher cancer risk [39]. The damaged bases have to be excised from the genome to avoid G:C to T:A transversions. Benzo[a]pyrene activity in the lung has also been associated with cytosine deamination [40].

Other natural environmental stresses

On top of the major contributors to DNA lesions – UV and IR – less common environmental sources do add up over time and significantly contribute to the mutagenic load and to overwhelming the DNA repair machineries. Exposure to toxins, heat, cold and oxygen deprivation have been shown to cause DNA damage in human cells. Hypoxia and local – tumor induced – low oxygen is linked to lower replication and translational activity in DNA repair genes, leading to a more unstable environment [41, 42]. Heat stress also inhibits DNA repair systems, in addition to that, it leads to the accumulation of 8-oxo-G, cytosine deamination and AP sites [43]. Exposure to harsh cold temperatures is correlated in plants with higher ROS and thus oxidative stress [44]. Finally, toxins are genotoxic agents used by microorganisms and fungi to defend themselves. Alfatoxin B1, for example, may lead to the formation of AP sites and other DNA lesions [45]. For humans, exposure to these toxins comes from contamination of food products [7].

Other man-made chemicals

To further add to the list of stresses creating DNA damage, there are many more man-made DNA damaging agent than the main ones mentioned above. N-nitrosamines found in tobacco form alkylated DNA bases [6]. The list goes on with man-made DNA intercalating molecules used for research or treatment. 4-nitroquinoline 1-oxide, has both carcinogenic and mutagenic properties [7]. DNA damage may indeed be induced chemically for treatment, especially in the case of chemotherapy. Cisplatin, for example, is a cross-link inducing chemotherapeutic drug [46].

Many other everyday products contain DNA damaging agents. Food preservatives, food additives, cosmetics, and most plant fertilizers and protection products [7]. The notorious sperm DNA damaging bisphenol A got known for disrupting endocrine activity and in turn triggering higher ROS stress [47].

The examples explained above are part of a non-exhaustive list, highlighting the existence of a myriad of ways to damage the DNA, with some prevailing sources. To these more common sources we may have to add multiple more rare chemicals, some of them acting in an indirect way by altering the balance of cell metabolism, inducing stress or creating deleterious environments. Viral or bacterial aggressions as well as physical stresses on cells causing tissue inflammation can also contribute to the DNA damage load [48]. The list of exogenous agents we expose ourselves to willingly – for food or leisure – is bound to keep growing as more studies reveal the intricacies of their effect on health.

1.2 DNA repair mechanisms: restoring DNA integrity

To restore the integrity of the DNA from the cumulated lesions, cells have evolved multiple repair mechanisms. Sometimes with overlapping functions. DNA repair mechanisms can come at a risk for cell viability. To allow an efficient safeguard of the genome the cells couple these repair pathways with mechanisms to slow-down and stall the progression of the cell cycle. Preventing cells from rushing to cell division unless the genome has been checked for its integrity. The cell's response to DNA damage consists then an initial damage sensing response and subsequent slowing-down of cell cycle followed by the actual repair processes [4, 49, 50].

The repair mechanisms have to cover a wide spectrum of substrates and sometimes lesions are difficult to repair due to an unconventional alteration. The basic arsenal of DNA repair mechanisms fulfills that description by having multiple independent mechanisms. Some of these have sub-pathways, which could be argued to have a backup role for one another. Although, it is possible for the core constituents of certain machineries to lend a hand to another DNA repair mechanism. The cross-talk and interplay between DNA repair mechanisms enable cells to reverse and repair a larger spectrum of lesions, both usual and rare, expected and unexpected.

From then on, most of the information will be distilled from studies of *Saccharomyces cerevisae* with rare mentions of the similarities with metazoans such as humans, and the occasional look at bacterial models. *S. cerevisae*, referred to as "yeast" or "budding yeast" has been the platform for many experimental discoveries and models in eukaryotic DNA repair. Its rather simple constituents and compliance make it an ideal lab subject. The results often give great insight into the human function when the mechanisms are not outright conserved in detail or in convergence of function [51-53].

1.2.1 Direct DNA repair by reversal

Some DNA modifications are countered by direct repair pathways, in which proteins reverse the modification of a damaged DNA base. The proteins engaged are often inactivated after the enzymatic reaction [1]. These pathways are generally directed to single base damage and most often do not require incision of the DNA backbone [5]. In the direct reversal reactions, the actual repair happens after recognition by complementarity between the specialized enzyme and a specific type of DNA damage. Recognition can occur through base pairing or shape recognition [4]. Though most events of direct DNA repair happen following the same basic principles, there are three major mechanisms [5].

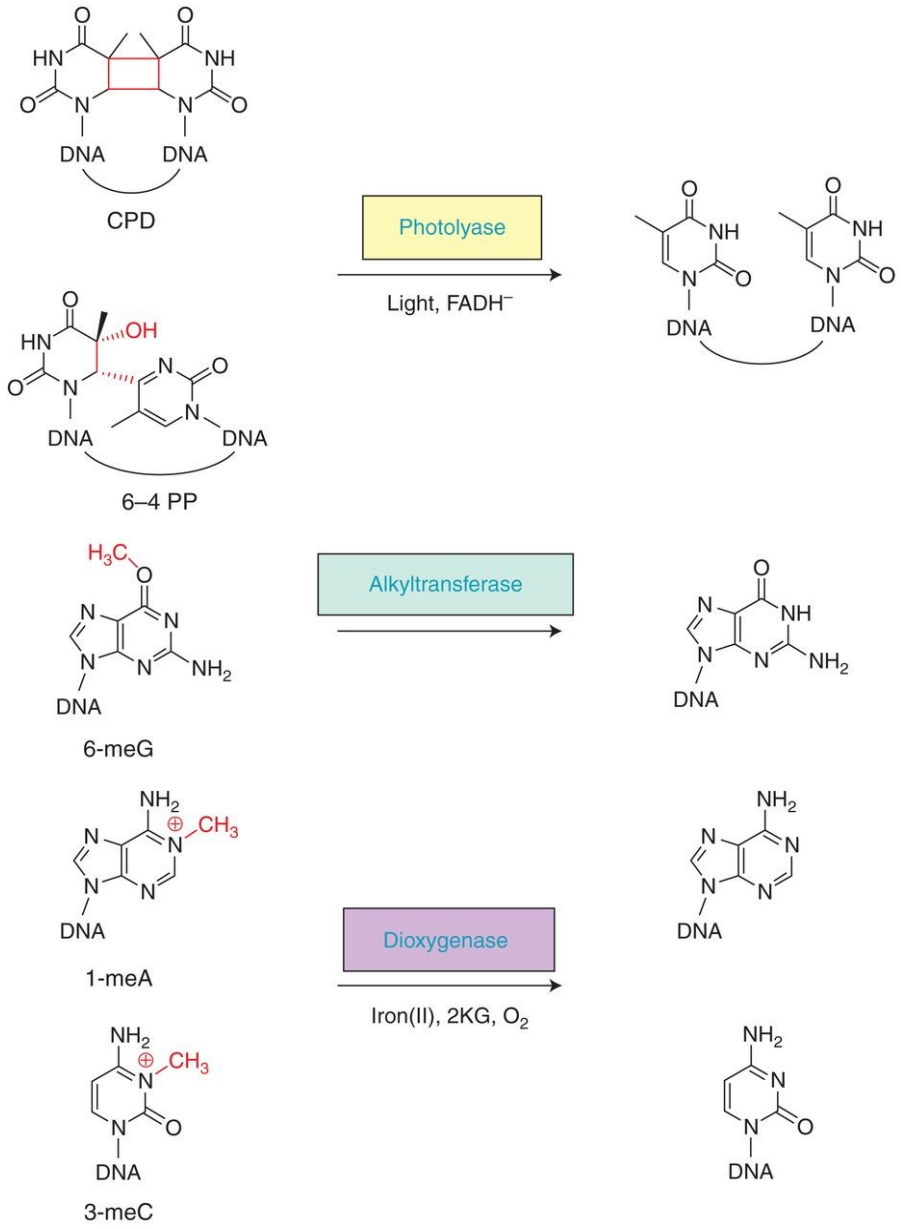

Figure 3. *Representation of direct DNA repair pathways, their main substrates and the corresponding single-use enzymes. By Yi and He in 2013 [5].*

1.2.1.1 Photolyases

A class of single-use enzymes called Photolyases use blue and near-UV light to reverse UV light induced damage via a photo-induced electron transfer from the essential cofactor Flavin adenine dinucleotide (FAD) located deep within the core of the protein [4, 5]. To allow this electron transfer, there must be direct contact between the protein and the damaged base [54].

UV light produces mainly two types of lesions: CPDs and 6-4PPs [5]. Similarly, there are two types of photolyases, each specific to a type of damage: CPD photolyases and 6-4 photolyases. The structures and reaction mechanisms of the two are similar [3]. These photolyases are not common in many species, especially metazoans. Specifically, placental mammals lack photolyases. Though, perhaps as an evolutionary keepsake, they express proteins named cryptochromes with high sequence and structural similarities to photolyases but lacking repair function. Rather, they set the circadian clock [3].

1.2.1.2 AGTs O6-alkylguanine-DNA alkyltransferases

Much more common than photolyases, O6-alkylguanine-DNA alkyltransferases (AGTs, or MGMT for methyl guanine transferase specifically) combat the deleterious effects of alkylating agents by reversing O6-alkylated DNA damage [5, 7]. AGTs remove alkylation adducts in a one step reaction by transferring it to a cysteine in their catalytic pocket [1, 7]. In accordance with the high frequency of occurrence of O6meG and its associated high mutagenicity and carcinogenicity [5], one of the most common AGT across species is O6-meG-DNA methyltransferase (MGMT). O6meG repair is alsmost exclusively handled by it even though nucleotide excision repair (see below) is a possibility [55]. Much like photolyases, MGMT recognizes damage by diffusion and shape recognition. Through recognition, the damaged base is flipped into the active site cavity where the methyl transfer happens to a cysteine. The protein then dissociates from the repaired DNA, but the methylcysteine is stable. AGTs become inactivated after the reversal of the lesion according to their single-use nature [3].

1.2.1.3 The AlkB family dioxygenases

In addition to the AGT-mediated reversal of O6-alkylated guanines a second pathway can reverse alkylation in N-alkylated base adducts that block Watson–Crick pairings by using AlkB-related α-ketoglutarate-dependent dioxygenases (AlkB) family enzymes [5, 7]. Much like the other direct DNA repair proteins, AlkB and related dioxygenases need to flip the damaged base out of the duplex for base adduct transactions. AlkB acts preferentially in ssDNA substrates [56]. The AlkB-catalyzed demethylation happens by oxidation of the aberrant alkyl group, which allows for cleavage of the N-alkyl group and restoration of the unmodified base [57].

1.2.2 Nucleotide Excision Repair (NER)

Nucleotide Excision Repair is the major repair pathway called onto for repair of bulky lesions such as CPDs and 6-4PP from UV radiation, benzo[a]pyrene adducts, or damage from chemotherapeutic agents [4, 7]. This multi-enzymatic system involves as many as 30 proteins in eukaryotes [58]. The basic principle is to remove a strip of around 30 nucleotides [59] containing the damaged base. The repair process ends when dsDNA integrity is finally restored using the undamaged strand as a template [60].

NER is well conserved among species [61]. In bacteria and eukaryotes, the nucleotide excision repair follows a similar path: the impaired base pairing [7] is recognized with a DNA binding protein: XPA or XPC (Xeroderma Pigmentosum, complementation group A and C) in humans, or its homologs in other eukaryotes. Stabilizing around the damaged area, these proteins then recruit TFIIH to unwind 20-30 base pairs. The unwound DNA is then substrate for a structure specific endonuclease with opposite flap-endonuclease activities. While XPG-ERCC5 cuts at 5'-flaps, XPF-ERCC1 will recognize 3'-flaps, both nucleases will thus operate incisions at 5' and 3' orientations of the unwound ssDNA bubble [4]. After the excision of the DNA stretch containing the lesion, the sliding clamp of the proliferating cell nuclear antigen (PCNA), together with replication factor C (RFC) will enable polymerases such as POL δ, POL ε or POL κ to synthesize a new DNA patch to fill in the gap. Either ligase LIG1 or XRCC1–LIG3 will finalize the repair by connecting the newly synthesized nucleotides to the incised dsDNA [7]. It is worth noting that some excision repair factors contribute to other processes such as TFIIH in transcription or RPA in recombination among other things [4].

This brief description of the events may not accurately reflect the key steps and proteins of these pathways which is why Figure 4, that brilliantly summarizes it was taken from Freidberg et al, 2001 [62] to further illustrate the details.

While studying the repair of UV-lesions, it was found that the transcribed strand was repaired at a faster rate the non-transcribing one [63-66]. This observation led to the identification of a specialized NER sub-pathway, the transcription-coupled repair (TC-NER), which couples the base damaged induced stalling of the RNA polymerase II with NER. In this specialized pathway, recognition of the damage is enforced by two specific factors, CSA and CSB (respectively cockayne syndrome WD repeat protein A or B also known as ERCC8 and ERCC6), which associate to stalled transcription sites to recognize the damaged bases and prime the recruitment of the core-NER factors [67]. Removal of the RNA polymerase II exposes the lesion site. At this point, TFIIH is recruited, and from then on, repair occurs following the same steps as those followed by the GG-NER (figure 4, right half, H to L) [7, 62].

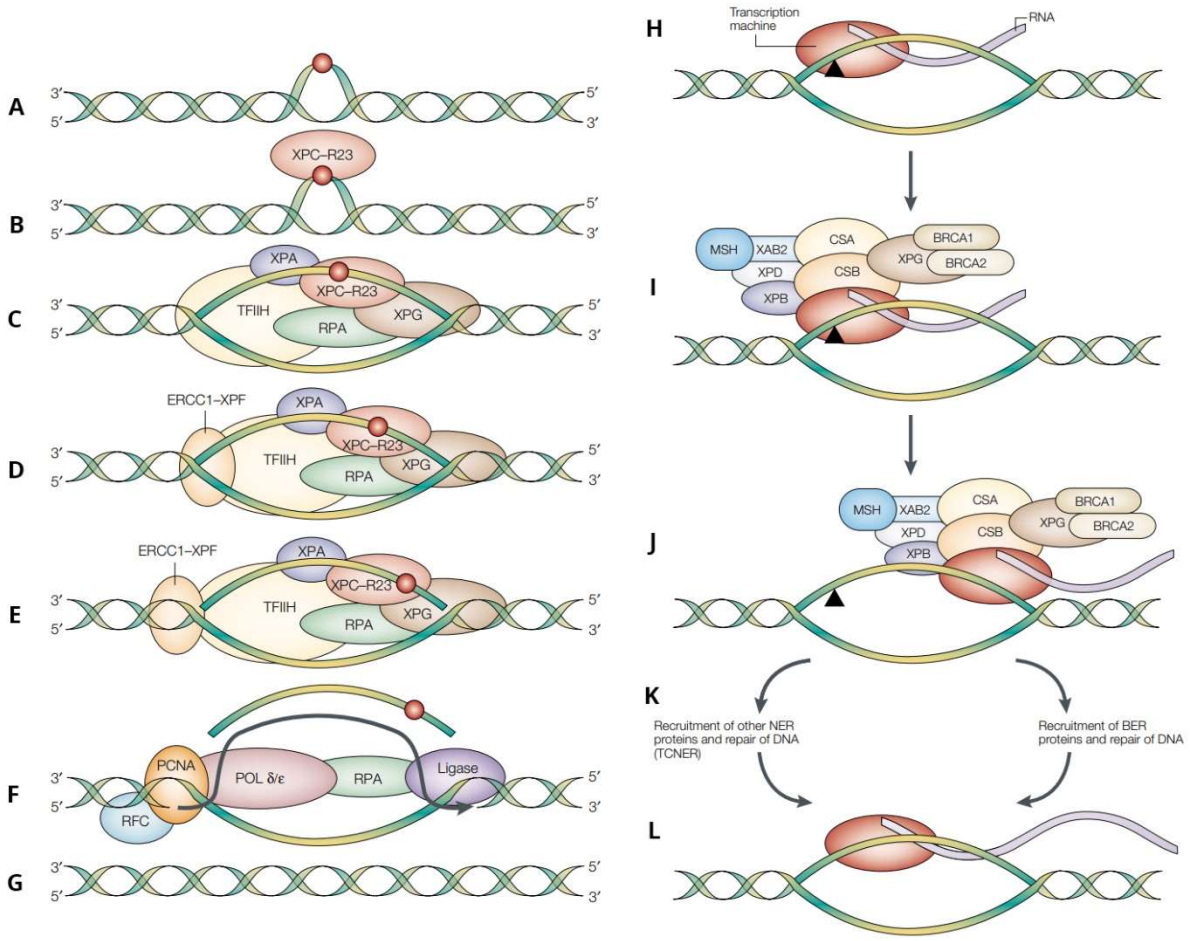

Figure 4*. GG-NER (left) and TC-NER (right) in humans from Friedberg et al. 2001 [62]* ***Left panel****: **A**: helix distorting base lesion (red circle) on duplex DNA. **B**: Damage recognition by XPC bound to HHRAD23B (R23). **C**: binding of XPA, RPA, TFIIH and XPG. TFIIH's helicase activity unwinds the DNA duplex around the base damage. This generates a bubble in the DNA. **D**: Binding of the ERCC1–XPF heterodimeric subcomplex generates a completely assembled NER multiprotein complex. **E**: XPG and ERCC1–XPF are duplex/single-stranded DNA endonucleases. XPG cuts the damaged strand 3' to the site of base damage. Conversely, ERCC1–XPF cuts 5' to the site of base damage. This bimodal incision generates an oligonucleotide fragment of around 27 to 30 nucleotides in length which includes the damaged base. **F**: This fragment is excised from the genome, concomitant with restoring the gap by repair synthesis with DNA pol δ or ε, as well as the accessory replication proteins PCNA, RPA and RFC. The covalent integrity of the damaged strand is then restored by DNA ligase. **G**: Collectively, these biochemical events return the damaged DNA to its native chemistry and configuration.* ***Right panel****: TC-NER. **H**: transcription road block by damaged base. **I**: Arrested transcription by RNA polymerase II recruits a large complex containing, among other proteins: CSA and CSB; the NER proteins XPB, XPD and XPG; BRCA1 and BRCA2; and a protein called XAB2 that binds to CSA. **J**: The stalled transcription machinery is removed from the fork. **K**: this provides access to proteins required for the completion of NER (or BER depending on the type of damage) **L**: after repair, transcription can begin anew.*

1.2.3 Base Excision Repair (BER)

Subtle modifications of DNA such as oxidized bases, alkylation and abasic single base damage, are not detected as significant distortions of the double helix [1] and thus will not be recognized by the NER toolkit. They can be corrected with minimal processing by Base Excision Repair (BER), a repair process mostly active in the G1 phase of the cell cycle [7, 60]. BER begins with a set of chromatin modifications around the damaged site, which allow recognition of specific base damage types by a DNA glycosylase [6]. The damage recognition mechanism of DNA glycosylases is similar to that of DNA photolyases [4].

DNA Glycosylases are either monofunctional or bifunctional, the latter combines glycosylase and β-lyase activity. Monofunctional glycosylases generate AP sites, which are directed to the short-patch-repair pathway, also known as single-nucleotide BER [6]. An AP endonuclease (APE1) cleaves the phosphodiester 5' bond of the AP site and the single nucleotide gap generated is filled by POL β and ligated by either LIG1 (DNA ligase 1) or a complex of LIG3 (DNA ligase 3) and XRCC1 (X-ray repair cross-complementing protein 1) [1, 6, 7]. These steps are illustrated in Figure 5, drawn by Simandi in 2017 [68]. Bifunctional glycosylases initiate what is known as the long-patch repair pathway, in which the gap is filled by a combination of DNA Polδ/ε, PCNA, and FEN1 that displace the strand 3' to the nick, producing a 2-13 nucleotide flap [69]. These events are followed by removal of the flap by an endonuclease and LIG1 ligation [7].

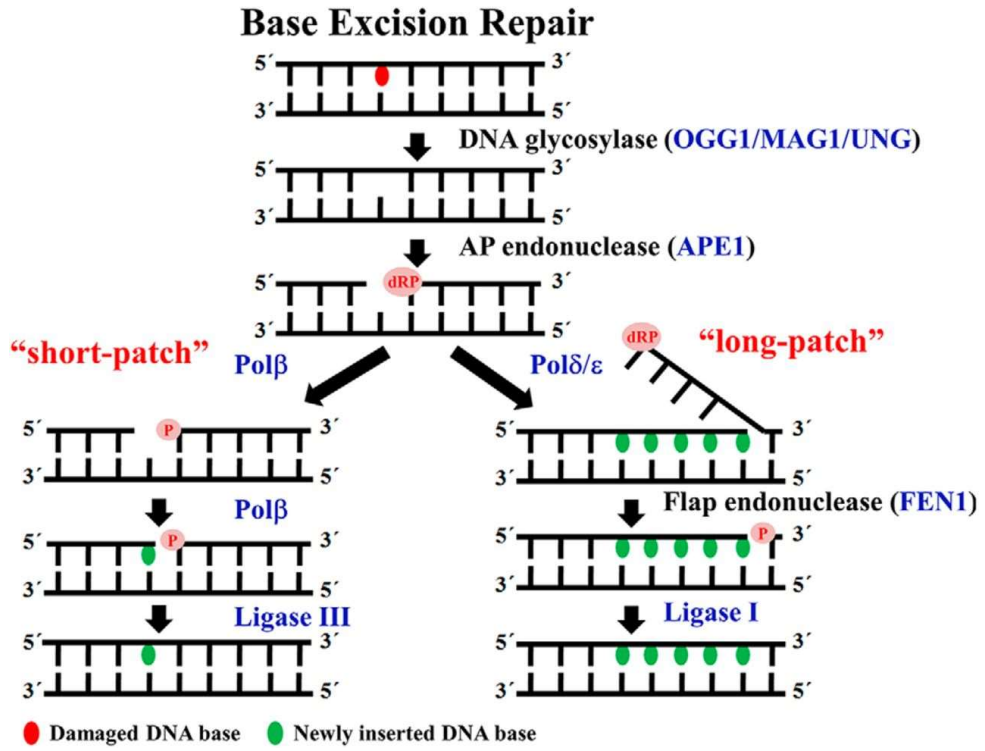

Figure 5. *Overview of the base excision repair by Simandi in 2017 [68]. Damaged or inappropriate bases are recognized and removed by DNA glycolysases, forming an AP site. These sites are cleaved by AP endonucleases, resulting in single-stranded breaks (SSBs). SSBs are processed by either "short-patch" (single nucleotide) or "long-patch" (2–10 new nucleotides) repair. Polß is the main polymerase that catalyses "short-patch" base excision repair.*

1.2.4 Mismatch repair (MMR)

Mismatch repair (MMR) is an evolutionarily conserved repair pathway that is estimated to contribute to replication fidelity by 100 to 1000-fold [70] by excising incorrect bases incorporated during DNA replication that escaped the proofreading of replication polymerases [60]. MMR involves a group of around 20 proteins with the generation of longer repair tracts compared to the 1-13 nucleotides replaced in the NER and BER pathways. On average, MMR will lead to the synthesis of up to 2kb of new DNA [71]. *Escherichia coli*'s mismatch repair has been extensively studied and is often used as a model. Other organisms have homolog proteins and follow the same basic principle, although the mechanisms of strand discrimination that allow MMR to determine the DNA strand that has to be used as template in eukaryotic organisms are completely different to those found in bacteria [72].

Identification of mismatches is performed by MutS. In most eukaryotes, it exists in two heterodimeric forms: MutSα (Msh2-Msh6 heterodimer) and MutSβ (Msh2-Msh3 heterodimer). While MutSα will recognize and initiate repair of single-base mismatches, MutSβ will be specialized in the removal of mismatches involving mis-aligned stretches, forming loops because of inserted or deleted bases. MutS heterodimers can scan DNA and trigger the recruitment of additional factors, as seen in figure 6. Those factors will allow strand-discrimination, unwinding of the DNA around the mismatch for the newly synthesized strand and its removal [73]. DNA synthesis will be used to replace the DNA stretch that contained the mis-aligned bases, either by POL δ in eukaryotes [74] or DNA pol III in bacteria [75]. While strand discrimination occurs in bacteria through the introduction of Dam methylation after replication to identify the template strand and protect it from MMR-mediated degradation [76], in eukaryotes, this strand discrimination is achieved by the presence of discontinuous nicks on the newly synthetized strand [73, 74] thus making the window to available MMR very limited in time. MutS-related heterodimers are found involved in other DNA repair processes, such as recombination, thanks to their ability to recognize and promote excision of un-aligned loops and flaps. Similarly, specialized heterodimers of the MutS-family (Msh4-Msh5) promote crossover formation during Meiosis [77]. The ability of MutS proteins to detect heterology is also critical to limit recombination between homeologous or non-identical sequences and prevent strand-exchange during DSB repair [78, 79].

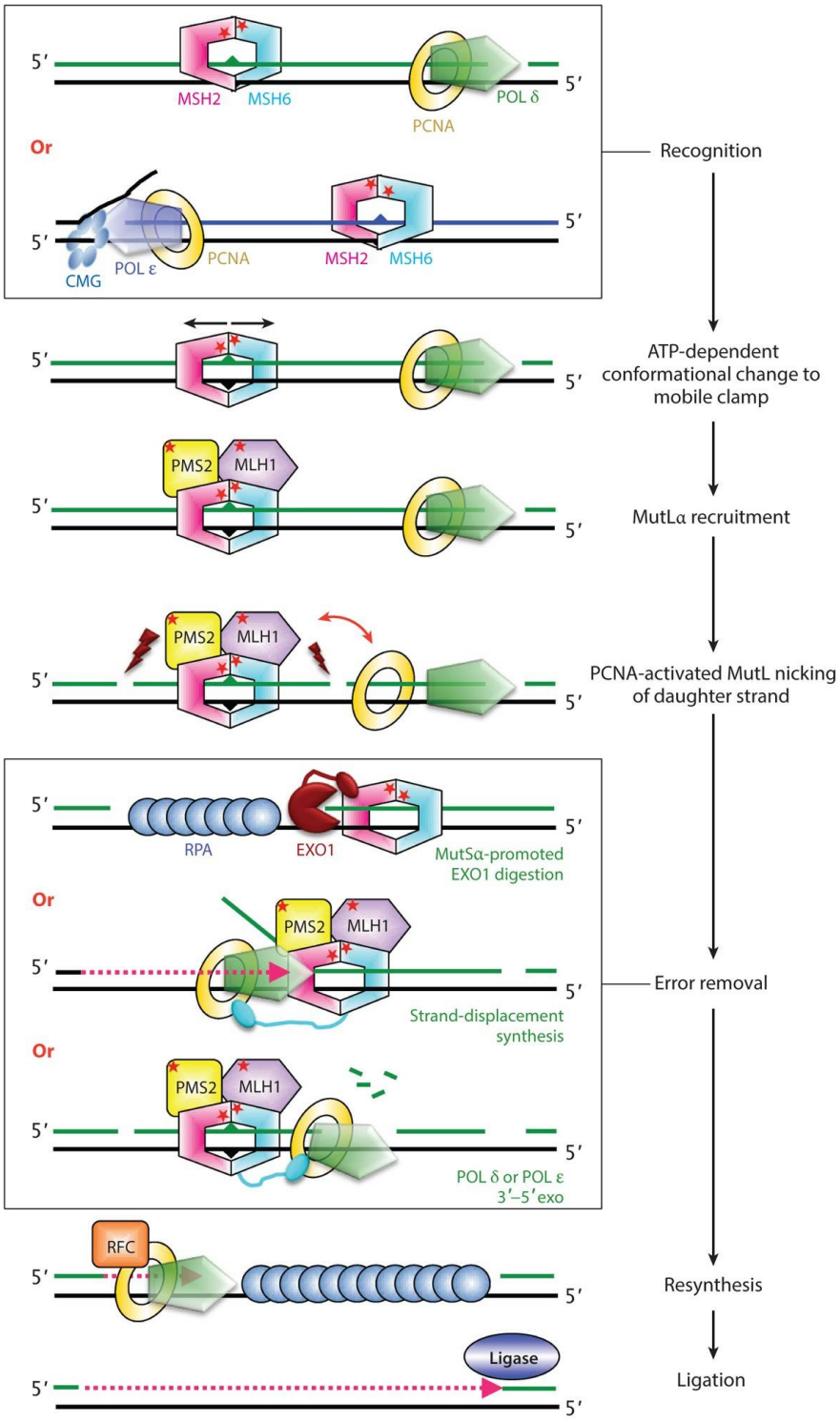

Figure 6. *Eukaryotic DNA mismatch repair (MMR) by Kunkel et al, 2015 [73]. The major MMR pathway initiates when MutSα (Msh2–Msh6) binds to a mismatch. This is followed by binding of MutLα (Mlh1 and Pms2 or yeast Pms1). PCNA activates MutLα to incise the nascent strand and the DNA ends are used for removing the replication error. After this, repair is completed by correct DNA synthesis and ligation.*

1.2.5 Post-replication repair mechanisms

When encountered during replication, damaged bases can act as a steric block to replicative polymerases and disrupt DNA synthesis. Considering the number of injuries on the genetic material that are sustained each day by an average dividing cell, replication forks are doomed to encounter fork stalling lesions at some point. Repairing them by direct reversal, BER or NER is undesirable in this context since stalling of the fork reveals ssDNA. Excision by any of these processes may form DSBs and result in fork collapse [80]. To avoid these potentially highly cytotoxic consequences, post-replicative repair mechanisms quite simply allow the replisome to by-pass the damaged bases. This can happen either by leaving the damage behind, using the opposite strand as temporary template for the replicative polymerase encountering the lesion (figure 7, right : Template switching, TS) or by synthesizing across the damage with specialized polymerases (figure 7, left: TransLesion Synthesis, TLS) [81].

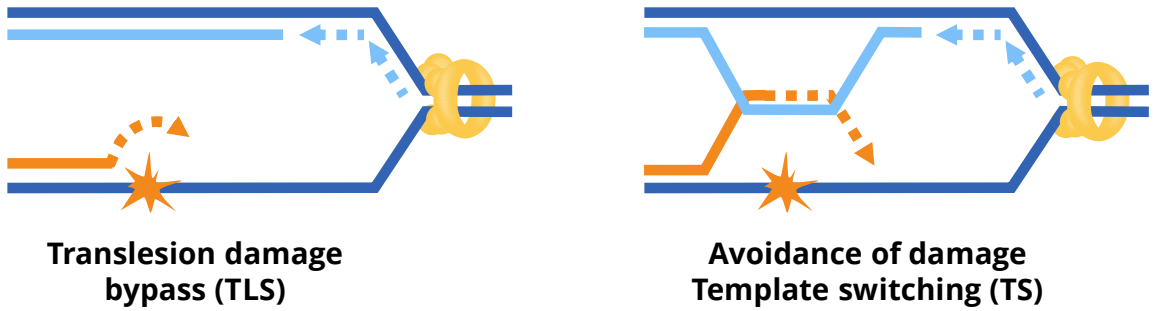

Figure 7. *Schematic illustration of the two main post-replicative pathways for tolerance of damaged bases. Orange star represents a bulky lesion. Adapted from Gao et al, 2017 [80].*

1.2.5.1 TransLesion Synthesis (TLS) damage tolerance

The Translesion synthesis (TLS) bypasses of the damage using specialized polymerases which are able to replicate past the obstructive lesion [6]. There are three major TLS polymerases RAD30 (η), Rev1, and ζ, in budding yeast and two additional TLS polymerases, κ and ι, in vertebrates [80]. The TLS polymerases are highly conserved and are very different from replicative polymerases: they lack exonuclease activity for proofreading and their smaller thumb and finger domain make fewer contacts with DNA. Replicative and translesion polymerases have very limited sequence homology and a different architecture [7] that enable them to accommodate even bulky lesions in their catalytic site and pair the incoming nucleotide in front of the distorted one [60]. Depending on the polymerase used, TLS outcome can be error free or produce a mismatched base pair, which can ultimately lead to mutagenesis, hence the idea of tolerating a mismatch rather than a damaged base. This process is thus also known as “DNA damage tolerance”.

The outcome of TLS is related to the type of DNA lesion and the polymerase involved. While some TLS polymerases will bypass many different lesions with a high rate of mispairing, others will rather recognize very specific substrates with a high degree of accuracy and insert the correct nucleotide. For example, POLη inserts two adenines on the strands opposing thymine dimers, allowing for error-free synthesis [82-84] but will be less efficient in bypassing other lesions. The risk associated with the TLS pathway is the elevated mutation rate that contributes to the gradual accumulation of mutations in somatic tissues [1].

1.2.5.2 Template switching

Template switching (TS) differs greatly from the principle of TLS as it is more akin to homology directed repair. In the context of replication, and in the event of a stalling lesions, TS is characterized by the use of the newly synthesized sister chromatid, present at close distance of the lesion site, to bypass the lesion and produce an error-free repair [85]. As a result of pairing between the nascent sister strands, an X-shaped intermediate will form at the vicinity of the stalled replication fork. Still poorly characterized, TS it is known to require some recombination proteins in yeast, in order to pair strands and the Sgs1-Top3-Rim1 (STR) complex to dissolve the intermediates [80].

1.2.6 Single strand break repair (SSBR)

Single strand breaks (SSBs) arising from oxidative damage, AP sites, erroneous TOP1 activity and other sources [7] are repaired by the single strand break repair (SSBR) pathway, a mechanism often considered a sub-pathway of BER because of the shared proteins between them [6]. The single strand break is detected by DNA-binding activated poly(ADP-ribose) polymerase 1 (PARP1) [7] that will modify several proteins around the break site including itself with Poly(ADP-ribose) (PAR) chains [33]. The PARylation will be critical for the recruitment of X-ray cross-complementing protein 1 (XRCC1), which in turn acts as a scaffold, stabilizing and recruiting additional SSBR proteins [6]. SSB ends might be damaged and could impair ligation. Prior to SSBR, they must be restored to a proper 3'-OH and 5'-P moieties for an efficient filling and ligation. Enzymes like Pol β, APE1 (as seen in BER), PNKP (polynuceotide kinase 3'-phosphate), Tyrosyl DNA phosphodiesterase 1 (TDP1) and Aprataxin (APTX) are used as accessory proteins depending on the nature of the damaged end [33].

Much like BER, SSBR can go down in either a short patch or a long patch synthesis step. The basic pathways of SSBR and the key proteins are represented in figure 8 designed by Caldecott in 2014 [33]. Most SSBs require the short patch repair where only one nucleotide will be synthesized [86, 87]. There, the gap filling is only carried out by POL β followed by LIG3 ligation [88]. In the long patch repair a ssDNA gap of multiple nucleotides is filled by POL β, in combination with POL δ/ε [7]. FEN1 removes the 5' displaced nucleotides [33] and the final step of ligation is carried out by LIG1, which will require the activity of PCNA and XRCC1 [7]. Another sub-pathway of SSBR, known as ribonucleotide excision repair (RER) is reserved for repair of erroneous incorporation of ribonucleotides in the DNA. This process functions much like the long-patch BER but making use of RNaseH2 for the first incision [89] and is illustrated as well in the rightmost part of figure 8.

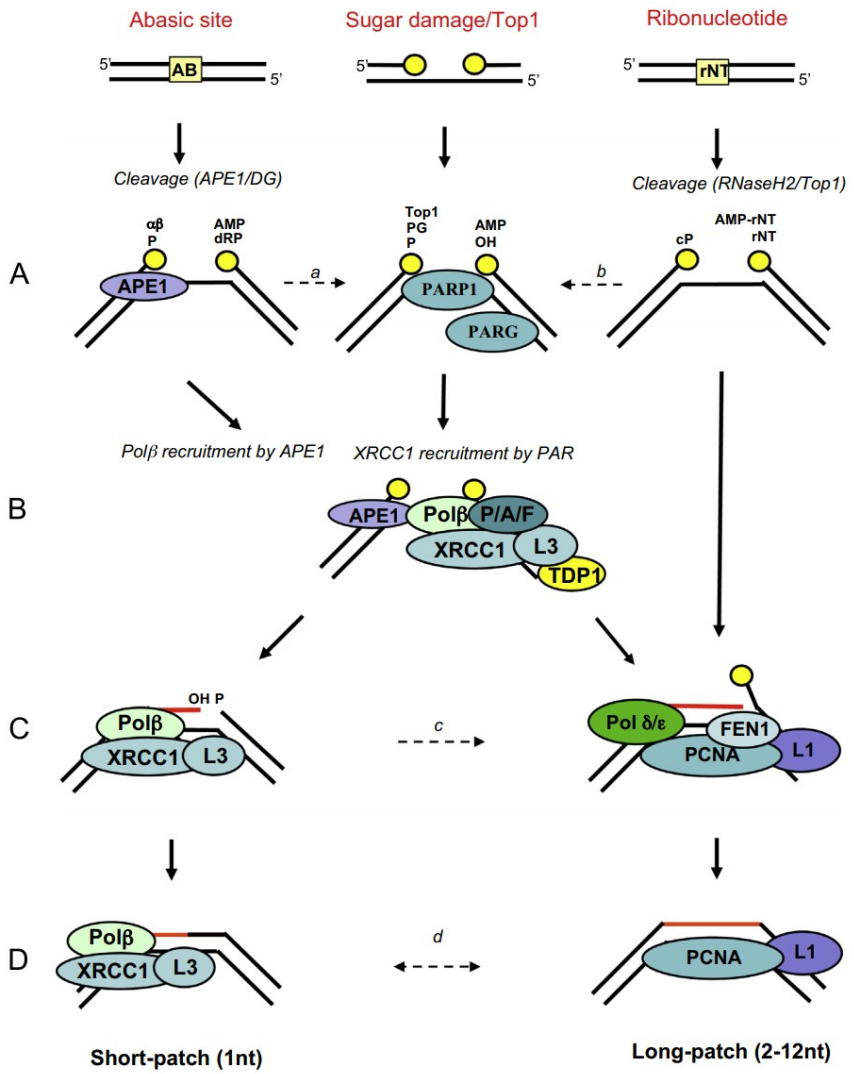

Figure 8. *Single-Strand Break Repair by Caldecott et al. in 2014 [33]. On the top are the main sources of SSBs.* ***[A]*** *Detection.* ***Middle****, 'Direct' breaks are detected by PARP1. This promotes recruitment of XRCC1 for DNA end processing. XRCC1 is joined by or complexed with Polβ and Lig3 and in addition either PNKP (P), APTX (A), or APLF (F).* ***Left****, in BER, SSB are intermediates. They do not require PARP1 for detection unless they become 'uncoupled' from the BER pathway (dotted line "a").* ***Right****, SSBs are intermediates of RER (created by RNaseH2) or products of abortive Top1 cleavage activity. It is unclear whether or not any of these SSBs are detected by PARP1 (dotted line "b").* ***[B]*** *DNA End processing.* ***Left****, In BER, APE1 remains bound to the SSB, enabling recruitment of Polβ (and associated XRCC1 complexes) via direct interaction with Polβ.* ***Middle****, at SSBs detected by PARP1, PAR synthesis results in rapid recruitment of XRCC1 protein complexes containing the enzymes necessary for repair of the damaged termini.* ***Right****, SSBs arising during RER contain 5'-ribonucleotide termini (rNT) and may be channeled directly into long-patch gap filling, avoiding the need for specialized end processing. However, SSBs arising at ribonucleotides via abortive Top1 cleavage activity harbor cyclic 3'-phosphate termini and are likely detected by PARP1 (dotted line "b").* ***[C]*** *Gap filling. Pol β replaces the single missing nucleotide at most SSBs (left, short-patch repair), but under some circumstances gap filling may involve incorporation of more than one nucleotide (typically 2–12 nt) by Pol β and/or Pol δ/ε (right, long-patch repair), resulting in displacement of a single-strand flap, which is then removed by flap endonuclease-1 (FEN1) in a reaction stimulated by PCNA (and possibly PARP1). No need for processing of the 5' end on the removed flap. This may take place if Polβ in BER struggles with 5' processing (dotted line "c").* ***[D]*** *DNA ligation. Short-patch and long-patch repair patches are primarily ligated by the XRCC1/Lig3α and PCNA/Lig1 complexes, interchangeably (dotted line "d").*

1.2.7 Double-Strand break repair

Compared to SSBs, double strand breaks (DSBs) happen less frequently but their potential for cytotoxicity is much higher. An important challenge of repairing a DSB is the fact that the genetic information at the break point must be preserved. Lesions at DNA bases or SSBs can be repaired making use of the opposing strand as a guide. At least two major pathways are dedicated to restoring DNA integrity after a DSB: either a quick ligation of the two ends in non-homologous end joining (NHEJ) or synthesis using a homologous template (homologous recombination or HR). The first option prevents the ends from promiscuously engaging other compatible ends in other genome positions. The second exposes the genetic information surrounding the break point in an attempt to find equivalent homologous copies of this code elsewhere and use it for synthesis and finally ligation. While NHEJ and its alternative joining pathways will be predominant in G0/G1 [17], homologous recombination will gradually take preeminence after replication takes place and sister chromatids are available to use as identical copies of the chromosomes experiencing breaks.

In the recent years, much attention has been placed in understanding how cells determine the pathway choice between NHEJ and HR, and other related minor sub-pathways, such as single-strand annealing and micro-homology mediated end joining (MMEJ). There is a competition between NHEJ and HR for recognition and processing of the DNA ends [90]. The initial processing of the ends will dictate whether those commit to ligation through NHEJ or initiate HR by transforming originally double-stranded ends into single-stranded 3' tails of DNA, the central substrate for the homology-driven repair. The conversion of ends into 3'-tails, also known as resection, is thus an irreversible commitment to HR [91].

A number of new actors have been recently described to regulate the protection of the ends, and the regulation of resection initiation, thus enabling NHEJ to be preeminently used in G1 and limiting HR mainly after replication by preventing the initial processing of ends into resection-bound intermediates [92-94].

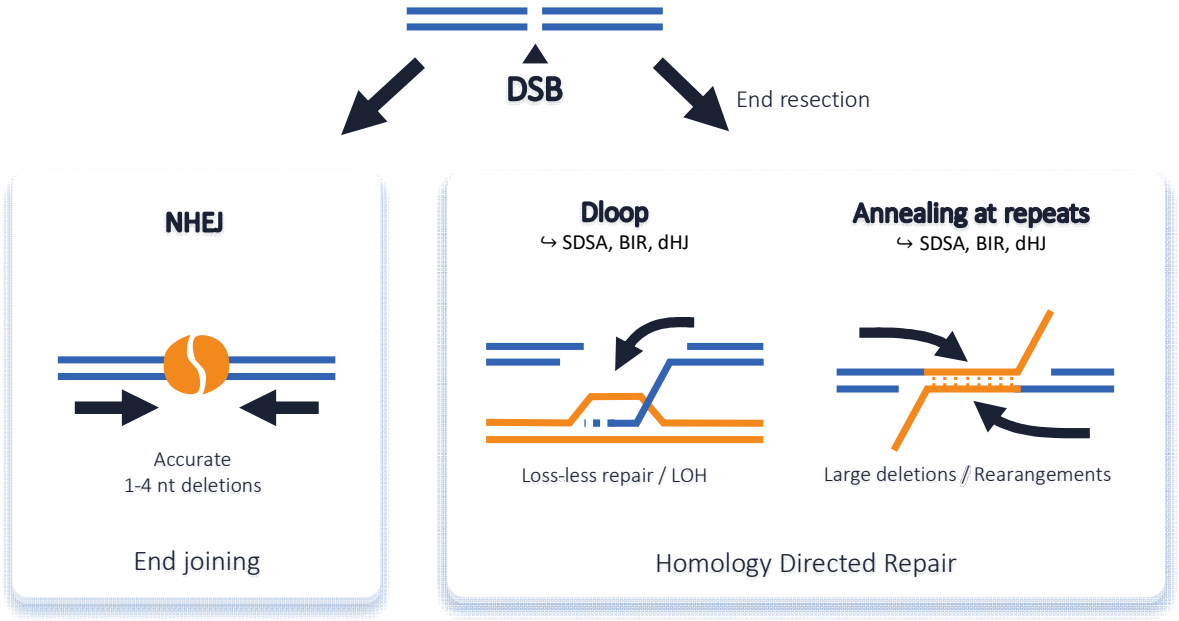

Figure 9. *Schematic representation of the branching sub-paths in DSB repair. The main separation occurs at the very start when DNA binding complexes compete between direct joining of the broken ends and initiation of resection.*

1.2.7.1 Non homologous end joining (NHEJ)

For DSBs with readily ligatable ends or ends requiring minimal processing to allow ligation, NHEJ is a quick and effective way to seal the broken DNA molecule. As its name suggests, in this repair process, both severed DNA ends are rejoined without searching for an homologous template to restore a potential loss of DNA information at the break point. While it was originally expected to be an extremely error-prone repair process, either by promoting ligation of non-reciprocal ends of DNA when multiple breaks are formed, or by slightly modifying the junction point with insertions and deletions, the classical NHEJ pathway is remarkably efficient and error-free, and ensures the genome integrity in response to breaks originated in cells at G1, when no perfect homology is available for the homology-driven repair processes [95-97]. That being said, the potential for errors in the ligation process of NHEJ still exists and impairments on the pathway will rapidly lead to accumulation of these insertions, deletions and potential translocations. Similarly, off-target NHEJ to eroded telomeres will be a source of un-wanted fusions between chromosome ends that normally are to be protected from the NHEJ pathway [98].

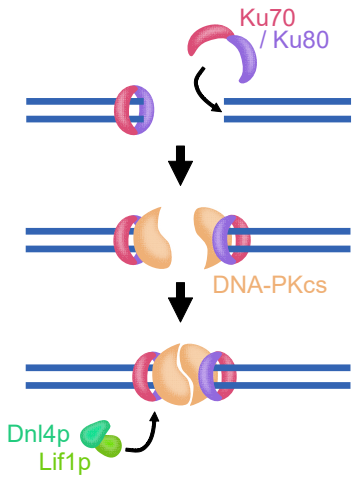

Figure 10. *Non Homologous End Joining adapted from Helleday et al. in 2007 [31].*

The core machinery of NHEJ assembles after the DNA binding of the KU heterodimer (Yku70p-Yku80p in budding yeast), which forms a ring that binds and stabilizes the DNA ends within seconds of the DSB formation [90]. This is illustrated in figure 10 adapted from Helleday et al in 2007 [31]. After this recognition by KU, a multi-protein complex know as the maturation complex forms at the DNA ends, containing the DNA-PK. The latter will auto-phosphorylate [31] and promote further recruitment of specialized players: Artemis, polynucleotide kinase 3'-phosphatase (PNKP), WRN helicase, PNKP-like factor (APLF) and Aprataxin [7]. When required, these factors will process the DNA ends by trimming, filling-in and removing end-blocks that may prevent ligation [95, 99, 100]. Finally, a third protein complex, the Ligation Complex, will form by the recruitment of the XRCC4 and XLF proteins, which in turn will promote the engagement of the specific NHEJ Ligase, Ligase 4 (yeast Dnl4 protein associated with Lif1) [90, 101, 102].

1.2.7.2 *Homologous recombination (HR)*

As mentioned before, the basic principle of HR is to restore the integrity of a broken DNA duplex by using the information stored in an intact homologous molecule of DNA. The interrupted genetic message at the break point is restored through DNA synthesis from the break point using the template as a guide. To achieve this goal, the ends have to be processed into ssDNA with a free 3'-end that will be used invade the template duplex and prime synthesis. Eventually, DNA synthesis from both ends will restore the remaining gaps that appeared when processing the ends. Ligation will ensue to complete the repair process. As illustrated in figure 11, HR is a complex pathway with shared steps in its initial processing of the break followed by a substantial diversity of sub-pathways to deal with DNA intermediates after strand-invasion and DNA synthesis begin.

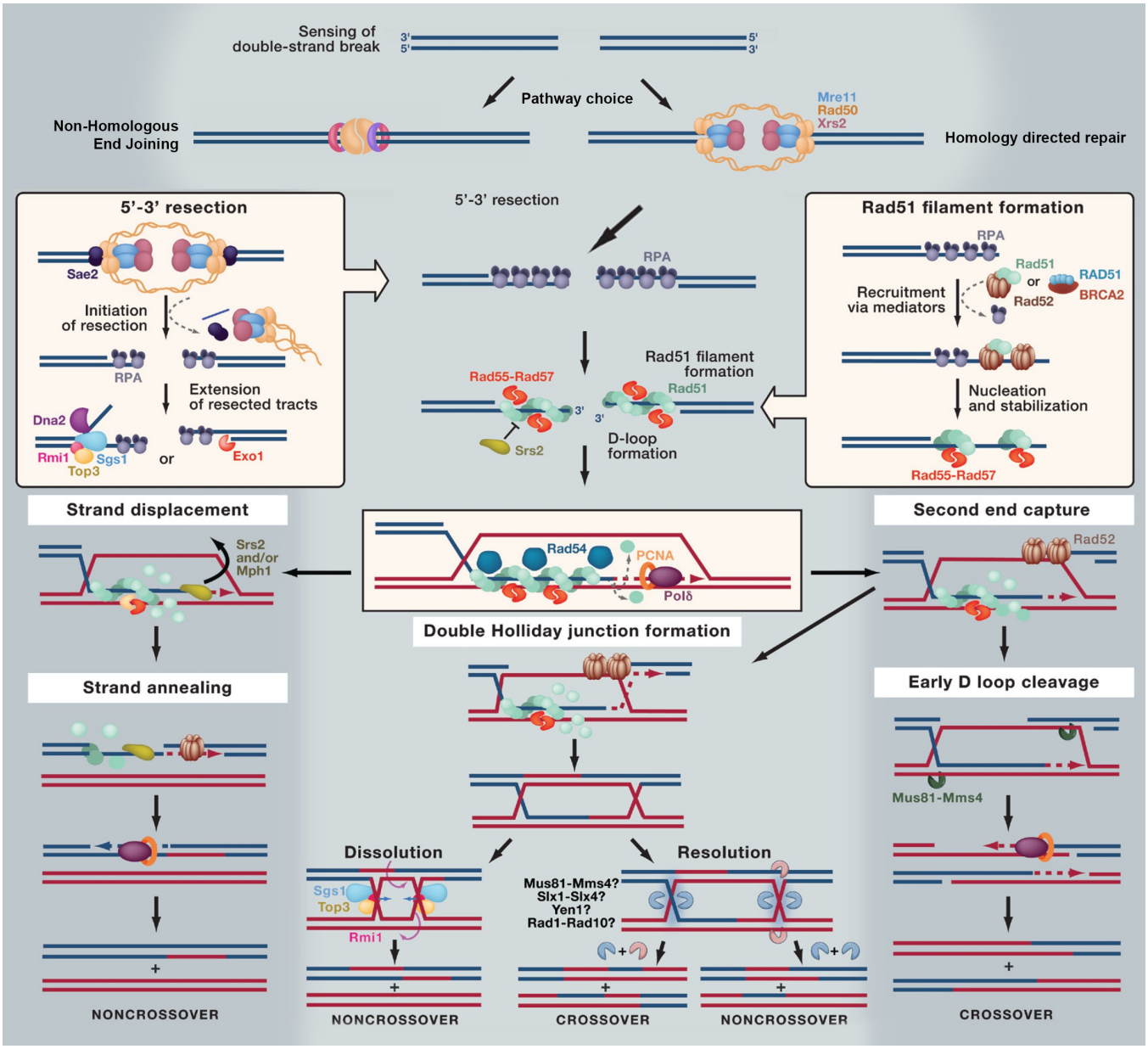

Figure 11. *Snapshot on homologous recombination by Mazón et al. in 2010 [103]. With minor modifications (top part) Schematic representation of the main steps described in the corpus.*

Processing of the DSB ends and commitment step

The recognition and processing of DSB ends will determine the choice of repair pathway between NHEJ and HR. The critical proteins that recognize the DSB to enable HR form a trimeric complex: the MRX complex. In yeast it is made up of Mre11, Rad50, and Xrs2 (figure 12). Its homolog is the MRE11-RAD50-NBS1 (MRN) complex in mammals [104, 105]. The MRX complex binds DNA ends directly and is the first HR factor to be detected at these ends, in competition with the NHEJ factors [106]. The whole complex stabilizes the two broken ends and prevents their degradation [105, 107]. Its core is composed of two Mre11 nuclease subunits associated to a dimer of Rad50, a protein of the structural maintenance of chromosomes (SMC) family [20, 108]. The presence of the Rad50 dimer is critical, it acts as a scaffold keeping the ends in close proximity. To initiate the processing of the ends and allow the resection of the dsDNA, the MRN/X complex will clip the ends by nicking one strand and releasing a short single-stranded fragment of DNA, leaving a 3'-overhang [109]. The clipping of the ends is the first step of the resection process that can then proceed with an extended resection via two alternative ways, using either the Exo1 exonuclease or the combined action of the Dna2 endonuclease and the Sgs1/BLM helicase, as seen in the bottom panel of figure 12.

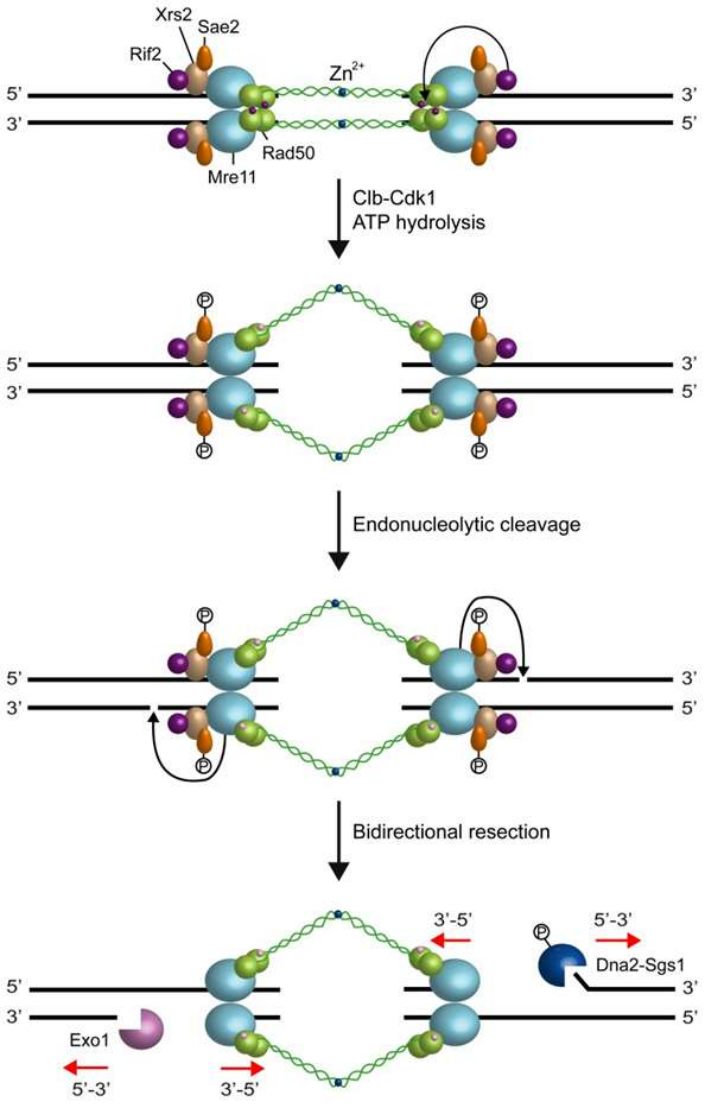

Figure 12. *Resection in yeast by Gobbini et al. in 2016 [20].*

DSBs occur all throughout the cell cycle, but end resection only happens in the S and G2 phase [92]. As mentioned before, Ku binding allows initiation of NHEJ and it also inhibits DNA end resection before the S phase [105]. But that competition for binding does not tell the whole story: one of the major factors for pathway choice between NHEJ and HR is the cell cycle phase [31]. Low Cdc28/CDK1 cyclin-dependent kinases activity in G1 limits end resection independently of Ku [92]. In yeast, CDK-mediated phosphorylation of Sae2/CtIP tips the balance of the competition between Ku and MRX in the favor of HR [110, 111]. Sae2 phosphorylation by CDK1 is thus critical to enabling the MRX clipping that initiates resection.

In mammals, other accessory factors can contribute to the pathway choice. BRCA1 and 53BP1 proteins will compete for the control of resection. While 53BP1 inhibits resection, a subset of BRCA1 can displace 53BP1 away from the DSB, preventing its action [112]. In G1 phase, 53BP1 localizes to DSBs, inhibits end resection and BRCA1 recruitment. In the G2 phase however, ATM/Tel1, recruited by MRN/X [106] will phosphorylate many factors including CtIP/Sae2 mentioned before and BRCA1, which will modulate the pathway choice in favor of resection and thus HR, by activating CtIP/Sae2 [7, 17].

As stated above, following the disassembly of MRN/X, CtIP/Sae2 and ATM/Tel1 [92] a long-range resection is performed by the unwinding of DNA via the Sgs1/BLM helicase in the STR complex associated with Dna2 nuclease activity or alternatively, by the processing of the ends with the Exo1 nuclease [92, 104]. Exo1 is a 5'-3' exonuclease most active on dsDNA substrates with a recessed 5' end, much like those created by the MRN/X complex and CtIP/Sae2. Similar to short-range resection, its long-range counterpart is controlled by CDK phosphorylation as Exo1 is a target of CDK1 and 2. Their phosphorylation of Exo1 during S and G2 promotes resection, thus tipping the pathway choice balance towards HR [113]. Additional factors play an important role to facilitate resection of the DNA ends, especially chromatin remodelers such as the yeast Fun30 and SWR1, that cooperate with either Exo1 or the STR and Dna2 by relaxing chromatin and allowing resection to proceed [105, 114].

As a result of resection, a large amount of 3'-ssDNA will be formed. This ssDNA will be bound by Replication Protein A (RPA), protecting it from degradation by nucleases [104] and preventing the formation of secondary structures [115]. RPA will also promote Exo1 action by preventing the latter from complexing with ssDNA and/or possibly degrading ssDNA [116, 117]. While Exo1 activity is promoted by RPA, Dna2 processing is completely dependent on it. RPA not only allows Dna2 recruitment but also promotes its 5' endonuclease activity [105]. Additionally, RPA interacts with Sgs1/BLM as well and promotes its unwinding activity [28]. Extensive resection will form ssDNA tracts ranging from a hundred to tens of thousands of nucleotides [107]. The long ssDNA tails will then be handed over to the recombinase Rad51 to form a neat helical filament that will be central for homology search and strand invasion reactions [115].

Rad51 nucleofilament formation

The binding of the evolutionary conserved Recombinase Rad51 to the ssDNA newly generated ssDNA is a key step in HR. It will result in the formation of a nucleoprotein filament – also known as the presynaptic filament – which will be the crucial intermediary allowing the next steps of HR to take place [118].

By definition, recombinases are conserved proteins that promote pairing, homology search and strand invasion during HR [104]. The RecA recombinase of *Escherichia coli* was the first recombinase identified, and most studies on its biochemical properties paved the way for the understanding of the HR pathway [119-121]. Rad51, the recombinase found in yeast and higher eukaryotes is part of the RecA superfamily. The deletion of Rad51 in yeast is viable, but cells harboring a deletion in the *RAD51*

allele are extremely sensitive to ionizing radiation and present defects in meiosis [122]. To perform its homology search and promote strand invasion, Rad51 has to bind and nucleate onto ssDNA and grow right-handed helical filaments on DNA [123]. The formation of the presynaptic filament induces an irregular DNA stretching [124] of up to 1.6 times for human RAD51 [125], which will become a critical property of the Rad51-bound DNA to enable homology search [126].

The nucleofilament formation is more akin to a two-step process rather than a gradual binding of RAD51 to ssDNA (figure 13). On the first phase – called nucleation – a few RAD51 monomers bind to DNA using their 3-4 nucleotide-binding sites. This creates sparse and isolated nucleation sites [127]. The nucleoprotein filament then grows during a second phase as new Rad51 is added to the bound monomers [128]. Rad51 is stable on ssDNA and able to mediate strand exchange, but only when bound to ATP [127]. Filament assembly is quite dynamic and ATP hydrolysis will enable Rad51 protein turnover and disassembly of the presynaptic filament. Several rounds of nucleation and filament growth will be required to obtain a productive nucleofilament able to start homology search [128].

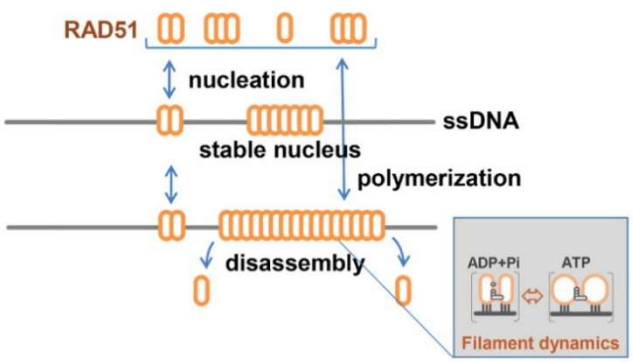

Figure 13. *Nucleation of human RAD51 on ssDNA by Subramanyam et al. in 2018 [128] The ATP bound RAD51 nucleoprotein filament is stably nucleated such that each RAD51 monomer binds three nucleotides which facilitates further polymerization of the nucleoprotein filament forming the active pairing unit in strand exchange reactions. Hydrolysis of ATP lowers the affinity of RAD51 for ssDNA and leads to turnover or disassembly of the nucleoprotein filament.*

A number of accessory factors will assist Rad51's formation of the nucleofilament. These are known as Rad51 paralogs and mediators. They help in overcoming the inhibitory role of ssDNA-bound RPA and ensure efficient filament formation [129]. On the other hand, negative regulators such as the yeast Srs2 helicase will try to dismantle and prevent Rad51 filament formation especially when recombination would prove toxic and unwanted for genome integrity [130-132].

In yeast, the main Rad51-mediator is the Rad52 protein. Its mutation completely prevents recombination in *S. cerevisae*, thus defining the RAD52-epistasis group, in which many other RAD genes involved in HR can be found, including RAD51 itself as well as RAD54, RAD55, RAD57 and RDH54 [122]. Nonetheless, RAD52 plays a minor and still poorly understood role in humans and higher eukaryotes, where most of its mediator functions are taken over by the BRCA2 protein [133]. In yeast, at the initial steps of HR, resected ssDNA wraps around the outer surface of the ring-shaped heptameric strucuture of Rad52, displacing RPA and allowing Rad51 to bind and start nucleation (figure 14) [134]. In humans however, BRCA2 mostly catalyzes this activity probably with some redundancy with RAD52 as highlighted by the synthetic lethality of simultaneous loss of RAD52 and BRCA2 [134-136].

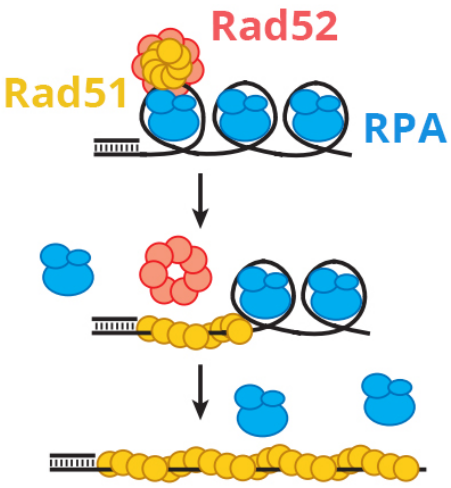

Figure 14. *Rad52-mediated replacement of RPA by Rad51. Figure altered from the original source by San Filippo et al. in 2008 [118] In its recombination mediator role, Rad52 forms a complex with Rad51 and delivers it to RPA-coated ssDNA to seed the assembly of the presynaptic filament. The polymerization of additional Rad51 molecules results in the further displacement of RPA from the DNA.*

While mediators favor the formation of the presynaptic filament and thus promote HR, disruptors balance the regulation. For instance, the yeast Srs2 helicase downregulates HR by dismantling Rad51 from ssDNA at an early stage. A similar function seems to be carried out by helicases RECQL5, PARI, and RTEL in humans and higher eukaryotes. Srs2 interaction with Rad51 triggers ATP hydrolysis causing Rad51 dissociation allowing RPA to re-populate ssDNA and further prevent subsequent Rad51 nucleation [137]. To oppose the inhibitory roles of anti-recombination factors, Rad51-paralogs like the Rad55-Rad57 heterodimer and the Shu complex (Psy3, Csm2, Shu1, and Shu2) counteract Srs2's action and stabilize the Rad51 filament [107, 138].

Homology search and synaptic complex

Once the presynaptic filament is assembled, it is able to explore duplex DNA molecules and browse for homology. Experiments with RecA show that this process happens through random collision [118, 139]. When homologous duplexes contact the nucleofilament, its stretching will facilitate the probing of dsDNA [140]. It is still undefined if there exist canonical or non-canonical base pairing through this homology pairing. Rad51 needs at least a 8nt pairing to achieve homology recognition [104]. The initial pairing is made up of paranemic joints, which are temporary and mostly A-T base pairing, possibly because A-T rich sequence flip out of the helix more readily to nucleate homology probing [141]. The three-stranded paranemic intermediate or synaptic complex can evolve to plectonemic joints with a topological intertwining of the strands on top of the base pairing, this invasion of the duplex DNA forms the displacement loop (D-loop) [110, 142, 143].

Strand invasion and D-loop formation

Having searched for homology, the presynaptic filament is able to align with one strand from the template duplex. If there is homology, the base pairing is shifted from the previous complementary strand to the new, invading, nucleoprotein strand. The transfer of base pairing is referred to as strand exchange [144]. This shift joins the two molecules and displaces the opposing strand, creating a bubble of ssDNA opposing the strand invasion. This three-strand structure is the D-loop and will be central for the finalization of the HR repair process, through divergent processing in several sub-pathways.

The Rad54 has been proposed to play critical co-factor role in the transition between of the synaptic complex to strand invasion [145]. While Rad51 can form D-loops *in vitro* by itself, the Rad54 translocase activity promotes the DNA remodeling of the three-strand synaptic complex by transiently opening DNA strands, which would allow pairing [146, 147]. The minute details of how Rad54 promotes strand invasion and displaces Rad51 from the 3'-termini of the invading strand to promote DNA synthesis are still under discussion. They most certainly involve Rad54's ability to bind to ssDNA-dsDNA transitions and branched structures, and its ability to bind Rad51 [143, 148, 149].

Rad54 promotes the probing of template DNA duplexes, all the while keeping a short precautionary distance with the potential template, allowing for homology checks. Rad54's motor activity converts Rad51 synaptic complexes into proper D-loops (figure 15) [143]. After Rad51 removal, DNA polymerases will be granted access to the resected end inside the D-loop to carry out DNA synthesis [150]. In yeast, DNA synthesis will be carried out by polymerase δ in the context of the D-loop, as well as lower fidelity TLS polymerases [107, 151, 152].

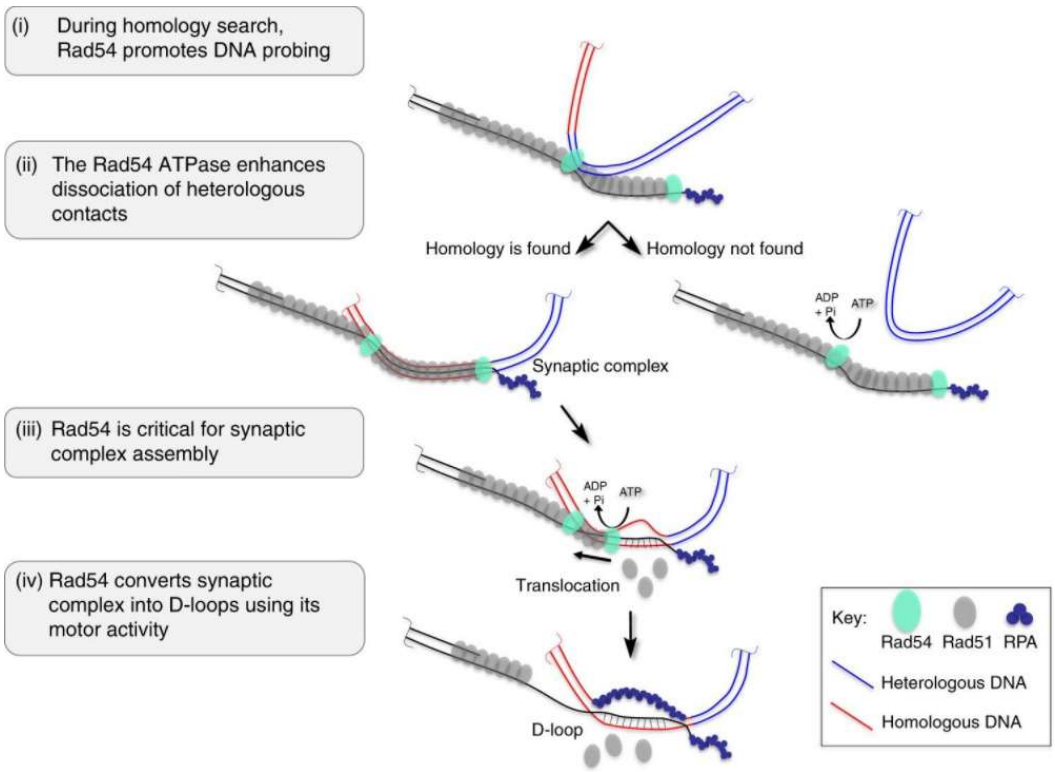

Figure 15. *model for homology search and D-loop formation by Tavares et al. in 2019 [143]. (i) During homology search, Rad54 promotes DNA probing. The invading DNA (light red) uses Rad54 to bridge the Rad51 filament to dsDNA during the homology search. Rad54 ATPase activity is not required but may enhance probing. (ii) Persistent associations with heterologous DNA (blue, right arrow) may be prevented or dissociated by Rad54 in an ATPase-dependent fashion. Rad54 ATPase exerts quality control to promote homologous pairing. (iii) Rad54 is required for synaptic complex formation without strict requirement for ATPase activity, and (iv) converts such complexes into D-loops dependent on ATP hydrolysis. Rad51 left on the ssDNA outside of the heteroduplex region after removal during heteroduplex formation may able to repolymerize back into the synaptic region. Note that this is a cartoon representation not meant to model the true scale and structure of the Rad51 filament or Rad54 protein arrangement in the depicted intermediates.*

During strand-invasion, the MMR machinery is known to participate in discriminating sister chromosomes' perfectly homologous sequences from merely similar or partially homologous sequences found elsewhere in the genome [153, 154]. A few mismatches drastically reduce recombination rates and crossover (CO) output thanks to the editing from the MMR proteins [155, 156]. Homeology rejection will avoid crossing-over sequences from non-sister alleles, which could lead to deleterious rearrangements [157].

D-loop maturation: Second end capture or D-loop displacement

After DNA synthesis has occurred at the 3'-termini of the DSB end in the D-loop, there are two main options for the repair process to follow: either the D-loop is dismantled by displacement of the invading-strand, in what is known as the synthesis-dependent strand annealing (SDSA) pathway (figure 16 top); or alternatively, the D-loop may mature by capture of the resected second end of the original DSB, that shares homology to its own displaced strand, in an annealing reaction requiring Rad52 in yeast [158] (figure 16 bottom). In that case, the intermediate is quite transient at first. Further DNA synthesis and ligation make it a covalent four-way intermediate that connects the two DSB ends and the homologous duplex DNA: the double-Holliday Junction (dHJ) [107, 159]. The maturation of the D-loop intermediate into a closed dHJ can also be described in the literature as the Double-Strand Break Repair (DSBR) pathway of HR [160], in a dichotomy of models trying to explain HR that has finally ended up in a single model including both original hypotheses as alternative sub-pathways depending on the fate of the D-loop intermediate (figure 11).

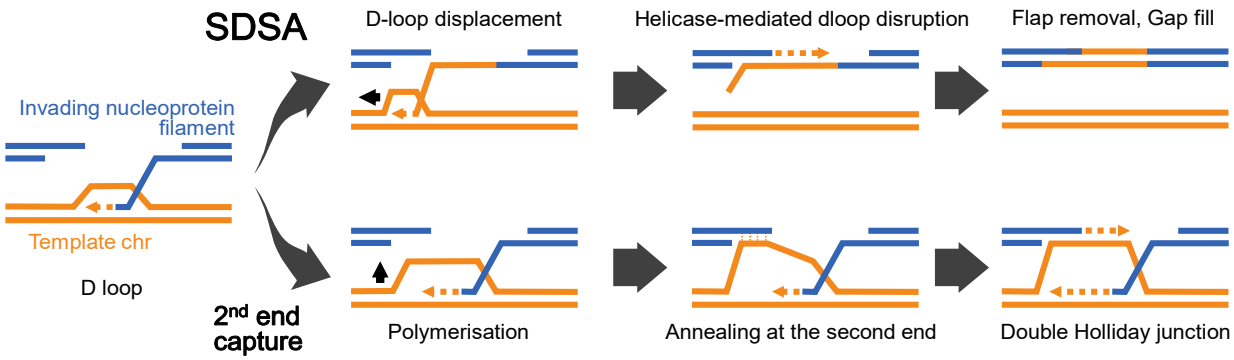

Figure 16. *Schematic representation of the branching paths following homology search and D-loop formation. The D-loop may be displaced allowing annealing to the break end with a non-crossing over outcome. The displaced strand of the D-loop may as well anneal to the opposite break end effectively forming a DNA quadruplex called a Double Holliday Junction. Representation mustered with data from [31, 161].*

Through the SDSA sub-pathway, the D-loop is dissociated. The DSB-end that originally invaded the template duplex is once more a free 3'-tail, but this time with an extended sequence obtained through the synthesis that occurred in the D-loop (figure 16). The newly acquired DNA sequence at the 3'-terminus will bear homology with the exposed ssDNA at the other DSB end. Thus, by annealing, both ends would form a gapped intermediate that will only require minimal processing by DNA synthesis and trimming of potential over-extended sequences in the form of 3'-flaps, to complete gap-filling by ligation (figure 16). With SDSA, the original broken chromosome arms are re-united in what is considered a non-crossover event (NCO). This prevents the exchange of one of the broken chromosome ends with the template DNA duplex [162].

SDSA requires the displacement of the invading strand after DNA-synthesis (figure 16), and this displacement will be a result of the enzymatic activity of helicases (figure 11) [162]. Srs2, Mph1 and Sgs1 within the STR complex are considered the major helicases in the yeast model able to displace D-loop intermediates and promote SDSA during HR [163, 164]. While Mph1 is well known to be able to displace D-loops, extended or not, Srs2 may as well promote SDSA by minimizing the possibility of dHJ formation and is also considered to be an anti-recombinase factor, that avoids excessive recombination in replication forks by channeling strand-invasion intermediates back to its previous un-invaded step [164, 165]. Both a Srs2 or a Mph1 mutation increases the amounts of COs, by channeling D-loop intermediates to the formation of dHJ and its intrinsic risk of resolving these structures with a CO [166]. The STR complex also limits formation of dHJ through early dissolution of D-loops *in vitro* and *in vivo*, in a process requiring Top3 activity and the presence of Sgs1 but not its direct helicase activity [167, 168].

Dissolution of the dHJ

If the D-loop matures into a dHJ, in order to release the covalently bound chromosomes, its processing will be linked to the occurrence of COs. The major processing pathway for dHJ joint molecules (JMs) consists of migrating both HJ until they meet, forming catenated intermediates, which are then released by a Topoisomerase nick to relieve the two DNA duplexes without crossing-over (figure 11 and 17) [169]. This is done through the cooperative action of the yeast helicase Sgs1 or BLM in humans, the type IA topoisomerase Top3/TopoIIIα and the accessory factor Rmi1/RMI(1-2). While Sgs1 unwinds the strands and pushes the two junctions to converge, the added tension of the supercoils that this unwinding generates is taken care of by the topoisomerase (figure 17) [107].

Of all topoisomerases, only type IA are able to deal with four way catenanes such as the ones encountered here by introducing a nick on the DNA. This allows strand passage and frees the duplexes from one another [169]. Rmi1 is a very well conserved oligonucleotide/oligosaccharide binding accessory factor, which promotes the dissolution reaction of JMs in complex with the two aforementioned proteins, forming what has been known as the "dissolvasome" or STR complex in yeast [170]. In the absence of Rmi1, the yield of the reaction of dHJ dissolution is minimal, highlighting its integral and critical role in the process [169]. The dissolution of the dHJ has been considered the pathway of choice for dHJ removal, that notion is in part linked to the severe phenotypes of cells deficient in the human homolog of Sgs1 – the BLM helicase – which display elevated levels of sister chromatid exchange [157]. Individuals with a BLM deficiency develop the cancer-prone Bloom disease, where the increase of COs and sister-chromatid exchanges lead to malignant transformation likely by the elevated number of loss of heterozygosity (LOH) and genomic re-arrangements that accumulate in somatic cells.

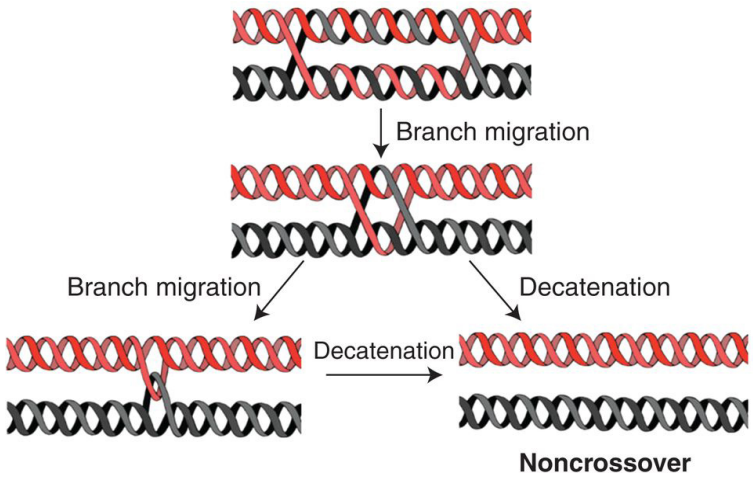

Figure 17. *dHJ dissolution schematic representation by Bizard et al. in 2014 [169]. Migration of the HJs toward one another. The fusion of the two HJs results in a hemicatenated intermediate. Decatenation of this intermediate regenerates the original DNA species present before the initiation of HR. Each strand engaged in the dHJ is reassociated with its original complementary strand, preventing exchange of genetic material between the two homologous sequences.*

Resolution of the dHJ

As an alternative to the dissolution pathway, dHJ structures that escape dissolution by the STR complex can be nucleolytically processed. dHJ cleavage can produce NCO as well as CO outcomes depending in the orientation of the cuts [104]. While a simultaneous cut on the inner or outer plane of the four-way junction will produce resolution without crossing-over, an alternative cut of one junction in the opposite plane to the other one will release a CO product where each side-arm of the chromosome bearing the original DSB has been exchanged to the corresponding side-arm of the template. In figure 18, the possible cuts are illustrated by triangles, the colors of which show which pair together to give rise to COs or NCOs.

The nucleolytic processing of the dHJ intermediates is performed by highly specialized nucleases able to discriminate the unique DNA structure of these intermediates. These structure-selective nucleases can act redundantly on the dHJ and other D-loop derived intermediates by recognizing the intact HJ, its nicked and incomplete HJ variants or an array of 3'-flap and 5'-flap DNA intermediates present at the D-loop and the transient D-loop with a captured the second intermediate. The slight differences in the specificity to these structures and the efficiency in its processing between the different structure-selective nucleases has helped propose models explaining how they can resolve post-D-loop HR intermediates at different stages (figure 11) [160, 171-173]. In yeast, Mus81-Mms4 (MUS81-EME1 in humans) and Yen1 (GEN1 in humans) have emerged as the two main players for the nucleolytic resolution of HR intermediates, with a secondary role for Rad1-Rad10 (XPF-ERCC4) in certain recombination situations involving ectopic sequences [173].

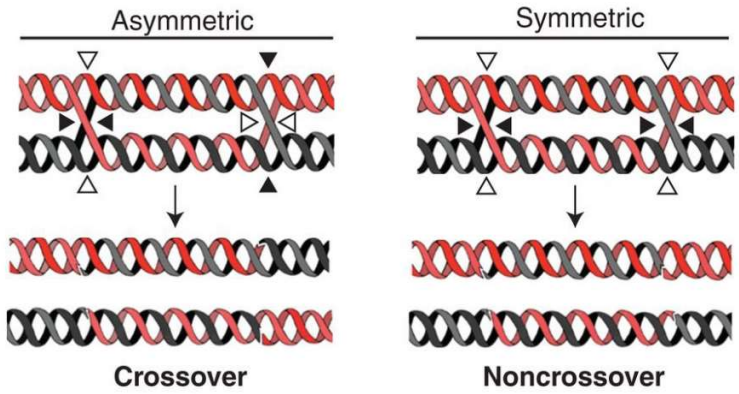

Figure 18. *dHJ nucleolytic processing representation by Bizard et al. in 2014 [169]. Each HJ of a dHJ is cleaved by a resolvase. Cleavage can be asymmetric or symmetric. This process can generate both CO and NCO products.*

Mus81-Mms4/EME1 was the first eukaryotic structure-selective nuclease described to have a role in the resolution of HR intermediates in the *S. pombe* model [174]. Its poor ability to cleave intact HJ *in vitro* and its asymmetrical cleavage of the junctions, leaving a small gap at the resulting linear products, pushed to revisit the models calling for the resolution of a closed covalent dHJ as the main intermediate resolved by nucleases [175]. The latter identification of the resolvase activity of the XPG family nuclease Yen1/GEN1 shifted the models again. Indeed, *S. pombe* does not contain an orthologue of Yen1, unlike *S. cerevisiae* and most of the higher eukaryotic organisms. Yen1/GEN1 is able to cleave intact HJs very efficiently and in a symmetrical cut in both opposite strands as expected from the canonical bacterial resolvases [176], and in the *S.cerevisiae* model, a simultaneous loss of Mus81-Mms4 and Yen1 is required to unveil a clear resolvase-deficient phenotype, including increased sensitivity to radiomimetic agents and IR, decreased formation of CO and chromosome segregation issues [177-179]. The current model, calls for a redundant function of Mus81-Mms4 and Yen1 in the

resolution of HJ and other HJ-related intermediates that mature from the D-loop through second-end capture (figure 11). Mus81-Mms4 is able to cleave early-HJ intermediates with still un-ligated ends, by recognizing the invading junction of the D-loop and the 3'-flap present at the front of the D-loop (figure 11). Yen1 would remain as the HJ resolution specialist that backs up for unresolved intermediates left behind by Mus81-Mms4 and the dissolution activity of the STR complex (figure 11). The secondary role of Yen1 is supported by the absence of phenotype of its single deletion in yeast as compared to fairly stronger phenotypes of single deletions of MUS81 or MMS4 [177, 178]. While the scaffolding protein Slx4 together with Slx1 was described to resolve recombination-like structures in the context of rDNA in yeast [180, 181], it showed no effect in the resolution of HR intermediates away from the rDNA context [182]. The identification of the SLX4 orthologue in humans allowed the characterization of this third structure-selective nuclease dealing with HJs in humans, able to cleave HJ canonically much like the Yen1 orthologue GEN1, in a coordinated action with MUS81-EME1. Indeed, in humans, MUS81-EME1 and SLX1 bind to the SLX4 scaffold to act in concert during the resolution of HJ intermediates, in a pathway redundant to that of GEN1 [183, 184].

As suggested before, there is an inherent risk of CO associated with the use of nucleolytic resolution in mitosis. How is it then that these pathways have been selected through evolution, when dissolution pathways ensure a better preservation of the genome integrity by preventing COs? Their function can read as a mere back-up for dissolution since absence of the Sgs/BLM dissolvasome leads to marked phenotypes of sister-chromatid exchange. However, in the absence of a cell's set of nucleases, and despite the presence of a functional BLM-led dissolution pathway, cells present a strong phenotype of chromosome mis-segregation, chromosome rearrangements and accumulation of recombination intermediates, both in yeast and humans [177, 178, 184]. An accurate study of the JMs accumulating in yeast cells devoid of Mus81-Mms4 and Yen1 led to the identification of a majority of single-HJ intermediates and un-conventional dHJ intermediates with gaps and nicks. These intermediates – collectively referred to as orphan-HJ – cannot be processed by the STR dissolvasome for they lack the required twin HJ that facilitate a TopoIII-catalyzed release [163, 185, 186]. Thus, nucleolytic cleavage could be seen as a back-up dis-entanglement of persistent JMs that are impervious to the STR complex that would accumulate because of incomplete D-loop maturation or inability to fill in the gaps of a dHJ.

Sub-pathways of HR are tightly hierarchized within the cell cycle. Nucleolytic processing and dissolution proteins are subject to waves of cell-cycle dependent post-translational modifications (PTMs) [187] to ensure dissolution is available in early G2/M and then shift to nucleolytic resolution later in division. Mus81-Mms4 is hyper-activated [188-190] through phosphorylation by Cdk1 and the Polo like kinase Cdc5. As for Yen1, it is called upon at the onset of Anaphase through similar phospho-dependent control [191], seemingly as a last resort before mitotic exit. Since Yen1 and its control are the central focus of this dissertation, these issues will be reviewed in depth in section 3.3.

1.2.7.3 Break induced Replication (BIR)

In the very dire situation where a DSB cannot be rejoined with the other broken end, the attempts of the cell to process the single-ended break by successive strand-invasions and D-loop extensions lead to a non reciprocal loss of heterozygosity by Break Induced Replication (BIR) where the invading strand is basically extended to the end of the template chromosome in order to grow back the lost chromosome arm [192]. BIR is a form of homology directed repair, and basically shares the initial steps of HR [193], even though it is strictly dependent on Pol32 subunit of Polymerase δ [194]. After the establishment of a D-loop, failure to engage a second end will trigger an extensive conservative DNA synthesis via a migrating D-loop, with lagging strand synthesis being primed on the nascent strand [192, 195, 196].

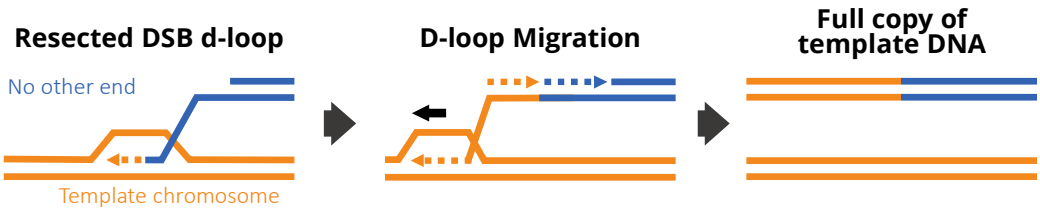

Figure 19. *Schematic representation of BIR from Symington et al. in 2014 [28].*

BIR can be seen as a pathological by-product of failed recombination that engages in processive D-loop extension when other options are unavailable. In that regard, is important to point out that BIR outcomes are often found in cells devoid of Mus81-Mms4 or Yen1 nucleolytic resolution, when monitoring those cells for outcomes of repair of a single DSB [177]. This suggests that BIR may also arise as a secondary product after mitotic catastrophe and chromosome breakage of DNA joint-molecule intermediates through cytokinesis and the extension of single-ended chromosome fragments in daughter cells [197].

1.2.7.4 Single strand annealing (SSA)

As stated before, resection initiation is the critical step preventing from NHEJ and driving the ends towards homology-directed. When there is homology in both resected ends, single strand annealing (SSA) can use this for annealing and repair to seemingly bypass HR. This is often possible between repeat sequences. The homology can be used by the Rad52 [109] and Rad59 [104] proteins to promote annealing before the Rad51 recombinase takes a hold of the ssDNA. Flap-endonucleases will trim the non-homologous tails that remain un-annealed, thusly allowing ligation of both ends at the expense of deletion of non-homologous sequences separating the repeats (figure 20) [198].

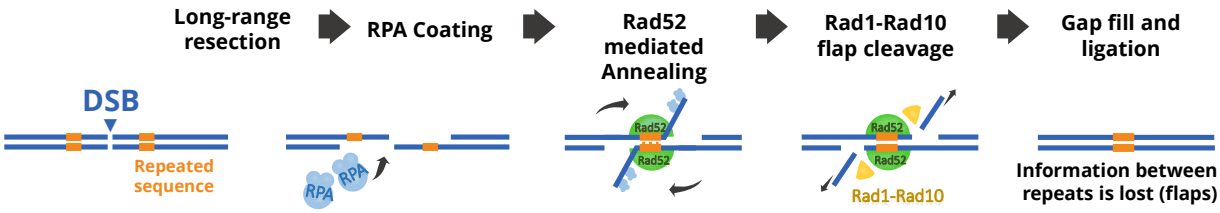

Figure 20. *Schematic representation of homology mediated SSA adapted from Helleday et al. 2007 [31]; Symington et al. 2014 [28]; Sallmyr et al. 2018 [198] Following long range resection, Rad52 (green semi-circles) interacts with RPA-bound ssDNA overhangs and aligns and anneals the repeated sequences. Superflous non-homologous 3' single strands overhang as flaps. They are cleaved by structure specific nuclease Rad1-Rad10 (yellow triangles). After that, gap fill and ligation are handled by unknown polymerases and ligases.*

While SSA efficiently deals with breaks exposing repeats with 200 bp homology or more, shorter homologies are not efficiently repaired [104]. The repair frequency drops significantly for repeats of <50 bp [199] until its bare minimum around 25 bp [198]. SSA is intrinsically mutagenic, leading to deletions of sequences between the repeats and the formation of dicentric chromosomes when inverted repeats are aligned and ligated [109, 118]. Subsequently, dicentrics forming by SSA can trigger translocations, deletions and duplications when they break at mitotic divisions [200]. However, metazoans and single cell organisms contain plenty of repeats in their genetic material. More than 10% of the human genome is comprised of repeat sequences [201]. Thus, this conserved process has its place within the multiple tools available for DNA repair and it has been shown to act in multiple species from yeast to humans [104, 202].

1.2.7.5 Micro homology mediated end joining

A side-pathway of NHEJ uses a very similar mechanisms to that of SSA to ligate ends showing very short homologies. While SSA can deal with a range of repeats between 200 an 25 nucleotides, this alternative pathway can subsist with homologies of only 25 to 2 nucleotides [198, 203, 204] hence its name: Micro-homology-mediated end joining (MMEJ).

When resection is at default and only a short overhang of 3'-ssDNA is formed, exposed micro-homologies can stabilize at DNA ends by annealing, which triggers this mode of repair [3, 198]. SSA and MMEJ do not only differ on the length of homology required, they also greatly differ mechanistically [202]. Specifically, there is no Rad52 requirement for MMEJ in either yeast or mammals for homologies under 14 nucleotides [205]. Annealing at microhomologies seems to be rather driven by the thermal stability of the annealed sequence itself [206]. In mammals, PARP1 stabilizes DSBs and competes with KU by an unknown mechanism that may somehow allow MMEJ [17, 198]. Accordingly, inhibition of PARP-1 with the inhibitor Olaparib disrupts MMEJ but not SSA [202].

MMEJ and SSA are often referred to as Alternative End Joining (Alt-EJ) mechanisms because they diverge from the canonical HR and NHEJ pathways by introducing a highly error-prone bias [202, 207]. Mostly considered as pathological pathways, Alt-EJ pathways only slightly contribute to overall DSB repair [198], but could be of increasing importance in mutant cells or upon mis-regulation or mutation of the canonical DSB repair pathways, thus promoting further cell transformation and cancer in human cells.

1.2.8 Inter-strand crosslink repair

Covalent links between opposite strands of double stranded DNA are highly cytotoxic and can disrupt many other cellular processes [208]. Since both strands are covalently attached, transcription and replication are arrested or can go into fork collapses and thus DSBs [4]. Due to the nature of the lesion, a simple excision and synthesis process is not sufficient and repair of this kind of damage entails a combination of repair pathways [1]. Components from the NER, TLS and HR machinery participate in the repair of ICLs, along with more than 13 proteins of the Fanconi Anemia (FA) group or its Fanconi Anemia-like homologs in the yeast model [23, 209, 210], as is illustrated in figure 21 below.

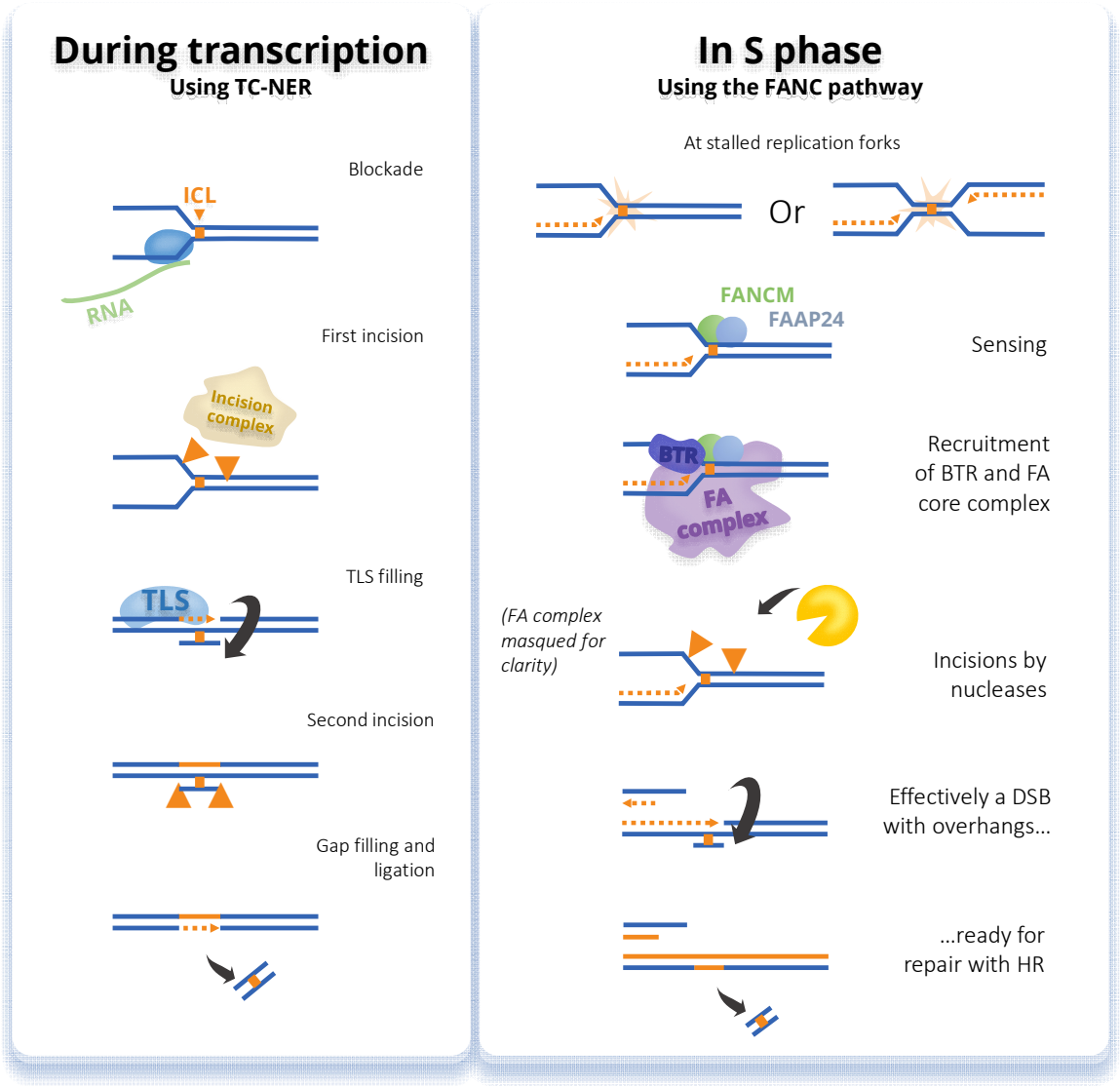

Figure 21. *Interstrand Crosslink Repair in humans, simplified. Adapted from Hashimoto et al. 2016 [208] with data and insight from Gourzones et al. 2019 [211] Left panel: In TC-NER repair, CSA and CSB help introduce the incision complex (XPA, XPG, RPA, TFIIH and XPF-ERCC1). TLS polymerases can be as κ, ζ, or REV1. Right panel: FA complex = FANCA, B, C, D2, E, F, G, I, L, FAAP20, FAN1; BTR = BLM-TOP3α-RMI1.*

As depicted in the figure above, ICL occurring in G1 will be mainly repaired by a combination of NER/TLS machineries, which will introduce flanking incisions to the ICL site to allow the flipping of the crosslinked base and an associated stretch of ssDNA. The gap will then be filled in by specialized TLS polymerases able to accommodate such a distorted template [208]. Crosslinks that arise during S phase and after are repaired through a specialized homology-driven pathway, making use of some Fanconi Anemia proteins. The core FANCM translocase recognizes ICLs and loads onto the chromatin forming the FA core complex [7] as seen in the right panel of figure 21. This FA core complex allows subsequent recruitment of nucleases that will unhook the ICL and collapse the stalled fork, leaving the damaged site to be corrected using homology directed repair [7, 212, 213].

1.2.9 The DNA damage checkpoint response

The repair of DNA lesions can vary in complexity depending on the type of lesions, the number of simultaneous lesions and the DNA repair pathways called upon. For instance, DSBs require complex DNA repair with alternative multi-protein and multi-step mechanisms. To ensure DNA integrity is fully restored, the cell triggers the activation of DNA damage checkpoints mediated by two key apical protein kinases: the yeast Mec1 (ATR in mammals) and Tel1 (ATM in mammals) [214]. While Tel1 activates the checkpoint when even minimally processed DNA ends are present, the Mec1 kinase will respond to the presence of ssDNA (figure 22).

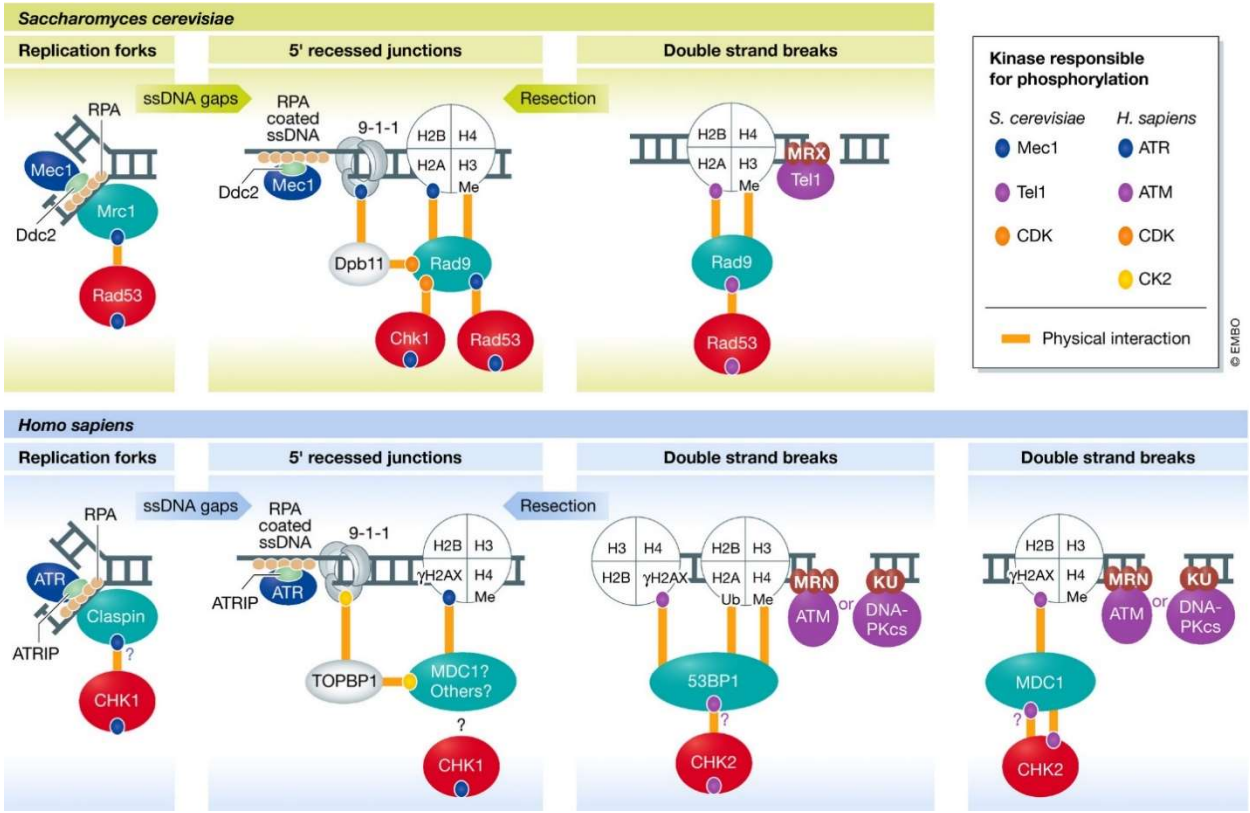

Figure 22. *Recruitment of DNA damage signaling kinases and adaptor proteins to DNA lesions: conserved features between budding yeast and humans. Figure by Lanz et al. in 2019 [215]. Phosphorylation and adaptor proteins play a key role in the recruitment of downstream checkpoint kinases. The colored ovals indicate phosphorylation events mediated by DNA damage signaling kinases (see kinase key). The orange lines indicate protein–protein interactions promoted by the indicated phosphorylation events (also methylation (me) or ubiquitination (Ub)). Activation of the downstream checkpoint kinases by the apical PIKK kinases requires adaptor proteins (outlined in green). In most cases, these adaptor proteins act as scaffolds to directly bind to and recruit the downstream checkpoint kinase. The model, mostly based on extensive work in yeast, posits that the recruitment of the downstream checkpoint kinase to the proximity of the apical PIKK kinase enables the phosphorylation and activation of the downstream checkpoint kinase. In addition to activating the downstream checkpoint kinase, phosphorylation events mediated by the apical PIKK kinases are critical for scaffold assembly, often promoting protein–protein interactions. Accordingly, a conserved feature of several adaptor proteins in budding yeast and humans is the presence of protein domains responsible for binding phosphorylated proteins (FHA and BRCT domains). Notably, other kinases such as CDK and CK2 also catalyze phosphorylation events involved in adaptor recruitment, although these events are often not induced by DNA damage. For DNA-PKcs, while this kinase has been implicated in the phosphorylation of H2AX and 53BP1, it does not seem to be involved in CHK2 phosphorylation.*

Binding of the MRX/N complex to the DNA ends promotes early recruitment of Tel1 by its direct interaction to the Xrs2 subunit (figure 22) [216-219]. The activation of Mec1 happens with further processing of DNA ends or the presence of long stretches of ssDNA, for example: in the form of gaps after a replication fork encounters a lesion or collapsed forks getting resected. Mec1 will be activated through its interaction to Ddc2 (mammalian ATRIP) and requires the presence of RPA bound to the

ssDNA (figure 22) [220, 221]. During DSBR, an initial Tel1 response will be replaced by a more sustained Mec1 response if the ends are processed through resection and enter the Homologous Recombination pathway (figure 22) [222, 223]. Once activated, the apical kinases will in turn phosphorylate downstream checkpoint kinases: Rad53, Chk1, and Dun1 in yeast (CHK2 and CHK1 in mammals). This second step catalyzes phosphorylation of mediators and effectors that trigger the cellular responses to DNA damage. Mediators include chromatin components like histone H2A, and repair factors like Rad9/53BP1, Sae2/CtIP, Dna2, or RPA (figure 22) [224].

By targeting chromatin and DNA repair factors, the checkpoint kinases promote the initial steps of recombination and control the extent of end-resection [114]. Moreover, a cascade of phosphorylation also targets cell-cycle factors that will ultimately halt cell cycle progression to allot time for repair to take place [225, 226]. Cell-cycle regulatory kinases like CDK, DDK and the Polo-like kinase Cdc5 (PLK1) are controlled directly or indirectly by the effector Rad53/Dun1 kinases as well as other critical players for the progression of mitotic cells as the proteins regulating dNTP pools and the stability of the replication forks [215]. In humans, the transcription factor p53 is a critical mediator of cell cycle arrest. It is directly modified by the signaling checkpoint kinases. The p53 mediated response is thus critical for DNA repair in humans. Mutations in these pathway are often associated to malignant transformation and cancer (reviewed in [227]).

1.2.10 A note on nucleolar rDNA and telomeres

Regions of the genome containing highly repetitive sequences are more susceptible to deleterious recombination and rearrangements. These loci include telomeres and the very repetitive rDNA region which is also highly transcribed. To avoid untimely recombination at these recombinogenic DNA regions, they are stored in nuclear compartments where recombination is basically suppressed. There, most Rad52-epistasis group proteins, checkpoint effectors and mediators are largely excluded. DSBs in rDNA are not left unrepaired, but Rad52 and downstream HR players only bind them after relocation of rDNA outside of the nucleolus. Rad52 exclusion from the nucleolus is mostly mediated by sumoylation. In the absence of Rad52 sumoylation, HR foci that form in the nucleolus lead to rDNA instability [228].

Similar to the rDNA loci, telomeres are compartmentalized into 6–8 clusters [229], which also prevent recombination and checkpoints in general. Telomeres can be considered as one ended DSBs. Being the natural end of a chromosome, they have to remain un-processed and not be recognized by repair mechanisms aimed at DSBs. Telomeres contain specific repeated sequences. One of the strands has a higher Guanine content and extends further than the C-rich strand. Bound by telomere protection proteins such as Rap1, the G rich strand can also form a tail that invades the upstream dsDNA in mammals [7, 109]. Some core components for telomere maintenance are actually actors of NHEJ and HR such as Ku and the MRX complex [230], acting in concert with the aforementioned telomere protection proteins specific to the G-tail and T-loop. Unprotected telomeres trigger the DDR and lead to deleterious recombination and chromosomal fusions.

Although full HR repair must be prevented at the telomeres, some HR recombination processes appear to be needed for proper telomere function. For instance, Rad51 and Rad52 are detected at telomeres at each replication round [231, 232]. Also, during replication, the HR machinery can lend a hand by restarting stalled replication forks that can accumulate at difficult to replicate sequence found at Telomeres. Finally, in the absence of telomerases, telomeres will shorten and trigger a response to use HR and BIR to elongate them [232].

1.3 Diseases linked to DNA repair deficiencies and DNA damage as therapeutic strategy

The necessity for DNA repair mechanisms was hinted at before by the sheer amount and diversity of DNA damage sustained on a daily basis. Moreover, the importance of the DNA repair pathways is dramatically highlighted by the number of human diseases linked to a deficiency in a gene associated to these repair pathways (table 1). Similarly, the cytotoxic potential of DNA damage has been used in therapeutic strategies to stop fast growing cells, especially in cancer treatment. The two edges of the DNA repair "sword" are thus intimately related.

Functional class	*S. cerevisiae*	*H. sapiens*	Associated disease(s)	Ref
End resection	MRX	MRE11-RAD50-NBS1	Nijmegen breakage syndrome; AT-like disorder	[233]
	Exo1	EXO1	Colorectal cancer	[234]
	Dna2; STR	DNA2-BLM-TOP3-RMI1-RMI2	Bloom syndrome	[235]
Adaptors	Rad9	53BP1, MDC1	Breast cancer	[236, 237]
	-	BRCA1	Breast cancer	[238]
Checkpoint signaling	Tel1	ATM	Ataxia-telangiectasia	[239]
	Mec1-Ddc2	ATR-ATRIP	Seckel syndrome	[240]
	Dpb11	TOPBP1	Breast cancer	[241]
Single-strand annealing Mediators	Rad52	RAD52		
	-	BRCA2-PALB2	Breast cancer	[238]
Strand exchange	Rad51	RAD51	Breast cancer	[242, 243]
Rad51 paralogs	Rad55-Rad57	RAD51B-RAD51C-RAD51D-XRCC2-XRCC3	Breast cancer	[244, 245]
Anti-recombinases	Srs2	FBH1, PARI		
	Mph1	FANCM	Fanconi Anemia	[246]
	-	RTEL1	Hoyeraal-Hreidarsson syndrome	[247]
Resolvases and nucleases	Slx1-Slx4	SLX1-SLX4	Fanconi Anemia	[248-250]
	Rad1-Rad10	XPF-ERCC1	Xeroderma pigmentosum	[251]

Table 1. *Evolutionary conservation of homologous recombination proteins and examples of related human diseases. Table slightly adapted from Symington et al. in 2014 [28].*

1.3.1 Mutations on DNA repair genes associate to cancer predisposition

Mutations of DNA repair core proteins and key players, interacting in many repair or checkpoint processes, lead to very severe conditions, when they are not outright essential and impair the embryonic development [6]. For example, neurodegenerative disorders result from a combinatorial failure of several DNA repair processes [7]. Other mutations, such as those that only impair sub-pathways or turn some DNA repair processes to a sub-optimal function, are better tolerated during development. However, by introducing genomic instability and increasing the mutational load, these mutations contribute to an elevated cancer risk [2, 7].

As summarized in table 1, there are a number of identified mutations in DNA repair pathways linked to diseases and syndromes associated with the development of cancer. This is the case of p53 signaling deficiencies that are common in a wide range of cancers and cause the Li-Fraumeni syndrome when associated to the germ-line [252]. It is relevant also to MMR deficiencies, which are linked to the Lynch syndrome, with an elevated frequency of nonpolyposis colorectal cancer [2, 3].

In some genetic syndromes, like Fanconi Anemia (FA), a group of genes that participate in the same DNA repair pathway can be the cause of the pathology with varying degrees of severity. Symptoms of FA, an autosomal recessive disorder, often include growth retardation, bone marrow failure and a cancer-prone phenotype with a high risk of myeloid leukemia [23]. Cells harboring mutations in one of the FA genes described so far are extremely sensitive to poly-alkylating agents and inter-strand crosslinks [253, 254].

It also common to find similar pathologies caused by mutations in alternative DNA repair pathways for the same type of lesions. As it is the case for the Xeroderma Pigmentosum disorder and its XP-variants, presenting photosensitivity and a high risk of light-induced skin cancers [4] as a result of faulty repair of UV-induced lesions [1]. While mutations in core components of the HR pathway and the NHEJ pathway are poorly tolerated, some mutations in HR-related genes have been identified as familial predisposition markers, tightly linked to hereditary ovarian and breast cancer [2] including mutations in BRCA1 and BRCA2 genes [3].

Proteins involved in the multiple sub-pathways of recombination can easily be backed-up by alternative processing modes, despite that, mutations in the RecQ helicases BLM and WRN associate to their respective Bloom and Werner syndromes where cancer predisposition is associated to the HR deficiencies and the increased number of chromosome exchanges and rearrangements [255, 256]. Some cancers originate by loss of expression of a critical gene, as the case for RB1 and retinoblastoma, are loosely associated to recombination in somatic cells, and they are strongly associated to loss of heterozygosity at the origin of the malignant transformation [257-259].

1.3.2 Mutations on DNA repair genes as therapeutic target

Transformation of normal cells into malignant cancer cells often involves the deregulation of classical cell functions including: the ability to respond to DNA damage through the DDR, a deregulated cell-growth with increasing replication-associated stress, a dysfunctional metabolism and higher levels of endogenous DNA damage. While all these malfunctions contribute to cell transformation, the mutations accumulated in the housekeeping functions of DNA repair can be exploited to kill cancer cells by inducing additional DNA damage [260, 261]. Even though DNA damaging agents are generally used to induce a broad spectrum of damage to all the cells indiscriminately, the preferential targeting of cancer cells is somewhat achieved because cancer cells divide and replicate their genome at a fast rate while the surrounding, normal cells, do not. Although unwanted side-effects are expected to result from widespread exposure to DNA damaging agents.

To further increase the efficiency and specificity of therapies using DNA damaging agents, the deficiencies of cancer cells in DNA repair systems and the molecular understanding of their function and regulation are to be exploited as a therapeutic advantage, in what is known as a synthetic lethality approach [262, 263]. Drug inhibition of alternative DNA repair pathways is used in cancers showing deficiencies for one given DNA repair function, specifically sensitizing cancer cells bearing these mutations as compared to the neighboring healthy cells. Until now, one of the most successful strategies of synthetic lethality that illustrate the potential of such strategies is the use of PARP inhibitors (olaparib, veliparib, niraparib or similar drugs) against cancers with BRCA1/2 mutations that showed promise mainly in the treatment of ovarian cancer [264-269]. These PARP inhibitors impair the PARP catalytic activity and compromise the BER/SSBR pathway, overwhelming BRCA1/2-deficient-cells with DNA damage they are unable to repair with the alternative NHEJ/HR pathways [270].

2 Modification by Ubiquitin and Ubiquitin-like peptides

Protein regulation is often achieved by post-translational modifications that alter its function and biochemical properties. Most of the well-characterized PTMs share the base principle of attaching a molecule to the target protein (phosphorylation, alkylation, glycosylation, acetylation). These modifiers are conjugated to the proteins in a covalent manner altering its charge, its surface and its overall properties. The reversible modification with small peptides of the Ubiquitin family constitutes a class of PTM that is widely used in the cell to control the fate of numerous proteins. Thus directing multiple pathways and biochemical processes [271]. Ubiquitin is a 76 amino acid long peptide (Figure 23) and as the name entails, it is ubiquitous [272, 273]. Its ubiquity implies, for one, that it is found everywhere within a cell and its influence can be found in many mechanisms. Second, it is a highly conserved protein, found in all eukaryotes, with strong sequence homology between species. Its ubiquity across species demonstrates its importance for basic cell functions, and it also suggests that the biological functions of this moiety are conserved [274].

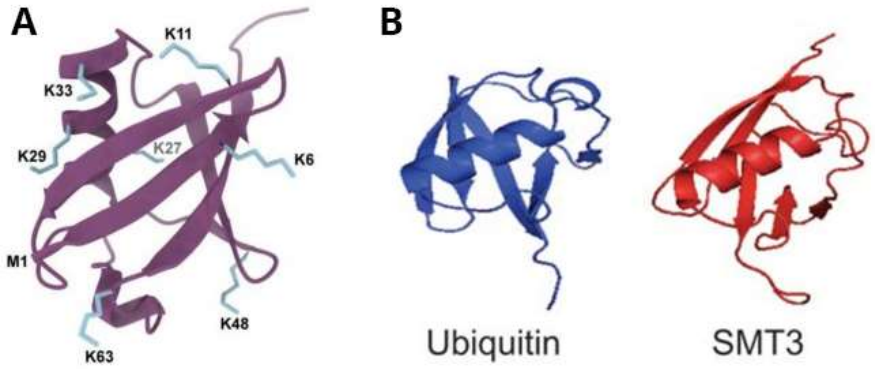

Figure 23. A: *Simplified representation of the 3D structure of ubiquitin with its lysines (K) and the first methionine residue (M1). Figure created by Dougherty et al. in 2020 [275]* ***B:*** *Ribbon drawing of ubiquitin and Smt3 by Alonso et al. in 2015 [276]. Orientation is inverted compared to A. The modifiers share a common secondary structure (βββααββαβ) that assembles into an ubiquitin-like fold.*

The ubiquitin modifier is characterized by its ubiquitin-fold or β-grasp fold, shared by all the UbL modifiers: a globular three dimensional structure [271] represented in the left panel of figure 23. Indeed, there are several ubiquitin-like (UbL) peptides that act in parallel to Ubiquitin and in a similar fashion. Ubiquitin and these UbL modifiers (Rub1/NEDD8, Atg8, Atg12, UFM1, ISG15, FUB1/FAU, Urm1, FAT10 or Smt3/SUMO) target their substrates thanks to a dedicated enzymatic conjugation machinery, which requires multiple steps to attach or detach the peptides with strong substrate specificity [277-279]. Ubiquitin and UbL modification cannot be lost spontaneously and will change the substrate's fate in multiple ways: altering the cross-recognition of the protein with itself and others, its solubility or its putative catalytic activity [274]. While at first, the main function associated with protein ubiquitination was proteasome signaling leading to protein degradation and recycling, many other functions have been associated so far with ubiquitination and modification with ubiquitin-like modifiers, including chromatin eviction or recruitment, substrate affinity changes for cross-interaction, building of protein complexes and much more [278].

Small Ubiquitin-like Modifier (SUMO or Smt3 in yeast) has little sequence homology with ubiquitin but shares a similar structure as seen in the right panel of figure 23. It is highly conserved across species. This suggests that sumoylation is quite distinct from ubiquitination and serves another signaling purpose.

2.1 Protein ubiquitination

A protein is ubiquitinated when an isopeptide bond is formed between the ε-amino group of one of its lysines and the carboxyl terminus of ubiquitin [274]. This conjugation is catalyzed by the sequential activity of 3 enzymes in the connected reactions of activation, conjugation and ligation [278], referred to collectively as the ubiquitination reaction (Figure 24). Prior to the ubiquitination reaction, ubiquitin needs to be processed from its inactive precursor form. In this maturation stage, dedicated proteases expose the double glycine motifs of ubiquitin C-terminus, making them available for conjugation. This precursor processing will also apply to all UbL modifiers [280].

It is also worth noting that, while ubiquitination most often happens on lysine residues of the substrate protein, other alternative ubiquitination sites such as serine, threonine and cysteine have been reported for some viral E3s [281].

2.1.1 Covalent bonding of the ubiquitin moiety to a substrate

The first step of an ubiquitination reaction is the activation of the ubiquitin moiety's C-terminus. It is catalyzed by the E1 enzymes that attach ubiquitin to an internal acceptor, a catalytic cysteine via a strong thioester bond in an ATP-dependent manner [278]. In yeast and mammals there is only one main E1 [277]. In *S. cerevisiae*, it is encoded by the UBA1 gene [278]. Therefore, activating enzymes are common to all ubiquitination reactions and do not bring any specificity to the mechanism. The bonding of ubiquitin to the E1s positions the "activated" ubiquitin in a favorable way to enable its transfer to the catalytic sites of the second enzyme of the reaction: the conjugating enzyme or E2 [274]. Different from other UbL modifiers, the ubiquitin pathway possesses a highly diversified set of available E2s. Thirteen E2 genes (UBCs) have been described so far in yeast, and many more in mammals, in striking difference with the single E2 (Ubc9) mediating all sumoylation reactions in yeast [277, 278].

After the conjugation step a third enzyme is required for the final transfer of ubiquitin to the substrates: ligases or E3 enzymes. This step is mostly essential for ubiquitination, but is not necessarily a requirement for the modification by other UbL modifiers [282]. In most situations, the E3 will merely promote the reaction by recruiting and positioning E2-Ub charged complexes in the compatible position for effective conjugation to the substrate. These E3 enzymes provide selectivity by having two separate binding domains. One is used to recognize the protein to be ubiquitinated and the other binds the E2-Ub [273]. The substrate interaction domain recognizes an ubiquitination signal, a specific sequence or structure in the substrate [274]. Positioning of the ubiquitination machinery via the aforementioned substrate-interaction domains will enable the E2-E3 complex to modify any suitable Lysine that lies in the vicinity of the catalytic site despite its amino-acid context. The high substrate selectivity of ubiquitination relies on the variety of the repertoire of E3s, able to identify and bind individual substrates via specific recognition sequences. These recognition signals are often related to ubiquitin-mediated protein degradation by the proteasome, as in the case of the D-box and KEN-box motifs found in several proteins, which are used as recognition sequences for ubiquitin ligases [283].

Naturally, there are multiple variations of E3 enzymes in eukaryotes. In mammals there are more than 600 E3s [277] while in yeast, there exist between 60 and 100 E3 [278]. The study of the multiple E3 enzymes identified in yeast led to the description of several major families with shared structural domains: the Really Interesting New Gene (**RING**) domain, the **U-box** domain, and the Homologous to

E6-AP Carboxy Terminus (**HECT**) domain [278]. U-box domains though are often considered as part of the RING family. In humans, a new RING between RING (RBR) class of E3 ligases has also been described [284]. The two major classes described in yeast: RING and HECT domain E3 act differently to catalyse ubiquitination. RING domain ligases position and activate E2 to promote the reaction. HECT domain E3s contain a catalytic domain with an active cysteine within the HECT-domain. This allows the formation of a thioester bond to the ubiquitin which is thus transferred from E2 to E3 prior to ligation to the substrate [278]. The specificity and numbers of E3 allow a great number of substrate and a targeted action at the same time. In addition to the specificity of E3s for a subset of substrates, phosphorylation, glycosylation, acetylation and hydroxylation can also alter the binding of substrates to their respective E3s [274].

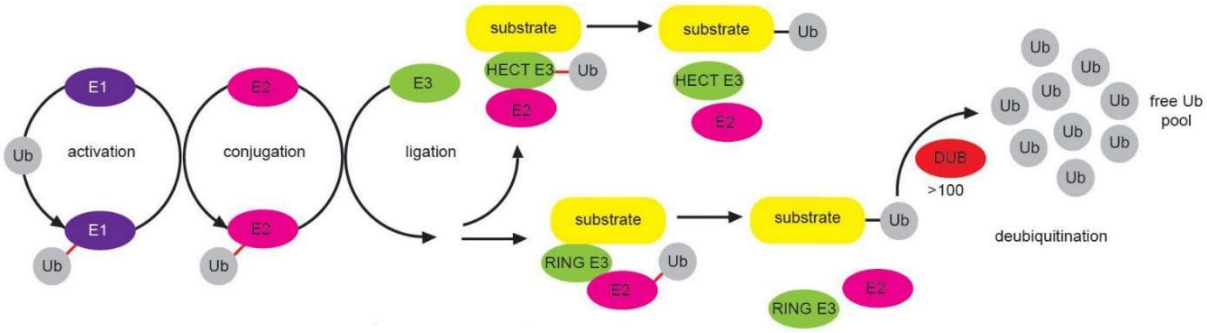

Figure 24. *Illustration of the basis of an ubiquitination reaction created by Kliza and Husnjak in 2020 [285].*

2.1.2 Multi- and poly- ubiquitination

Ubiquitin is conjugated to lysines on the target proteins. Similarly, ubiquitin itself bears lysines and can thus be ubiquitinated [286]. All seven lysines (K6, K11, K27, K29, K33, K48, and K63) found in ubiquitin (Figure 25) can be conjugated to other moieties creating chains with a variety of branching options [277]. The N-terminal Methionine can also be modified increasing the variety of poly-ubiquitin chains that can be obtained forming yet another type of chain, a linear chain [279]. Mono-ubiquitination and multi-mono-ubiquitination are the result of the attachment of single monomers of ubiquitin to either one or multiple lysines on the substrate (Figure 25) [273]. The addition of ramified or linear chains of ubiquitin will be described as poly-ubiquitination, and these chains can form after or before the conjugation to the substrate protein [274].

E2 enzymes can be specific to the synthesis of a certain type of poly-ubiquitin chains. Yeast's Ubc13, for instance, only synthesizes K63 chains through its heterodimer form with Mms2, which allows the active site access the lysine K63 of ubiquitin only [278]. Interaction between various E2 and E3 may thus determine how the substrate will be modified by either mono- or poly- ubiquitination. Further control is potentially established by N and C-terminal extensions of E2 enzymes which could regulate association with the E3 [274].

All the combinations of ubiquitin modification in different Lysines can occur for a given protein: grouping different chains of poly-ubiquitination or mixing mono and poly-ubiquitinated lysines. All these offer new layers of signaling and thus multiply the possible outcomes for the ubiquitin-modified substrate (Figure 25) [287]. These variable patterns of ubiquitination are seen *in vivo* when pulling down ubiquitinated substrates. Immunoblotting of these proteins reveals a smear or a ladder of various molecular weights indicative of the multiple possibilities granted by the ubiquitination pathway [288].

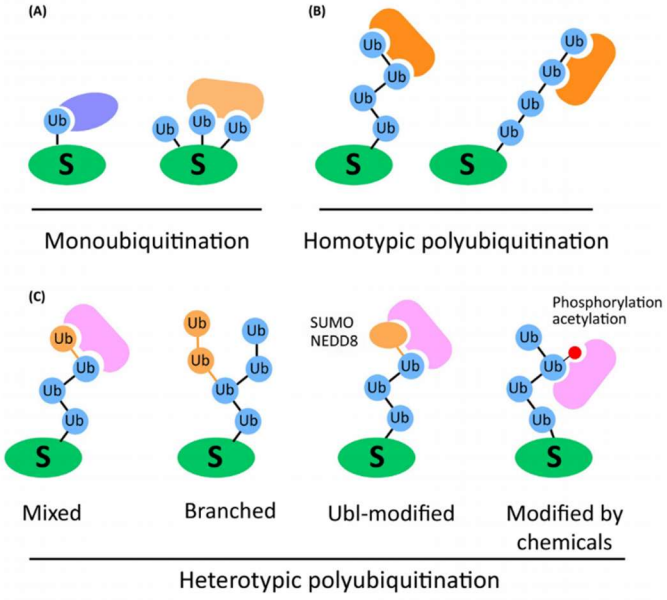

Figure 25. *The Different Types of Ubiquitin (Ub) Linkages and their Post-Translational Modification by Small Molecules. A figure by Kwon and Ciechanover in 2017 [289].* ***(A)*** *Monoubiquitination (left) and multi-monoubiquitination (right). Purple and orange shapes are possible interaction with proteins bearing ubiquitin binding domains specific to a spatial orientation of the moieties.* ***(B)*** *Homotypic polyubiquitination.* ***(C)*** *Heterotypic polyubiquitination. On the left: a mixed ubiquitin chain with varying lysine residues targeted. Middle left: branched chains by modification of ubiquitin at 2 or more sites. Middle right: Ubiquitin conjugated to UbL modifiers. Right: additional layers of control with PTMs on ubiquitin.*

2.1.3 Additional layers of control: PTMs targeting the ubiquitin modifier

Even if it functions as a modifier, ubiquitin is a protein first and can be in turn modified. As mentioned before, ubiquitin is also subjected to ubiquitination to give rise to chains. It can also receive a myriad of additional PTMs [279] including Ser/Thr phosphorylation [290] or acetylation [291] and other ubiquitin-like modifiers [279]. PTMs altering the substrate of ubiquitination can modify the interaction between E3s; and substrates containing other modifications at different sites may behave in different ways once ubiquitinated [274]. All these potential modifications increase the complexity of the ubiquitin chains and its associated signaling purpose in the cell.

2.1.4 De-ubiquitination

Ubiquitination is a covalent but reversible modification, and thus requires another specific machinery dedicated to cleaving ubiquitin from the modified substrates in order to recycle it and turn off the ubiquitin-mediated signaling. Multiple specific proteases can mediate this cleavage and are collectively known as ubiquitin-specific proteases (UBPs) or de-ubiquitinases (DUBs) [277]. In yeast, there are about 20 different DUBs [292]. To this day, their role is still poorly understood. They seemingly lack the substrate recognition specificity found in E3 ligases [277]. While some DUBs are tasked with recovering ubiquitin from conjugates on their way to degradation, thus playing a role in maintaining ubiquitin levels in the cell [278]; another DUB duty is to activate the modifiers from their precursor forms as mentioned before [293]. DUBs can also degrade poly-ubiquitin chains or edit the chain topology [279], possibly adding a variation to the message carried by the original ubiquitin modification on the target protein [273].

2.2 Protein Sumoylation

2.2.1 The SUMO modification reaction

SUMO is a very conserved UbL modifier and thus shares properties with the ubiquitin monomer. SUMO peptides have high structural similarities with ubiquitin even though they have a limited similarities in sequence of only around 20% and different charge distributions [277]. The similar 3D structure and ubiquitin fold [294] can be seen in the B part of figure 23. Yeast have a single SUMO gene, coding the protein Smt3 [295] while plants and vertebrates possess several SUMO encoding genes [277].

Like ubiquitin, SUMO is successively activated and conjugated to a substrate protein. The first activation stage is also handled by a unique E1: the heterodimer Aos1-Uba2 in yeast [296]. As for the conjugating E2 enzyme: a single enzyme has been described to carry out this reaction. In yeast, this enzyme is Ubc9. Similarly to what has been described for the ubiquitin pathway, it binds SUMO directly and transfers it to the target protein [274]. The E3 ligating enzymes can improve conjugation, however, there is no clear dependency on a ligase enzyme for the reaction to take place [274].

E3s are sometimes dispensable both *in vitro* and *in vivo* and the single E2 enzyme Ubc9 is able to aptly conjugate SUMO to an acceptor lysine in a given sequence context. Indeed, sumoylation occurs most frequently at lysines surrounded by a defined consensus sequence [295]. These are mostly found in disordered regions or extended loops that lay outside of the more conserved globular domains of the target protein. They are made up of a ψKX(D/E) motif with amino acid preceding the lysine mostly being large and hydrophobic and being often preceded or flanked by negatively charged aminoacids like Glutamic and Aspartic acid [297-299]. This motif mediates a direct interaction with the Ubc9 catalytic core, and is often flanked by additional sequences, which facilitate the interaction with Ubc9 [300, 301]. Several variants of this consensus have also been described, such as those replacing the negatively charged acidic residues with phosphorylation sites also known as a phosphorylation-dependent SUMO motif, the negatively charged amino acid dependent SUMO motif and finally the N-terminal hydrophobic cluster SUMO motif [300]. The existence of a consensus sequence for sumoylation, which is often conserved from substrate to substrate, helps in predicting sumoylation sites *in silico* even though a number of sites evade this consensus and constitute non-canonical sumoylation sites [302].

The ability of Ubc9 to modify its substrates with little help from the E3 ligases suggests that the role of these ligases rather lies in controlling the access of substrates to Ubc9. Either by tethering the enzyme to specific sub-cellular locations, or by locally increasing the concentration of substrates by affinity interactions and cross-recognitions defining which pools and sets of proteins are going to be modified [300, 303]. Most E3 ligases described so far are members of the Siz/PIAS family containing a characteristic zinc-finger SP-RING domain, which is responsible for the Ubc9 recruitment [304-306]. The known E3s ligases in budding yeast all belong to this family: Siz1, Siz2, Mms21 and the meiosis-specific Zip3 [307]. Within these SP-RING ligases, Siz1 and Siz2 – and the human PIAS family – have a SAP domain, which allows non-specific DNA targeting besides a more substrate-specific interaction via a PINIT domain [308]. For this reason, both Siz1 and Siz2 are often located in and around chromatin, helping in restricting specificity of sumoylation to proteins localized there, as is the case for the well-known Siz1-dependent sumoylation of PCNA [309]. The other yeast SP-RING E3s, Mms21 and Zip3, lack both SAP and PINIT domains [310]. Yet, these latter E3s are specifically localized as well by being part of multi-protein complexes such as the DNA repair Smc5-Smc6 complex and the meiotic synaptonemal complex, respectively [307, 311-314].

2.2.2 Poly- and Multi- sumoylation and additional PTMs

Much like ubiquitin, UbL modifiers are proteins and can be modified by other PTMs, including sumoylation. In yeast, the K11, K15 and K19 lysines of Smt3 are known to be used for the formation of chains, most likely because of their position in the vicinity of consensus motifs [315]. Other lysines can also be sumoylated, at least *in vitro*, to form different chains on top of the three normally found *in vivo* [316]. Poly-sumoylated substrates have been found to be important for chromatin-related signaling and transcription control. This was shown using mutant Smt3 forms unable to establish these chains [317]. Recent work in yeast and humans have implicated the use of chains of SUMO in centromere organization, SMC complex regulation, DNA repair, the DDR, meiosis, replication initiation and most likely much more [318-320]. In addition to these functions, poly-sumoylation is also related to the cross-targeting to ubiquitination via Sumo-targeted Ubiquitin Ligases (STUbL) that often bind and ubiquitinate its substrates thanks to the presence of poly-SUMO chains in the substrate protein [321].

2.2.3 SUMO group modification

Sumoylation differs from other PTMs, including ubiquitination, by most often targeting groups of proteins rather than selected substrates. In the context of DNA repair, for instance, the SUMO machinery collectively modifies HR proteins following exposure to DNA damaging agents [322]. However, *in vivo* examples suggest that sumoylation can also be used for specific targeting of selected substrates such as PCNA that is modified in the same lysine by both SUMO and Ubiquitin in a competitive way, thus determining the DNA repair pathway choice for replication stalling lesions [288].

This is in line with SUMO E2 being enough for reactions sometimes. This machinery is able to target groups displaying consensus sequences without substrate specificity for each and every one of them.

2.2.4 De-sumoylation and ULP proteases

Sumoylation is a reversible process as well. It is to be reversed by the protease-mediated cleavage of SUMO catalyzed by specific proteases or de-sumoylases. In yeast, de-sumoylases Ulp1 and Ulp2 remove the moiety from target substrates to enforce a turnover and turn off the response related to this modification [277]. Ulp2 deals mostly with SUMO chains [319]. The importance of these SUMO-specific proteases does not end at a mere turnover mechanism. Deletion of these has grave phenotypic consequences which allow experimental recognition of the mechanism they play a role in [318].

2.3 Sumo-targeted ubiquitination

Ubiquitin-like modifications are not always mutually exclusive for a given substrate. Often there exists some cross-talk and successive modifications by more than one UbL moiety on the same substrate. A first example of this type of interplay lies in the competition, which can occur between the SUMO and Ubiquitin machineries for the same substrate lysine, as well as with other PTMs such as methylation and acetylation. For example, sumoylation limits the poly-ubiquitination of IkappaBalpha – an inhibitor of the NF-κB transcription factor – and thus its degradation by blocking the target lysine residue [323].

As it was mentioned prior, its quite possible to have UbL modifiers modifying ubiquitin chains [324]. Another side of this interplay can be found in SUMO targeted ubiquitin ligases (STUbLs). These enzymes are E3 ligases of the RING type, that specifically target previously sumoylated proteins thus cherry-picking a subset of modified proteins within the general protein pool [279]. STUbLs recognize their substrates by using either scattered or clustered motifs that bind to SUMO: SUMO interacting motifs (SIMs), that will be described in more detail further below [321, 325, 326].

In *S. cerevisiae*, two STUbLs have been described to date. Ris1, that plays a role in mating-type switching [327, 328] and Slx5-Slx8, a heterodimer [329] which localizes to nuclear DNA repair foci [330, 331]. Binding of Slx5-Slx8 to chains of SUMO stimulates the ubiquitination output on the protein and the chain itself. Loss of this STUbL in yeast triggers an accumulation of sumoylated products [330]. This shows that STUbLs target sumoylated proteins preferentially to trigger their degradation, thus contributing to the regulation of their activity. Though new roles are still being described, like involvement in the DDR [332]. Uls1 is considered to be another STUbL because of its similarities with Slx5-Slx8. Indeed, it binds SUMO monomers and chains. It also bears an E3 RING domain. Most interestingly, in absence of Uls1, highly sumoylated proteins accumulate [327, 333]. Sadly, ubiquitin ligase activity of Uls1 has yet to be demonstrated [334]. There are other RING-type ubiquitin ligases, such as yeast Rad18, that bear SIM consensus motifs, suggesting that there may be more STUbLs to uncover [327, 332, 335-337].

2.4 Cross-protein interaction using SUMO and Ubiquitin recognition motifs

While the actual event of ubiquitination or sumoylation is a covalent modification of a target protein, there can be non-covalent interactions between a protein and a partner containing ubiquitin or UbL modifiers. These interactions are by definition transient, and mediated by specific sequences or interaction motifs [338].

2.4.1 Families of ubiquitin-binding domains

The ubiquitin machinery is characterized by a remarkable dynamism and a variety of outcomes. The large amount of E3s explains the high substrate selectivity. However, a link is missing in the chain to explain how this system can signal so many proteins to do that many different things. Small peptide stretches on receptor proteins mediate a non-covalent binding to ubiquitin. This allows the recognition of ubiquitinated substrates with high specificity. These amino acid sequences are called Ubiquitin Binding Domains (UBDs). Though it can be strong, more often than not the binding is quite weak [339].

UBDs can be arranged in families given their recognition basis. Interestingly, a single class of UBD is much more widespread than the others: α-helical UBDs are the largest family, including ubiquitin associated (UBA), ubiquitin-interacting motif (UIM), coupling of ubiquitin conjugation to endoplasmic reticulum degradation (CUE) and many more. UBA domains were the first to be described; they bind mono-ubiquitin *in vitro* and mediate protein-protein interactions [340-345]. The UIM is found in trafficking proteins that transport ubiquitinated substrates. CUE and UIM are known to sometimes be a requirement for the ubiquitination of the proteins bearing them [346-352], as do some members of the second largest family of UBD: the zinc finger based binding domains [353]. There are many more

types of UBD to list, and most likely new ones that remained uncharacterized [354]. Of note: Ubiquitin binding motifs (UBM), which are found in DNA polymerases involved in DNA repair [355]. The Ubc fold of E2 enzymes can also be considered as such. Indeed, E2s bind non-covalently to ubiquitin during chain elongation [339, 356].

Overall, the effect mediated by UBDs seems rather varied. While some help in the regulation of auto-ubiquitination, others allow context-sensitive recognition of ubiquitinated substrates. This can be used for scaffolds and platforms that help in the assembly of repair complexes.

2.4.2 The SUMO-interacting motif (SIM)

SUMO interacting motifs (SIMs) are found throughout species and are defined by a robust consensus sequence [357]. Some SIM types have a sequence and architecture that resembles that of certain UBD [346, 358], attesting of their similar principle of action.

Most SIMs are defined by a hydrophobic core of four amino acids, typically rich in V, I or L such as "[V/I]-x-[V/I]-[V/I]". Many other arrangements and dispositions exist. This hydrophobic core fits into the hydrophobic groove on the SUMO surface. SIMs are often flanked by a stretch of 3-4 acidic or polar residues, which interact with basic residues on the surface of SUMO [359-363] as illustrated in figure 26, a human example of simulation of a SUMO-1/SIM interaction. The side amino acids are often susceptible to phosphorylation, altering the ability of the SIM to recognize and bind SUMO depending on the phosphorylation status [357]. It is worth noting that with the growing number of validated SIMs it has become easier to predict potential new SIMs *in silico*. Current algorithms used to predict these motifs are remarkably accurate [357]. Nonetheless, the sometimes loose consensus calls for validation of these predicted SIMs to see if they are relevant *in vivo*.

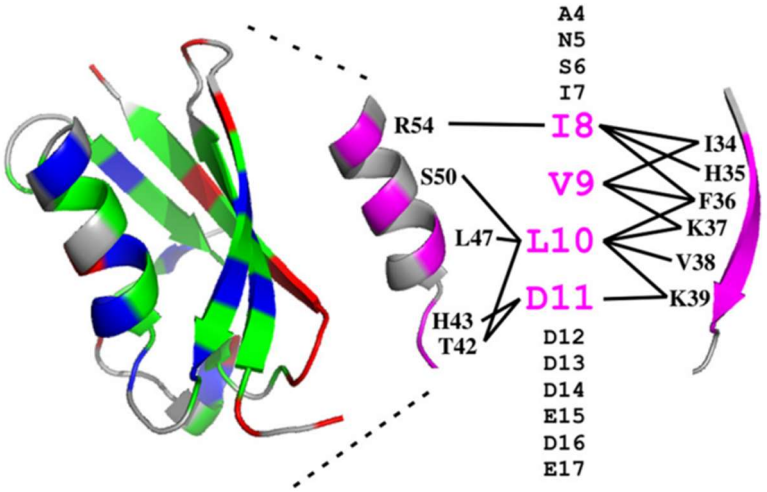

Figure 26. *Example of binding of the scaffold protein DAXX on SUMO-1 (left) via its N-terminal SIM (amino acids in column) Parts of SUMO-1 are shown as isolated elements with residues that receive intermolecular interaction from SIM-N highlighted in magenta. Each line represents the presence of at least one intermolecular Nuclear Overhauser Effect. Figure by Escobar-Cabrera et al. in 2011* [364].

SIMs are often found in multiple copies in proteins, seemingly to interact with poly- or multi-sumoylated partners. Most SUMOylation substrates and enzymes of the SUMO pathway are found among the SIM- bearing proteins, thusly enforcing the notion that a cooperative and grouped sumoylation occurs for a given number of related proteins involved in the same pathway or cell process [300, 305]. Actually, the SUMO mediated protein-protein interactions are often associated with the actual sumoylation of the two interacting proteins [337, 365].

The SUMO to SIM interaction is reportedly weak. This could be considered a feature in context-sensitive and transient processes that involve the dynamic interactions of a few proteins, such as HR [366]. The presence of SIMs also is determinant for the targeting of a specific subset of proteins. This is especially the case for STUbLs such as the aforementioned Slx5-Slx8 and Uls1 or the Cdc48 segregase that benefits from the SIMs of its cofactor Ufd1 to recognize sumoylated substrates to extract them from chromatin [367-370].

2.5 Ubiquitin and SUMO effects and consequences

The precise signaling and the dynamic nature of ubiquitin-related processes make them a powerful tool for most cellular processes. As research endeavors go further and further, the importance of ubiquitination and sumoylation seems to be better appreciated and found to be essential to numerous basic cell processes.

2.5.1 Molecular effects of Ubiquitination and sumoylation

The main molecular effect of ubiquitination and sumoylation, as for most PTMs, is the alteration of protein surfaces, shifting their interaction landscape and thusly transforming their normal behavior. These modifications can target lysine residues in competition with other PTMs, including concurrent PTMs such as methylation or acetylation. One molecular role of both ubiquitination and sumoylation will be to antagonize another PTM effect [371], as it is reflected in the fine tuning of transcription factors [372, 373].

The modification can also alter the protein surface of a given interaction domain, thus interfering with the interaction of the substrate to another component of a complex [286, 374]. But most usually, the combined effect of ubiquitination or sumoylation in a substrate and the presence of specific binding motifs (ubiquitin or SUMO) in other proteins will enable the interaction of the modified substrate with a given partner protein or group of proteins.

Another molecular effect of SUMO and ubiquitin is its chaperone-like role, which is hinted at by the development of a SUMO tag toolkit for protein solubilization in recombinant protein expression [375]. The use of such tags to help production of soluble proteins in *E.coli* came from the experimental observation that insoluble proteins may fold properly when fused to ubiquitin or SUMO [376, 377]. Interestingly, the correct folding of recombinant proteins survives the cleavage of the SUMO tag, suggesting an actual – direct or indirect – chaperone-like function for SUMO [378].

2.5.2 Biological functions of Ubiquitination and sumoylation

The presence of ubiquitination, especially in the form of poly-ubiquitin chains is mostly associated to proteasomal degradation [279]. Components of the proteasome machinery will use ubiquitin chains as binding-partners to direct proteins to proteolytic degradation. A controlled ubiquitination thus serves the role of deciding when a protein or a subset of a protein pool should be degraded. Sometimes allowing the removal of inhibitory factors in cell processes such as transcription and gene expression, but also in cell cycle regulation, chromosome segregation or the switching off of multiple other

pathways and biological processes [278, 379-381]. Not all poly-ubiquitination events will trigger degradation. Sometimes, it will depend on the type of side-chains. For instance, while K11 and K48 ubiquitin chains target proteins to the proteasome for degradation, K63 chains seem rather directed at assembly of complexes in DNA repair [382].

Growing evidences of sumoylation of different proteins pinpoint its multiple roles in various cellular processes. Our knowledge of the sumoylation function has basically been associated to the description of sumoylation targets, lacking insight of the precise effect of sumoylation on these targets. In yeast and in mammalian systems, some proteins are well known to be sumoylated. Septins were one of the first groups of proteins to be characterized as substrates of Siz1. Absence of this SUMO ligase leads to the deficient disassembly of septin rings after cytokinesis [383] and in humans, deficient septin sumoylation has also been shown to lead to defective septin bundle formation and cytokinesis problems [295, 384]. Nucleolar proteins have also been shown to be sumoylated, including most of the components of the RENT complex [385, 386], and together with the sumoylation of the proteins of the Condensin and Cohesin complexes and Topoisomerases (Top1 and Top2) highlight an important role of sumoylation in an ordered segregation of the highly transcribed and repetitive region of the rDNA thus allowing an unperturbed mitotic exit [303, 387]. Often, sumoylation is intimately associated to SUMO-targeted ubiquitination. An important role of the STUbL lies in clearing some protein complexes from sensitive nuclear positions, as is the case for Rap1 sumoylation and its targeted removal by Uls1 [388], or the Slx5-Slx8 mediated degradation of factors such as: Siz1 [389], centromeric histone Cse4 [390], spindle positioning Kar9 [391], and most likely many more targets yet to uncover as is exemplified by the wide ubiquitination events mediated by Slx5-Slx8 in “ubiquitin hotspots” aimed at remodeling chromatin [392].

Together with the aforementioned proteins, a growing number of sumoylation targets have been described among the different proteins involved in the DNA damage response and DNA damage repair pathways [393, 394]. Both a wave of ubiquitination and sumoylation occur after DNA damage to presumably help recruit DNA repair proteins [395]. Likewise, an increase in DNA damage leads to a noticeable increase in sumoylation of various DNA repair proteins [396]. The role of ubiquitination in chromatin remodeling also contributes to the DNA damage response by modulating the transcription activity and avoiding conflicts between replication, repair and transcription. Similarly, the turnover of all the factors involved in the response is ensured by the ubiquitin-linked proteasome activities often coupled to SUMO-targeted turnover [277].

Ubiquitination has been reported to help in the regulation of all the main DNA repair processes such as NER, BER, ICL repair, TLS and DSBR [277]. The paradigmatic example of such role is the control of the pathway choice between TLS and Template switching after replication fork stalling, dictated by the ubiquitination status of PCNA [397]. Interaction of PCNA to downstream factors will depend on whether it is mono- or -polyubiquitinated in reactions mediated by Rad6-Rad18 and Mms2-Ubc13-Rad5[398]. PCNA is also sumoylated at the same lysine, further controlling the access of repair factors to prevent illegitimate recombination and promote replication resumption and repair[288]. Another example can be found during NHEJ, where repair will only proceed if the Ku heterodimer is timely removed after ubiquitination of Ku80 with K48 chains signaling for its degradation [277]. In the same complex, Ku70 has been reported as being sumoylated by Siz1/Siz2 to promote its binding to DNA [399].

Homologous recombination is one of the DNA repair pathways where more proteins seem to respond in different ways to sumoylation-based regulation. During its initial resection steps, the resulting ssDNA

tails will trigger a wave of Siz2-dependent sumoylation [400]. A few key players of HR are sumoylated [396]. Among these key players, Rad52 sumoylation lowers its DNA binding activity and signals for its degradation [401]. Inhibiting sumoylation of Rad52 seems to render it hyperactive [228, 401-403]. The ssDNA binding protein RPA has also been shown to be both ubiquitinated and sumoylated during DNA damage responses [404, 405]. While the small portion of the protein pool that is ubiquitinated seemingly corresponds to the chromatin-bound part of the RPA pool [406], sumoylation of RPA has been associated with promoting the binding of Rad51 to ssDNA [404].

Sumoylation is also implicated in the recruitment of HR proteins associated with DNA damage occurring in a context when HR might be deleterious, especially during replication. In that context, sumoylation will control recruitment of helicases Srs2 and Sgs1 as well as other factors related to Smc5-Smc6 [407-410]. While sumoylation can directly promote functional interactions and the access to substrates during DNA repair, another common target for sumoylation is the control of the localization of these factors, as seen with Rad52. Similarly, attachment of ubiquitin chains on 53BP1 can also promote its recruitment at sites of DNA damage [411]. Both modifications are also important to control the HR protein pools, as highlighted by the control of Exo1 levels [412], of which excessive amounts trigger SUMO-mediated degradation [413].

To sum up, the influence of ubiquitination and sumoylation in DNA repair is widespread although not fully characterized. The selected examples highlight the possible effects of these modifications on DNA binding, activity, levels of active protein, localization and protein-protein interactions. The effects described so far paint a clear picture of the expected effects of sumoylation in newly identified ubiquitinated or sumoylated proteins.

2.5.3 Ubiquitin and SUMO associated diseases

The widespread action of ubiquitination across most cell processes is highlighted by the myriad of diseases stemming from dysfunctions in part of the ubiquitination machinery. For instance, it has been linked to neurodegenerative diseases, immunity and cancer [414]. Several genes known to have a link in Parkinson's disease encode direct components of the ubiquitin signaling pathway [415]. One of these genes codes the most studied of the human RBR E3 ligases, which has recently been described as an Ubiquitin E3 ligase, linked to mitophagy [284].

As for sumoylation, recent research efforts point to similar ties of sumoylation deficiencies and devastating neurodegenerative conditions such as Huntington's and Parkinson's diseases, associated to the formation of protein aggregates [416, 417] and to Cardiovascular diseases [418]. Finally, and not surprisingly, loss of sumoylation enzymes, as stressed before, leads to impaired double-strand break repair and increased sensitivity to DNA damaging agents like UV, IR and MMS. Thus loosely connecting sumoylation deficiencies to DNA repair associated diseases such as cancer [396, 419, 420].

3 Yen1's contribution to Homologous Recombination

3.1 The Yen1/GEN1 nuclease and its biochemical properties

3.1.1 The quest for a canonical resolvase in eukaryotes

The first evidence of nucleolytic resolution of homologous recombination intermediates came with the identification of T4 endonuclease VII, an enzyme capable of cutting joint plasmids generating un-branched duplex products that could be religated [421]. Shortly after, followed the identification of equivalent enzymatic activities in cell extracts of both *Escherichia coli* and *Saccharomyces cerevisiae* with an analogous ability to process HJ intermediates [422-425]. The bacterial activity was soon assigned to the RuvC protein, acting in concert with the branch migration activity mediated by RuvA and RuvB proteins [426-429]. In bacteria containing these enzymes, RuvC dimers bind the junction and cut symmetrically in a sequence-specific manner. These findings set the canon of what is now identified as "Resolvase" activity. Characteristic of an enzyme capable of cleaving a Holliday Junction with two nearly simultaneous incisions at symmetrical points in the two strands, generating two linear fragments directly available for re-ligation. While the resolution activities in bacteria had been established, the initial activities identified from yeast extracts were ultimately assigned to the activity of a mitochondrial enzyme: the Cce1 resolvase. From that moment on, a quest began to identify resolvases in other organisms and especially in humans.

In that context, the first evidence of resolvase activity in mammalian cells came with the analysis of crude extracts from cells and tissues [425, 430], followed by the purification of the first classical HJ resolvase activity from mammalian cells [425]. Ultimately, this HJ resolvase activity was referred to as *ResA*, with enzymatic properties compatible with what had been observed for the RuvABC canonical bacterial resolvase. The enzyme responsible for that activity remained elusive.

The identification of a first candidate able to encode the HJ processing activity in eukaryotes, the Mus81-Eme1 heterodimer in *Scizosaccharomyces pombe* and human cells [174, 431, 432] was received with a huge controversy. The initial characterization of the biochemical activity of Mus81-Eme1 complexes purified *in vivo* revealed their ability to cleave mobile HJs, but in a non-canonical manner generating asymmetric and non-ligatable linear duplexes [174, 433]. Indeed, the human MUS81-EME1 heterodimer, expressed and purified from bacteria, lacked activity towards HJ substrates *in vitro* [432]. Further characterization of the yeast Mus81-Mms4/Eme1 pointed to a preferential substrate specificity for flap substrates [432, 434]. Moreover, while phenotypically, *MUS81* mutants showed a strong meiotic phenotype in *S. pombe*, with a stark decrease in spore viability and chromosome segregation defects, and also presented a decreased number of both mitotic and meiotic COs [160, 435, 436]; the mutations of *MUS81* in either budding yeast or higher eukaryotic models lacked any strong phenotype in meiosis or DSB repair [437-441].

At last, the identification of the first bona fide nuclear resolvases in eukaryotes – compatible with the *ResA* activity previously identified in extracts – was the result of a colossal effort of purification from human tissue culture cell extracts, performed in parallel with a screen on a yeast protein-fusion library [176]. As a result, the Yen1 and GEN1 orthologues were identified as the first canonical resolvases in yeast and mammals respectively. GEN1 was identified with a serial purification of fractions from tissue cells cultivated in large amounts. The yeast orthologue Yen1 was found by screening a collection of epitope-tagged yeast ORFs enriched with low abundance proteins that were absent from the original commercially available collection. Immunoprecipitated proteins were tested for resolution of synthetic

HJ structures leading to the identification of Yen1, besides the already characterized Cce1 and Mus81-Mms4 nucleases [176]. The absence of Yen1 in the commercial TAP-fusion library probably delayed its discovery for several years in a typical serendipity situation.

3.1.2 Yen1/GEN1: a class IV XPG/Rad2-family nuclease

Yen1 and GEN1 are members of the Rad2/XPG family of well-conserved structure-selective nucleases [176, 442-444]. GEN1/Yen1 makes up a new fourth class of Rad2/XPG nucleases, with the other three classes showing slightly different DNA substrate preferences in relation to their role in diverse pathways of DNA repair and DNA maintenance [445, 446] (Figure 27).

The 3 other classes of the Rad2/XPG family are: the Flap EndoNuclease FEN1 class, the EXO1 class and the XPG class. [447]. The functions of these are loosely connected by their substrate selectivity, as well as their ability to recognize flexible or bendable regions in DNA. The defining member of the super-family, the NER factor XPG/Rad2/ERCC5, recognizes the bubble formed around the distorted base pair during NER, where it is able to recognize the 5'-flap of the bubble and cleave it. FEN1 is involved in Okazaki fragment processing during DNA replication, where it cleaves the 5'flap substrates, thus removing the primers required to prime its synthesis. EXO1 is a 5'-to-3' exonuclease with important roles in MMR and HR [445, 446, 448, 449].

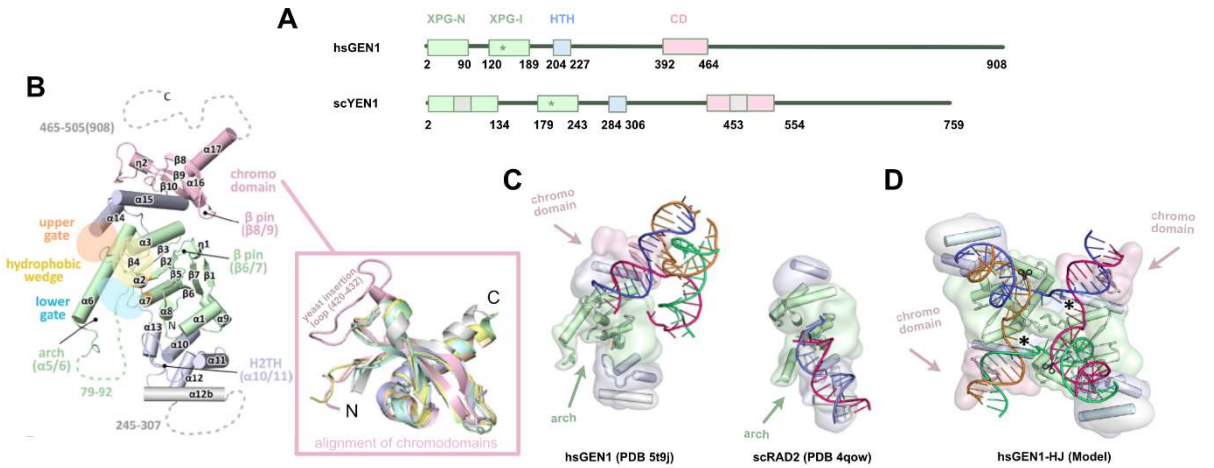

Figure 27. *Architecture of human GEN1. By Lee et al. in 2015 [450]* ***A:*** *Domain architecture of S. cerevisiae Yen1 and human GEN1 with the main domains represented at relative sequence positions 'CD' chromodomain, 'HTH' helix-turn-helix.* ***B:*** *Secondary structure elements of the catalytic core of GEN1. Dotted lines represent parts that are not resolved in the crystal structure. The numbering follows a unified scheme for the Rad2/XPG family for α-helices, β-sheets and 310-helices (η).* ***C:*** *Structural comparison of Rad2/XPG family nucleases. Proteins are shown in a simplified surface representation with important structural elements in cartoon representation and DNA in ladder representation.* ***D:*** *Model for the dimerization of GEN1 upon binding to a HJ substrate. The monomers interlock via both arches (α4-α6) and the hydrophobic wedges (α2-α3) contact each other.*

A common feature for all Rad2/XPG members is the presence of a core conserved domain, where the catalytic activity resides, accompanied by an N-terminal domain (XPG-N), an internal domain (XPG-I) and a C-terminal conserved Helix-two-turn-helix (HtH) domain. The rest of the Ct-distal protein length is a variable region where most of the regulatory motifs are found (figure 27 A). While the interaction between these nucleases and the branched DNA region is mostly mediated by the XPG-N and XPG-I domains, the HtH domain plays an important role in stabilizing the DNA binding by making contact with the duplex DNA portions of the substrates [446, 451].

In a striking and defining difference to the other classes of XPG family members, the primary protein sequence of Yen1 contains – in addition to the well conserved XPG-N, XPG-I and HtH – an additional conserved chromodomain motif important for DNA interaction and substrate selectivity [450] (Figure 27 A). In general, chromodomains are used to target proteins to the chromatin as well as to facilitate protein-protein interaction or dimerization (reviewed in [452-458]). In GEN1/Yen1, the chromodomain serves a structural role to securely bind DNA, but also for targeting and regulatory functions, as highlighted by the presence of several CDK1 sites in an insertion loop at the chromodomain of Yen1, further discussed below (Figure 27) [459, 460].

The structure of GEN1 bound to a HJ structure confirmed how the main DNA-binding interface is found at the conserved XPG-domains. The chromodomain interacts by loosely contacting a DNA strand by matching its peptide surface to the DNA backbone contour in a sequence unspecific manner [450]. The active site of both GEN1 and Yen1 is found at the conserved domains, and mutations in either GEN1 (D30N, E134A E135A) or Yen1 (E193A E194A) generated a loss of the cleavage activity on both HJ and 5' flap substrates [176, 450]. To achieve coordinated cleavage of the HJ opposite strands, Yen1/GEN1 dimerizes upon binding to the DNA substrate as indicated by the increase of the hydrodynamic radius compared to the protein alone [461, 462]. Another structural property of the GEN1/Yen1 protein that possibly singles out this class of enzymes as compared to the other XPG proteins is the presence of an arch structure that can clamp a single-stranded DNA overhang [450]. Rather than forming a "cap" structure as observed in the FEN1 protein, in GEN1 this arch points away from the DNA providing a "lower gate" (Figure 27), these structural variations can explain the GEN1/Yen1 broad activity on 5'-flap DNA structures as well as HJ intermediates [450] .

3.1.3 The nuclease structure-selectivity of Yen1/GEN1

The whole process that led to the identification of the Yen1/GEN1 nuclease was guided by the quest for a canonical resolvase in eukaryotic cells and especially in mammals. As thoroughly explained before, the archetypical activity of such enzymes is the resolution of four-arm Holliday Junctions. These substrates can be monitored for resolution *in vitro*, in assays using different types of synthetic HJ made with complementary oligonucleotides allowing or preventing branch migration by introduction of small heterologies in the arms [463].

The identification of both human GEN1, and the yeast orthologue Yen1 was thus based on the characterization of its ability to cleave HJ with the introduction of symmetrical cuts on the two opposites sides of the HJ, thus generating a linear duplex that can be ligated [176]. This very same ability of GEN1 to cleave synthetic HJ was also identified in its Drosophila orthologous Gen protein [464] and is a conserved feature in all the other class IV Yen1/GEN1 orthologues that have been identified and characterized.

Besides their canonical activity in resolving HJ, Yen1/GEN1 were also shown to be able to cut – although with less efficiency – 5'-flap intermediates presenting or not dsDNA at the displaced splayed DNA arms (figure 28) in yeast, humans as well as in plants and flies [176, 464-467]. Contrary to that, no cleavage activity was detected for the *GEN1* orthologue of *C. elegans*, which only showed activity with a synthetic HJ *in vitro* [466]. While the cleavage of the Flap-containing DNA structures might require a single monomer of Yen1, two monomers of Yen1 are required for HJ cleavage. The protein is mainly detected as a monomer in solution and will dimerize, as explained before, at the HJ prior to the nucleolytic processing [171]. In fact, the studies with the *Drosophilia melanogaster* dmGEN suggest that HJ cleavage is slowed down by the necessity for homodimerization prior to Yen1 symmetrical nucleolytic processing [464] (figure 28).

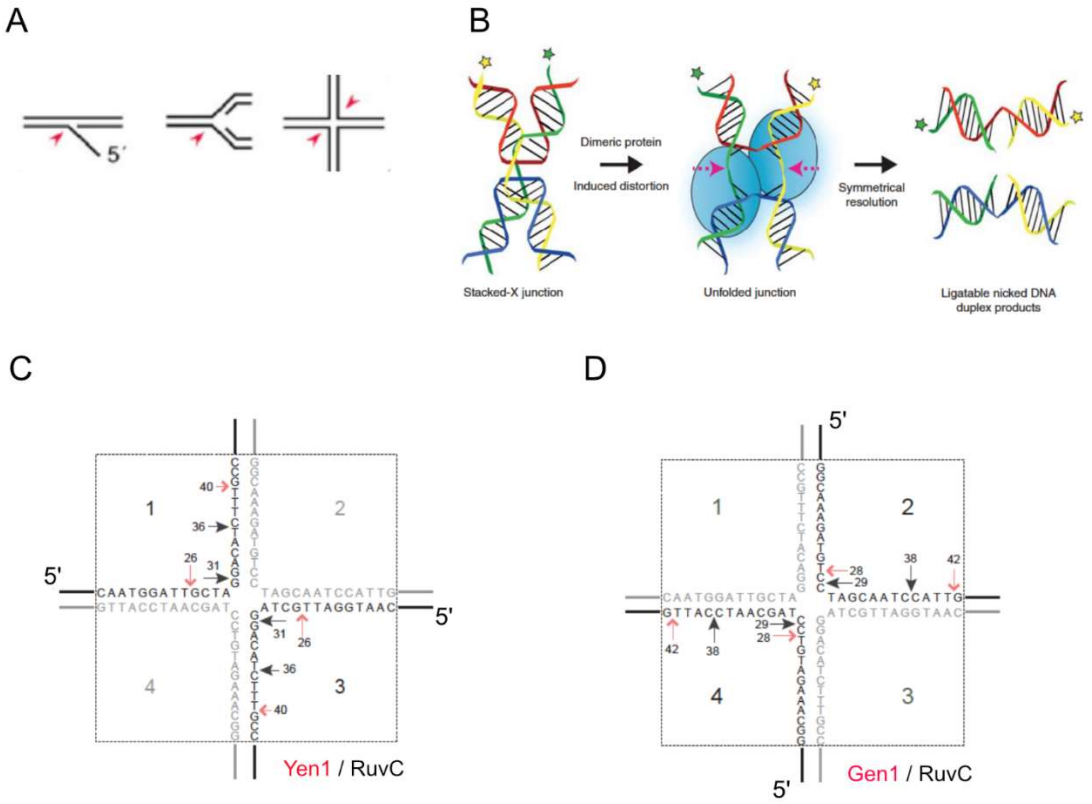

Figure 28 A: *specific substrates of Yen1/GEN1 with triangles showing the incision sites. Adapted from Schwartz Heyer in 2011 [171]* ***B:*** *Canonical mechanism of Holliday junction resolution by Wyatt and West in 2014 [468].* ***Left:*** *Antiparallel stacked-X Holliday junction with twofold symmetry.* ***Middle:*** *dimerization of a canonical resolvases induces structural changes to the junction on binding, causing the junction to unfold. Resolution occurs by the introduction of two coordinated and symmetrically related nicks in strands of like polarity at, or very near, the branch-point.* ***Right:*** *Symmetrical resolution gives a pair of nicked DNA duplexes, each of which can be directly repaired by nick ligation. Asterisks signify a given strand of DNA.* ***C and D:*** *Detail of symmetrical cuts introduced by Yen1 (C) and GEN1 (D) adapted from reference by Ip et al. in 2008 [176].*

3.2 Yen1 as a critical player for Genome stability

JMs are formed as intermediates of DNA repair processes that promote genomic integrity and survival. They are however, in themselves, a threat to the cell. Indeed, an unprocessed residual JM can lead to chromosome segregation defects if not outright aneuploidy [460]. The timely removal of JMs is paramount to any dividing cell. Yen1 is part of the toolkit that can process these chromosome links, making it a key player for DNA repair and chromosome segregation.

3.2.1 Yen1 processes DNA intermediates redundantly with Mus81-Mms4 in mitotic cells

A deletion of YEN1 is not especially deleterious for cells. Study of *yen1Δ* single mutants did not find them especially sensitive to IR, Hydroxyurea (HU) or MMS [177, 178]. However, simultaneous deletion of mus81 and yen1 leads to a synergistically increased DNA damage sensitivity, suggesting both proteins target a shared subset of DNA repair intermediates. In a way, they can complement for each other [177, 178]. The synergistic effects of simultaneous loss of Mus81-Mms4 and Yen1 were further illustrated by an array of phenotypes including a much slower doubling time of the double mutant

compared to the single mutants. This particular phenotype was extremely exacerbated in diploid strains containing the simultaneous deletion of both nucleases [177]. Observation of the cells growing in the absence of both nucleases is described by the presence of a large portion of morphologically abnormal cells, stalled at G2/M and presenting typical features of increased cell death and abnormal chromosome segregation [177, 178]. Indeed, FACS analysis of asynchronous populations showed a higher amount of G2 cells for the *mus81Δ yen1Δ* mutant compared to the wild type or any of the single mutants [177]. The slow growth and aberrant cell morphology was observed in the absence of any external damage, suggesting that the two nucleases are not only needed in dire conditions.

3.2.1.1 Loss of Yen1 is associated with increased chromosome mis-segregation and genome instability

A more specific evaluation of the chromosome segregation in the nuclease-deficient cells was key to identifying a marked increase in chromosome mis-segregation. Segregation defects were present in the absence of external DNA damage sources and exacerbated after treatment with genotoxic drugs like MMS. They involved both sister-chromatid or chromosome homologues [177, 178]. Most of the burden of mis-segregation was dependent on Rad51, and thus associated with the processing of recombination intermediates. However, a significant mis-segregation phenotype was retained in the absence of Rad51 suggesting a mixed origin of the DNA intermediates being targeted by the redundant activity of the nucleases. Some intermediates would originate from under-replicated or hard-to-replicate regions, that can still present branched structures at the mitosis onset, preventing correct chromosome separation in the daughter cells [177].

The archetypical function of resolvases is the resolution of HJs. It was thus to be expected that the simultaneous loss of both nucleases would phenotypically result in a decrease of CO during the repair of DSBs. Infering from the models of HR, in the absence of nucleolytic processing, one would expect that the JMs would be channeled into dissolution pathways. Thus, the expectation is to witness an increase of NCO parallel to the reduction in CO. It came as a surprise to notice that, in the first studies using cells lacking both Mus81-Mms4 and Yen1, displayed a very minor phenotype in recombination assays using single DSBs both in haploid cells with an ectopic donor, and diploid cells [177, 469]. Further analysis demonstrated that indeed, in the absence of Yen1 and Mus81-Mms4, CO are reduced, but instead of producing a concurrent increase in NCO outcomes, JMs are channeled to repair by BIR instead [177]. Resolution in the context of limited homology – as the situation presented in the widely used ectopic recombination assays – proved more difficult to dissect. The XPF/ERCC1 nuclease Rad1-Rad10 was demonstrated to be able to process HR intermediates that originate during ectopic recombination by cleaving D-loop intermediates that are not still fully ligated as dHJs, and might present heterology barriers [470]. Taken together, the results on CO formation clearly suggested the presence of specific DNA intermediates during the HR-mediated repair of DSBs that are refractory to the dissolution by Sgs1/BLM complexes. These seem to accumulate during mitosis in cells devoid of nucleolytic resolution [163, 185].

3.2.1.2 In vivo substrates of Yen1 : orphan HJ and underreplicated fork intermediates

The nucleolytic resolution of Holliday Junctions has often been studied with the bias of the bacterial models and the well-established role of the RuvABC protein complex. The discovery and characterization of the STR-mediated dissolution pathway “de-throned” the nucleases from their central role in the models to a mere safeguard role during mitotic recombination. Nonetheless, the

aforementioned studies using the double *mus81Δ yen1Δ* nuclease-deficient yeast mutants strongly suggested a specialized role for the nucleolytic-cleavage. Moreover, two-dimensional neutral-neutral agarose gel electrophoresis analysis showed clear evidence of JM accumulation in *mus81Δ yen1Δ* cells after exposure to MMS. Further highlighting the pending question of identifying what type of intermediates were specifically left unresolved in this genetic background despite the presence of functional STR complexes [163, 177, 185].

Two research endeavors shed light on the nature of the intermediates that accumulate in these nuclease-deficient conditions [163, 471]. Combining neutral and denaturing two-dimensional DNA electrophoresis analyses, these undertakings clearly demonstrated that a subset of JM, containing either single HJs or nicked HJs, accumulate when cells lack resolvases [163, 471]. These substrates, collectively named orphan HJ [185], lacking the two HJ of a dHJ canonical HR intermediate, cannot be dissolved by the convergent branch-migration and Topoisomerase-mediated release catalyzed by the STR complex (figure 29).

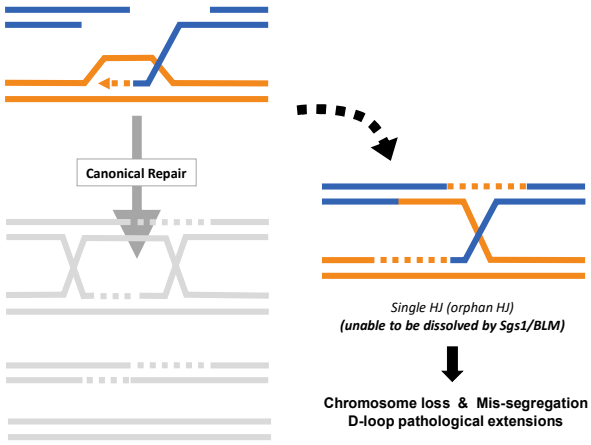

Figure 29. *Schematic representation of abortive repair resulting in residual orphan HJs.*

The origin of such intermediates can be linked to incomplete processing of HR intermediates after second-end capture (figure 29), likely because of modifications at the end of the original DSB or by the presence of other inhibitory modifications on DNA during the annealing of the second end or the maturation into a fully ligated dHJ [163, 185]. Some of these intermediates, containing nicks and discontinuities [163, 471] can also be associated to replication-derived structures. The role of Yen1 in processing replication-associated structures has been additionally illustrated after exploring the synthetic lethality between Yen1 and Dna2 [472]. Dna2, which was mentioned prior in this text, is quite important in budding yeast for it has many functions: it promotes DSB end resection in HR alongside Exo1 and is also known to cut occasional RPA covered ssDNA flaps during replication. When Dna2 is absent, its functions in alleviating fork stalling associated structures induce a persistence of replication-borne JMs until mitosis, ultimately leading to segregation problems. Yen1 thus becomes a critical player to resolve these persistent fork-derived intermediates [472]. These results further abound in presenting Yen1 as a “chromosome segregation” player, monitoring chromosomes before mitosis exit. Yen1 enables the timely removal of different types of DNA-intermediates that hamper chromosome separation when mitosis progresses through anaphase and telophase.

3.2.2 Yen1 regulation: a dual control in space and time

3.2.2.1 Yen1 as a substrate of cell-cycle regulators Cdk1 and Cdc14

Amongst other PTMs, waves of phosphorylation and de-phosphorylation are common in controlling DNA repair enzymes. HR nucleases are no exception. The first evidence of this regulation was the finding that Mus81-Mms4 activity was kept low in G1/S and specifically hyperactivated Mms4 in G2/M. These phosphorylation events are coordinated by cell cycle dependent kinases Cdc5 and Cdc28/Cdk1. The phosphorylated form of Mus81-Mms4 is more active for HJ cleavage than the dephosphorylated form. Shortly after, Yen1 was found to be controlled in a similar cell-cycle dependent manner, which will be discussed thoroughly in this section. Importantly, the hierarchical activation of the nucleases as a back-up and last resort option is coordinated with an early activation of helicase functions, as has been recently demonstrated for Sgs1 (Figure 30) [185, 188, 190, 191, 473, 474].

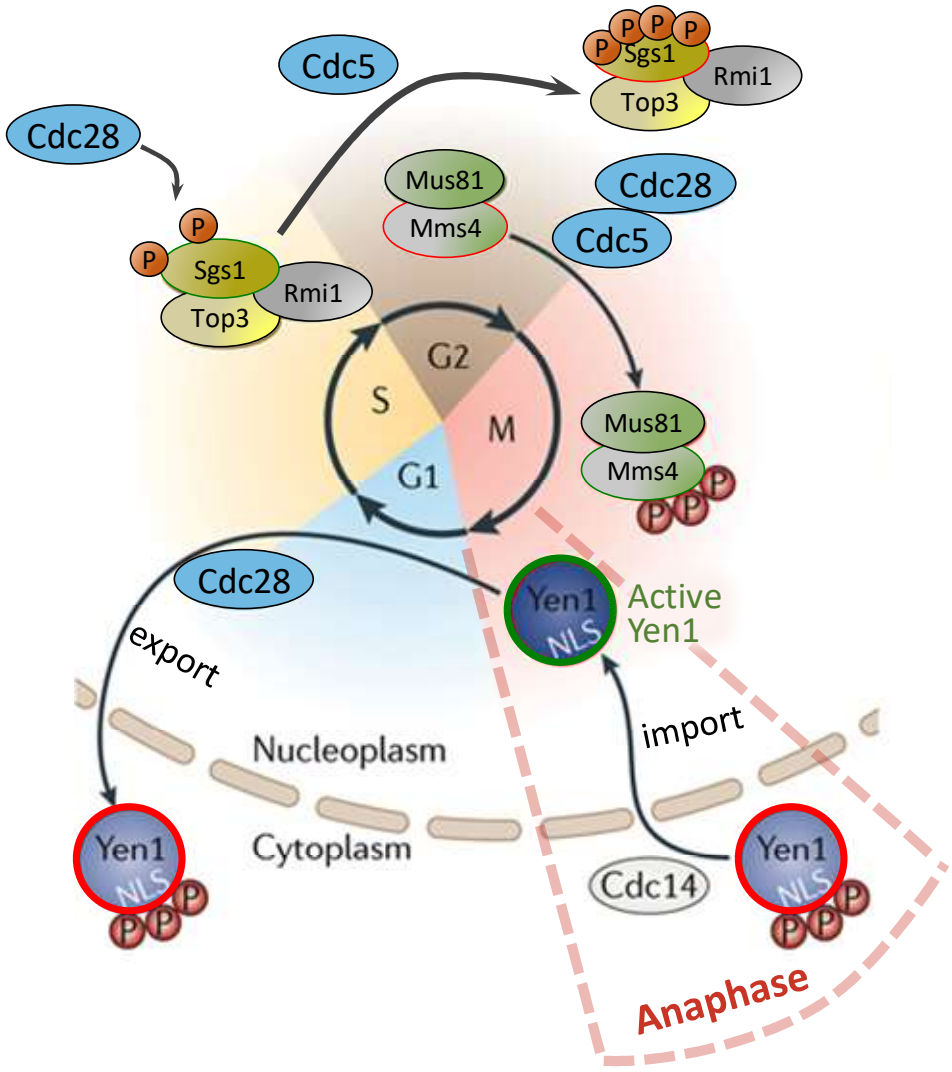

Figure 30. *Activation of the main HR players and pathways along the cell cycle in Saccharomyces cerevisiae. Figure slightly modified from source: Dehé et al. in 2017 [475]. Sgs1-Rmi1-Top3, Mus81-Mms4 and Yen1 are activated through cycles of phosphorylation (P) and dephosphorylation. Active enzymes are outlined in green and inactivated ones in red.*

3.2.2.2 *Yen1 is phosphorylated by CDK1 (Cdc28-Clb5 or Cdc28-Clb2)*

Yen1 contains nine consensus Cdk sites distributed all along its sequence. These match the consensus for Cdk with a Ser-Pro motif. For eight out of them, the sequence matches the extended consensus Cdk site S-P-X-K/R. Though they are found from the C to the N terminus, Yen1's Cdk sites are mainly clustered in three groups (figure 31), a feature that is common for bona fide regulatory Cdk motifs.

A first confirmation of the Cdk-substrate nature of Yen1 was given by proteome-wide approaches [476] where Yen1's phosphosites were recovered. Yen1 proved to be a good substrate for the S-phase Cdk1 complex Cdc28-Clb5 *in vitro* [477]. In extensive mass-spectrometry analyses using immuno-precipitated Yen1 from cell-extracts, six out of the nine consensus Cdk sites were verified as phospho-residues [459, 460].

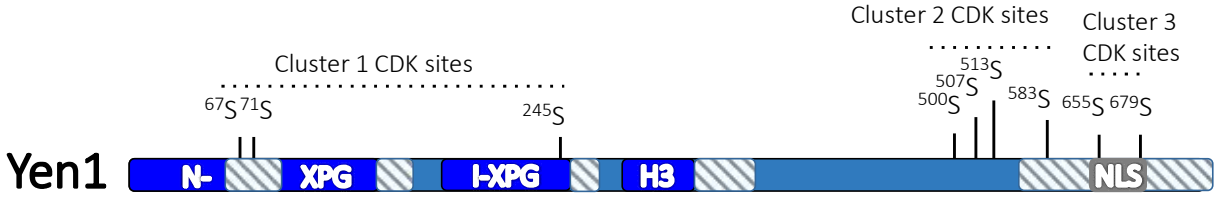

Figure 31. *Schematic representation of Yen1 protein and its CDK/Cdc14 sites by Talhaoui et al. in 2016 [185]. The conserved functional domains of Yen1 are depicted in solid dark blue, while other conserved domains are shown in solid turquoise. The three clusters of Cdk1 phosphorylation sites are indicated. Cluster 2 sites in the central part of the protein play a role in the inactivation of Yen1 during S-phase and G2 by decreasing its affinity to the substrate when they are phosphorylated. Cluster 3 sites are present embedded into the nuclear localization signal (NLS).*

The phosphorylation of Yen1's Cdk sites was also browsed by western blotting protein extracts of cells harboring epitope-tagged Yen1 versions. The retardation shift of the protein was slightly apparent in normal SDS-PAGE gels but was made evident using the specific phos-tag reagent that binds to phosphorylated proteins, increasing the retardation of the protein mobility during SDS-PAGE migration [459, 460]. Analysis of protein extracts from synchronously growing cells as well as cells arrested in different cell phases demonstrated a dynamic Yen1 phosphorylation occurring preferentially in S and early G2/M phase, while G1 arrested cells showed a form of Yen1 migrating further, lacking phosphorylation [459, 460].

The presence of phosphorylated forms was rapidly correlated to a fluctuation on the biochemical activity of Yen1 recovered from different cell-cycle phases [459, 460]. Immunoprecipitated Yen1 from cells in S-phase showed low levels of nuclease activity. On the contrary, those from cells in late mitosis were efficient in processing synthetic HJ substrates [190, 459, 460]. Replacement of the nine Serines of the Cdk sites to Alanine resulted in an active Yen1 protein (referred to as: Yen1-9A [459] or Yen1^{ON} [460]), further stressing the inhibitory nature of Cdk-phosphorylation. Besides Cdc28-Clb5, Clb2-Cdc28 was also shown to phosphorylate Yen1, opening the possibility of a differential affinity of the two Cdk1 complexes for specific sites or cluster of sites as the cell-cycle advances from S to G2 phase [459].

3.2.2.3 *Yen1 is specifically dephosphorylated by the Cdc14 phosphatase*

In *S. cerevisiae*, Clb-CDK are key orchestrators of mitosis through phosphorylation of a large panel of proteins during the M phase. The reversal of these PTMs is essential for mitotic exit [478, 479]. Around anaphase, a transition in phosphorylation levels takes place, mediated by the Cdc Fourteen Early Anaphase Release (FEAR) network [387, 480]. The Cdc14 phosphatase is released and directly dephosphorylates a number of Clb-CDK targets [481] including the anaphase promoting

complex/cyclosome, which directly destructs anaphase inhibitors such as Clb-CDK. Early release of Cdc14 by the many proteins composing the FEAR network is essential for timely segregation of all chromosomes [478, 482].

Out of the nine Cdk sites in Yen1, four of them were predicted to be optimal targets *in silico* for the Cdc14 phosphatase (S500, S507, S655, and S679). The activity of Cdc14 on synthetic peptides containing these sites was further confirmed [459]. Moreover, the clear transition from a phosphorylated form of Yen1 to the dephosphorylated one was shown to occur at the actual cell-cycle stage of the onset of Anaphase, when Cdc14 is known to trigger a dephosphorylation wave as part of the FEAR-response [480]. Cdc14's involvement in Yen1 regulation was further stressed genetically and biochemically [459, 460]. Yen1 was shown to immunoprecipitate with a catalytically impaired form of Cdc14 [460] that is stabilized when bound to its substrates. Yen1 phosphorylation detected from immunoprecipitated or *in vitro* phosphorylated samples, was shown to be reversed by the addition of purified Cdc14 phosphatase [459, 460]. Genetically, cells growing in a *cdc14*-1 background were shown to accumulate the phosphorylated form of Yen1 when shifted to the non-permissive temperature, as expected for substrates of the early anaphase onset FEAR response [480]. Interestingly, cells arrested using the mitotic exit kinase cdc15-1 allele at non permissive temperature showed an initial Yen1 dephosphorylation since Cdc14 was allowed to kick in, followed by re-phosphorylation at later points of the arrest in agreement with the already reported re-activation of Cdk1 in cdc15-1 arrested cells.

3.2.2.4 Yen1 phosphorylation modulates its activity and localization

Yen1 is most definitely regulated by phosphorylation and dephosphoryation throughout the cell-cycle. Remaining inhibited in its activity during the S-phase and most of G2/M in its fully phosphorylated form, Yen1's activity window starts at the onset of anaphase through the activation of the FEAR-response and its key phosphatase Cdc14 that triggers dephosphorylation. These fluctuations on the phosphorylation status of Yen1 have implications for its substrate recognition and its biochemical activity and for its actual subcellular localization to the nucleus [459, 460, 483] that in concert, ensure an efficient suppression of Yen1 activity before anaphase.

Cdk1 phosphorylation controls Yen1's nuclear localization

Prior to the full identification of the regulatory roles of Cdk1/Cdc14, Yen1 was identified as a protein capable of shuttling between the nucleus and the cytoplasm under the regulation of Cdk1 signals [483]. Using *in silico* algorithms, a core of basic residues constituting a putative NLS overlapping to Cdk-consensus sites were identified at the C-terminal region of Yen1 and other proteins [483]. Yen1's NLS was further validated and shown to respond to its Cdk-status. While the protein remained mostly nuclear after inhibition of Cdk1 by using *cdc28*-as alleles, it shuttled to the cytoplasm in cells morphologically in S-phase [483]. Moreover, Yen1 nucleocytoplasmic shuttling was dependent on Importin-alpha and the export activities of the karyopherin Msn5. In a *msn5* mutant, Yen1 was constitutively localized to the nucleus, indicating that the nuclear export of the phosphorylated form of Yen1 is mediated by this protein [483]. Using different epitope tag GFP-Yen1 versions or analyzing mutants by immune-staining, the mutants containing phospho-deletion replacements (Ser-to-Ala) at one or both Cdk1-sites overlapping the motifs of the bipartite NLS of Yen1 (S655 and S679) showed constitutive nuclear localization [459, 460, 483]. It is worth noting though, that the phospho-mimicking replacements did not achieve a full cytoplasmic localization, suggesting that while the replacement inhibits Msn5 export in part, it possibly left the import activities by Importin-alpha un-altered. In full agreement with the required Cdk1-phosphorylation for nuclear export, inactivation of Cdc14 by using the *cdc14*-1 thermosensitive allele also induced Yen1 nuclear accumulation [191].

Cdk1 phosphorylation lowers Yen1 substrate recognition

Initial studies with immuno-precipitated Yen1 clearly pointed to a decreased activity of the phosphorylated form of Yen1 over synthetic HJ substrates. The relative contribution of the different clustered Cdk sites was further investigated, using phospho-mimick substitution in each of the three clusters of Cdk1 sites of Yen1. Mimicked constitutive phosphorylation of the central cluster of Cdk1 sites was enough to prevent full activity of Yen1 [459]. That observation was complemented with mobility shift assays that demonstrated a decreased substrate affinity of the phosphorylated Yen1 and its phosphomimick mutants [460] pointing to a inhibitory role of the Cdk1 phosphorylation at the central cluster of Cdk1 sites for the recognition of HJ substrates. The central Cdk1-sites are mostly clustered in Yen1's chromodomain. As stressed before, this domain is shown to contact DNA by loose interactions that can be modified in strength by the additional net charge introduced by phosphorylation in these residues [450]. Moreover, these Cdk1-sites cluster in a loop motif that is absent in the equivalent human GEN1 chromodomain, thus clearly pointing to a specific and adapted regulator role.

Yen1 double-layered inhibition prevents off-target cleavage of replication intermediates

The very restricted window where Yen1 activity is allowed in the nucleus seems to be intimately related to its broad substrate recognition. Indeed, the $Yen1^{ON}$ allele showing unrestricted nuclear localization and substrate recognition, displayed increased sensitivity to DNA replication damage suggesting an off-target activity of Yen1 when granted access to the chromatin during S-phase at the moment when replication forks expose splayed DNA intermediates with accessible 5'-flaps that can be cleaved by Yen1 as demonstrated *in vitro* [176, 460].

3.2.3 The resolution activity of Yen1 in meiosis

Meiosis is a time for the cell where interplay and exchange between chromosomes is promoted both to foster genetic variability and to ensure the chromosome reduction from diploid cells to haploid gametes. Nucleases are thus needed to ensure proper segregation during meiosis. COs are not only intended but also promoted in this case. However, the generation of COs in the first meiotic division will rely into a specialized player, MutLγ, which is central to the resolution of the meiotic obligated COs [484-486]. In yeast, as in other organisms, the set of mitotic nucleases used in HR are mostly used as back-up and repair enzymes for remaining junctions, especially during the second meiotic division. They play a minor part for spore viability. Indeed, Yen1 is also under the control by Cdk1 and Cdc14 in meiosis, which will prevent its use during Prophase I. If Yen1's regulation is overridden by mutation of the Cdk sites, Yen1 will basically turn into an over active nuclease and can rescue the spore viability in yeast lacking the other nucleases. Unrestrained Yen1 activity is overall detrimental to spores though, as it happens prematurely and alters the spatial distribution of COs across chromosomes [485].

3.2.4 Human GEN1 control by nuclear exclusion and phosphorylation

When it was first identified, GEN1 was recovered as full-length. However, an N-terminal fragment of roughly 60KDa lacking the less-conserved C-terminal part of the predicted protein [176, 462], Gen1 1-527, exhibited an increased activity compared to the full length GEN1 [176]. It was then hypothesized that this truncation was probably the active form of the enzyme, released after proteolysis of the full-length protein. The Gen1 1-527 truncation retained the ability to suppress phenotypes in fission yeast strains deficient in either Mus81 or Rqh1 (BLM) [487].

Characterization of the regulatory mechanisms of the yeast Yen1 orthologue switched the focus to understanding GEN1 regulation. Making use of the information gathered from Yen1, it is no surprise to find that GEN1 is exported out of the nucleus as well, for most of the cell cycle [190]. A first difference emerges in the fact that for humans, the nuclear envelope breaks down during the M phase. GEN1 therefore does not need to be imported back into the nucleus. In fact, its shuttling is strictly one way. GEN1 is only exported out of the nucleus.

One could assume that, similarly to Yen1, GEN1's activity would be regulated by its putative CDK sites. GEN1 does contain at least eight CDK consensus target sites, and subsequent studies showed that the protein was phosphorylated in these sites in a CDK-dependent manner [461]. Accordingly, a phosphorylated form of GEN1 can be observed on phostag gels of M-phase synchronized cells extracts. However, comparing *in vitro* activity of S and M phase GEN1 yielded little to no difference in activity. Treatment by λ phosphatase did not alter this result. GEN1's activity seems relatively constant during the whole cell cycle. Mutation of all putative CDK sites of GEN1 showed no difference in chromatin interaction, *in vitro* activity nor CO output [461]. GEN1's control differs from that of Yen1 in having no dependency on phosphorylation waves. Rather, localization seems to be the main form of control over GEN1.

While it was known that GEN1 is cytoplasmic [190, 488] further experiments showed that this was due to nuclear export receptors recognizing GEN1's Nuclear Exclusion Signal (NES) a Leucine-rich deca peptide between L660 and L669 at its C-terminal region. Inhibition of a major nuclear exporter led to higher amounts of nuclear GEN1. The timeframe was narrowed down to a unique event of export in telophase. The NES was identified by dicing up GEN1 in small polypeptides fused to GFP. Only one of these displayed true export from the nucleus and its sequence seemingly contained a NES consensus sequence. Mutating GEN1's NES with the inclusion of a synthetic NLS forced GEN1 to enter the nucleus before the nuclear envelope breakdown. The protein remained nuclear all over the cell cycle, presenting phenotypes reminiscent of the constitutively active Yen1 version with deleted Cdk1-sites [461]. Constitutively nuclear GEN1 reduces the deleterious effects of MUS81 and BLM depletion but seems to lack deleterious side-effects for replication fork intermediates as those found with the unrestricted copy of Yen1 in yeast [460, 461].

3.2.5 Additional yet uncharacterized modifications for Yen1/GEN1

The basic principles of Yen1 double-layered spatio-temporal regulation by Cdk1 and Cdc14 have been characterized in depth. Although, broad mass-spectrometry data suggest additional Yen1 regulatory motifs remain unexplored. For instance, multiple phosphorylation sites in the C-terminus of Yen1 were identified, but did not match Cdk-consensus. Together with still uncharacterized partners, these sites may help explain some uncharted facets of Yen1's control [190, 460, 473].

Ubiquitination and sumoylation are two common and rather prevalent modifications for proteins involved in the DNA repair processes (as thoroughly described in section 2 of this introduction). Using a biochemical screen, Yen1 was also detected among sumoylated proteins in a candidate approach that looked at 179 DNA repair associated proteins [396]. Similarly, a GEN1 sumoylated motif was also identified in wide-screening of samples [489] suggesting a putative role for sumoylation in the control of Yen1/GEN1 proper function in the cell.

4 Results: Characterization of the SUMO covalent modification of Yen1 and its non-covalent binding to SUMO

The experimental approaches and results of this thesis work will be presented in this chapter with the insertion of two publications. The first publication came about from a collaborative effort with the laboratory of Steve Brill at Rutgers University (NJ, USA). It was published in Nature communications in 2018 during my first year of PhD. I contributed with several experiments as exposed in the article's contributions listing. The second article, presented as a submission manuscript, is the result of my main experimental contributions, with the help of I.Talhaoui in biochemistry and molecular biology experiments.

The full description of the experimental approaches and results will be found in the articles and their associated figures and supplementary data. To facilitate the intertwining of both articles and delineate the main hypotheses that guided both works I have added a brief summary of the main findings of the articles as an introductory note that will help guide the reader on the analysis of the data provided by each of the articles.

4.1 Yen1 resolvase is a SUMOylation substrate of Siz1/Siz2 and is controlled by the sumo-targeted ligase Slx5-Slx8

As stressed in the previous sections, the repair of dsDNA breaks by HR entails the formation of joint-molecule intermediates that can prevent proper chromosome segregation during mitosis. The removal of such intermediates is achieved by overlapping pathways where two nucleases, Mus81-Mms4 and Yen1 take central stage ensuring their nucleolytic cleavage during the G2/M cell phases where they gradually become activated and recruited to the nucleus, in a fashion thoroughly described in sections 1 and 3 of this dissertation. In this work, we have demonstrated that in addition to the already characterized modes of control over the Yen1 nuclease elicited by Cdk1 and Cdc14, Yen1 is further regulated by sumoylation and ubiquitination.

In vivo, Yen1 becomes sumoylated under conditions of DNA damage in a manner dependent on the redundant roles of ligases Siz1 and Siz2 (Figure 32 page 82). Indeed, Yen1 was recovered from denaturing pull-downs using Histidine tagged Smt3, as observed in the western blot analyses shown in Figure 32, and presented a pattern of modification compatible with either poly- or multi-sumoylation. The recovery of sumoylated Yen1 was lost in cells deficient for both Siz1 and Siz2 E3 SUMO ligases, suggesting an overlapping role for these ligases in modifying Yen1. The use of reverse experiments, with immuno-precipitation of Yen1, drew the same conclusions (Figure 32 e) and the sumoylation reaction were reconstituted *in vitro* as well (Figure 32 F).

Yen1 is also a substrate of the STUbL Slx5-Slx8, with which it interacts as shown in figure 33 page 84. Slx5-Slx8 is able to modify Yen1 in reconstituted reactions (Figure 34 page 85), and in its absence, Yen1 presents very subtle phenotypes including a persistence of Yen1 foci when observed by microscopy

(figure 35 page 87). The persistence of Yen1's foci in slx8Δ cells correlates with the parallel observation of a more persistent fraction of Yen1 accumulating in cycloheximide chase experiments, where Yen1 depletion is observed at the transition between G1 and S, at the same time interval when the protein is relocated to the cytoplasm.

Slx5-Slx8-dependent ubiquitination of Yen1 was shown to occur mainly at K714, the very last C-terminal lysine available for modification in Yen1. Mutation of this lysine reproduces phenotypes similar to the deletion of slx8Δ in terms of foci persistence and Yen1 accumulation in cycloheximide chases. The mutant was reported to generate increased crossover formation during DSB repair as well. This apparent gain-of-function of Yen1 was also observed with the ability of the K714R mutants to suppress chromosome segregation defects in a mus81Δ background (Figure 37 page 91).

Overall, this work highlights the regulation of Yen1 by sumo-targeted ubiquitination to remove a subset of the protein from its nuclear sites of activity at the transition into the next S-phase. Deregulation of these pools induced increased Yen1 availability to cleave intermediates, resulting in suppression of Mus81-Mms4 defects for chromosome segregation and crossover resolution. Importantly, the work paved the way for a more comprehensive understanding of how sumoylation of Yen1 could probably assist in the nuclease function, a question that was mainly addressed in the second article of this thesis work.

4.1.1 Abstract

The repair of double-stranded DNA breaks (DSBs) by homologous recombination involves the formation of branched intermediates that can lead to crossovers following nucleolytic resolution. The nucleases Mus81-Mms4 and Yen1 are tightly controlled during the cell cycle to limit the extent of crossover formation and preserve genome integrity. Here we show that Yen1 is further regulated by sumoylation and ubiquitination. *In vivo*, Yen1 becomes sumoylated under conditions of DNA damage by the redundant activities of Siz1 and Siz2 SUMO ligases. Yen1 is also a substrate of the Slx5-Slx8 ubiquitin ligase. Loss of Slx5-Slx8 stabilizes the sumoylated fraction, attenuates Yen1 degradation at the G1/S transition, and results in persistent localization of Yen1 in nuclear foci. Slx5-Slx8-dependent ubiquitination of Yen1 occurs mainly at K714 and mutation of this lysine increases crossover formation during DSB repair and suppresses chromosome segregation defects in a *mus81Δ* background.

"Slx5-Slx8 ubiquitin ligase targets active pools of the Yen1 nuclease to limit crossover formation"

An article by Ibtissam Talhaoui, Manuel Bernal, Janet R. Mullen, Hugo Dorison, Benoit Palancade, Steven J. Brill & Gerard Mazón.

This article originally published in Nat. comm. 9, Article number: 5016 (2018) on the 27th of November 2018 is presented here in manuscript format. In Annex 1, at the end of this document, the original publication of this article can be found for reference.

4.1.2 Introduction

Homologous recombination (HR) is a key repair pathway for the maintenance of genome integrity. HR is involved in the repair of double-strand breaks (DSB) generated by endogenous or exogenous sources of DNA damage and it plays an important role in the repair of damage associated with DNA replication [28]. A variety of DNA joint molecules (JM) form during the different steps of the HR pathway and these are sequentially matured into novel intermediates or dismantled by different specialized proteins to prevent their persistence into mitosis. Failure to resolve joint-molecule intermediates results in chromosome segregation defects [28, 163, 490, 491]. In yeast, the helicase Sgs1, together with Rmi1 and Top3, mediates the dissolution of double Holliday Junctions (dHJ) to ensure a non-crossover outcome [490, 491], and similar NCO outcomes are generated by helicases such as Mph1 or Srs2 [163, 164, 492]. In contrast to the dissolution pathways, nucleolytic processing of recombination intermediates can result in reciprocal crossovers (CO), with the risk of loss of heterozygosity (LOH), or chromosome translocations, both of which are genome-destabilizing events [28, 493].

Nucleolytic processing of HR intermediates is strictly controlled and appears to be used as a last option to cope with orphan HJs and other intermediates that cannot be dissolved by the Sgs1-mediated pathway [163, 471]. Whereas Mus81-Mms4 is hyper activated in late G2/M phase by Cdc5- and Cdc28/CDK1-dependent phosphorylation of Mms4 [188, 190, 494], Cdc28 phosphorylates Yen1 to prevent its activity and nuclear localization until anaphase [459, 460]. In anaphase, the Cdc14 phosphatase gradually dephosphorylates Yen1, and this late activation of Yen1 ensures that persistent recombination intermediates are resolved before mitotic exit [459, 460]. Although CO levels are minimized by the late activation of nucleases, their windows of activity are likely to overlap with those of DNA helicases that dissociate intermediates to form NCOs. It is thus possible that another layer of control is required subsequent to chromatin binding to prevent the use of nucleases when other factors are available. The tight regulation of these nucleases also highlights the risk of their uncontrolled activity in other cell-cycle phases, and suggests that their turnover might be enforced to remove active pools from the nucleus when they are no longer needed.

Regulation by coupling of the small ubiquitin-like modifier (SUMO) [296] has emerged as a potent means to fine tune the amount and activity of specific pools of proteins, especially during DNA-mediated transactions [495]. In *Saccharomyces cerevisiae*, the enzymes involved in SUMO conjugation are the E1 Aos1-Uba2 activating enzyme dimer, the E2 conjugating enzyme Ubc9, and a limited set of E3 ligases (including Siz1, Siz2 and Mms21) that provide substrate selectivity [304, 313, 496]. Although protein sumoylation regulates multiple cellular activities, it has been shown to be especially important during the DNA damage response [400, 497, 498]. Important players of the HR pathway are found among the sumoylated DNA repair targets, including Rad52, PCNA, RPA and Sgs1 [130, 288, 396, 400, 403, 408]. Some lines of evidence link sumoylation to specific pathways that locally target repair factors to degradation by the action of SUMO-targeted ubiquitin ligases (STUbLs) [330, 332] to prevent the toxic effects of their persistent activation. Two STUbLs are thought to operate in *S.cerevisiae*, the Slx5-Slx8 complex [329, 499] and the Uls1 protein [328, 500]. Mutations in *SLX5* and *SLX8* result in slow growth or lethality in combination with components of the SUMO metabolic pathway [501] highlighting its role in regulating sumoylated proteins. The *SLX5* and *SLX8* genes were originally identified by their requirement for the viability of *sgs1*Δ cells [502], and this lethality is partially explained by the accumulation of sumoylated substrates in the *sgs1*Δ background.

In this work we explored the hypothesis that there is crosstalk between Slx5-Slx8 and Yen1. We demonstrate that Yen1 is a sumoylation target and that Slx5-Slx8 participates in its regulation by ubiquitination of its lysine 714. Slx5-Slx8 prevents persistent accumulation of a fraction of Yen1

associated with sites of activity in late G2/M and helps maintain the balance between pro- and anti-crossover pathways during HR.

4.1.3 Results

Yen1 is sumoylated after DNA damage via Siz1/Siz2

STUbLs have been shown to recognize sumoylated substrates [332], including certain nuclear proteins that participate in the DNA damage response [330]. Because Yen1 was identified in a screen for sumoylated proteins following DNA damage [396], we analyzed how Yen1 is sumoylated *in vivo* and whether it interacts with Slx5-Slx8.

To detect the Yen1 post-translational modification of Yen1 by SUMO and ubiquitin (Ub), we tagged the endogenous gene with a single C–terminal HA epitope. The *YEN1-HA* allele was judged to be functional as it showed no effect on the methyl-methane sulfonate (MMS) sensitivity of a *mus81*Δ strain (Figure 39a - Supplementary Figure 1a). Further, Yen1-HA immunoblots revealed phosphorylated and unphosphorylated forms with the expected cell-cycle regulation [460] (Figure 32a).

Using a 6xHIS-Smt3-expressing plasmid [503], we performed a Histidine pull-down experiment to detect Yen1 among the sumoylated proteins. Sumoylated Yen1 was detected as a faint signal in the eluates of unperturbed cells (Figure 32b, extended exposure) and the recovery of sumoylated Yen1 was not greatly increased by inhibiting proteasomal degradation by treatment with MG132 (Figure 32b). However, after MMS treatment, we recovered a clear ladder of sumoylated Yen1 forms whose abundance increased in the presence of MG132 (Figure 32b).

The Yen1-SUMO conjugates migrated as a doublet of two discrete bands near 120 KDa (Figure 32b), these forms shifted when using a different tagged version of Smt3 further confirming their sumoylated nature (Figure 39 - Supplementary Figure 1). We also observed higher MW bands may be due to multiple sumoylations or chains of SUMO or Ub. The major bands detected from pull-downs resemble those detected following *in vitro* sumoylation assays where immunoprecipitated Yen1-HA was incubated with purified Smt3-3KR, E1 (Aos1-Uba2) and E2 (Ubc9) enzymes (Figure 32c, figure 39 - Supplementary Figure 1c). Sumoylation under mild MMS treatment was also detected with Yen1-HA immunoprecipitation after lysis in denaturing conditions of cells with induced expression of Yen1-HA but endogenous levels of Smt3 (Figure 32d). We did not detect significant Yen1 sumoylation in pull-downs from *siz1Δ siz2Δ* double-mutant strains confirming the requirement of these E3 ligases *in vivo*. Interestingly, one of the two major Yen1 sumoylation bands disappeared in the *siz1*Δ single mutant pull-down, suggesting some sites have a strong preference for Siz1 as E3 ligase (Figure 32e).

To complement our *in vivo* observations, we tested whether highly purified Yen1 produced in *E. coli* was a substrate for sumoylation *in vitro*. A sumoylation reaction consisting of Smt3, Aos1-Uba2 (E1), Ubc9 (E2), and Siz2 (E3), triggered the formation of Yen1 products that migrated as a ladder of bands with a more intense band at 120 KDa similar to the major forms observed *in vivo* (Figure 32f). Increased concentrations of Siz2 stimulated Yen1 sumoylation, which occurred at a lower yield in the absence of E3 (Figure 32f, g). Similar to what has already been reported for other proteins [401, 504], we observed increased Yen1 sumoylation *in vitro* in the presence of its DNA substrate (Figure 32g). We conclude that the Yen1 forms detected following *in vitro* sumoylation are largely reminiscent of those detected *in vivo* (Figure 32b). The fact that Yen1 sumoylation is stimulated by MMS treatment suggest that it is a response to substrates that accumulate during DNA damage.

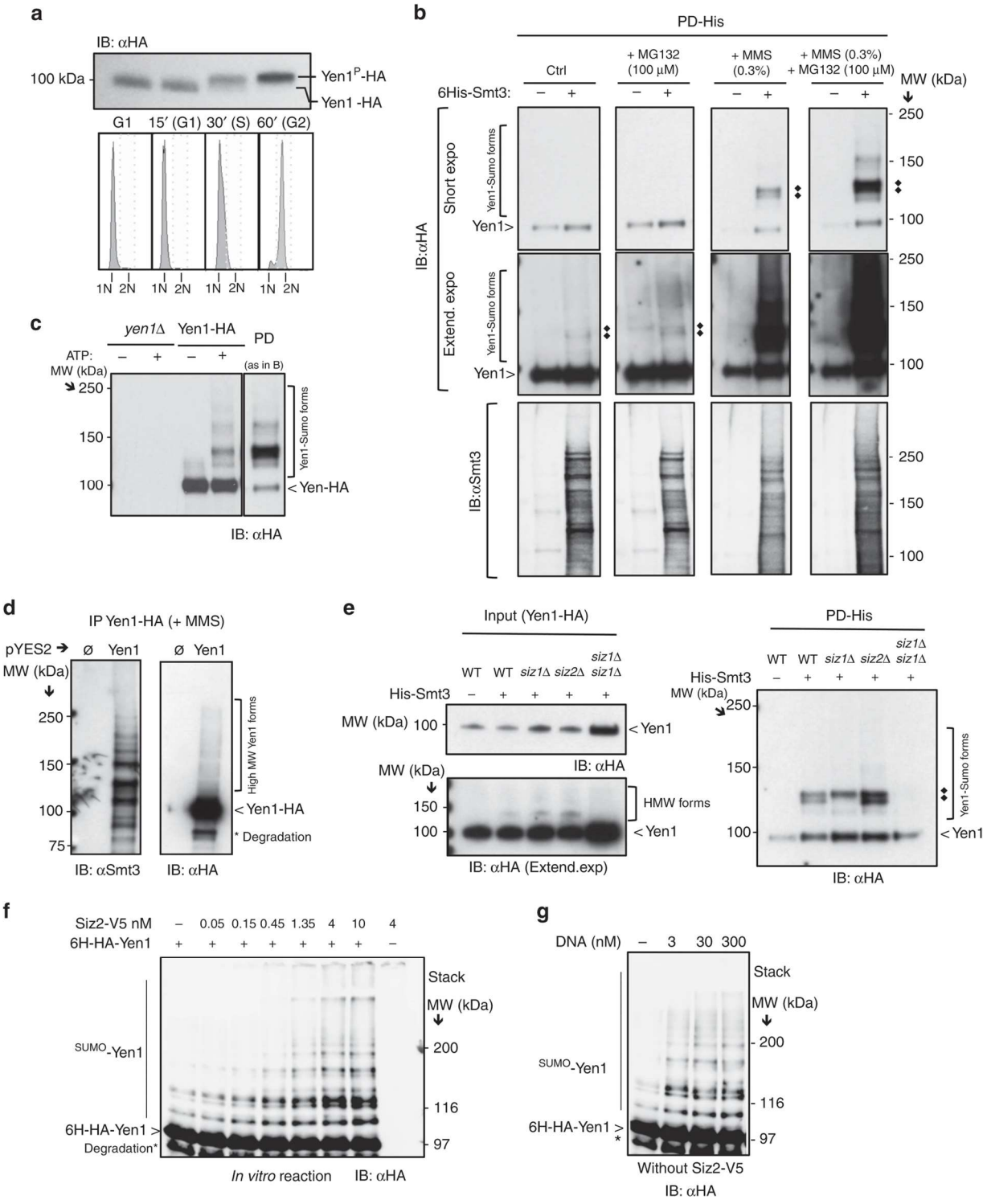

Figure 32. *Yen1 is sumoylated in vivo and in vitro.* ***a*** *A wild-type chromosomally tagged YEN1-HA strain was synchronized with alpha factor and released into fresh medium to observe phosphorylation of Yen1 by immunoblot (upper) and progression through the cell cycle by FACS (lower).* ***b*** *Wild-type strains expressing Yen1-HA, with (+) or without (−) pCUP-6xHIS-Smt3, were subjected to MMS challenge followed by denaturing Ni-NTA pull-down and immunoblot analysis. Yen1 was detected by anti-HA (top and middle) and a prominent sumoylated doublet is indicated (black rhombus). Membranes were also probed with anti-Smt3 (bottom). Note that un-sumoylated Yen1 binds to Ni due to a histine-rich region.* ***c*** *Yen1-HA was overexpressed in wild-type asynchronous cells, immunoprecipitated with anti-HA, eluted by HA peptide competition and mixed with Aos1-Uba2, Ubc9, and Smt3-3KR in the presence or absence of ATP. After immunoblotting with anti-HA sumoylated forms were detected in the presence of ATP that migrate at similar sizes to those detected in the PD experiments shown in* ***b*** *(far right duplicate for comparison). A control reaction was made with HA-immunoprecipitation of a yen1Δ strain eluted with the same amount of HA peptide.* ***d*** *yen1Δ cells expressing Yen1-HA from a Gal-inducible plasmid or harboring a control plasmid were subjected to MMS treatment (0.03%), and extracts were immunoprecipitated using anti-HA prior to immunoblotting with anti-Smt3 (left)*

or anti-HA (right). ***e*** *Indicated strains (WT, siz1Δ, siz2Δ, or siz1Δ siz2Δ) with (+) or without (−) pCUP-6xHIS-Smt3 were subjected to pull-down analysis of Smt3 as in* ***b*** *in conditions of MMS damage and eluates were analysed by immunoblot. The input used for PD was immunoblotted to allow normalization and comparison between strains (bottom).* ***f*** *Purified recombinant 6His-HA-Yen1 protein was incubated under sumoylation conditions with the indicated concentrations of Siz2 followed by immunoblotting with anti-HA. Asterisk indicates breakdown products of Yen1 carried from purification.* ***g*** *Sumoylation reactions were performed as in* ***f*** *but with increasing amounts of synthetic Holliday junction DNA, 458 nM Yen1 and in the absence of Siz2. All experiments were independently replicated at least three times and images are representative of the reproducible results obtained.*

To test whether substrate recognition is important for sumoylation of Yen1 *in vivo*, we introduced amino acid substitutions in the four central CDK1 sites to generate phospho-deleted or phospho-mimic alleles. Previous work has shown that phospho-mimic mutations in the central CDK1 sites of Yen1 impair substrate cleavage and reduce its association with DNA [459, 460]. However, analysis of Smt3 pull-downs following MMS treatment showed no significant difference in sumoylation compared to the wild-type Yen1 (Figure 39d - Supplementary Figure 1d). To directly test the possibility that the Yen1 sumoylation is stimulated by its substrates, we analysed Smt3 pull-downs from a *dna2Δ pif1* strain. It has been shown that Yen1 is important in eliminating replication-dependent recombination intermediates in this strain [505]. Compared to wild-type, more abundant sumoylation was observed in *dna2Δ pif1* cells (Figure 39d - Supplementary Figure 1d). This supports the idea that sumoylation of Yen1 occurs in a context where Yen1 activity is required.

Yen1 is a substrate of the Slx5-Slx8 ubiquitin ligase

Having established that Yen1 is sumoylated, we next investigated whether the Slx5-Slx8 STUbL recognized and further processed the modified protein. To determine whether Yen1 and Slx5 physically interact or are in proximity in the nucleus, we used the bimolecular fluorescence complementation (BiFC) approach [506]. Cells expressing the complementary VN-Yen1 and VC-Slx5 epitope-tagged proteins displayed fluorescent signal in discrete foci (Figure 33a), similar to what has been described for another Slx5-Slx8-substrate interaction [391]. The BiFC interaction was nuclear as determined by introducing a Nup49-mCherry marker (Figure 33a). The Yen1-Slx5 interaction was confirmed using a pull-down approach. Cells containing the *YEN1-HA* allele were transformed with a pYES2 plasmid expressing GST-Slx5 under a galactose inducible promoter or an empty vector as control. After induction of GST-Slx5, cell extracts were applied to a glutathione column and Yen1 was specifically detected in the eluates (Figure 33b). Finally, the association of Slx5 with Yen1 was further confirmed by a two-hybrid assay where DBD-Yen1 bound AD-Slx5 (Figure 33c). These data indicate that Yen1 and Slx5 are in close proximity and may physically interact in yeast.

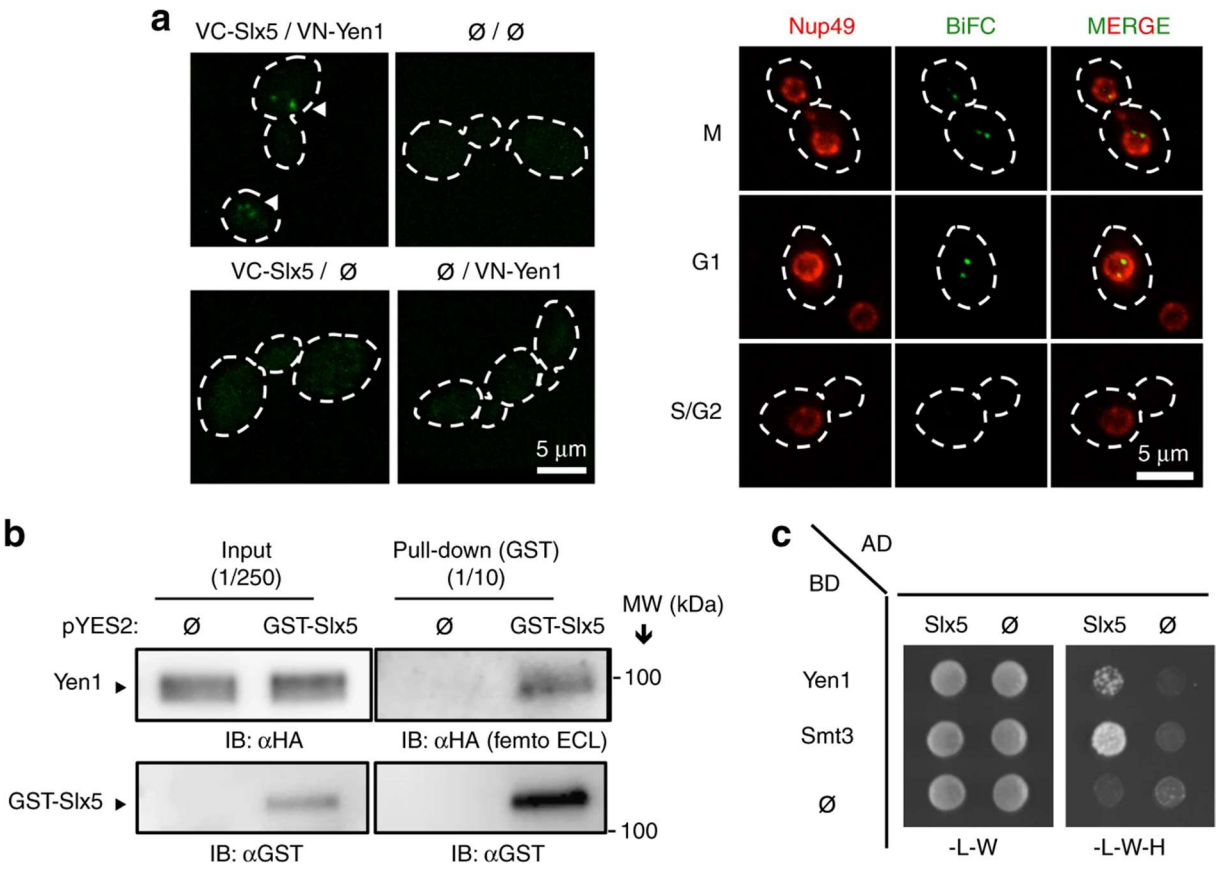

Figure 33. *Yen1 interacts with Slx5–Slx8 in the nucleus.* ***a*** *Diploid strains carrying one allele of galactose inducible VC-Slx5 and VN-Yen1 with wild-type copies of YEN1 and SLX5 in the homologous chromosomes were observed by live microscopy. BiFC (white arrows) signal denotes an interaction between the two BiFC (Venus) epitopes. Control diploids lacking one or both of the epitope-tagged proteins (ϕ) were used to substract background signal. A plasmid carrying Nup49-mCherry was transformed on the diploid strain harboring VC-Slx5/VN-Yen1 to visualize the nuclear perimeter. BiFC interactions were only detected in the nuclear compartment.* ***b*** *Cells carrying either an empty vector or a pYES2 plasmid expressing GST-Slx5 under galactose control were grown in selective media and induced with galactose for 3 h. Lysates were then applied to a glutathione-sepharose column. After washing, the bound proteins were eluted and immunoblotted with α-HA (upper) or α-GST (lower).* ***c*** *Two-hybrid assays were performed with strains carrying the indicated activating domain (AD) or DNA binding domain (BD) fusions. Strains were grown in selective media lacking leucine (L) and tryptophan (W) prior to spotting on media lacking histidine (H) to detect a positive interaction. Experiments were independently replicated three times and images are representative of the reproducible results obtained.*

The fact that Yen1 is sumoylated and interacts with the STUbL component Slx5 prompted us to investigate whether it was ubiquitinated by Slx5-Slx8. We first asked whether Slx5-Slx8 could directly recognize Yen1 as substrate by reconstituting the ubiquitination reaction *in vitro*. Combined with the E1 (Uba1) and E2 (Ubc5), Slx5-Slx8 ubiquitinated Yen1 producing a major band around 110 KDa and a less intense ladder of higher MW bands (Figure 34a). No ubiquitination was detected when using a RING mutant of Slx5 in the reaction (*slx5-6*), and no cross-reacting products were detected by the anti-HA antibody when Yen1 was not added to the reaction, further confirming the specificity of detection of the Yen1 ubiquitinated forms (Figure 34a). Ubiquitination was stimulated by the presence of DNA (Figure 34b), suggesting that DNA enhances ubiquitination but is not essential for the reaction. Although Slx5-Slx8 is able to ubiquitinate Yen1 *in vitro* in the absence of prior sumoylation we cannot exclude the possibility that sumoylation is required for ubiquitination *in vivo*.

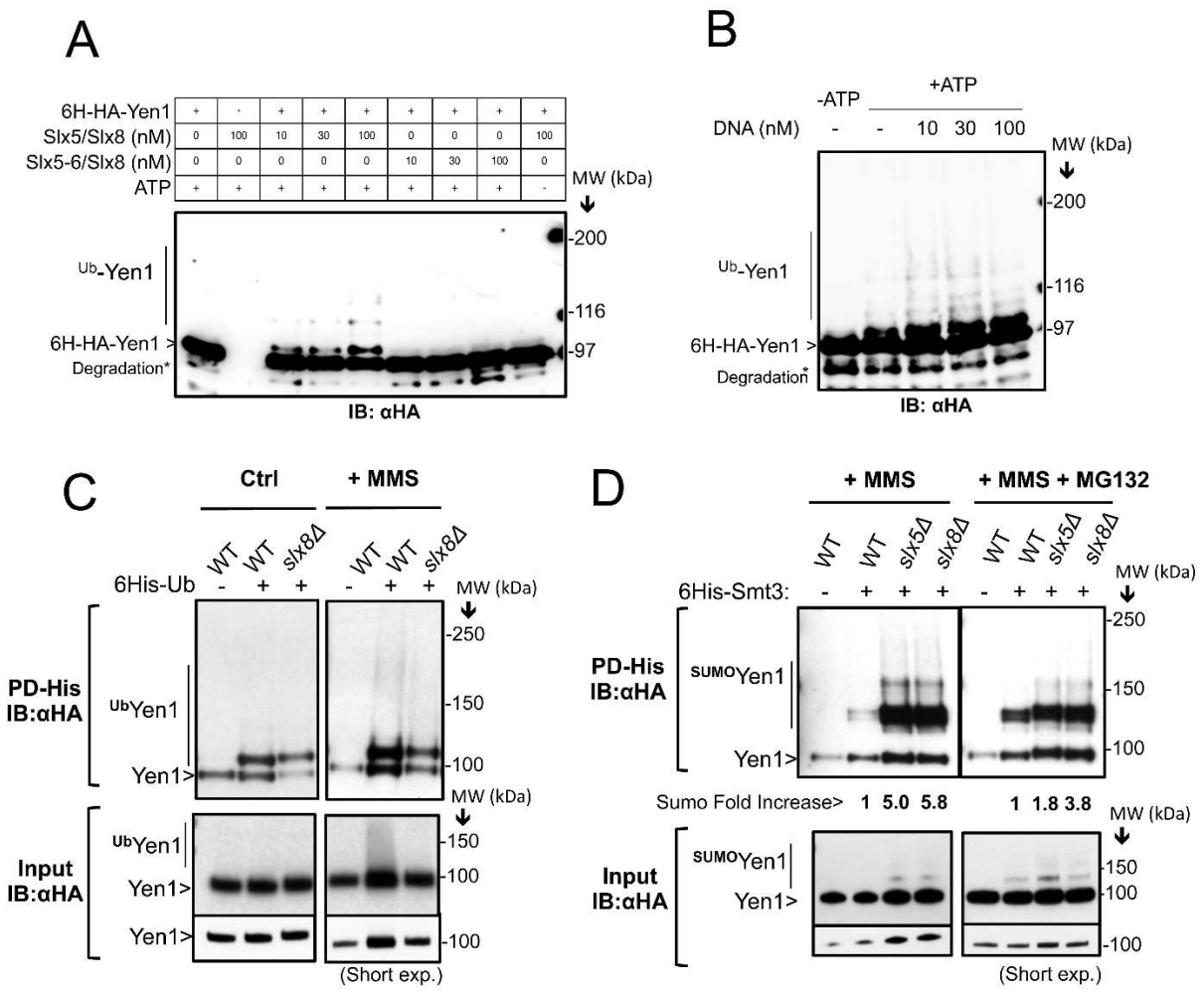

Figure 34. *Yen1 is a direct substrate of the Slx5–Slx8 ubiquitin ligase.* ***a*** *H6-HA-Yen1 (916 nM) was ubiquitinated in vitro in the presence of the indicated concentrations of either Slx5/Slx8 or the RING mutant Slx5–6/Slx8 and 0.2 µM DNA. Control lanes with H6-HA-Yen1 in the absence of E3 and Slx5/8 in the absence of Yen1 are shown. Breakdown products of Yen1 are marked with an asterisk.* ***b*** *The ubiquitination reaction was performed as above but with 50 nM Slx5–Slx8 and increasing amounts of DNA.* ***c*** *Strains expressing 6xHis-Ub were subjected to different growth conditions and lysed to pull-down ubiquitinated proteins under denaturing conditions, input Yen1-HA levels were controlled to allow comparisons.* ***d*** *Smt3 denaturing pull-downs were performed in wild type, slx5Δ, or slx8Δ cells (all in a pdr5Δ background) after growth in the presence of MMS. The fold increase in the sumoylated fraction indicated at the bottom of the gel is an average of three trials. Inputs were controlled in each trial to allow comparison of the eluted sumoylated proteins.*

To determine whether the *in vivo* ubiquitinated Yen1 was dependent on Slx5/Slx8, we employed a pull-down approach. Using a 6xHIS-Ub expression plasmid we detected mono-ubiquitinated Yen1 in the pull-down eluates and a faint ladder of poly-ubiquitination (Figure 34c). Yen1 ubiquitination was not largely increased under MMS treatment of cells and was not importantly altered after *slx8*Δ deletion (Figure 34c). From the results obtained it is difficult to estimate the contribution of Slx5/8 to the Yen1 ubiquitination *in vivo* that also possibly involves another general turnover pathway that mask the modification of a small fraction of Yen1 by Slx5/8 as already observed for other substrates [507].

We then explored the possibility that Slx5-Slx8-mediated degradation of Yen1 would target the sumoylated version of this protein. To this aim, we asked whether inactivation of Slx5-Slx8 affected the stability of sumoylated Yen1 detected after MMS treatment. Wild-type and cells harboring deletions of either *SLX8* or *SLX5* expressing 6xHIS-Smt3 were collected after exposure to MMS 0.3%.

After Smt3 pull-down, an increase in the sumoylated Yen1 fraction (≈5-fold) was detected in the *slx8*Δ and *slx5*Δ strains (Figure 34d). Treatment with the proteasome inhibitor MG132 reduced the differences in the recovery of the sumoylated fractions between the wild-type and the *slx5*/*slx8* mutants suggesting that this increase might be due to the combined effects of more DNA damage in the absence of Slx5/Slx8 [508] and decreased removal in these strains of sumoylated proteins [509], including Yen1.

slx8Δ cells present persistent Yen1 foci

We next addressed the possible impact of Slx5-Slx8 impairment on the dynamics and function of Yen1. The cell-cycle regulation or degree of Yen1 phosphorylation was not grossly altered by deletion of *SLX8* (Figure 35a). An *slx8*Δ single deletion showed no increase in MMS sensitivity when combined with *yen1*Δ, although *yen1*Δ displayed the known synergistic defect when combined to *mus81*Δ (Figure 35b). A subtle increase in sensitivity for the *slx8*Δ *yen1*Δ mutant was detected with the radiomimetic drug Zeocin, but this was not as pronounced as the synergistic effects of *slx8Δ mus81Δ*.

To identify potential defects in the nuclear transport and distribution of Yen1 in the absence of Slx5-Slx8 we GFP-tagged Yen1 at its N-terminus, where we previously obtained positive BiFC data (Figure 33). After mildly inducing GFP-Yen1 from a plasmid in a strain carrying Hta1-mCherry and a fully functional *YEN1-HA* endogenous allele cells were judged to be healthy and we observed the expected cellular distribution of wild-type Yen1 with its nuclear exclusion occurring at S-phase (Figure 40 - Supplementary Figure 2).

Compared to wild type, *slx8*Δ cells were three times more likely to display Yen1 foci (Figure 35c, fig 39 - Supplementary Figure 2). To characterize the phenotype, cells were classified as containing no focus, 1-2 foci per cell, more than 2 foci and rare events with abnormal features (Figure 35d, fig 39 - Supplementary Figure 2). The *slx8*Δ cells showed foci of all classes in G2/M, and there was a dramatic increase in cells with 1-2 foci in G1 phase.

Yen1 foci may reflect accumulation of non-degraded or chromatin-associated protein, resulting from faulty nuclease activity or impaired turnover. We compared foci formation in wild type and *slx8*Δ cells to those formed in cells carrying the nuclease dead Yen1^{E193A,E195A} (Yen1ND). As expected, Yen1ND also showed higher foci accumulation compared to wild type suggesting that GFP-Yen1 reflects, at least partially, dynamics of an active protein. However, Yen1ND did not accumulate foci in G1 as observed in *slx8*Δ cells (Figure 35d). We used video microscopy to determine the duration of the foci before they were dispersed. The *slx8*Δ Yen1 foci were about three times more stable (30.4 min) than those detected in wild-type cells (12.3 min) and 50% more stable than Yen1ND (20.9 min) (Figure 35e). This supports the idea that foci accumulation due to faulty nuclease activity is different from that detected in a strain devoid of Slx5/8. The average intensity of these foci, compared to the nuclear average intensity, was not increased between the different strains.

A closer analysis by video microscopy time-lapses allowed us to observe the disappearance of nuclear signal in cells morphologically in G1 by following the intensity of GFP in both the nuclear and cytoplasmic compartments (Figures 35f, fig 40 - Supplementary Figure 3). Although most of the signal present in the nucleus was transferred and diluted into the cytoplasm we observed a decline in overall signal during cytoplasmic re-localization (Figures 35f, fig 40 - Supplementary Figure 3). This suggests that a wave of degradation occurs in a small window of time after nuclear exclusion (at the G1 to S transition). Compared to cells with no focus at the G1-S transition, cells with a focus showed increased nuclear signal for a larger time suggesting its rate of re-localization and degradation is altered (Figure 41 - Supplementary Figure 3).

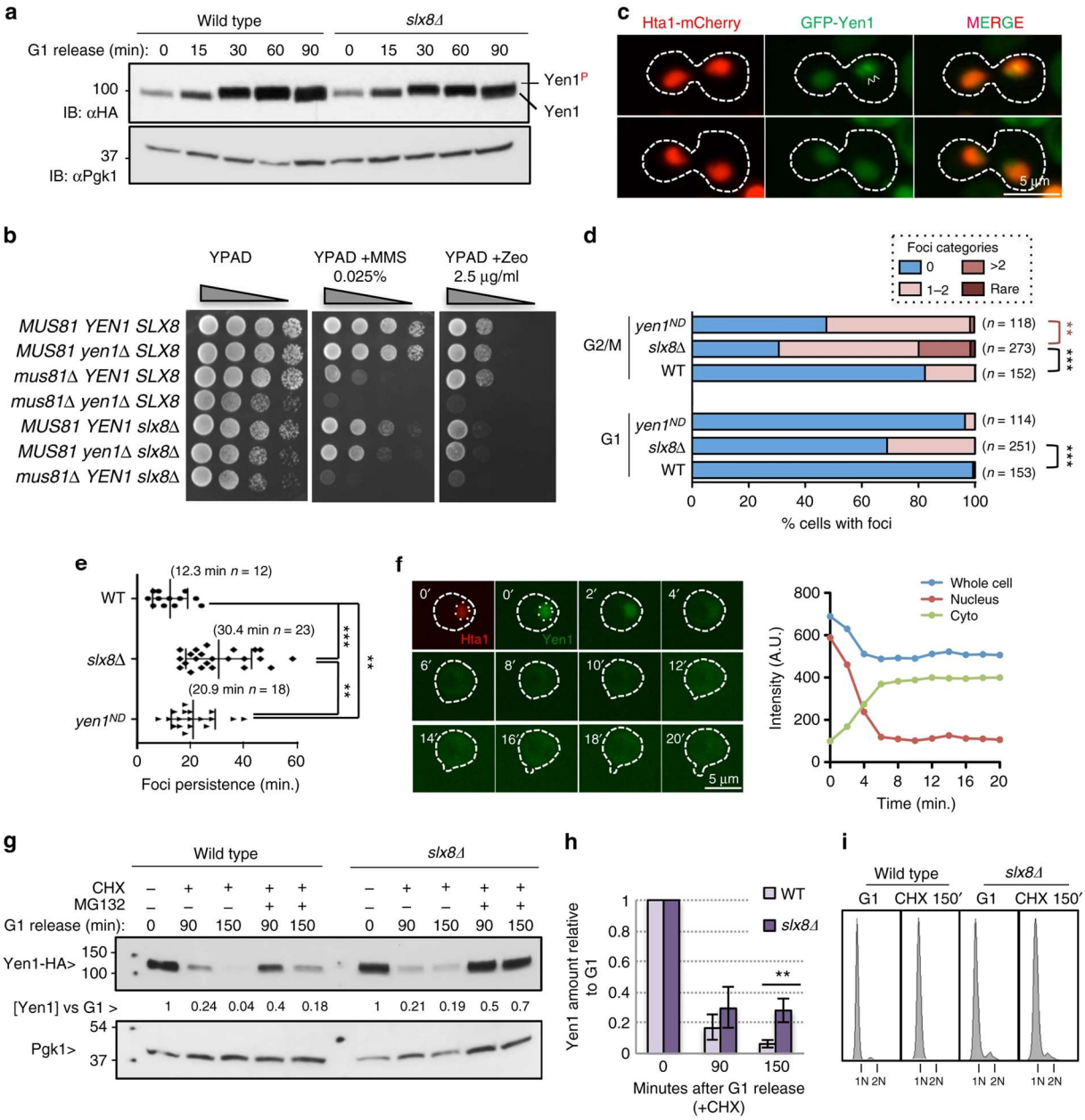

Figure 35. *Deletion of SLX8 alters the nuclear distribution and turnover of a fraction of Yen1.* ***a*** *Wild type and slx8Δ cells were synchronized in G1 and released to observe the phosphorylation of Yen1 as a function of cell-cycle progression.* ***b*** *Serial dilutions of the indicated strains were spotted onto YPAD media containing different genotoxins.* ***c*** *Cells with an endogenous HTA1-mCherry carrying plasmids expressing wild-type GFP-Yen1 were observed microscopically after a short induction of the fusion protein. Shown are cells presenting normal nuclear localization (lower) or presenting foci (white arrows, upper).* ***d*** *G1 and G2/M cells of the indicated genetic backgrounds were microscopically examined as in* ***c*** *and classified according to the number of foci they displayed. The graphs show the percentage of cells in each category. The total number of cells individually scored from three video recordings are indicated as (n). Categories were subjected to the Fischer's exact test, asterisks denote significant levels at P < 0.001(***) or P < 0.005(**).* ***e*** *The duration of foci in the indicated genetic backgrounds was measured by video-microscopy analysis. The mean ± s.d. of the duration time and n are indicated, error bars denote s.d. Asterisks refer to significance at the P < 0.05 (**) and P < 0.001 (***) levels in unpaired two-tailed Student's t-test.* ***f*** *Cells expressing GFP-Yen1 and Hta1-mCherry were observed by video-microscopy in 2′ time-lapse frames. GFP total intensity of the whole cell, the nucleus and the cytoplasm was determined for 5 z-planes and used to calculate the total GFP intensity in each compartment. The graph displays the time course of GFP intensity in a single cell* ***g*** *The indicated pdr5Δ strains, that are permeable to MG132, were synchronized in G1 and subjected to cycloheximide (CHX) treatment during their release from G1 arrest. Where indicated, cells were pre-treated with MG132 for 30 min before, and during release in the presence of CHX. PGK1 was used to normalize the amount of Yen1.* ***h*** *Quantitation of the fraction of Yen1, compared to G1, remaining at the indicated times after release into CHX. The mean ± s.d. of triplicate assays is shown; statistically significant difference in unpaired two-tailed Student's t-test is indicated (**P < 0.05).* ***i*** *FACS analysis of cells at the beginning and at the end of the CHX treatment.*

The Slx5-Slx8 Ub ligase is known to target substrates that are subject to stage-specific degradation as well as constitutive turnover [332]. Thus, a possible explanation for the accumulation of Yen1 in foci that persist until G1 in the *slx8*Δ mutant, is that Slx5-Slx8 targets only a fraction of Yen1. To test this hypothesis we further determined whether Yen1 is degraded at the G1-S transition as suggested by the microscopy time-lapse experiments by performing a cycloheximide chase experiment on cells synchronized in G1 (Figures 35g, h, i). Under these conditions, we detected the disappearance of Yen1 following release from G1 (Figure 35g). The degradation of Yen1 was at least partially dependent on the presence of a functional proteasome as MG132 largely prevented the degradation. In the absence of Slx8, 20-30% of Yen1 (relative to its G1 level) persisted 150 min after addition of cycloheximide, a time at which the protein was completely degraded in wild-type cells. These data show that while Slx5-Slx8 plays a role in Yen1 turnover, it is not the only pathway targeting Yen1 for degradation.

Yen1 localizes to the nucleolus in the absence of DNA damage

It has been previously reported that *slx8*Δ induces a larger amount of DNA damage by interfering with the control of multiple targets associated with DNA repair [508]. Slx5-Slx8 co-localizes to sites of stalled replication or to Rad52 foci [508], suggesting that its deletion will impair the normal function of replication and recombination and generate multiple sites of damage. Contrary to this view, we detected only 1-2 Yen1 foci in the majority of *slx8*Δ cells; this result suggests that Yen1 clusters specifically in a nuclear region that may experience more spontaneous damage.

We speculated that Yen1 accumulates in the absence of exogenous DNA damage in the nucleolus, where rDNA loci often generate DNA structures that are substrates for Yen1 activity [471]. Indeed, most of the Yen1 foci detected in *slx8*Δ cells, where foci appeared in a large fraction of cells, co-localized with the Sik1 and Nop1 nucleolar markers (Figures 36a, fig 41 - Supplementary Figure 4). In wild-type cells, the foci also accumulated in the nucleolus and also localized adjacent to the rDNA array on chromosome XII (Figure 36b), indicating that Yen1 normally resides there. Slx5-Slx8 localizes to nucleolar sites [508], and accordingly, we often detected interaction by BiFC of Slx5 and Yen1 adjacent to nucleolar stained regions (Figure 42b - Supplementary Figure 4b). Interestingly, we also detected Yen1 foci associated with lagging chromatin between the nuclear masses in a number of *slx8*Δ cells (Figure 42c - Supplementary Figure 4c). This suggests that Yen1 is associated with chromatin regions that are having difficulty segregating, where the nuclease may act to resolve joint-molecule intermediates.

After Zeocin or MMS treatment, wild-type and *slx8*Δ cells accumulated foci in larger numbers than untreated cells. But in *slx8*Δ cells, many of these foci failed to diffuse significantly after 3.5 h (Figures 36c, d). Furthermore, when *slx8*Δ cells carrying a Sik1 nucleolar marker were treated with Zeocin or MMS we found that some foci induced after the drug challenge de-localized from the nucleolus (Figures 36e, f, fig41 - Supplementary Figure 4), demonstrating that foci are dynamic and can be formed at other undetermined nuclear sites.

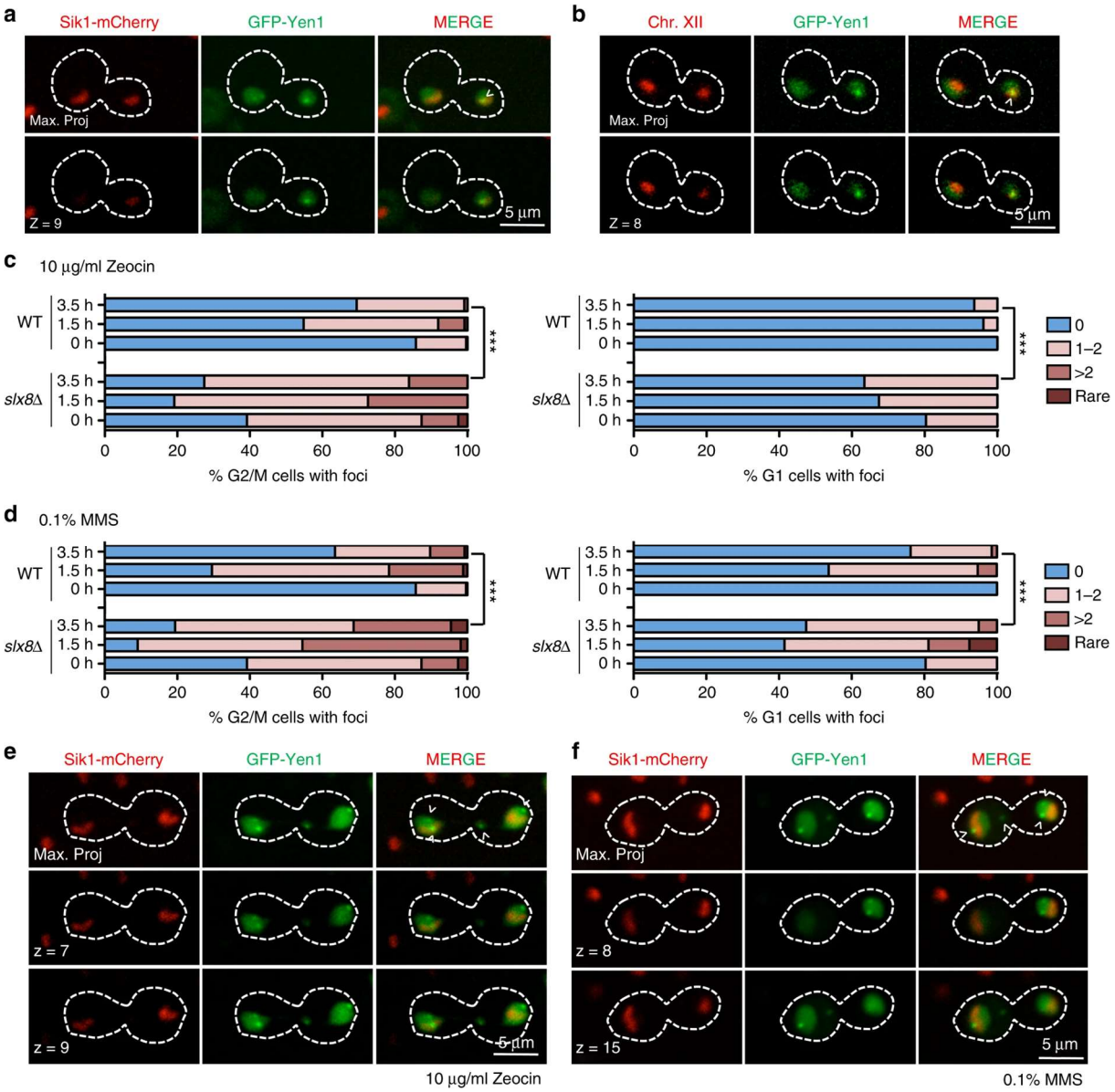

Figure 36. *Yen1 foci are dynamic and localize preferentially to nucleolar sites in the absence of DNA damage.* ***a*** *slx8**Δ** cells carrying a SIK1-mCherry endogenous marker and an inducible GFP-Yen1 expressing plasmid were observed after short induction of the fusion protein. The white arrow denotes co-localizing signal of GFP-Yen1 with Sik1-mCherry.* ***b*** *Wild-type cells carrying a TetO-TetR array tag on chromosome XII and an inducible GFP-Yen1 expressing plasmid were observed after short induction of the fusion protein.* ***c*** *Cells were subjected to acute challenge with Zeocin (0.01 mg/ml) and observed during their recovery as in Fig. 4. Cells displaying the designated categories of GFP-Yen1 foci were scored at the indicated time points. The total number of cells analysed (n) from two independent recordings were as follows: WT 0 h (n_{G1} = 81, $n_{G2/M}$ = 267), WT 1.5 h (n_{G1} = 78, $n_{G2/M}$ = 124), WT 3.5 h (n_{G1} = 110, $n_{G2/M}$ = 118), slx8Δ 0 h (n_{G1} = 107, $n_{G2/M}$ = 79), slx8Δ 1.5 h (n_{G1} = 40, $n_{G2/M}$ = 73), slx8Δ 3.5 h (n_{G1} = 52, $n_{G2/M}$ = 62).* ***d*** *Cells were subjected to an acute challenge with 0.1% MMS and for foci were observed as in* ***c****. The total number of cells analysed (n) from two independent recordings were as follows: WT 0 h (n_{G1} = 81, $n_{G2/M}$ = 267), WT 1.5 h (n_{G1} = 95, $n_{G2/M}$ = 98), WT 3.5 h (n_{G1} = 139, $n_{G2/M}$ = 137), slx8Δ 0 h (n_{G1} = 107, $n_{G2/M}$ = 79), slx8Δ 1.5 h (n_{G1} = 53, $n_{G2/M}$ = 55), slx8Δ 3.5 h (n_{G1} = 40, $n_{G2/M}$ = 67).* ***e*** *slx8Δ cells carrying SIK1-mCherry were observed after Zeocin challenge to determine GFP-Yen1 co-localization. White arrows indicate GFP-Yen1 foci.* ***f*** *slx8Δ cells were observed as in* ***e****, but were subjected to MMS treatment. White arrows indicate GFP-Yen1 foci. Images are representative of the reproducible results obtained after three independent trials. Statistical significance at P < 0.0001 in Fischer's exact test at 3.5 h recovery points is indicated by asterisks in* ***c*** *and* ***d.***

Lysine^{714} is the main Slx5/8 target in Yen1

In order to identify the lysine residues in Yen1 that are targeted by Slx5-Slx8, we performed a mass-spectrometry of immunoprecipitated Yen1-3xFLAG following exposure of cells to MMS. We recovered a peptide harboring a modification consistent with the presence of ubiquitin on the lysine 714. Although the score was below the level of significance, we generated an endogenous replacement with the allele *yen1-K714R*-HA.

Our previous experiments with ubiquitin pull-downs showed that Yen1 was not exclusively ubiquitinated by Slx5-Slx8 *in vivo* (Figure 34c). Therefore, we tested the lysine mutant by *in vitro* ubiquitination using Slx5-Slx8 and recombinant Yen1-K714R. As shown in Figure 37a, the K714R mutation prevented Yen1 ubiquitination *in vitro*, supporting the identification of K714 as a target for the ubiquitin ligase. As expected, pull-down analyses with the strains harboring Yen1^{K714R} did not eliminate the recovery of ubiquitinated Yen1. This is likely due to the presence of overlapping pathways of ubiquitin-mediated turnover of Yen1. However we can nonetheless see a decrease in overall ubiquitination in the K714R mutant (Figure 37b).

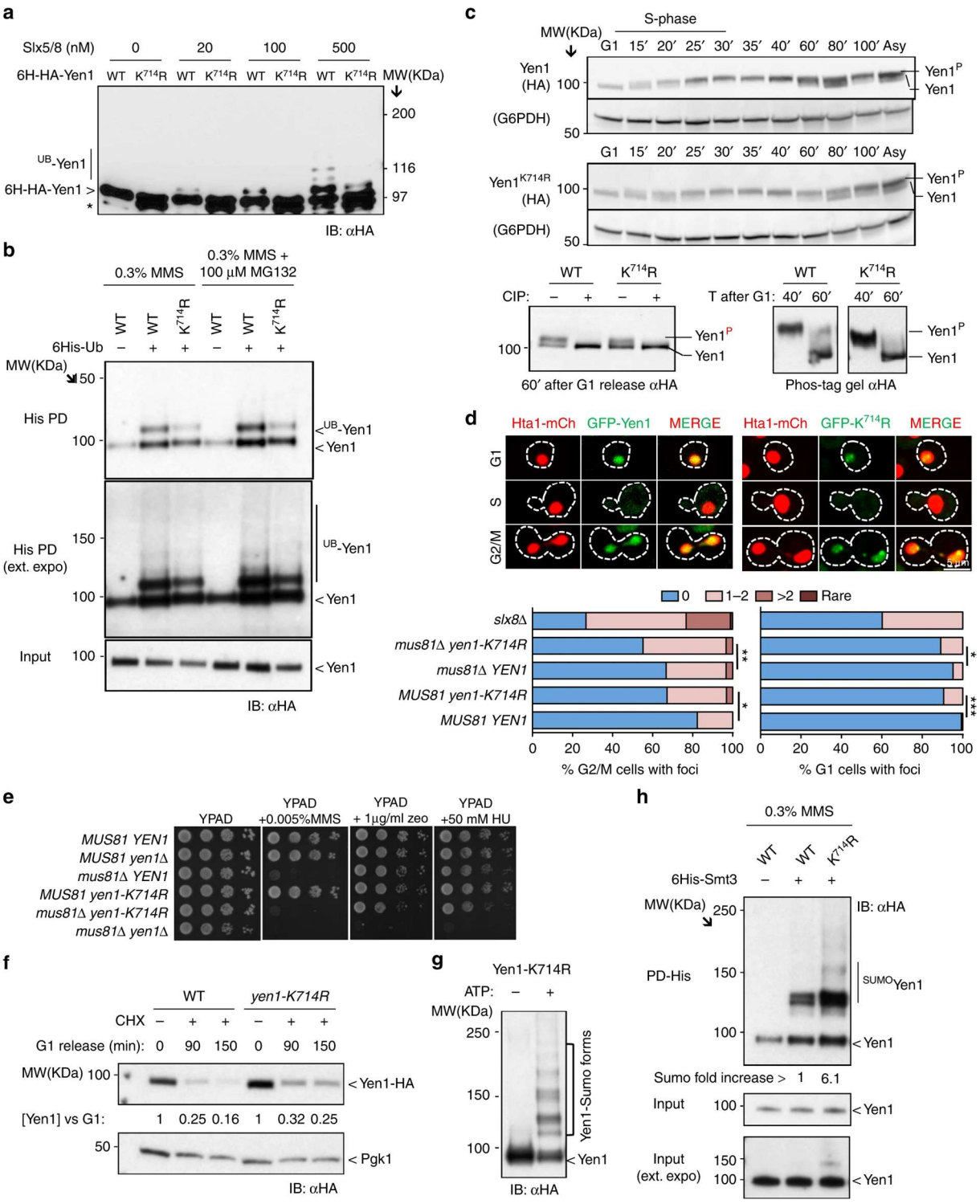

Figure 37. *K714 is ubiquitinated by Slx5–Slx8.* ***a*** *Recombinant 6xHIS-HA-Yen1 and the mutant 6xHIS-HA-Yen1-K714R (916 nM) were subjected to in vitro ubiquitination as in Fig. 3a.* ***b*** *6xHis-Ubiquitin pull-downs were performed on cells expressing 6His-Ub and carrying endogenous Yen1-HA or its variant Yen1-K714R-HA following treatment with the indicated genotoxics.* ***c*** *Strains carrying endogenous Yen1-HA or its K714R variant were synchronized with alpha factor in G1 and proteins extracted at indicated time points after G1 release and immunoblotted with anti-HA. At time points where Yen1 is modified by CDK1, extracts were subjected to phosphatase treatment (CIP+) and also subjected to phos-tag gel separation.* ***d*** *Strains carrying HTA1-mCherry and the indicated GFP-Yen1 expression plasmids were examined microscopically as in Fig. 4c to assess the presence of the proteins. Foci were quantified as a function of cell-cycle phase, which was determined by cell morphology. The total number of analysed cells (n) and independent video recordings (VR) were as follows: WT (nG1 = 105, nG2/M = 153, VR = 3), yen1-K714R (nG1 = 106, nG2/M = 64, VR = 3), mus81Δ (nG1 = 294, nG2/M = 337, VR = 3), mus81Δ yen1-K714R (nG1 = 203, nG2/M = 306, VR = 3), slx8Δ (nG1 = 166, nG2/M = 172, VR = 3). Statistical differences were estimated by the Fischer's exact test and significance is indicated by*

asterisks P < 0.05(*), P < 0.005(**), P < 0.001(***). e Sensitivity to the indicated genotoxics was determined by spotting serial dilutions of different strains on the indicated media. f Cycloheximide chase experiment showing persistence of Yen1 after a G1 release in the presence of CHX. g Immunoprecipitated Yen1-K714R-HA was eluted and the protein was sumoylated with Aos1-Uba2, Ubc9, and Smt3-3KR in the presence or absence of ATP. Samples were de-phosphorylated with CIP before loading. h 6xHIS-Smt3 pull-downs were performed on cells expressing 6HIS-Smt3 and carrying YEN1-HA or its variant yen1-K714R-HA under conditions of MMS treatment as indicated. The average fold enrichment is indicated at the bottom of the blot.

Foci distribution and sumoylation in yen1-K714R

To determine the effect of the K714R mutation, we initially assessed its cell-cycle regulated localization and activity. Yen1 is phosphorylated by Cdc28 (Cdk1) in S-phase and is de-phosphorylated by Cdc14 at anaphase [510]. No major difference could be detected when analyzing the mutant *yen1-K714R* as compared to wild type (Figures 37c, fig 42 - Supplementary Figure 5). Nuclear shuttling of Yen1^{K714R} was identical to wild-type Yen1, with S-phase exclusion occurring in both strains (Figure 37d). Interestingly, we detected a modest increase in Yen1^{K714R} foci in undamaged conditions, further increased in a *mus81*Δ background (Figure 37d), suggesting the persistence of Yen1^{K714R} foci is specifically observed if there are increased substrates. This increase in foci in the *yen1-K714R mus81*Δ double mutant did not result in increased DNA damage sensitivity (Figure 37e, fig 42 - Supplementary Figure 5), however, suggesting that locally accumulated Yen1^{K714R} retained the ability to complement the loss-of-Mus81 nuclease. A cycloheximide chase experiment with the *yen1-K714R* strain resulted in the detection of a more persistent Yen1 fraction 150 min after G1 release (Figure 37f) that is in agreement with the observation of increased Yen1 foci. Yen1-K714R was still sumoylated both in *in vitro* assays with immunoprecipitated Yen1-HA or in pull-down experiments (Figures 37g, h). The modified forms recovered from pull-downs were more abundant in the mutant strain compared to the wild type suggesting that the lysine substitution triggers stabilization of the Yen1 sumoylated fraction similarly to the effects observed in the experiments with *slx8*Δ and *slx5*Δ cells (Figure 34).

Increased crossover formation in yen1-K714R cells

To test possible gain-of-function effects of Yen1^{K714R} we measured mitotic CO levels. A gain-of-function of Yen1 would likely increase the rate of CO resolution during DSB repair without affecting sensitivity to DNA damaging agents. To test this hypothesis, we used the diploid strain able to screen CO/BIR levels after an I-SceI-induced DSB [177]. Introduction of -1xHA tagged Yen1 in these strains did not affect the CO levels previously reported [470] and were within experimental variation. As expected for this assay, the *mus81*Δ strain showed a slightly reduced CO level that was further reduced in the *mus81Δ yen1Δ* strain, along with a parallel increase in BIR (Figure 38a). Surprisingly, when introduced alone, Yen1^{K714R} increased the overall CO levels above those of wild type. Further, when *yen1-K714R* was combined with *mus81*Δ, instead of a decrease in CO levels as expected for a loss-of-function *YEN1* allele, we observed a nearly twofold increase in COs compared to *mus81*Δ alone (Figure 38a). These CO levels are above those expected for wild type and consistent with a gain-of-function phenotype.

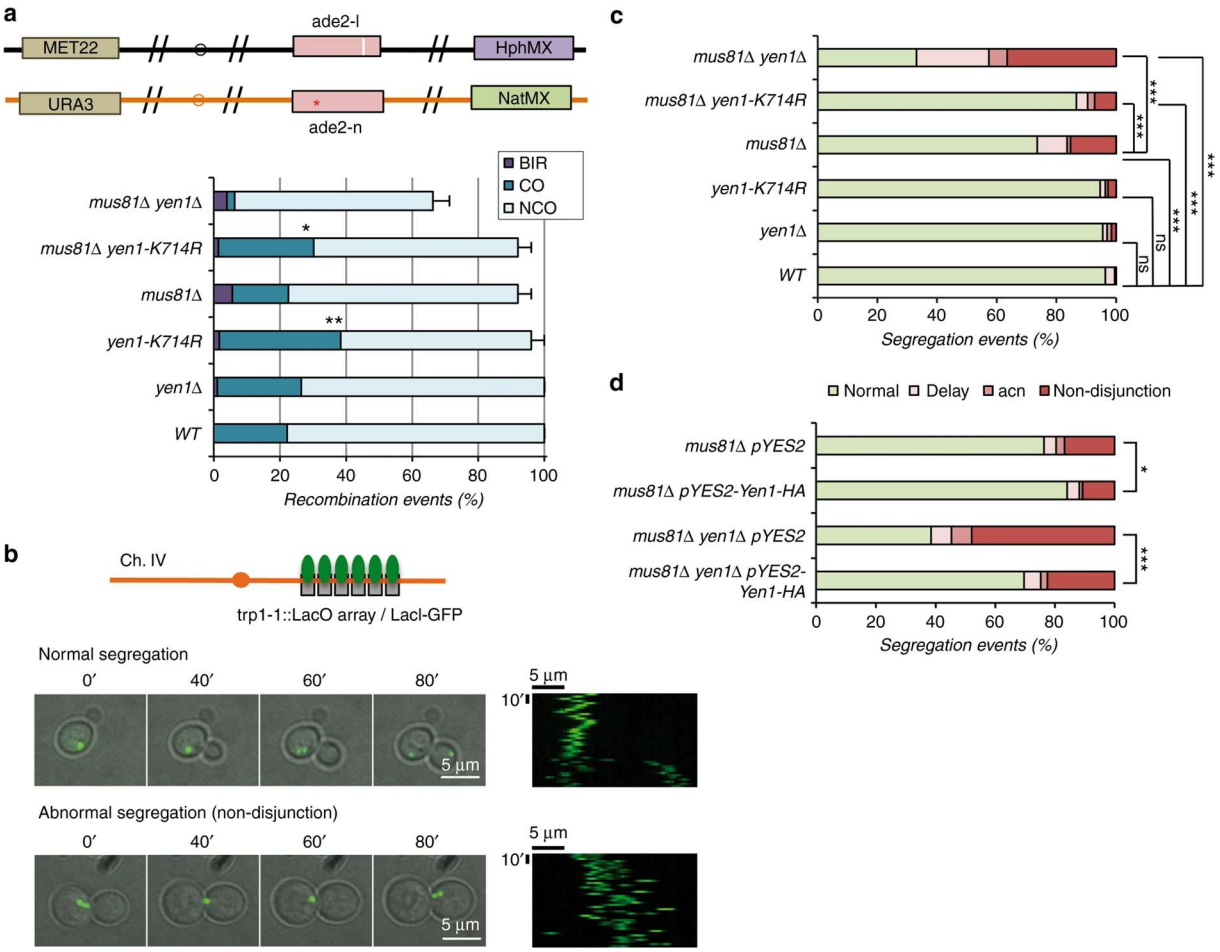

Figure 38. *Yen1-K714R increases COs and suppresses spontaneous chromosome segregation defects in mus81Δ cells.* ***a*** *Diagram explaining the Chr. XV DSB-induced crossover reporters. Recombination outcomes were scored in white/red sectored colonies of the indicated strains and normalized to its plating efficiency (PE). The number of independent experiment trials (T) and the total number of recombination events scored (n) were as follows: WT (T = 6, n = 158), yen1Δ (T = 9, n = 538), mus81Δ (T = 5, n = 168), mus81Δ yen1Δ (T = 9, n = 160), yen1-K714R (T = 5, n = 230), and mus81Δ yen1-K714R (T = 5, n = 230).* ***b*** *A strain harboring a lacO/GFP-LacI array tag on chromosome IV was followed by video-microscopy to discriminate chromosome segregation in timely manner from aberrant segregation. Images display a typical normal and aberrant segregation and its respective kymograph.* ***c*** *GFP foci of the indicated strains were observed by video-microscopy and chromosomal segregation was scored as to whether it displayed a proper phenotype (normal) or one of three types of defective phenotypes (non-disjunction, delay, and aberrant chromosome number (acn)). The total number of cells analysed (n) and independent video-recordings (VR) were as follows: WT (n = 606, VR = 3), yen1Δ (n = 133, VR = 3), yen1-K714R (n = 131, VR = 3), mus81Δ (n = 259, VR = 5), yen1-K714R mus81Δ (n = 448, VR = 3) and yen1Δ mus81Δ (n = 289, VR = 3).* ***d*** *Segregation events scored as in* ***c*** *were determined for mus81Δ and mus81Δ yen1Δ strains containing a pYES2 plasmid expressing Yen1-HA under Galactose-inducible control or an empty pYES2 and subjected to acute over-expression of Yen1-HA or the equivalent mock induction prior to the recording of the video-microscopy. The total number of cells analysed from three VRs were as follows: mus81Δ (+pYES2) n = 245, mus81Δ (+pYES2-Yen1) n = 391, mus81Δ yen1Δ (+pYES2) n = 117, mus81Δ yen1Δ (+pYES2-Yen1) n = 218. Statistically significant differences in* ***a*** *between CO and other outcomes and in* ***c*** *and* ***d*** *between normal and abnormal categories were determined by the Fischer's exact test, asterisks refer to significance at the P < 0.001(***), P < 0.005(**) or P < 0.05(*).*

yen1-K714R suppresses segregation defects of mus81Δ

One effect of the failure to repair recombination intermediates is the accumulation of joint-molecules in mitosis that lead to mis-segregation of chromosomes and ultimately an increase or decrease in chromosome number. The *mus81Δ yen1Δ* strain display such segregation defects even in the absence of DSBs induced by exogenous sources [177]. In order to test the *yen1-K714R* mutant for a gain-of-function phenotype, we devised an improved assay for chromosome segregation fidelity. Genetic systems that monitor mis-segregation have the limitation of looking at viable endpoints and cannot

recover unviable ones. We therefore chose to look at real-time chromosome segregation by using a fluorescent array tag on chromosome IV (Figure 38b, fig 43 - Supplementary Figure 6). Using this approach we confirmed that *mus81Δ yen1Δ* cells are severely impaired in chromosome segregation (Figure 38c). Segregation defects were observed in 35% of *mus81*Δ single mutants, and more than 60% of *mus81*Δ *yen1*Δ cells (Figure 38c). Under the same conditions, *yen1*-K714R partially suppressed the *mus81*Δ defects (Figure 38c). The ability of Yen1^{K714R} to suppress *mus81*Δ defects is further evidence of a gain-of-function phenotype consistent with the idea that more spontaneous joint-molecule intermediates are resolved in cells expressing Yen1^{K714R} than in wild-type cells. Because elevated Yen1 expression has been shown to suppress *mus81Δ* phenotypes [511], we compared the effect of Yen1 over-expression to the phenotypes of the *yen1-K714R* mutant. Expression of plasmid borne wild-type Yen1-HA, suppressed *mus81Δ* segregation defects to levels similar to those observed in a *mus81Δ yen1-K714R* strain (Figure 38d). Thus, even though Yen1-HA protein levels were extremely high following induction (see Figure 45b - Supplementary Figure 7b), suppression was no better than that achieved by endogenous levels of Yen1K714R. Interestingly, long-term high-level expression of Yen1 appeared to be deleterious to *mus81Δ* cells. Chronic but mild over-expression of Yen1-HA (0.1% galactose induction) resulted in *mus81*Δ cells that were more sensitive to MMS than their un-induced counterparts even though Yen1-HA expression was only slightly higher than endogenous levels (Figure 45 - Supplementary Figure 7).

4.1.4 Discussion

Nucleolytic processing of recombination intermediates by Yen1 has been proposed to be an option of last resort that is needed to prevent chromosomal segregation defects and genome rearrangements in mitosis [512]. Accordingly, Yen1 has a tightly controlled operational window that is limited to the anaphase – telophase period of mitosis. Here, it removes the last intermediates that physically connect the chromosomes [185, 510]. Although the window of Yen1 activity is known to rely on cell-cycle driven phosphorylation and de-phosphorylation [459, 460], we establish here for the first time a new layer of control involving Slx5-Slx8 dependent ubiquitination of Yen1 (see model in Figure 46 - Supplementary Figure 8). Slx5/8 targets a minor fraction of Yen1 that is detected as a more persistent pool associated with nucleolar or active sites on the chromatin (Figures 35 and 36). We have identified K714 as the major target of Slx5-Slx8 (Figure 37). The fact that significant levels of ubiquitinated Yen1 were recovered from *slx8*Δ cells, is in full agreement with reports that other Slx5/8 targets are redundantly targeted by alternative ubiquitination pathways to ensure rapid destruction in different contexts or sub-nuclear compartments [507, 513, 514].

Our analysis of the transition between G1 and S phases clearly indicates that there is a wave of Yen1 destruction before S-phase entry, when most of the previously nuclear protein is targeted for proteasomal degradation (Figure 35). Our data suggests this is a general turnover pathway that is not controlled by Slx5/8. This pathway degrades most of the Yen1 pool, similar to what has been described for other Slx5/8 targets [514]. One plausible explanation for why Slx5/8 targets such a minor fraction of Yen1 is that it can be quickly degraded, or evicted from the nucleus before S-phase starts. In agreement with such a hypothesis, we see a fraction of Yen1 that remains un-degraded in cycloheximide chase experiments performed in cells that are synchronized in G1. The amount of Yen1 that remains un-degraded is about 20% of the total found at the beginning of the experiment, although this may reflect an increased amount of Yen1 associated with chromatin or active sites in cells devoid of Slx5/8 [508, 515]. Under wild-type conditions, we might expect the fraction of Yen1 being targeted by Slx5/8 to be more transient. Our data are also compatible with a SUMO-independent role of Slx5/8

in targeting Yen1 (Figure 34). SUMO-independence has previously been observed in certain Slx5/8 substrates. These substrates are thought to be targeted by Slx5/8 binding to sumoylated partner proteins [391] or to substrate structural features that mimic SUMO [514].

Sumoylation has been proposed as a mechanism to rapidly form protein complexes under stress conditions [400], or to recruit factors that need to associate at precise cellular localizations in a timely constrained manner [516]. We speculate that Yen1 is sumoylated in stressful situations, and that Slx5/8 ubiquitination ensures any remaining Yen1 that is strongly associated with DNA at the end of G1 will be effectively degraded before replication starts. In such a hypothesis, sumoylation would not be a pre-requisite for Slx5/8 targeting, but sumoylated Yen1 would be targeted due to its preferential association with DNA or chromatin regions that preclude it from being exported or degraded at S-phase similar to what has been described for proteins associated with the kinetochore [391]. Although, we consider it unlikely, our data does not exclude the possibility that Slx5/8 ubiquitination does not directly trigger Yen1 degradation, but only influences its local association with other partners or its DNA substrates. For example, the extended nuclear persistence of a limited Yen1 fraction could also result from its association with nuclear sites that are inhibitory to a general mechanism of degradation that has yet to be described and is responsible for eliminating the majority of the Yen1 protein before S-phase.

The fact that Yen1 is regulated by multiple mechanisms, including phosphorylation, nuclear exclusion, and protein turnover, suggests that Yen1 inhibition is especially important for preventing DNA damage during DNA replication when structures generated at the replication forks may be a substrate for Yen1 cleavage. In agreement with this hypothesis, hyperactive forms of Yen1 that are constitutively nuclear ($Yen1^{ON}$) sensitize cells to high doses of MMS [460]. This has been interpreted as an increased sensitivity to conditions where forks stall more frequently. Similarly, we can detect a suppressive effect linked to over-expression of Yen1, but chronic mis-regulation of Yen1 levels sensitizes cells and causes deleterious side effects (Figure 38, fig 45 - Supplementary Figure 7), whereas we did not detect an increased sensitivity to MMS in *yen1*-K714R cells. It is important to keep in mind that redundant controls are probably able to restrict Yen1 activity if overall levels are not largely altered, but these controls may not be sufficient to cope with a chronic over-expression of the nuclease. With moderate excess of Yen1, the protein may still become dissociated from chromatin and exported prior to S-phase and it can still be phosphorylated by CDK1 to inhibit its activity thus explaining limited impacts in MMS sensitivity. Nonetheless, we see a striking increase in CO formation with the *yen1*-K714R allele following a DSB, suggesting that the Slx5/8 control plays an important role in maintaining the preference for the use of NCO pathways (Sgs1- or Mph1-dependent pathways) whenever these factors are available. It is known that Slx5/8 is needed to allow re-localization of DSBs to nuclear pores [325] and could thus regulate the ability of repair factors to gain access to the intermediates of DSB repair [325, 517]. We suggest that Slx5/8 may be responsible for clearing Yen1 from DNA intermediates where Sgs1- is already recruited, or for limiting Yen1's ability to associate to these intermediates. The fact that the K714R mutation allows increased recovery of sumoylated Yen1 (Figure 37) raises the interesting possibility that sumoylation favors Yen1 activity over other proteins capable of dismantling joint-molecule intermediates. Slx5-Slx8 may regulate access of different proteins by removing sumoylated Yen1 from DNA intermediates if its recruited in the presence of NCO determinants like Sgs1.

Mapping of the multiple sites of Yen1 sumoylation will be required to determine whether sumoylation is strictly required for Yen1 functions *in vivo,* and whether different sites or levels of sumoylation influence its binding to known partners, or proteins yet to be described. Should any potential "sumo-less" mutants, bearing multiple lysine replacements, be neutral with respect to Yen1's protein folding,

it would be possible to draw conclusions on the effect of sumoylation on Yen1's localization and nuclease activitiy. Similarly, a more extended study on the biochemical activities of *in vitro* fully-sumoylated Yen1 will help test whether sumoylation alters Yen1's specificity for its different substrates.

Yen1 has a specific role in dealing with replication intermediates that are usually handled by Dna2 [505] and it plays a role in suppressing the accumulation of JM intermediates that originate in the rDNA locus [471]. These JM contain either orphan HJs or D-loop -derived intermediates that do not mature into dHJs, and thus are not dissolved by the BLM ortholog Sgs1 and its associated proteins [163, 471]. Slx5/8 could thus ensure that Yen1 is only used as the last option even in situations when recruitment has been enforced by a sumoylation cascade [400]. If the human GEN1 ortholog is regulated similarly, we expect that mutations equivalent to the K714R identified here may recapitulate the hyper-crossover phenotypes we observed without a major effect on cell viability. Such mutations might be found to have a cancer predisposition phenotype due to its increased genome instability. Defects in GEN1 turnover would be expected to give rise to a phenotype similar to that of impaired BLM helicase, or a defect in factors enforcing NCO pathways. The redundancy in the pathways of nucleolytic resolution during HR in humans [518] makes it difficult to determine a precise role of GEN1 mutations in cancer predisposition, with scarce evidence to date [519-521]. However, should the active pools of GEN1 be similarly regulated in human cells, it may be possible to identify mutations that destabilize the balance between CO and NCO outcomes.

4.1.5 Materials and methods

Yeast Strains and Growth Conditions

S. cerevisiae strains and plasmids used in this study are listed in Supplementary Tables 1 and 2. The *YEN1*-HA allele was generated by inserting a FactorXa cleavage site and a single -HA epitope at its C-terminus using PCR amplification with a dedicated oligonucleotide. Mutants in the different designated loci where either obtained by crossing or by gene replacement with the indicated selective cassettes. Cells were typically grown in YP (1% yeast extract; 2% peptone) or SC media with 2% glucose or alternatively with 2% raffinose or 2% galactose in strains under inducible conditions. A modified medium (SC with 0.17% YNB without ammonium sulfate, 0.1% proline and 0.003% SDS) was used for the cycloheximide and MG132 assays and for the Smt3/Ubi pull-down assays. Methyl methane sulfonate (MMS, Sigma), Zeocin (Zeo, Invitrogene) and hydroxyurea (HU, Sigma) were added to YPD medium at the designated doses for DNA damage sensitivity assays.

Western Blot analyses

Proteins were extracted by the TCA (Trichloroacetic acid) method if not stated otherwise. Samples were loaded into 7.5% or 4–15% gradient Tris-Glycine BioRad stain-free pre-casted gels for routine analysis. Samples from pull-downs analyses were loaded into 3–8% gradient NuPAGE Tris-Acetate gels (Invitrogen). Gels were transferred to PVDF membranes using a semi-dry transfer machine (BioRad) and hybridized on TBST 5% milk with the appropriate antibodies. Antibodies were used at the suggested dilution: anti-HA-HRP (3F10, Roche) 1:1000 (1:500 for pull-down analysis), anti-Ubiquitin (P4D1, Biolegends) 1:1000, anti-Smt3 (provided by B.Palancade) 1:2000, anti-G6PDH (A9521, Sigma) 1:20,000, anti-Pgk1-HRP (22C5D8, Abcam) 1:10,000, anti-GST-HRP (GERPN1236, Sigma) 1:5000. When required, HRP-conjugated secondary antibodies from Cell Signaling (anti-Mouse-HRP, anti-Rabbit-HRP) were used at 1:10,000 dilution. Western blots were revealed with WesternBright ECL solution (Advansta) or WesternBright Sirius HRP subsrate if required (Advansta). Blots were cropped in order to arrange figures without any lane substitution and conserving the area with immunoblotting signal (examples of uncropped images are available in figure 47 - Supplementary Figure 9).

Microscopy and Cell Biology Methods

Live cell imaging was performed with a Spinning Disk Confocal Microscope (CSU-W1, Yokogawa), with an electron multiplying charge device camera (ANDOR Zyla sCMOS) and a x60/1.35 numerical aperture objective at 30°C. Cells were mounted on agarose pads as described [522] and imaging recorded 15 z-sections with 0.5 µm spacing. Image acquisition was performed using Fiji (ImageJ) [523]. Cells were grown in synthetic complete medium without uracil (SC-URA 2% raffinose), GFP-Yen1 was induced in a short burst with 30 min with Galactose at 2%, followed by addition of Glucose at 2%. DNA damage acute exposures (MMS 0.1% or 10 µg/ml Zeocin) lasted 15 min at room temperature following arrest of GFP-Yen1 expression. After the acute DNA damage, cells were washed once with fresh SC-URA 2% glucose and held for 30 min at 30 °C in this medium, whereas aliquots were removed at the indicated times. Cells showing an accumulation of spots were measured at maximum projection of the GFP channel. Statistical analysis was performed using Fisher's exact test to determine the level of significance between two categories and $\chi 2$ to compare more than two categories and consistency between trials.

Cycloheximide chase experiments

Cultures grown in SC complete modified media (0.1% proline 0.017% YNB w/o ammonium sulfate) were diluted to OD 600 = 0.2 and synchronized with alpha factor (3 µM) for 2 h. At G1 release, cells were treated with cycloheximide (250 µg/ml) in fresh media and when indicated cells were pre-treated with MG132 (100 µg/ml) 30 min before G1 release. At every given time point 1 ml of culture was removed and frozen in presence of 25 mM sodium azide. Proteins were extracted by the TCA method and analyzed by 7.5% SDS-PAGE and western blot.

Pull-downs and Immuno-precipitation

For 6xHIS-Smt3 and 6xHIS-Ubi4 pull-downs, strains containing the expression vectors or the control plasmid were grown in SC-LEU modified medium (0.1% proline, 0.17% YNB without ammonium sulfate). Cells were allowed to grow to OD 600 = 0.3 when $CuSO_4$ was added at 100 µM final concentration in a volume of 100 ml. After 1 h MMS was added to 0.3% and cells were collected 3 h later. For cultures inhibited for proteasome degradation MG132 was added to 100 µM 2 h before collecting the cells. Cells where lysed under denaturing conditions and SUMO or ubiquitin-conjugated proteins where isolated basically as described [383, 503, 524, 525] with the modifications detailed in Supplementary methods section. In GST-pull-downs cells were lysed in IP buffer (40 mM Tris-HCl (pH 7.5), 10% Glycerol 0.1% NP40 150 mM NaCl) and cleared lysates bound to Glutathione Sepharose (GE Healthcare). After washes, proteins were eluted directly in Laemmli buffer. For the detection of sumoylated Yen1-HA forms by immunoprecipitation cells were lysed in TCA buffer by bead-beating at 4 °C. After centrifugation, precipitated proteins were washed once in cold acetone and then, pellets were resuspended in denaturing-IP buffer (0.5 M Tris-base, 6.5% SDS, 100 mM DTT, and 12% glycerol) and heated during 20 min at 65ºC before centrifugation at 16,000g for 10 min. Each 45 µl of soluble protein were diluted in 1.5 ml of RIPA buffer (50 mM Tris (pH 7.5), 150 mM NaCl, 5 mM EDTA, and 1% Triton X-100) containing protease inhibitors (EDTA free, Roche) and applied to anti-HA conjugated Agarose (Pierce), the bound fraction was eluted in Urea-loading buffer (8 M urea, 200 mM Tris-HCl (pH 6.8), 1 mM EDTA, 5% SDS, 0.1% bromophenol blue and 1.5% DTT).

Protein purification and in vitro assays

HIS6-tagged recombinant proteins were produced in *E. coli* BL21-RIL cells as described [370]. Proteins were purified on a 1 ml His-Trap column using an AKTA FPLC (GE Healthcare). The peak fractions were identified by SDS-PAGE, pooled, and dialyzed to buffer A (25 mM Tris-HCl (pH 7.5), 1 mM EDTA, 0.01% NP40, 1 mM DTT, 10% glycerol, and 0.1 mM PMSF) containing 300 mM NaCl and stored at −80 °C. Ub, Uba1, and UbcH5 were obtained from Boston Biochem.

In vitro full reconstituted sumoylation and ubiquitination assays with recombinant 6H-HA-Yen1 were performed in the presence of 20 mM HEPES (pH 7.5), 5 mM MgCl2, 2 mM ATP, 5 µM ZnSO4, and 0.1 mM DTT. Sumoylation reactions were incubated at 30 °C for 40 min and contained 10 nM Aos1/Uba2, 60 nM Ubc9, 0–10 nM Siz2-V5, 1.5 µM His6-Smt3-G98, and 0.7 µM Yen1 in a total volume of 20 µl. Ubiquitination reactions were incubated at 30 °C for 30 min and contained 10 nM Uba1, 60 nM Ubc5, 0–500 nM Slx5–Slx8, and 1.5 µM Ub in a 20 µl reaction. Where present, Holliday junction DNA, comprised of four 49-nt oligonucleotides, was added at 0.2 µM.

In *in vitro* Sumoylation assays with Yen1-1xHA from yeast, Yen1 was immunoprecipitated from cell lysates in native IP buffer using anti-HA conjugated Agarose (Pierce) and the protein was eluted with HA peptide (Sigma) competition. Eluates were subjected to SUMO conjugation as described [503].

DSB-induced ade2 recombination assay

The diploid recombination assays were performed basically as described [470]. Briefly, diploid strains containing 2 hetero-alleles of *ade2* are cleaved in its *ade2*-I allele by induction of I-SceI and allowed to repair under non-selective conditions (YPD) to give rise to either ADE2 or *ade2*-n repair products in three types of colonies (red, white and sectored). Outcomes were scored as in [470] by assigning to each colony the recombination events that correspond to the repair of the two sister-chromatids. A more detailed overview is available at the Supplementary methods section.

Contributions

G.M. obtained funding and designed the experimental plan. G.M., S.J.B., M.B., and I.T. designed experiments. I.T. contributed to Figs. 1, 3, 4 and 6, Supplementary Figures 1, 5 and 8; M.B. contributed to Figs. 4, 5, 6 and 7 and Supplementary Figures 1, 2, 3, 4, 6 and 7; H.D. contributed to Fig. 2 and Supplementary Figure 4; S.J.B. and J.M. contributed to Figs. 1, 3 and 6; G.M. contributed to Figs. 1, 4, 6 and 7, and Supplementary Figures 1, 5 and 8, strain crossing and constructions; B.P. contributed to Fig. 1 and shared reagents and strains. G.M. wrote the paper with major contributions from B.P. and S.J.B.

Acknowledgements

We thank LS Symington, M Hall, S Marcand, K Dubrana, S Leon, S Dokudovskaya, O Gadal, and S Biggins for generous gifts of yeast strains and plasmids. We thank LS Symington for critical reading and comments on the manuscript. We thank J. Rouviere for assistance in the setting of sumoylation assays. This study was supported by a starting grant to G.M. from the joint program of the CNRS and INSERM (ATIP-Avenir), a grant to G.M. from Gustave Roussy Foundation funded from donations from Natixis, grants from Fondation ARC pour la Recherche sur le Cancer and Ligue Nationale Contre le Cancer (LNCC) to B.P. and a grant from the National Institutes of Health to S.J.B. (GM101613). G.M. is a full-time INSERM researcher at the CNRS. M.B. has benefited from a post-doctoral funding from the LNCC.

4.1.6 Supplementary materials and methods

Yeast Strains and Plasmids

S. cerevisiae strains used in this study are listed in Table S1. Strains were generated by crossing and are derivatives of the W303c background. The Yen1-HA allele was generated by inserting a FactorXa cleavage site and a single -HA epitope at its C-terminus using PCR amplification with a dedicated oligonucleotide. Full length YEN1-HA was transformed into a *yen1*Δ::KlURA3 strain followed by counter-selection on 5-FOA to insert the allele in the endogenous locus. Positive clones were confirmed by sequencing and back-crossed to a wild-type W303c strain. The pYES2-GFP-Yen1 plasmid was obtained by cloning the GFP-Yen1 allele from pGAD-GFP-Yen1 [483] into pYES2-TOPO2 vector. Vectors expressing Yen1-HA or Yen1-3xFLAG were generated by inserting a PCR fragment of Yen1 with the tag and restriction sites into pYES2 opened by *HindIII* and *NotI*. Mutations in Yen1 were generated by PCR mutagenesis and introduced into the endogenous locus by transformation and gene replacement with a full-length YEN1 ORF PCR product into a *yen1*Δ::KlURA3 strain. Mutants in the different designated loci where either obtained by crossing or by gene replacement with the designated selective cassettes. Plasmid pNJ7766 contains the 6xHIS-1xHA-Yen1 insert in pET21a for expression of N-terminal-tagged Yen1 in *E.coli*.

Smt3 and Ubi4 denaturing pull-downs

Strains containing the 1346 plasmid (pCUP1-6xHIS-Smt3) or the control plasmid were grown in SC-LEU modified medium (0.1% proline, 0.017% YNB without ammonium sulfate), allowing direct MG132 treatment. Overnight cultures were diluted in 100 ml to an OD600=0.2 in the same medium but containing 0.003% SDS. Cells were allowed to grow to OD600=0.3 when CuSO4 was added at 100 µM final concentration. After 1hr MMS was added to 0.3% and cells were collected 3hrs later. For cultures inhibited for proteasome degradation MG132 was added to 100 µM 2 hrs before harvesting the cells. Cells where lysed under denaturing conditions and SUMO or ubiquitin-conjugated proteins where isolated as described [383, 503, 524] with the following modifications. Cells were precipitated 30 min on ice in 10% TCA, and lysed with glass beads for 20 min at 4°C. After centrifugation, the pellet was washed with cold acetone, and then we resuspended the pellet in guanidine buffer containing 6 M guanidium-HCl, 20 mM Tris-HCl (pH 8.0), 100 mM Na_2HPO_4, 10 mM imidazole, 100 mM NaCl, 0.1% Triton X-100, 0.05% Tween-20, 10 mM β-mercaptoethanol, 100 µM MG132 and 50 mM NEM (N-Etyl-Malemeide) and incubated the sample 1 hour at room temperature on rotating platform. After centrifugation at room temperature during 10 min at 16,000 g, the lysate was incubated for 2.5 hours with agarose nickel-nitriloacetic-acid beads (Agarose Ni-NTA ; Qiagen) previously equilibrated with guanidine buffer. The matrix was then washed three times with Guanidine buffer and three times with urea buffer containing 8 M urea, 100 mM Na_2HPO_4 (pH 6.3), 10 mM Tris-HCl (pH 8.0), 0.1% Triton X-100, 10 mM β-mercaptoethanol and 100 µM MG132. Samples were routinely treated with CIP phosphatase to allow a clearer detection of sumoylation and ubiquitination. Beads were dried before proceeding to elution in HU buffer composed by 8 M urea, 200 mM Tris-HCl (pH 6.8), 1 mM EDTA, 5% SDS, 0.1% bromophenol blue and 1.5 % DTT. Samples were heated at 65°C for 20 min. Eluates were loaded in 3-8% NuPAGE Tris-Acetate gradient gels. After transfer, membranes were processed for immuno-detection and finally stained with Ponceau Red to confirm sample loading. Input samples served as control in standard SDS-PAGE gels for equivalent expression of Yen1-HA.

DSB-induced ade2 recombination assay

Diploid strains containing 2 hetero-alleles of ade2 that are cleaved by I-SceI and repaired to give rise to either ADE2 or ade2-n repair products in three types of colonies (red, white and sectored) were grown in YP-R (2%) Overnight. Cultures were diluted and let grow to exponential phase when the DSB was induced by addition of Galactose at 2%. Cells were immediately plated in YP-D (2%) and grown for 3 days. Colonies were scored as solid red, solid white and sectored and replica plated to YP-D containing Hygromycin (SIGMA), Nourseothricin (Werner BioAgents), both antibiotics and to SC-URA-MET and SC-ADE (Raffinose 2% Galactose 2%). Non-recombinants were detected and excluded from analysis by papillation growth in YP-D and growth as ADE2 reversion in SC-Ade+Raff+Gal. Outcomes were scored by assigning to each colony the recombination events that correspond to the repair of each of the two sister-chromatids. A colony retaining heterozygosity for *Nat* and *Hph* was scored as two NCO events while a sectored colony with reciprocal LOH was scored as one NCO and one CO event. Recombination outcomes are presented relative to the YP-Gal (galactose) versus YP-D (glucose) PE of the strains (mean ± SD). To better address PE, cells were deposited by micromanipulation in both media plates and colony growth was scored after 3 days. Statistical significance was determined by Fisher's exact test between two categories with the indicated N (number of chromatid outcomes) shown in the legend. All strains were induced independently at least three times (see number of trials) and the results of each induction were pooled to calculate the distribution of events.

4.1.7 Supplementary figures

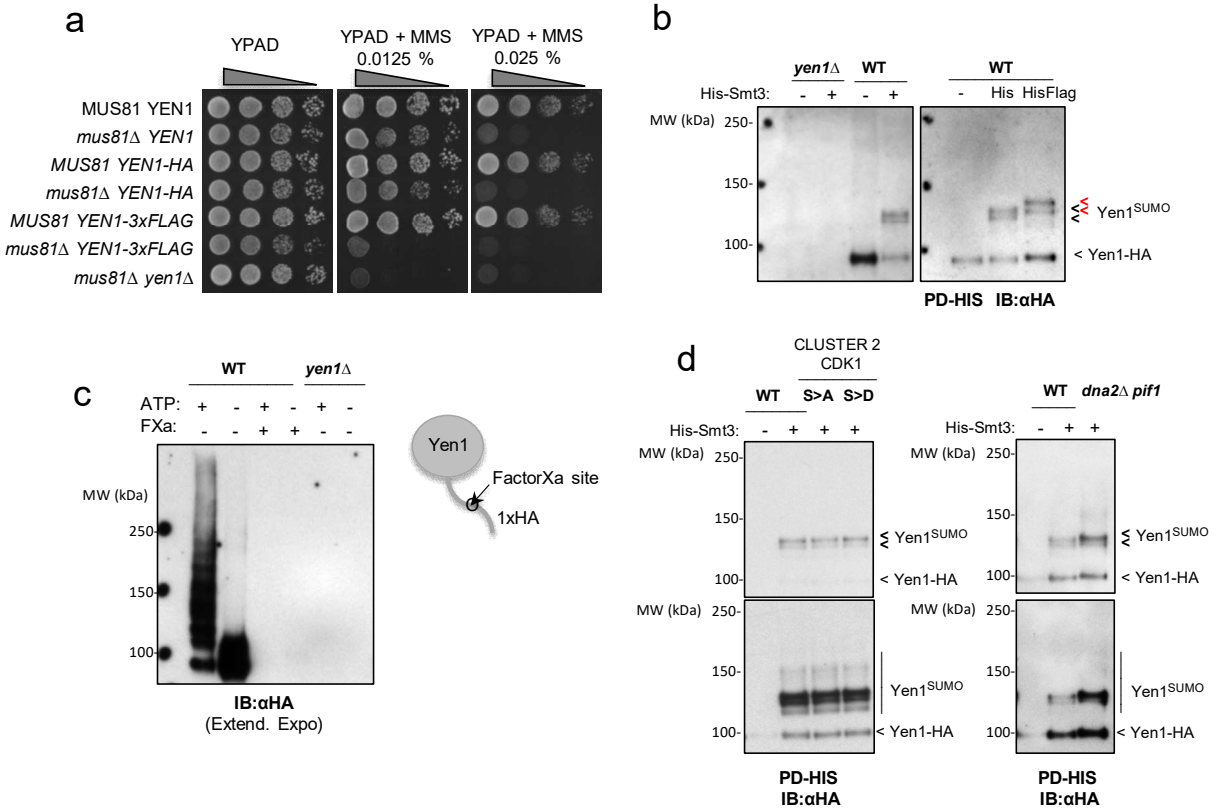

Figure 39. Supplementary Figure 1. A*) Strains carrying either a wild-type YEN1 locus or an endogenous replacement with the epitope tagged YEN1-HA or YEN1-3xFLAG were combined to mus81Δ and sensitivity to MMS was monitored with growth of serial dilutions in plates with the indicated doses of MMS.* ***B)*** *Smt3 denaturing pull-down under MMS treatment (0.3%) was performed from either a yen1Δ or wild-type strain expressing either empty, 6xHis-Smt3 (His) or His-Flag-Smt3 (HisFlag), small amont of PD was loaded to allow detection of the different bands of Yen1 sumoylation without saturation (dark marks for his-Smt3 or red marks for his-flag-Smt3)* ***C)*** *Yen1-HA was overexpressed in wild-type asynchronous cells and equivalent growth was made in an empty yen1Δ strain, extracts were immuno-precipitated with anti-HA, eluted by HA peptide competition and mixed with Aos1-Uba2, Ubc9 and Smt3-3KR in the presence or absence of ATP. When indicated, reactions were subjected to Factor Xa (FXa) treatment to remove the –HA tag.* ***D)*** *Smt3 denaturing pull-down under MMS treatment (0.3%) was performed from a wild-type strain and strains containing the Alanine or Aspartic substitution of four Serines of the CDK1 sites of cluster 2 [191]. Second gel compares wild-type with dna2Δ pif1 strain that results in an average (N=2) fold increase of 3.3 ±0.5 (SD) in the sumoylated fraction for the mutant strain.*

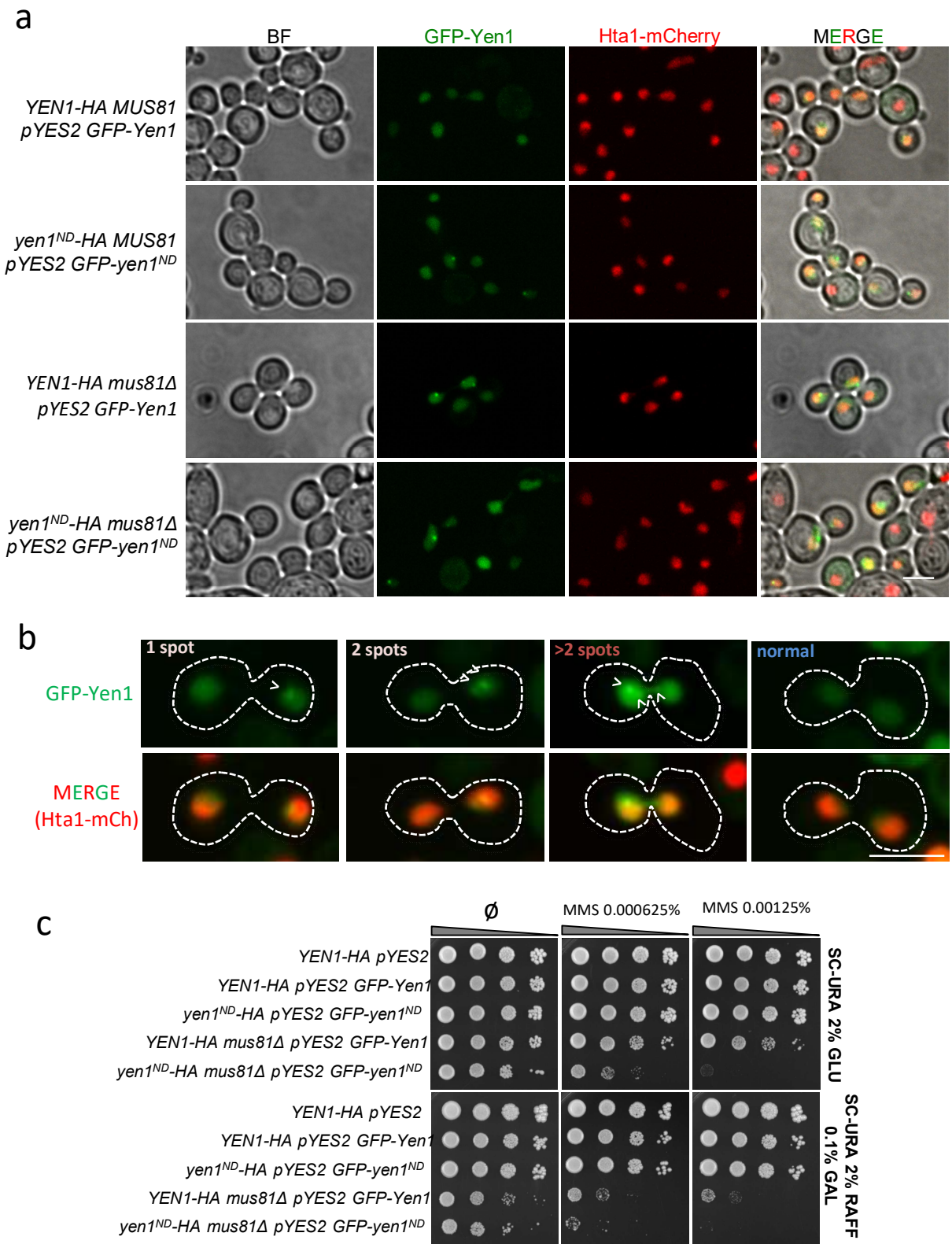

***Figure 40. Supplementary Figure 2**. **A**) Representative fields of strains expressing GFP-Yen1 on a short burst and its co-localizing signal with chromatin (Hta1) **B)** slx8Δ cells showing intra-nuclear foci that were categorized as 1-2 foci, >2 foci, normal or rare events (not included in the other categories) **C**) Strains used in microscopy were monitored for sensitivity to MMS under chronic low expression.*

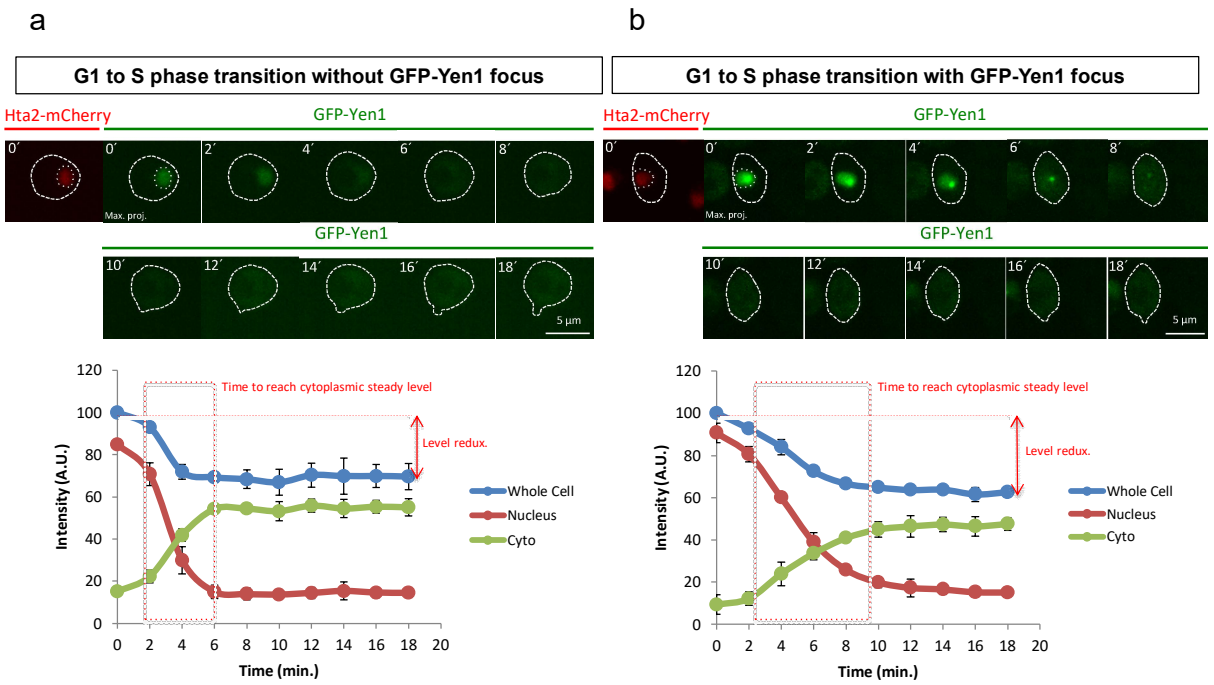

Figure 41. Supplementary Figure 3. (a) *Sequential images taken every 2 min of a cell expresing GFP-Yen1 during the re-location of GFP-Yen1 to the nucleus and associated graph showing the total intensity (normalized to 100%) of whole cell and both nuclear and cytoplasmic compartments for each time point.* ***(b)*** *2' time-lapse of a cell containing one focus during its GFP-Yen1 nuclear to cytoplasm re-distribution and associated graph (as in A). Graphs display the average intensity and SD (N=3).*

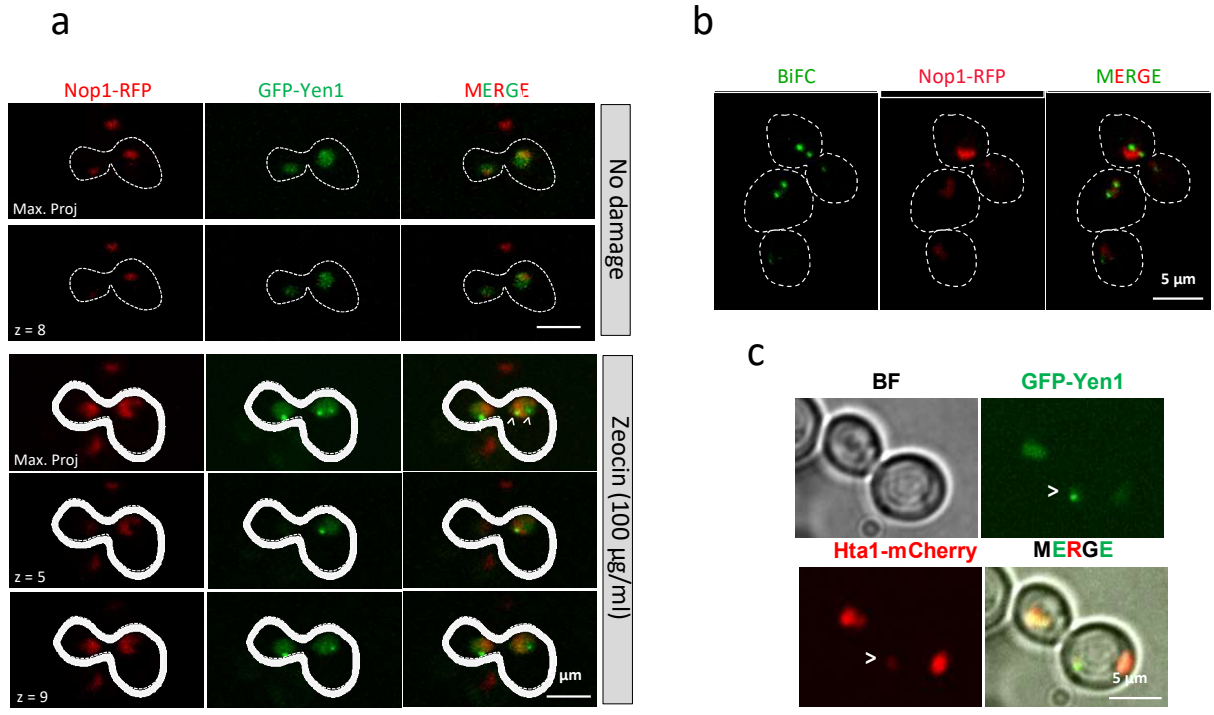

Figure 42. Supplementary Figure 4. (a) *Co-Localization of GFP-Yen1 and the Nop1-RFP nucleolar marker in normal and Zeocin challenge conditions. Co-localizing signal of Nop1 can also be detected with BiFC signal between Yen1 and Slx5.* ***(b)*** *Co-localization of BiFC signal of the Slx5-Yen1 interaction with the Nop1 nucleolar marker.* ***(c)*** *Representative image of a GFP-Yen1 focus localized to chromatin still not completely segregated in a slx8Δ cell (white arrow).*

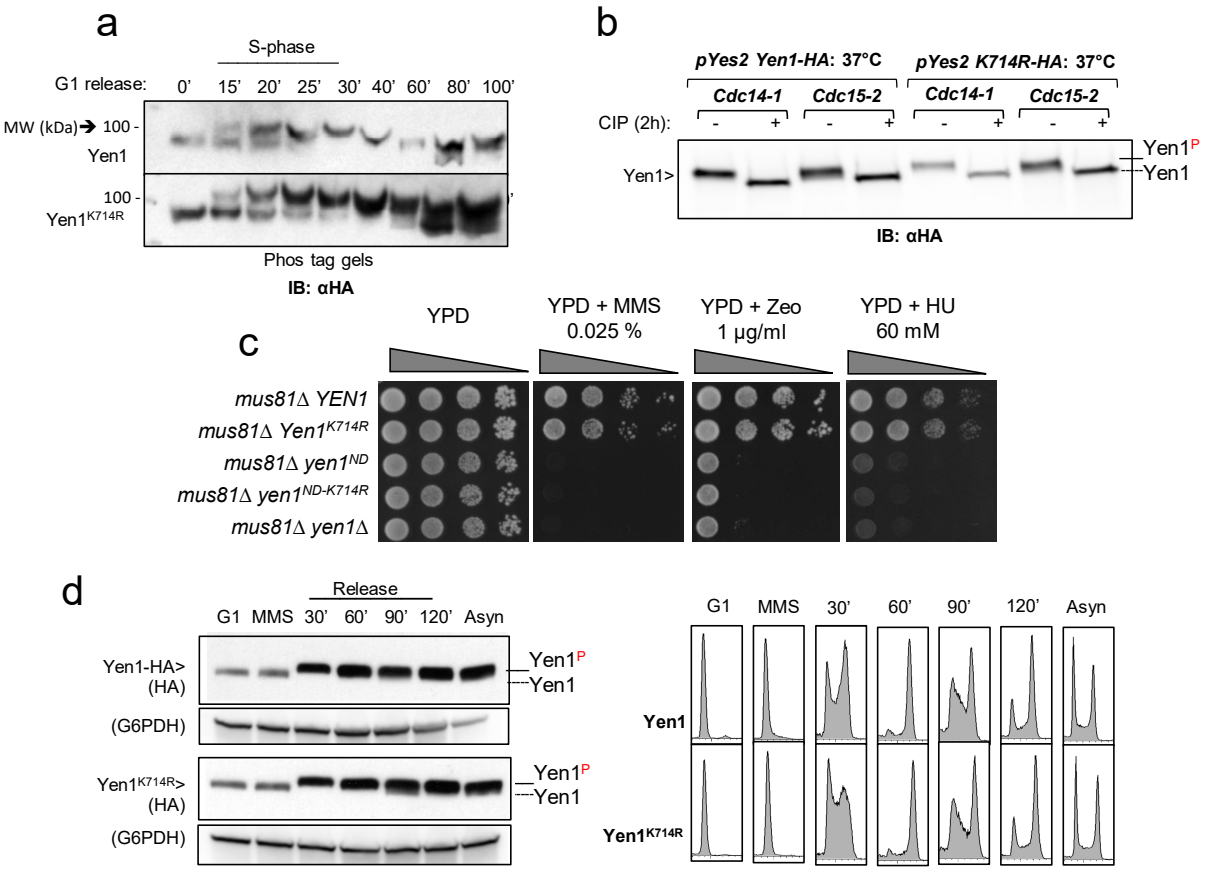

Figure 43. Supplementary Figure 5. (a) *PAGE phos-tag gel comparing phosphorylation status of a wild-type and a yen1-K714R strain during a time course after G1 release.* ***(b)*** *cdc14-1 or cdc15-3 cells were arrested at restrictive temperature and protein extracts were either mock treated or treated with CIP phosphatase to reveal the extent of Cdc14- sensitive phosphorylation in both wild-type and yen1-K714R strains.* ***(c)*** *Indicated strains (carrying a nuclease-dead ND allele of Yen1 combined or not with the K714R mutation) were subjected to a spot-test sensitivity assay by dropping serial dilutions in plates with the indicated genotoxics.* ***(d)*** *Cells arrested in G1 were released in MMS (0.1%) containing media for 10' and washed out of drug and let recover in fresh YPD, samples at indicated points were analyzed by western-blot and flow-cytometry to monitor the MMS recovery.*

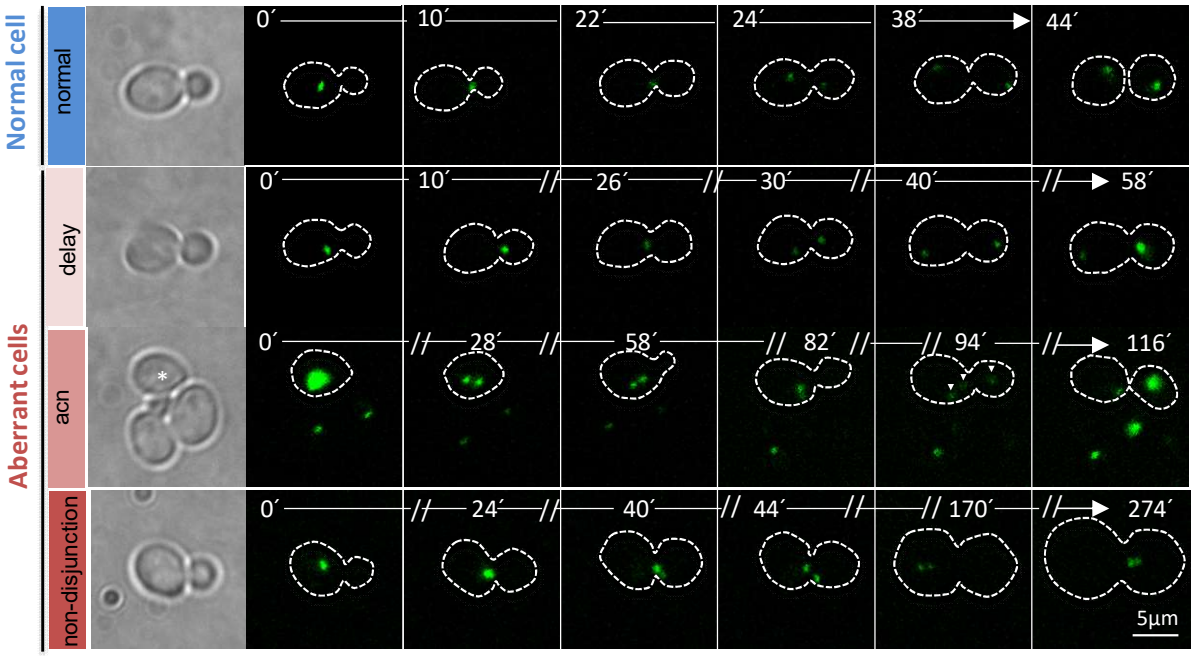

Figure 44. Supplementary Figure 6*. Images of representative cells from the 4 different categories used to analyzed proper segregation by video-microscopy (using the LacI-GFP-LacO array). Note the time lapses are not equivalent and delayed and non-disjunction events have significant increases on the time between frames that illustrate its phenotype (acn, aberrant chromosome number).*

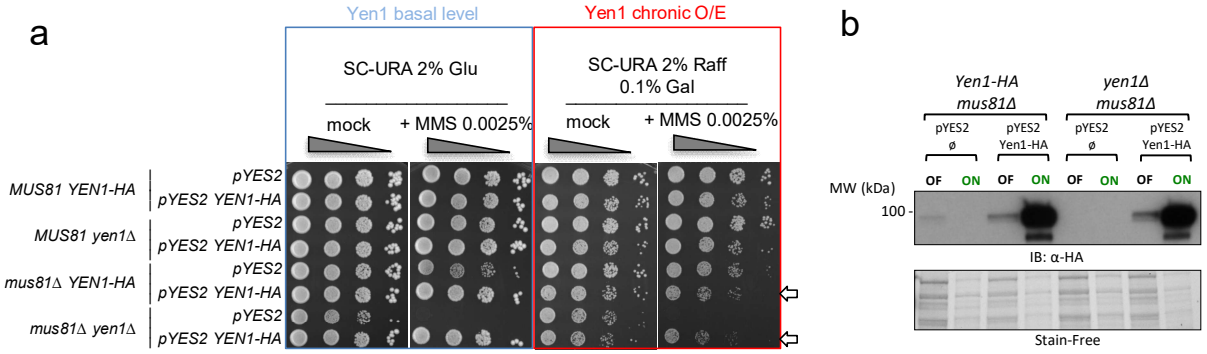

Figure 45. Supplementary Figure 7*. (**a**) Strains carrying either a pYES2 empty vector or a pYES2-Yen1-HA expression vector were spotted in selective media with or without 0.0025% MMS in conditions allowing basal expression (Glucose repression) or chronic over-expression of YEN1 (Induction with Galactose). (**b**) Analysis by western blot of the expression level of strains used in the segregation assay with acute O/E of Yen1-HA in Figure 7.*

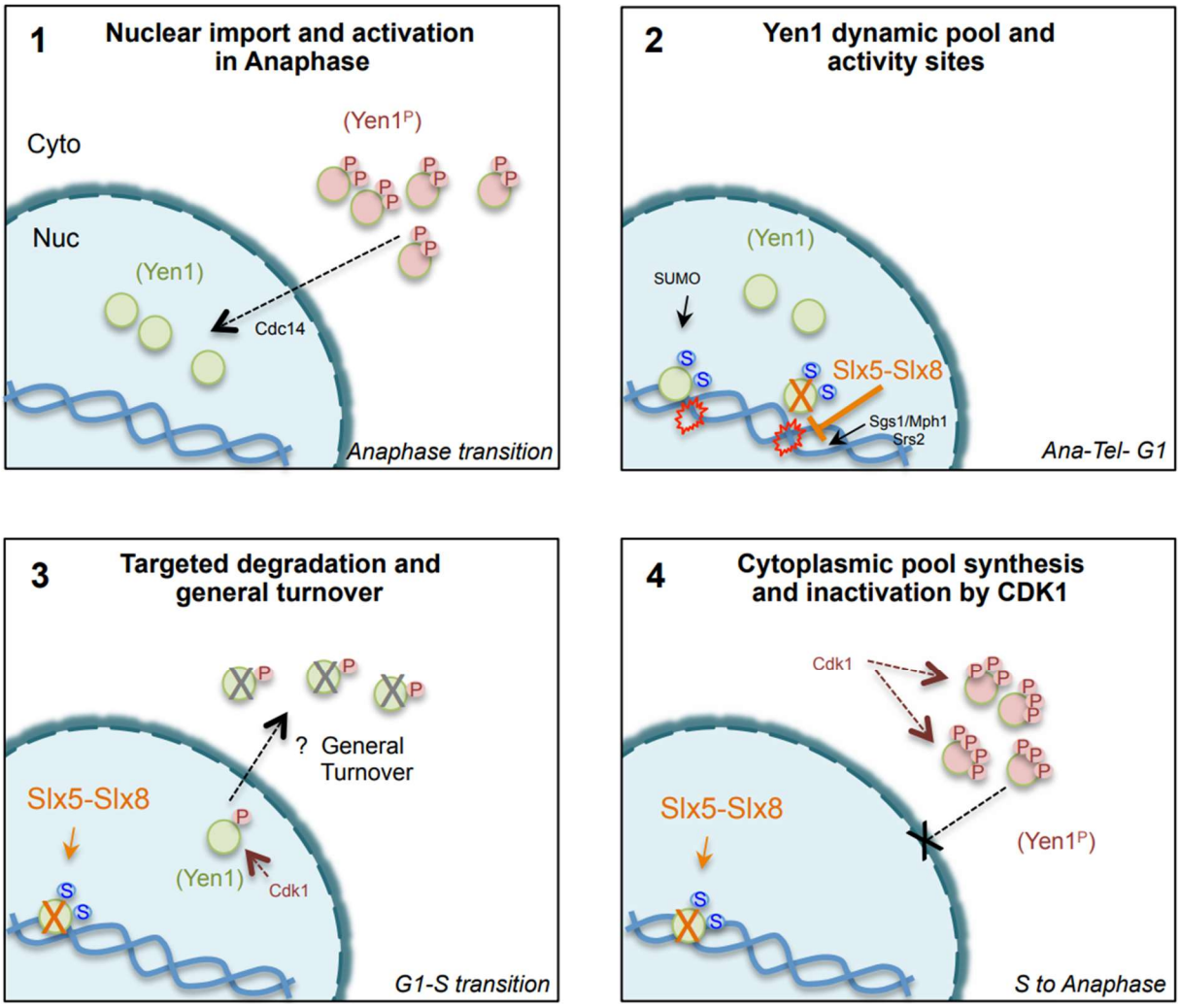

Figure 46. Supplementary Figure 8. Model explaining the role of Slx5-Slx8 in targeting the active fraction of Yen1 for degradation*. At Anaphase transition (1), the cytoplasmic pool of Yen1 (pink circles) is still phosphorylated by Cdk1 and remains excluded from the nucleus. The action of Cdc14 enables active forms of Yen1 (green circles) to enter the nucleus and be recruited at its active sites with a putative role for sumoylation (2). Slx5-Slx8 removes Yen1 from active sites reducing the time of its association in competition with other HR factors (Sgs1, Mph1, Srs2) (2). After mitosis the Yen1 pool remains nuclear until Cdk1 gradually phosphorylates Yen1 at the entry of S-phase (3). During the G1-S transition the Yen1 pool is targeted to degradation in parallel to its nuclear exclusion (3) and the newly synthesized pool remains cytoplasmic after Cdk1 phosphorylation (4). Any Yen1 that remains in the nucleus is targeted by Slx5-Slx8 to allow its degradation and prevents its persistent accumulation in the nuceus at the S-phase (4).*

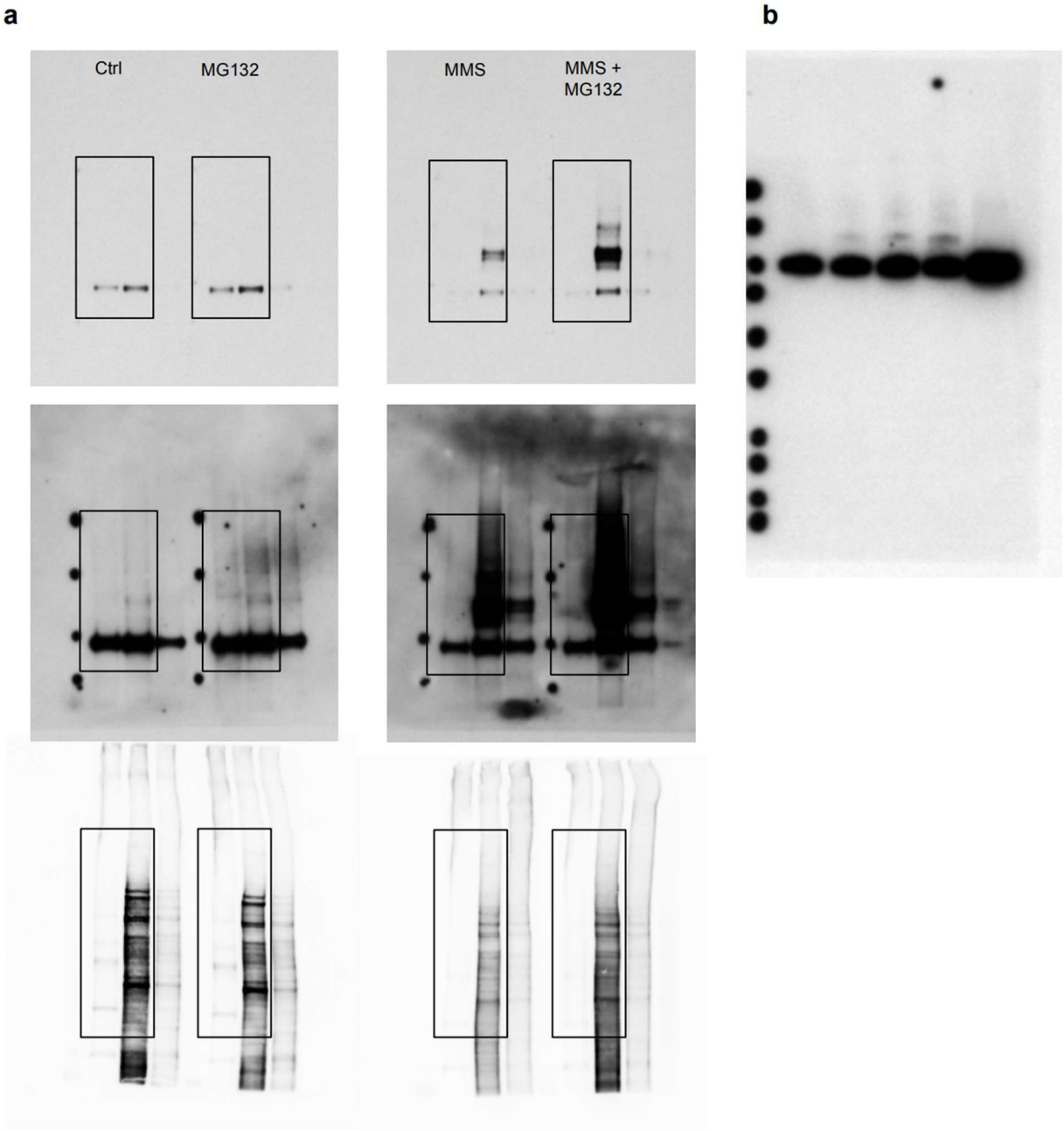

Figure 47. Supplementary Figure 9. a) *Uncropped immunoblot images from Figure 32 panel b. Squares show the cropping limits used to generate the images in display in panel b.* ***b)*** *Uncropped blot used in Figure 32 panel e input control.*

4.1.8 Supplementary table

Supplementary Table 1. Yeast strains

Strain	Genotype*	Source or reference
Strains for general purpose		
GM77	*MAT**a** ADE2 ura3Δ::HphMX*	LSY2307-7B [177]
GM104	*MAT**a*** ADE2 mus81Δ::KanMX ura3Δ::HphMX	LSY2307-1D [177]
GM58	*MAT**a*** ADE2 yen1::HIS3 ura3Δ::HphMX	LSY2307-6D [177]
GM47	*MATα ADE2 yen1::HIS3 mus81Δ::KanMX*	LSY1801-1D [177]
GM84	*MAT**a** ADE2 yen1Δ::klURA3* ura3Δ::HphMX	This study
GM93-5D	*MATα ADE2 yen1Δ::klURA3 mus81Δ::KanMX*	This study
GM98-4B	*MAT**a** ADE2 YEN1-HA ura3Δ::HphMX*	This study
GM98-7B	*MATα ADE2 YEN1-HA mus81Δ::KanMX ura3Δ::HphMX*	This study
GM481-2A	*MAT**a** ADE2 YEN1-HA mus81Δ::KanMX ura3Δ::HphMX*	This study
GM230-9	*MAT**a** yen1-K714R-HA ura3Δ::HphMX*	This study
GM240-8B	*MAT**a** yen1-K714R-HA mus81Δ::KanMX ura3-1*	This study
GM398-8	MAT**a** yen1- S500A S507A S513A S583A -HA ura3Δ::HphMX	This study
GM569-4	MAT**a** yen1- S500D S507D S513D S583D -HA ura3Δ::HphMX ura3-1	This study
GM395-5C	*MAT**a** ADE2 yen1::HIS3 ura3-1*	This study
GM395-14C	*MAT**a** ADE2 yen1::HIS3 mus81Δ::KanMX ura3-1*	This study
GM481-3D	*MAT**a** ADE2 YEN1-HA slx8Δ::KanMX ura3Δ::HphMX*	This study
GM481-9B	*MAT**a** ADE2 YEN1-HA mus81Δ::KanMX slx8Δ::KanMX ura3Δ::HphMX*	This study
GM548-6A	*MAT**a** ADE2 yen1::HIS3 slx8Δ::KanMX ura3-1*	This study
GM399-5	*MAT**a** ADE2 yen1-E193A E195A-HA (ND) ura3Δ::HphMX*	This study
GM410-1B	*MAT**a** ADE2 yen1-E193A E195A-HA (ND) mus81Δ::KanMX ura3Δ::HphMX*	This study
GM424-1A	*MAT α ADE2 yen1-E193A E195A K714R-HA (K714R ND) ura3Δ::HphMX*	This study
GM424-4B	*MAT**a** ADE2 yen1-E193A E195A K714R-HA (K714R ND) mus81Δ::KanMX ura3Δ::HphMX*	This study
GM198-1B	*MAT**a** ADE2 YEN1-3xFLAG ura3Δ::HphMX*	This study
GM198-6D	*MAT**a** ADE2 YEN1-3xFLAG mus81Δ::KanMX ura3Δ::HphMX*	This study
GM563-3B	*MATα ADE2 YEN1-HA slx5Δ::NatMX*	This study
GM529	*MAT**a** ADE2 yen1::HIS3 pdr5Δ::HphMX*	This study
GM548-1B	*MAT**a** ADE2 YEN1-HA pdr5Δ::HphMX*	This study

GM548-17A	*MAT**a** ADE2 YEN1-HA slx8Δ::KanMX pdr5Δ::HphMX ura3-1*	This study
GM571-9B	*MAT**a** ADE2 YEN1-HA slx5Δ::KanMX pdr5Δ::HphMX ura3-1*	This study
GM575	*MAT**a** ADE2 yen1-K714R-HA pdr5Δ::HphMX ura3-1*	This study
GM635	*MAT**a** ADE2 YEN1-HA siz1Δ::KanMX pdr5Δ::HphMX ura3-1*	This study
GM636	*MAT**a** ADE2 YEN1-HA siz2Δ::KanMX pdr5Δ::HphMX ura3-1*	This study
GM672-9C	*MAT**a** ADE2 YEN1-HA siz1Δ::KanMX siz2Δ::KanMX pdr5Δ::HphMX ura3-1*	This study
Strains for cell biology		
GM23	MATα his3-11:pCUP1-GFP12-LacI12:HIS3 trp1-1:256LacO:TRP1 lys2Δ bar1 ipl1-315-Flag:KanMX	SBY1372 [526]
GM304-11C	*MATa* ADE2 Yen1-HA his3-11:pCUP1-GFP12-LacI12:HIS3 trp1-1:256LacO:TRP1 ura3Δ::HphMX	This study
GM371-10A	*MATa* ADE2 *yen1-K714R*-HA his3-11:pCUP1-GFP12-LacI12:HIS3 trp1-1:256LacO:TRP1 ura3Δ::HphMX	This study
GM304-6A	*MAT*α ADE2 Yen1-HA mus81::KanMX his3-11:pCUP1-GFP12-LacI12:HIS3 trp1-1:256LacO:TRP1 ura3Δ::HphMX	This study
GM249-2D	*MAT*α ADE2 *yen1-K714R*-HA mus81::KanMX his3-11:pCUP1-GFP12-LacI12:HIS3 trp1-1:256LacO:TRP1 ura3Δ::HphMX	This study
GM120-12A	*MAT*α ADE2 yen1::HIS3 mus81::KanMX his3-11:pCUP1-GFP12-LacI12:HIS3 trp1-1:256LacO:TRP1 ura3Δ::HphMX	This study
GM120-12B	MATα ADE2 yen1::HIS3 his3-11:pCUP1-GFP12-LacI12:HIS3 trp1-1:256LacO:TRP1 ura3Δ::HphMX	This study
GM524-2C (G)	*MATα ADE2 YEN1-HA hta1-mCHerry::HphMX (+pYES2-GFP-Yen1)*	This study
GM524-10A (G)	*MATα ADE2 YEN1-HA slx8Δ::KanMX hta1-mCherry::HphMX (+pYES2-GFP-Yen1)*	This study
GM564-1B (G)	*MATα ADE2 YEN1-HA slx5Δ::NatMX hta1-mCHerry::HphMX (+pYES2-GFP-Yen1)*	This study
GM374 (G)	*MATα ADE2 Yen1-K714R-HA hta1-mCherry::HphMX (+pYES2-GFP-yen1-K714R)*	This study
GM392 (G)	*MATα ADE2 YEN1-HA mus81Δ::KanMX hta1-mCherry::HphMX (+pYES2-GFP-Yen1)*	
GM556 (G)	*MAT**a** ADE2 yen1-EE-HA hta1-mCherry::HphMX (+pYES2-GFP-yen1-EE)*	This study
GM525	MAT*α* ADE2 GFP-RAP1::LEU2 SIK1-mRFP::KanMX	yKD939 [527]
GM531-1B (G)	MATα ADE2 *YEN1*-HA SIK1-mRFP::KanMX (+ pYES2-GFP-Yen1)	This study
GM560-12D (G)	MAT**a** ADE2 *YEN1*-HA *SIK1*-mRFP::KanMX *slx8Δ*::KanMX (+ pYES2-GFP-Yen1)	This study
Strains for crossover monitoring		
LSY2205-24D	*MATα ade2-I lys2::GAL-ISCEI his3::HphMX4 yen1::HIS3*	[177]
LSY2202-42A	*MAT**a** ade2-n his3::NatMX4 met22::klURA3 yen1::HIS3*	[177]

LSY2205-77B	*MAT**a** ade2-I lys2::GAL-ISCEI his3::HphMX4 mus81::KanMX6 yen1::HIS3*	[177]
LSY2202-19D	*MATα ade2-n his3::NatMX4 met22::klURA3 mus81::KanMX6 yen1::HIS3*	[177]
GM379-4C	MATa YEN1-HA ade2-I lys2Δ::pGal-ISceI his3Δ::HphMX	This study
GM379-13C	*MATα YEN1-HA mus81Δ::KanMX ade2-I lys2::GAL-ISCEI his3::HphMX4*	This study
GM387-22B	*MATα YEN1-HA ade2-n his3::NatMX4 met22::klURA3*	This study
GM387-5A	*MAT**a** YEN1-HA mus81Δ::KanMX ade2-n his3::NatMX4 met22::klURA3*	This study
GM244-1B	*MAT**a** yen1-K714R-HA ade2-I lys2::GAL-ISCEI his3::HphMX4*	This study
GM243-9A	*MATα yen1-K714R-HA ade2-n his3::NatMX4 met22::klURA3*	This study
GM243-3B	*MAT**a** yen1-K714R-HA mus81Δ::KanMX ade2-n his3::NatMX4 met22::klURA3*	This study
GM244-7A	*MATα yen1-K714R-HA mus81Δ::KanMX ade2-I lys2::GAL-ISCEI his3::HphMX4*	This study
Strains for BiFC (BY4741 and BY4742 backgrounds)		
GM540	MATa KanMX::pGAL::VN-Yen1 his3Δ1 leu2Δ0 met15Δ0 ura3Δ0	This study
GM541	MAT*α* KanMX::pGAL::VC-Slx5 his3Δ1 leu2Δ0 lys2Δ0 ura3Δ0	This study
Strains for Two-Hybrid		
PJ69-4a	*MAT**a*** trp1-901leu2-3.12 ura3-52 his3-200 gal4Δ gal80Δ LYS2::GAL1-HIS3 GAL2-ADE2 met2::GAL7-lacz	Stan Fields Lab [528]
Pj69-4alpha	*MATα* trp1-901leu2-3.12 ura3-52 his3-200 gal4Δ gal80Δ LYS2::GAL1-HIS3 GAL2-ADE2 met2::GAL7-lacz	Stan Fields Lab [528]
Construction with tetO-chr XII		
LSY2282-1B	MATa ADE2 ura3:3xURA3 - tetO x112, TetR-mRFP yen1::HIS3	derived from W6956-24D (Rodney Rothstein Lab)
GM109-15C	MATα Yen1-HA mus81Δ::KanMX ura3:3xURA3-tetOx112 TetR-mRFP	This Study
GM518	MATa his3-Δ1, leu2-Δ1, ura3-Δ0 ade2-801 lys2-801, LYS2::TETR-GFP, nup49Δ::HphMX, inter YLR188w-YLR189c::ura3::TetO-NATMX (+ pASZ11-NupNop)	HBT28_1a [529]
GM562-5C	MAT*α ADE2 YEN1-HA* inter YLR188w-YLR189c::ura3::TetO-NatMX TetR-RFP *ura3*Δ::HphMX met17s his3?, leu2? (+ pYES2-GFPYen1)	Cross of HBT28_1a with 109-15C and 2 re-cross on 109-15C

*If not stated otherwise strains background is the W303 genotype (*his3-11, 15 leu2-3, 112 trp1-1 ade2-1 can1-100*), only mating type and differences from the standard genotype are listed. Specific strains in other backgrounds are defined.

Supplementary Table 2. Plasmids

Plasmid	Description
pNJ7766-Yen1	*pET21a derivative encoding 6xHIS-HA-Yen1 (IPTG inducible)*
pNJ7766-yen1-K714R	*pET21a derivative encoding 6xHIS-HA-yen1-K714R(IPTG inducible)*
pYES2	*pYES2 (URA3) empty vector, GAL inducible*
pYES2-Yen1-HA	*pYES2 (URA3) derivative, GAL inducible expressing wild type Yen1-HA*
pYES2-yen1-K714R-HA	*pYES2 (URA3) derivative, GAL inducible expressing yen1-K714R-HA*
pYES2-Yen1-3xFLAG	*pYES2 (URA3) derivative, GAL inducible*
pYES2-GFP-Yen1	*pYES2-TOPO (URA3) derivative, GAL inducible*
pYES2-GFP-Yen1$_{ND}$	*pYES2-TOPO (URA3) derivative, GAL inducible*
pYES2-GFP-yen1-K714R	*pYES2-TOPO (URA3) derivative, GAL inducible*
pRS315	*empty vector (LEU2)*
p1346	*Cu inducible (LEU2) encoding 6xHIS-Smt3 (from B. Palancade)*
pJM421	*Cu inducible (LEU2) encoding Ubi4*
pJD421	*Cu inducible (LEU2) encoding 6xHIS-Ubi4*
pOA-Slx5	*AD fusion with Slx5 (TRP1), derived from pOAD (from Stan Fields)*
pBDB-Yen1	*DBD fusion with Yen1 (LEU2), derived from pOBD2 (from Stan Fields)*
pUN100-mCherry-NOP1	*pRS305 derivative (LEU2) encoding mCherry-NOP1 (constitutive) (from O. Gadal)*
p1028-NUP49-mCherry (LEU2)	*pRS305 derivative (LEU2) encoding mCherry-Nup49 (from B.Palancade)*
p1069 His-Flag-Smt3 (LEU2)	Gal inducible (LEU2) encoding His-Flag-Smt3
pYES2 GST-Slx5	*pYES2-TOPO (URA3) derivative, GAL inducible expressing the fusion protein GST-Slx5*

4.2 Yen1 contains SUMO-interacting motives that guide its subnuclear localization and enable its proper role in resolving DNA joint-intermediates

In the second article inserted in this results section, we followed up the results showing Yen1 as a sumoylation substrate to convey the possible roles of such SUMO targeting for the functions of Yen1. The scanning of the protein for relevant features associated to sumoylation uncovered the presence of SUMO-interacting sites, that were further verified to mediate direct interaction to Smt3 in two-hybrid classical tests as well as more elaborated pull-down assays (Figure 48 page 115). We focused then in the characterization of the phenotypical effects of mutations in these motives, for both the persistence or lack thereof, of Yen sumoylation and its classical phenotypes made apparent in a genetic background lacking the overlapping role of the nuclease Mus81-Mms4 (Figures 49, 51-54).

SIM mutants kept most of the original control signatures of a wild-type Yen1. Indeed, controlled nuclear localization with nuclear exclusion in S-phase, phosphorylation by Cdk1 and dephosphorylation at the entry of Anaphase were all unchanged. Although we detected a decreased ability of cells expressing the SIM-deficient Yen1 variants to back-up Mus81-Mms4 functions in the presence of radio-mimetic or fork stalling drugs (Figure 49 page 117) and during normal chromosome segregation (Figure 53 page 121). All these shortcomings in the SIM mutants of Yen1 were associated to a decreased number of foci, and thus assigned to deficient localization (Figure 52 page 120).

Our conclusion is that the inability to interact with SUMO via the SIMs impair Yen1 localization at relevant sites of activity containing joint-molecules. In addition, its mis-localization prevents full sumoylation of Yen1 and suppresses the requirement for a Slx5-Slx8 targeting of the sumoylated subset of Yen1, resulting in a rapid clearing of the protein during cycloheximide chase experiments with cells at the G1-S transition (Figure 52).

“SUMO-mediated recruitment allows timely function of the Yen1 nuclease”

A document for submission by Hugo Dorison, Ibtissam Talhaoui and Gerard Mazón.

4.2.1 Introduction

The DNA integrity of the genomes is constantly exposed to multiple challenges either from endogenous or exogenous sources of DNA damage. Cells have evolved multiple DNA repair pathways to keep the genome stability, Homologous Recombination (HR) being one of the most critical pathways to specifically counter the deleterious DNA double-strand breaks and other problems in the DNA integrity arising during replication. As the HR pathway operates, different DNA substrates and intermediates are formed that physically inter-connect separate DNA molecules crating a joint-molecule (JM) intermediate. These intermediates are a threat to the successful segregation of chromosomes and are to be dismantled during mitosis by different specialized proteins acting in concert to prevent segregation defects and genome rearrangements. In yeast, the dissolution pathway mediated by the complex of Sgs1- Top3-Rmi1 (STR) ensures the disentanglement and release of double Holliday Junctions (dHJ) and two other helicases, Mph1 and Srs2, act early on in the pathway preferentially over D-loop intermediates to reduce the number of joint-molecule intermediates and ensure the completion of the recombinational repair without crossing-over between the DNA templates involved. Opposed to these non-crossover (NCO) pathways, the nucleolytic processing of these JM intermediates can result in reciprocal crossovers (CO), with the risk of genome rearrangements and loss of heterozygosity (LOH) events [28, 493].

Given the risk for genome stability of a nucleolytic processing of HR intermediates, the different actors able to cleave these intermediates are strictly controlled and used as an option of last resort in DNA substrates not previously dismantled by the action of helicases [163, 471]. Two major nucleases are involved in the nucleolytic processing of recombination intermediates in the yeast model, Mus81-Mms4 and Yen1 [177]. The Mus81-Mms4 nuclease plays different roles at replication forks, and is gradually hyper-activated by Cdc5- and Cdc28/CDK1-dependent phosphorylation of Mms4 to peak its activity in late G2/M [188, 190, 494] where it associates with the Slx4-Dpb11 scaffold[530], its broad substrate recognition enables Mus81-Mms4 to cleave 3'-flap containing DNA substrates and Holliday Junctions, preferentially when they are still nicked or not completely ligated [434]. Its hyper-activation in late G2 and its broad substrate specificity positions Mus81-Mms4 in a critical role to cleave both captured D-loop and early HJ intermediates, possibly targeting these intermediates that can't complete full conversion to a dHJ and thus remain inaccessible to processing by the STR complex [163]. As mitosis progresses, the Cdc14 phosphatase will trigger the reversal of the inhibitory Cdc28-mediated phosphorylation of Yen1 in turn allowing its nuclear localization and its proper substrate recognition [459, 460]. This late activation of Yen1 at the anaphase entry ensures that all remaining recombination intermediates, especially those that escaped dissolution by STR or cleavage by Mus81-Mms4, are resolved before mitotic exit [459, 460]. To ensure the clearing of Yen1 nuclease from the nucleus in the subsequent S-phase, and prevent off-targeted activity directed to 5' flap containing DNA intermediates, Yen1 is additionally controlled by a sumo-targeted degradation mediated by the Slx5-Slx8 ubiquitin ligase, further limiting the potential of crossover formation [531].

Protein covalent modification with the small ubiquitin-like modifier (SUMO)[296] is an important mechanisms to fine tune DNA-mediated transactions during the DNA damage and repair responses [400, 495, 497, 498]. In *Saccharomyces cerevisiae*, Sumoylation occurs in a multi-step reaction involving the E1 Aos1-Uba2 activating enzyme dimer, the E2 conjugating enzyme Ubc9, and three possible E3 ligases (Siz1, Siz2 and Mms21), with some redundancy of Siz1 and Siz2 for its substrates [304, 313, 496]. Several players of the HR pathway, besides the nuclease Yen1, are also found among the sumoylated DNA repair targets, including Rad52, PCNA, RPA and Sgs1 [130, 288, 396, 400, 403, 408]. Sumoylation is able to influence biological processes in different ways. Proteins can be mono-sumoylated, multi-sumoylated or poly-sumoylated, and the modification will re-design the protein

surfaces allowing changes in protein activity, or in its way it can interact with other proteins. One of the best-described effects of protein Sumoylation is the enabling of interaction with other protein partners in a bait-to-prey fashion using sumo as the moiety that is recognized by a specific domain in the partner protein, called a SUMO Interacting Motif (SIM). These motifs are found throughout species and according to its amino acid composition can be classified in several families of consensus sequences [357]. Most SIMs can be defined as a core stretch of four amino acids with a majority of hydrophobic residues (typically rich in V/I/L). This hydrophobic core fits into the hydrophobic groove on the SUMO surface and is often flanked by a stretch of 3-4 acidic or polar residues in the SIM sequence that interact with basic residues on the surface of SUMO [359-361, 532]. SIM types showing the flanking stretch of acidic residues present thus a similar architecture to that of ubiquitin interacting motives (UIM) that also show a stretch of polar residues flanking the more loosely hydrophobic core [346, 358]. SIM motifs are able to interact with mono or sumoylated proteins and can be usually present in tandem dispositions, probably helping interact with multiple sumoylated lysines or with a poly-sumoylated lysine in the interacting protein [300, 516, 532]. Interactions by sumo-SIM partnerships are extremely labile and can be easily induced and curbed down by altering the Sumoylation status of the involved proteins, this flexibility allows a quick building of protein complexes in response to changing stress conditions in the cell [400, 516]. The build up of these protein complexes by sumo-mediated recruitment via SIM is generally associated to the actual sumoylation of the two proteins involved [337, 365], and it was thus not surprising to identify in Yen1, which is sumoylated [531], several putative sumo interacting motifs. In the present study we define two functional SIMs in Yen1 C-terminal region that play important roles in the nuclease sub-nuclear localization and its function alleviating the persistence of chromosome-segregation challenging joint-molecules through the end of mitosis.

4.2.2 Results

Yen1 contains two functional SUMO-binding motifs (SIM) at its C-terminal region

As stressed before, sumoylated proteins are able to transiently interact with a variable strength to other proteins containing "sumo-interacting" motives. These motives consist in a stretch of aminoacids with a core of aliphatic residues, often flanked by three or more aminoacids with a negative charge or susceptible to become phosphorylated [357]. We inspected the Yen1 sequence through available algorithms [357] to detect SIM motifs and we identified at least three interesting hits in the primary sequence of Yen1 (Figure 48A). To validate the presence of such motives in Yen1 we performed a two-hybrid analysis with Smt3 as bait and either wild type full-length or truncated versions of Yen1 as a prey (Figure 48B). The ability to interact with sumo in the two-hybrid assay was only retained by the C-terminal part of Yen1 (aminoacids 354 to 759) and mutations in two putative SIMs present in that half of the protein completely abolished the interaction. A mutation in the first SIM, a type r motif [357] with a core at aminoacids 636 to 642 and a flanking stretch of acidic residues was indeed sufficient to almost completely impair the binding to Smt3 in the two-hybrid assay (Figure 48B). Interestingly, this motif is highly conserved across Yen1 in other fungi and is very reminiscent of SIMs found in the Slx5, Rad18 and Elg1 proteins (Figure 55 – Supplementary figure 1) [337, 515, 533].

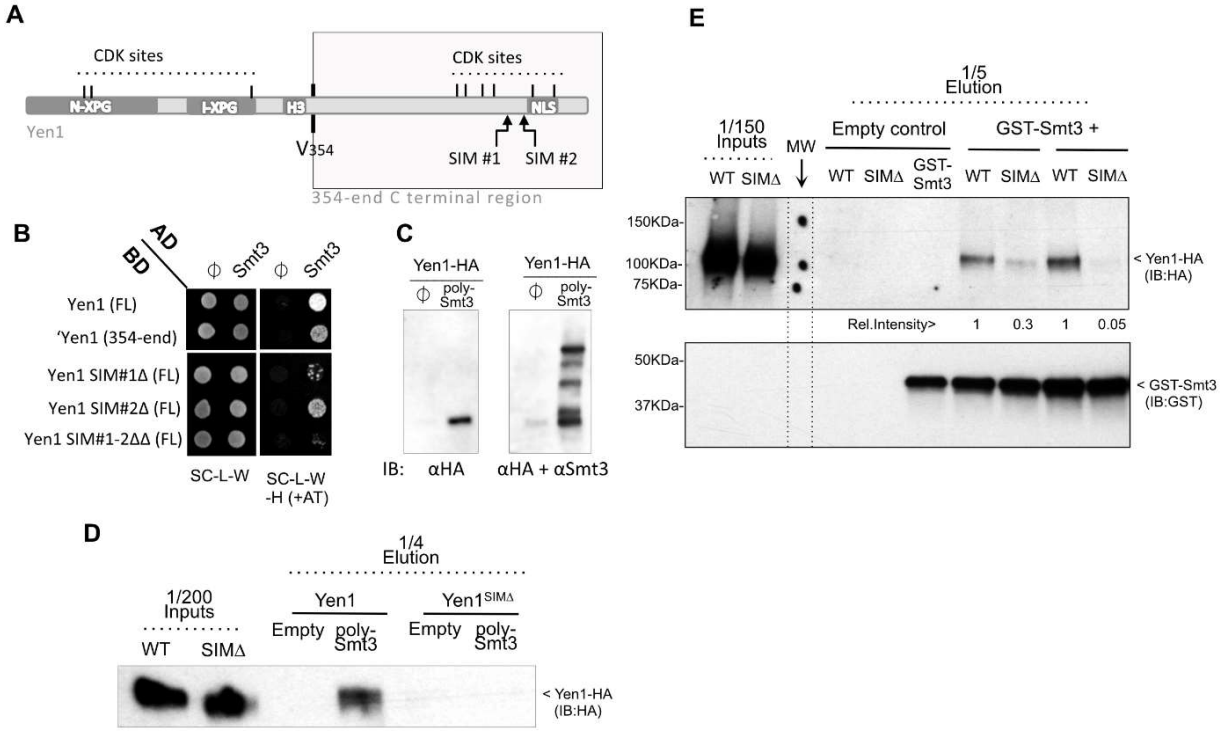

Figure 48. *Yen1 contains two Sumo Interacting Motifs (SIMs) in its C-terminal domain* ***(A)*** *Diagram showing the conserved domains of Yen1 and the positions of the regulatory Cdk1-phosphorylation sites bundled in three clusters (two last clusters merged) [191]; Amino acid 354 shows the cut-off point for truncated forms of Yen1 in Two-Hybrid assays; the two identified candidate SIMs are shown near the nuclear localization sequence (NLS).* ***(B)*** *A Two-hybrid assay was performed with strains carrying the indicated Activator Domain (AD) and DNA Binding Domain (BD) plasmids to test interaction of Yen1 to Smt3 (SUMO) and the Yen1 critical domains for such interaction. Mutations D635A D636A D637A for SIM1 and V675A E677A for SIM2 were introduced to test the putative SIMs. Strains were grown on selective media lacking Leucine and Tryptophan and spotted in selective media also lacking Histidine to reveal interaction of the proteins fused to the AD and BD domains. Non-specific interactions were minimized by the addition of 3-aminotriazole (AT) [534].* ***(C)*** *A SUMO-retention assay was performed where poly-Smt3 chains of multiple sizes generated in vitro were immobilized to a Cobalt Ni-NTA matrix and mixed with equal amounts of either Yen1 or the Yen1 mutated in its putative SIMs. After letting Yen1 interact with the poly-Smt3 coated matrix, the matrix was eluted in denaturing conditions and the eluates inspected by western blot for the presence of Yen1 (anti-HA, left panel) and the pre-bound Smt3 chains (right panel).*

Even though the mutation of consensus SIM sites abolishes the interaction, the two-hybrid assay is based in the detection of growth by activation of metabolic pathways and can not clearly distinguish between a covalent sumo interaction to Yen1 and a non-covalent binding of a sumoylated protein or a poly-sumo chain to Yen1. Even mutations to Smt3 preventing covalent modification of proteins would have an impact to eventual partners of Yen1 with the question of covalent or non-covalent binding of Smt3 to Yen1 remaining unanswered. To better assert the nature of the interaction lost in our mutants and thus validate the SIM sites, we decided to generate an affinity column containing poly-sumo chains to test whether they have the ability to non-covalently bind to Yen1 and thus capture the protein in a retention assay (Figure 48C). We generated Smt3 chains by adding Aos1-Uba2 and Ubc9 in a reaction with purified 6xHis-Smt3 [531], the resulting poly-sumo chains were dialyzed and used to bind to a Cobalt Ni-NTA matrix, the poly-Smt3 coated matrix was used to test retention of Yen1-1xHA (Figure 48C). While the column retained the wild-type Yen1, the recovery of the SIM mutant ($Yen1^{SIM\Delta}$) was greatly decreased (Figure 48D), thus confirming that Yen1 binds non-covalently to sumo chains and that the two identified SIMs increase the ability of Yen1 to bind to Smt3 non-covalently. We further confirmed the non-covalent binding of Yen1 to Smt3 by using a common pull-down approach [337]. GST-Smt3 was over-expressed and purified from bacteria, and bound to a Glutathione resin, purified Yen1 or its mutant SIM variant were then allowed to bind to the pre-bound GST-Smt3, and after several washes, the column content was eluted in denaturing conditions and inspected by western blotting (Figure 48E). Again, Yen1 was detected in the eluates, but was much less retained (5-30% compared to wild-type) when bearing mutations in its SIMs (Figure 48D). While the GST-Smt3 column may indicate the ability of Yen1 to bind to monomers of Smt3 through its SIMs, the packed dispositions of GST-Smt3 in the column can also be mimicking a poly-sumoylated chain and contact Yen1 simultaneously in multiple SIM sites.

Strains carrying a SIM-defective variant of Yen1 display increased sensitivity to DNA damage

We next aimed to understand the effect of the mutations in the SIM motifs on the ability of Yen1 to be normally regulated by Cdk1/Cdc14 and shuttled timely to the nucleus. We introduced the mutant Yen1 variants in the endogenous locus and determined its cyclic phosphorylation by synchronizing cells in G1 and analysing the mobility of the protein at different time points after its release (Figure 49A). All the mutants displayed a normal cycle of phosphorylation in S-phase followed by gradual de-phosphorylation (Figure 49A) with a slight variation in the total amount of the protein all across cell-cycle phases. Given the proximity of Yen1's SIMs to its NLS, a C-terminal GFP fusion of the Yen1 mutants was also monitored to see if any gross defect occurred for its nuclear shuttling. Both single and double SIM mutants presented nuclear exclusion in S-phase as the wild-type and were nuclear in late mitosis and G1 (Figure 49B).

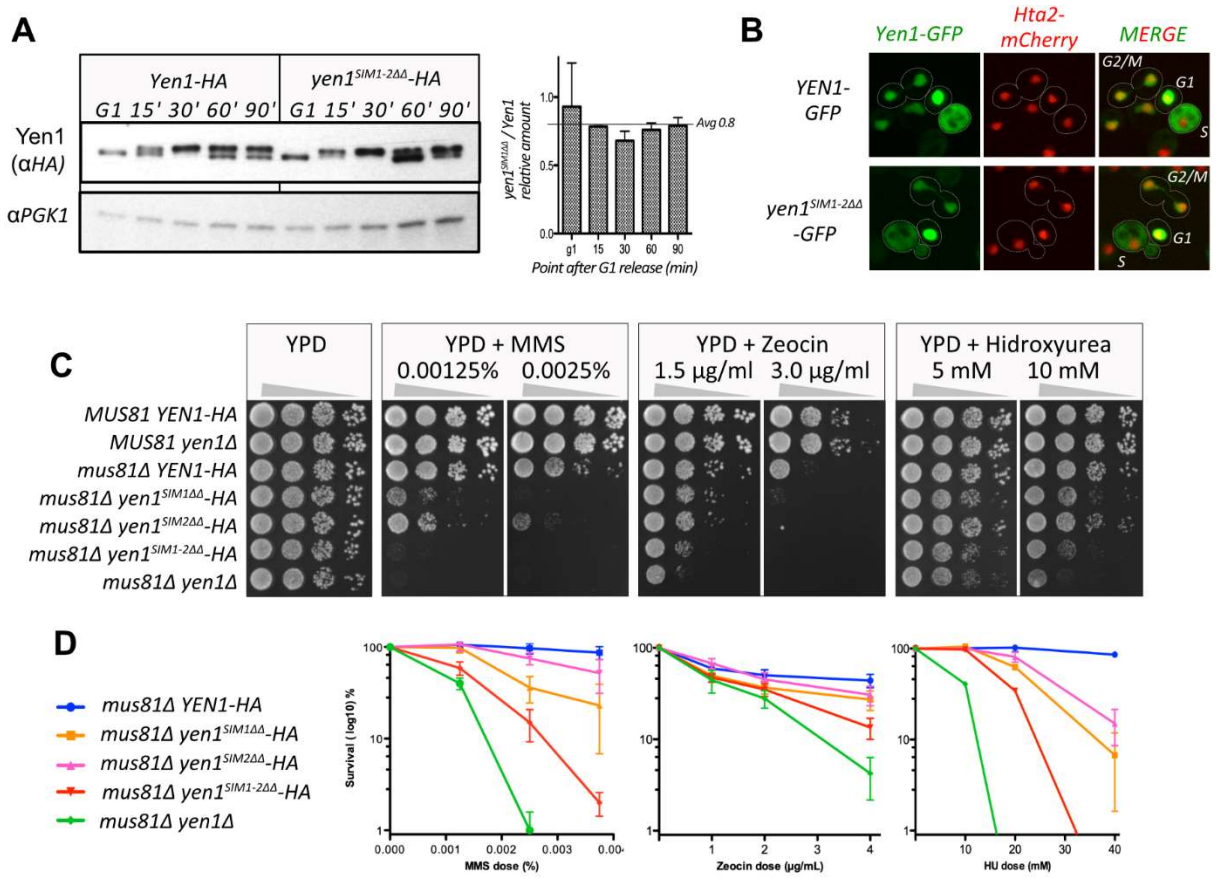

Figure 49. *Mutation in Yen1 SIMs has no impact to its CDK1 regulation and nuclear shuttling but sensitizes cells to DNA damage* ***(A)*** *Strains with a chromosomally inserted copy of –HA tagged wild-type Yen1 or its double SIM mutant (Yen1^{SIMΔΔ}) were synchronized with alpha factor and released into fresh medium to monitor the modification of the protein through the cell cycle by immunoblot (left). Both unmodified and phosphorylated Yen1 are indicated. Average levels of endogenous Yen1 were normalized with PGK1 in triplicate experiments (right).* ***(B)*** *Cells carrying an endogenous histone Hta2-mCherry marker and chromosomally –HA tagged versions of Yen1 wild type and Yen1^{SIMΔΔ} were transformed with a plasmid carrying an equivalent version of Yen1 fused with GFP at its C-terminal region. Cells were grown on selective media and observed using a spinning-disk microscope after a brief induction with galactose. Shuttling of the protein from cytoplasm to the nucleus can be observed in representative fields displaying cells with nuclear excluded Yen1 (S-phase and early G2-M) and nuclear localized Yen1 (anaphase to G1).* ***(C)*** *Sensitivity to different DNA damaging agents and drugs was determined by spotting serial dilutions of strains carrying different Yen1 mutants in its SIM in a MUS81 deleted background for the indicated media.* ***(D)*** *Survival curves to the agents tested in (C) were established by counting colony forming units of the different strains after plating in YPD containing the indicated doses of drugs in replicate trials. Survival was normalized per trial with its respective control YPD counts and the average % survival is plotted in the graphs (+/- SEM). Statistical significance was estimated by the student T-test at P<0.05.*

Next we asked whether the presence of an endogenous copy of the SIM mutants would compromise the ability of Yen1 to back-up for the functions of Mus81-Mms4 [177]. The mutants were introduced into a *mus81*Δ background and tested for its sensitivity to an array of DNA damaging agents (Figure 49C and D). Cells with a double mutation *mus81Δ yen1Δ* are extremely sensitive to MMS at low doses, and they also present a moderate sensitivity to the radiomimetic drug Zeocin and to the replication stalling drug Hydroxyurea (HU) [531], both a mutation in the first SIM and the double SIM mutant significantly increased the sensitivity of a *mus81*Δ strain to MMS, while mutation in the second SIM alone did barely increase this sensitivity (Figure 49). Similar results were observed with Zeocin and HU but with less marked differences to the *mus81Δ* single mutant (Figure 49C and D).

Mutation on the SIMs of Yen1 does not impair its nuclease activity

To understand if the defective phenotypes we detected with the SIM mutants were related to a faulty nuclease activity we decided to verify the Yen1 activity *in vitro* using a synthetic Holliday Junction [535] as a substrate. Immuno-precipitated Yen1 was added to cleavage reactions, and we compared the yield of HJ cutting for either the wild-type Yen1 and the SIM defective mutant Yen1$^{SIM1\text{-}2\Delta\Delta}$. The nuclease activity was undistinguishable for both the wild-type and the mutant, that were able to linearize the HJ substrate at similar rates (Figure 50). Alteration of the SIM motifs at the C-terminal part of the protein seems thus not to alter the cutting efficiency of Yen1, whose nuclease and conserved XPG domains are present at the N-terminal part of the protein (Figure 48), the test nonetheless did not take into account the disposition of the junction in a chromatin context in the cell.

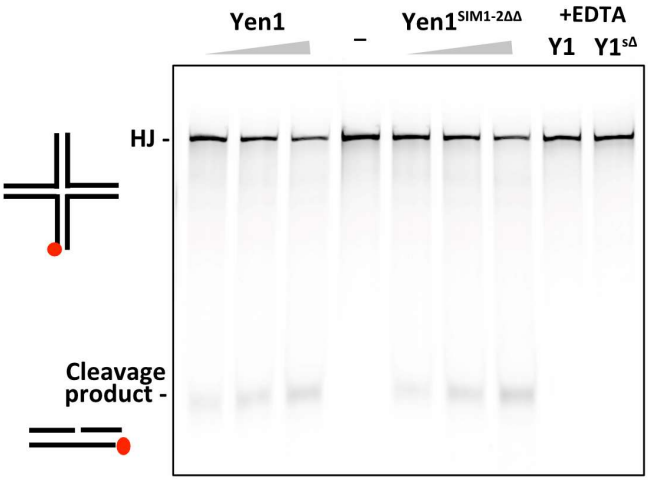

Figure 50. *Nuclease activity of Yen1 is not affected by mutation in its SIMs. Activity of Immuno-precipitated Yen1 was tested in a re-constituted cleavage reaction using synthetic Holliday Junctions (HJ) made with oligonucleotides and labeled with Cy5. The DNA products were run in non-denaturing PAGE and revealed by the fluorescence of the Cy5 labeled oligonucleotide. Controls were run to determine the size and apparent size of linear and four-way HJ substrates, respectively.*

Yen1 covalent Sumoylation is reduced in the SIM mutant in vivo

In other sumoylated DNA repair proteins containing functional SIMs, the mutation of these motives has an impact in the ability of the protein to be directly sumoylated [337, 365]. We decided to test if that was indeed the case for Yen1, which we have previously characterized to be sumoylated [531]. We compared the sumoylation levels of the wild-type and the SIM-defective Yen1 mutants by performing denaturing pull-downs of His-tagged Smt3 (Figure 51). Yen1 sumoylation peaks when cells are exposed to high MMS doses [531] and we reproduced Yen1 sumoylation in these conditions for the wild-type protein (Figure 51). Nonetheless, the fraction of sumoylated Yen1 in the mutant in either the first SIM motif or the double mutant in the two SIM motives was greatly reduced in conditions with similar input levels (Figure 51). The mutations introduced to inactivate the SIM sites do not contain any lysine substitution, to confirm that the lack of Sumoylation was not due to the absence or un-accessibility of Sumoylation-target lysines in Yen1, we decided to test the mutant protein in an *in vitro* Sumoylation reaction. After a reaction of the SIM mutant of Yen1 with Aos1-Uba2 and the conjugating enzyme Ubc9, a normal Sumoylation pattern was detected with the same ladder of bands of increasing size (Figure 51). While the yield of the reaction was slightly lower in the mutant, the presence of the SIMs mutations does not preclude modification of any of the Lysines targeted by the Sumoylation machinery.

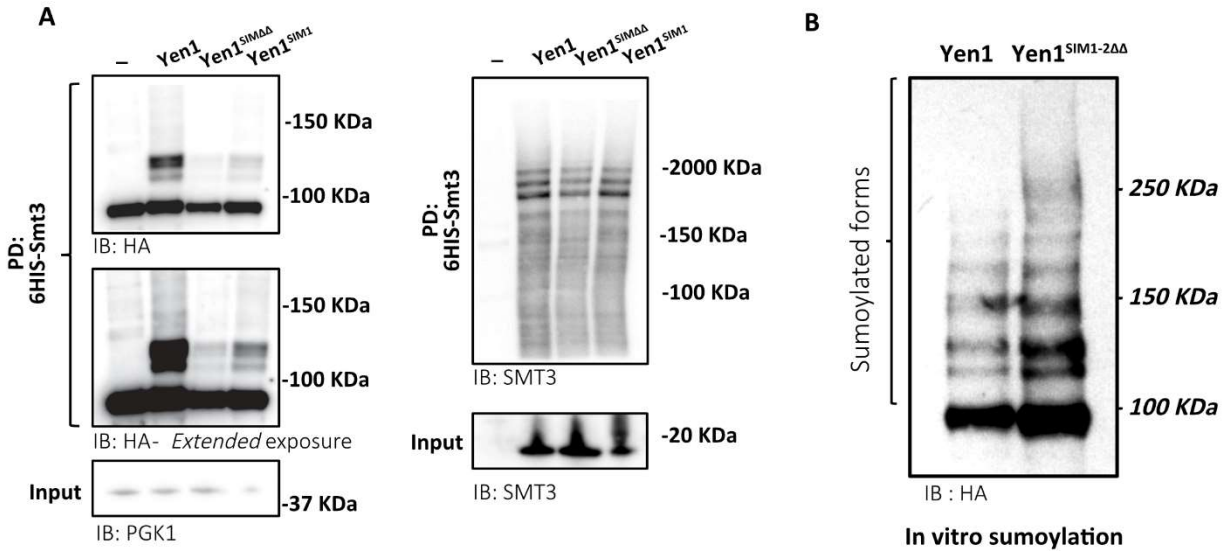

Figure 51. *The mutation of Yen1's SIMs prevents Yen1 sumoylation in vivo.* ***(A)*** *Strains carrying endogenous copies of -HA tagged wild type Yen1, Yen1$^{SIM1\Delta}$ and Yen1$^{SIM\Delta\Delta}$ mutants, with (+) or without (Ø) the plasmid pCUP-6xHIS-Smt3, were grown in the presence of MMS. Cells were lysed and lysates subjected to a denaturing Ni-NTA pull-down followed by immunoblot analysis. Yen1 was detected by anti-HA (top-left). Membranes were subsequently probed with anti-Smt3 (Bottom-left). Prior to Ni-NTA pull-down, input samples were taken from the lysates and were analyzed by immunoblotting for the levels of Smt3 induction (Right) and relative protein amounts (Anti-PGK1) of each lysate (Bottom-left).* ***(B)*** *Purified Yen1-HA and Yen1$^{SIM\Delta\Delta}$ mutant variant were subjected to an in vitro sumoylation reaction containing Aos1-Uba2, Ubc9 and Smt3-3KR and subjected to Tris-Acetate PAGE for comparison of their sumoylation patterns after immunoblotting with anti-HA.*

Yen1 localization to spontaneous and induced sites of activity is impaired in the SIM mutants

Sumoylation and interaction with SIMs has been proposed as a way to enforce a cascade of interactions to foster recruitment of factors to specific subcellular locations [516]. We decided to determine if the impairment of the Yen1 SIMs was somehow altering the normal behaviour of Yen1 by studying its ability to cluster in foci that are observed to occur either spontaneously or induced by DNA damage [471, 531]. C-terminal GFP tagged versions of Yen1 were compared for its foci distribution and we observed a sharp decrease of the number of cells displaying foci for the SIM1 mutant and the double-SIM mutant (Figure 52B, Figure 56 – Supplementary figure 2), barely recapitulating the phenotypes observed for its sensitivities to MMS (Figure 49). The number of cells showing spontaneous foci in a wild-type strain ranges around 10%, while only 3% of either the SIM1 or the double mutant displayed foci in strains with a functional Mus81-Mms4 (Figure 52B). The effect was more marked when observing the spontaneous foci in a *mus81Δ* strain where cells displaying foci decreased from 30% to 3-4% in the presence of the SIM mutant Yen1 variants (Figure 52B). These foci were equally decreased in the presence of exogenous damages, suggesting that Yen1 SIMs are equally important to properly localize the protein to spontaneous damaged sites and sites of exogenous damages (Figure 52C). We have demonstrated in a previous work a role for the Slx5-Slx8 Sumo-targeted ubiquitin ligase in the removal of a subset of Yen1 from the nucleus, as a result, cells defective in Slx8 show a persistence of Yen1 foci, which are detected in large numbers even in the presence of functional Mus81-Mms4. Slx5-Slx8 ubiquitin ligase is able to target Yen1, and its deletion induces the accumulation of a subset of the nuclease that can be detected as an increased number of Yen1 foci and a more stable fraction of Yen1 during a cycloheximide chase from cells released from a G1 arrest in media with this inhibitor of protein synthesis [531].

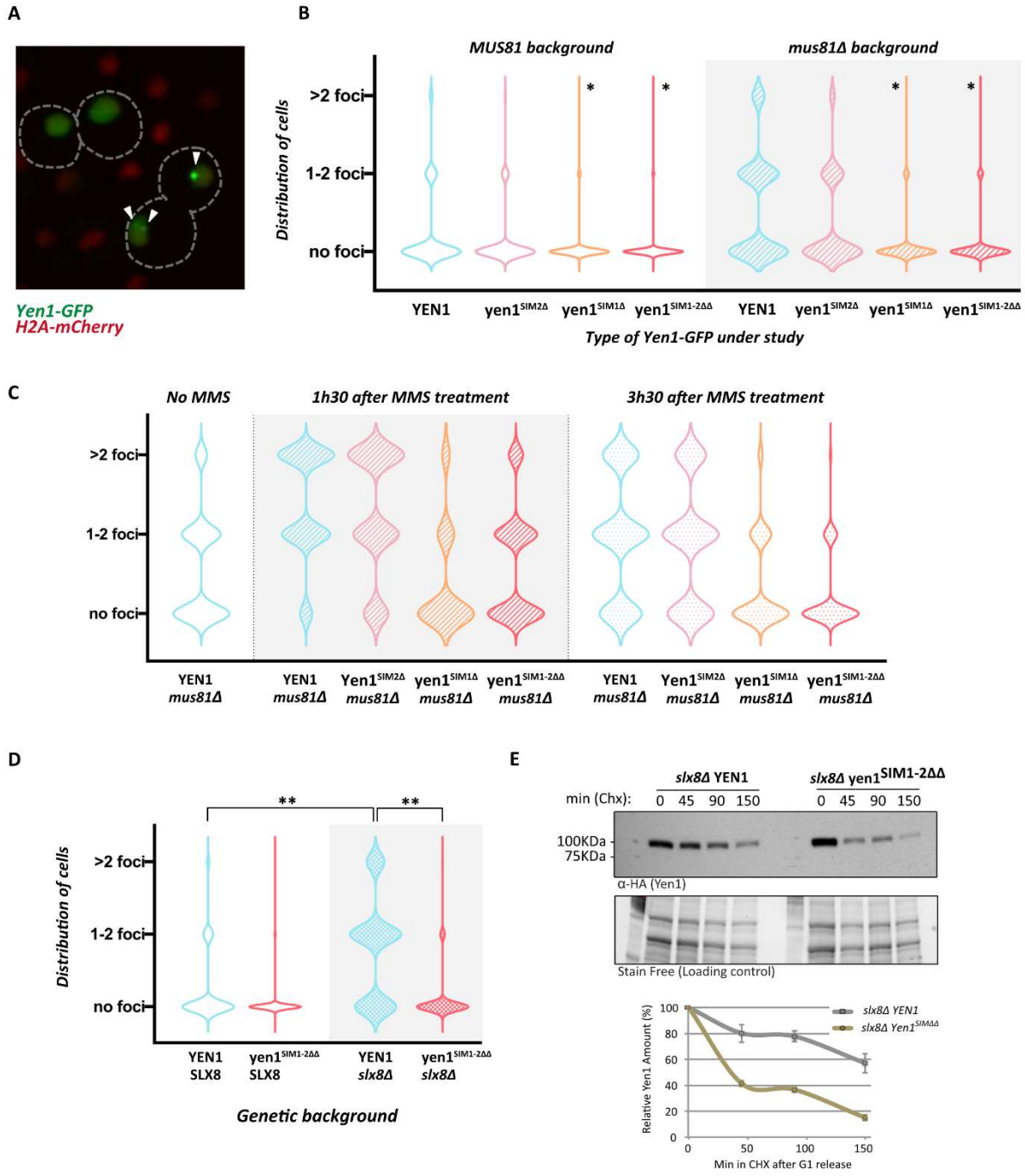

Figure 52. *Mutation in the SIMs of Yen1 prevent foci accumulation in G2/M.* ***(A)*** *Cells with an endogenous Hta2-mCherry and YEN1-HA expressing Yen1-GFP observed under a spinning-disk microscope after a brief induction with galactose. The white triangles denote the presence of Yen1-GFP foci.* ***(B)*** *Chromosomally tagged Yen1-HA wild type and SIM mutants in the indicated genetic backgrounds and carrying the corresponding Yen1-GFP expressing plasmid were observed under the microscope after a brief induction. Pictures of several fields were taken for each trial and cells were classified according to their cell cycle phase and the presence or absence of Yen1 foci. Violin Plots display the distribution of G2/M cells showing: no foci, 1-2 foci or more than 2 foci for each strain. Counting was performed for over 400 distinct G2/M cells for each strain over several independent trials.* ***(C)*** *Cells from the indicated genotypes were treated with MMS (0.1% for 15min) and observed 1h30 and 3h30 after release into fresh media without MMS. Violin plots display the distribution of cells presenting Yen1-GFP foci as in (B), the untreated mus81Δ cells plot is shown as reference.* ***(D)*** *Cells containing a deletion on SLX8 were observed for their distribution of foci of the different variants of Yen1-GFP. Violin plots display the distribution of cells as in (B).* ***(E)*** *Cells from the indicated genotypes were arrested in G1 and released in the presence of cycloheximide with samples being taken at the indicated time points. Total protein extracts were inspected by immunoblot for the presence of Yen1-HA and their intensity quantified relative to the loading control obtain by stain-free imaging (BioRad), relative amounts of Yen1 are plotted in the graph to facilitate comparison. Statistical significance for foci distribution difference was estimated by the Fischer exact test and asterisks denote p<0.05 compared to wild-type.*

We wondered if the absence of proper localization in the SIM mutant would prevent Yen1 accumulation in the absence of Slx5-Slx8. According to our expectations, a deletion of *slx8*Δ in the strain bearing the mutations in the Yen1's SIMs did not increase the number of Yen1 foci, thus suggesting mis-localization of Yen1 in the mutant strain prevents the need for Slx5-Slx8 targeted removal (Figure 52D). Moreover, in a slx8Δ background, the mutant protein was degraded during a cycloheximide chase faster than the wild-type protein (Figure 52E) indicating that the lack of accumulation of Yen1 at nuclear sites does also dispense a targeted removal of this subset of the nuclease, that is removed timely even in the absence of sumo-targeted ubiquitination by Slx5-Slx8.

Unpaired sumo-directed localization induces an increase in untimely chromosome segregation

The presence of both *mus81*Δ and *yen1*Δ deletions makes cells synergistically sensitive to drugs like MMS, and also increase their spontaneous number of chromosome mis-segregations monitored either by dedicated genetic systems [177, 470] or by a direct observation of fluorescent-tagged chromosomes during mitotic divisions [531]. We compared the mitoses of single *mus81*Δ cells to that of cells carrying *mus81*Δ and the allele with the two mutated SIMs. Similar to what we could observe in a *mus81Δ yen1Δ* control strain, *mus81*Δ cells with the mutated Yen1 SIMs displayed an increased number of segregation issues. Plotting the segregation timings of each cell in a violin plot graph shows how most of the cells manage to divide in a similar time interval as that observed for the *mus81Δ* cells carrying a Yen1 wild-type allele. Nonetheless, a sub-population of lagging cells appears, which still manage to complete G2/M, albeit with a delay (Figure 53B). Introducing the SIM mutations in Yen1 in cells with a *mus81Δ* background results in a segregation phenotype similar to that observed in *mus81Δ yen1Δ* cells, with a larger number of cells with a lagging segregation and roughly 30% of the cells unable to resolve its segregation within the time of video-microscopy observation (2hrs), classified as non-disjunctions (Figure 53B).

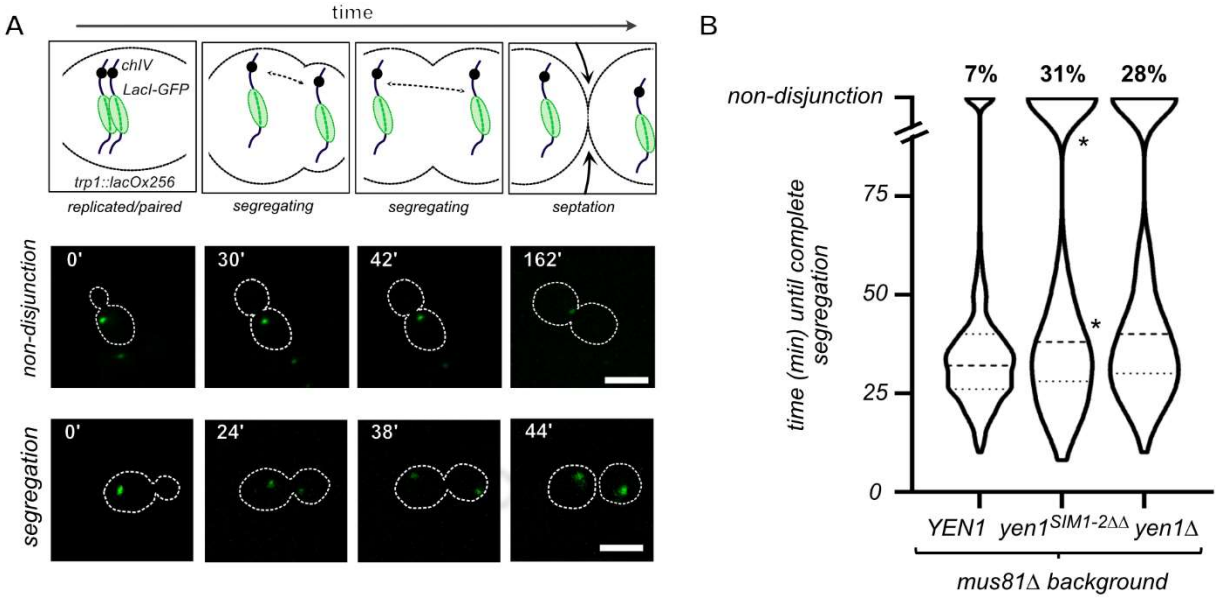

Figure 53. *Mutation of the SIMs of Yen1 impacts the chromosome segregation in mus81Δ cells.* ***(A)*** *Diagram showing representative drawings of chromosome segregation in cells harboring a lacO/GFP-LacI array tag on chromosome VII. To discriminate cells with a timely chromosome segregation from those presenting different types of aberrant segregation (delayed segregation, non-disjunction and aberrant chromosomal numbers) a 2h limit of observation was implemented, the time intervals to achieve full GFP-dot separation into daughter cells was determined for each individual cell observed, and cells un-segregated at 2hrs were classified as non-disjunctions. Two sets of representative actual images of a normal segregation pattern and a non-disjunction pattern are shown below the diagram.* ***(B)*** *Over 400 cells per strain were individually counted and are represented in violin plots according the time spent to segregate the lacO/lacI array. Statistical relevance of the differences observed was determined by the Fischer exact test at P<0.05.*

Mutation in the SIM of Yen1 reduces the formation of crossing-over

To finally browse the implication of the presence of a defective sumo-interacting Yen1 allele for the actual resolution of recombination intermediates, we decided to analyze the level of crossing-over (CO) formation in two widely used tests that estimate the CO levels after a single DSB formation [163, 177, 469]. In accordance with the increased sensitivity to different DNA damaging agents observed for the Yen1 allele carrying the SIM mutations when combined with a *mus81Δ* background (Figure 49), we detected a decreased formation of crossovers in this strain after the induction of a single DSB in a diploid tester strain [177], half-way to the phenotype observed with a double mutant carrying both deletions in *mus81*Δ and *yen1*Δ (Figure 54A). The decrease in crossover formation was paralleled by a slight increase in BIR events (Figure 54A). Using an ectopic recombination assay [469], we detected a decrease in viability after the induction of an HO cut site in chromosome II in the *mus81*Δ *yen1*$^{SIM1\text{-}2\Delta\Delta}$ strain, already signaling a defective crossover resolution resulting in a number of unviable events. This survival decrease probably reflects a BIR increase that in this test leads to lethality by the loss of essential genes in the chromosome II distal arm. The number of crossovers quantified by southern blotting analysis of the survivors showed a nearly 50% reduction in the crossover yields, as previously reported for a strain carrying both deletions in *mus81*Δ and *yen1*Δ [163] (Figure 54B).

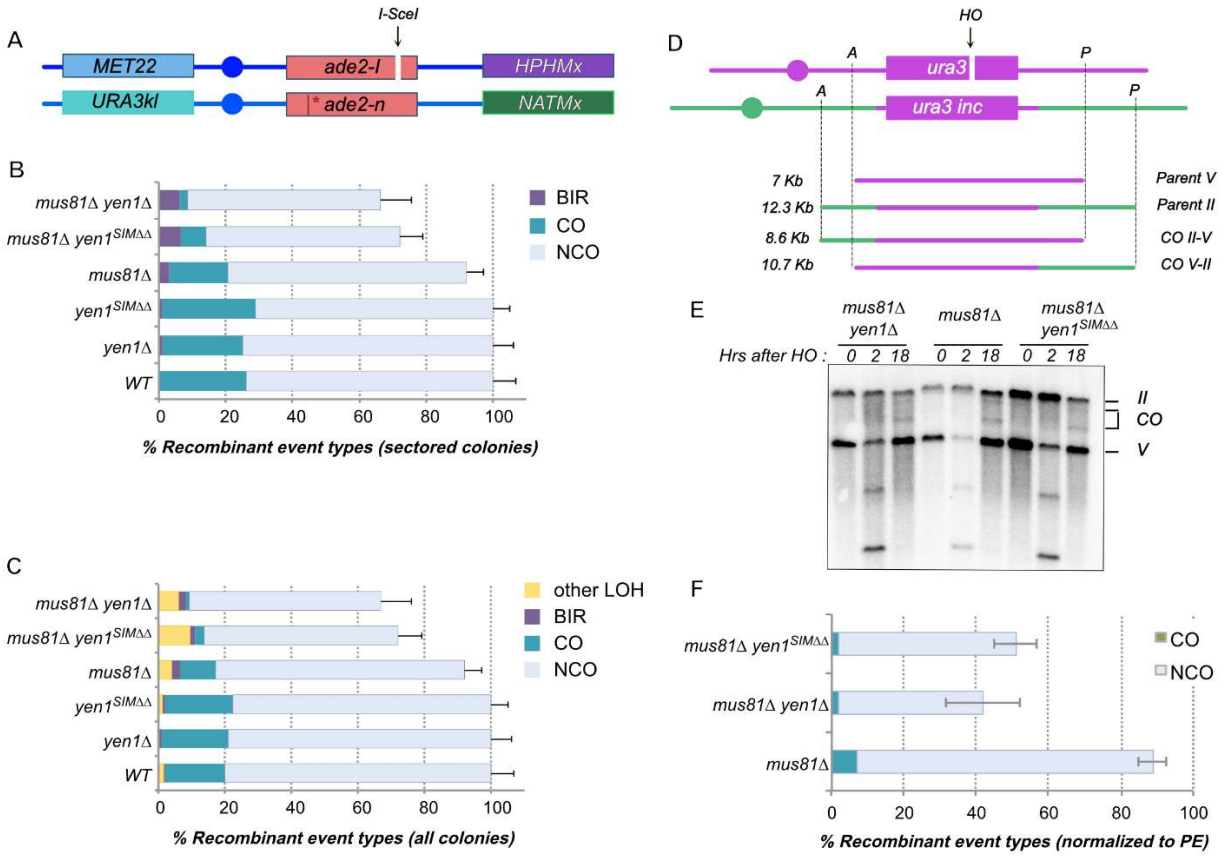

Figure 54. *Crossover formation is impaired in cells containing the SIM mutant version of Yen1.* ***(A)*** *Diagram showing the ch XV based DSB-induced recombination reporter.* ***(B)*** *Graphs summarize recombination outcomes in either red-sectored colonies or all types of colonies* ***(C)*** *combined with the indicated strains and normalized to their Plating Efficiency (PE). Statistical significance was determined by the Fischer exact test at P<0.05.* ***(D)*** *Diagram showing the ch II-V based ectopic DSB-induced recombination reporter and its expected outcomes during physical analysis by southern blotting* ***(E)*** *with a probe at the URA3 locus.* ***(F)*** *Quantification of three independent southern blot analyses is plotted relative to PE (Galactose vs Glucose). Statistical significance was determined by the Student T-test at P<0.05.*

4.2.3 Discussion

In the present work we aimed to understand whether the Yen1 nuclease depends on interactions with sumoylated partners to be able to act accurately and promptly on its substrates. We have demonstrated that in addition to being sumoylated [531], Yen1 is also able to interact non-covalently to sumoylated chains and sumo monomers through at least two sumo-interacting motifs in its C-terminal region (Figure 48). These SIMs mediate interaction to SUMO in either a classical two-hybrid assay or pull-down assays (retention assays) with either immobilized GST-Smt3 or pre-polymerized poly-(6HIS)-Smt3 coupled to a NiNTA Cobalt resin (Figure 48). Although our experiments point to a non-covalent interaction of Yen1 to SUMO in these experiments, we also have demonstrated that the absence of such interaction in a mutant variant of Yen1 modified in critical residues of its SIMs leads to a nearly complete loss of direct sumoylation of Yen1 when analysed by denaturing pull-downs from cell extracts (Figure 51).

Previous reports suggested covalent sumoylation occurring in the C-terminal region of Yen1 was responsible for the Smt3-interaction detected in a two-hybrid assay [536], our results are in agreement with the original observation of a C-terminal motif mediating a Smt3-interaction but our retention experiments and the absence of interaction of our rather limited set of mutations in two SIMs point to a non-covalent nature of such interaction. Nonetheless, the intimate relation between non-covalent interaction to sumo and sumoylation makes it difficult to assert whether one precedes the other, our *in vitro* sumoylation assays suggest that the protein lacking its SIMs is still able to interact to the sumoylation machinery and be sumoylated at similar rates compared to the wild-type (Figure 51) but this reaction might be prevented by a faulty localization via SIMs to the sites where the sumoylation enzymes are already working in a given cell. While the absence of the SIMs in Yen1 has no effect in its catalytic activity (Figure 50), we have detected a sub-optimal function of these mutants in the cells, leading to phenotypes of chromosome mis-segregation and DNA damage sensitivity similar to those observed for a null mutant in combination with a deletion of the somehow redundant cell's major resolvase activity mediated by the heterodimer Mus81-Mms4 [177]. Indeed, these phenotypes correlate with the inability of the SIM mutants of Yen1 to properly localize in mitotic cells in previously characterized sub-nuclear localizations as foci, mainly at the vicinity of the nucleolus when cells are not exposed to exogenous DNA damage [531] (Figure 52). The impaired localization not only seems to induce a sub-optimal function of Yen1 in response to spontaneous damages under normal growth conditions, but also decreases the number of crossing-over that can be observed after single DSB induction in two different settings (Figure 54). Our initial efforts to identify the partners that interact through SUMO with Yen1 have not been conclusive enough to determine the composition of the sumo-mediated complex including Yen1. One hypothesis is that group modification [516] is responsible for a local enrichment of multiple sumoylated proteins together with free Smt3 and the sumoylation machinery when persistent recombination intermediates are somehow revealed during anaphase. It is possible that the condensation of chromosomes and the forces that pull them to the opposite spindle poles may contribute to the recruitment of factors through these group modification mechanisms. It is thus of great interest to continue studying Yen1 functional interactions and overlaps, in conditions that are greatly transient an ephemeral, and determine which other factors ensure prompt Yen1 recruitment to its activity sites during its anaphase activity window thus influencing the delicate balance between chromosome segregation and genome integrity.

4.2.4 Materials and Methods

Yeast Strains and Growth Conditions

S. cerevisiae strains used in this study are derivatives of the W303c background and are listed in Table S1. The Yen1-FX-GFP allele was made by inserting a Factor X site and the GFP epitope from pGAD-Yen1GFP[483] between amino acids D753 and S754 at the C-terminus of Yen1 using dedicated oligonucleotides and was cloned into TOPO-pYES2 (Invitrogen) to allow controlled expression by Galactose induction. Mutants in the different designated loci where either obtained by crossing or by gene replacement with the indicated selective cassettes. Cells were typically grown in YP (1% yeast extract; 2% peptone) or SC media with alternatively 2% glucose, 2% raffinose or 2% galactose in strains under inducible conditions. A modified medium (SC with 0.17% YNB without ammonium sulfate, 0.1% proline and 0.003% SDS) was used for the Smt3 pull-down assays.

Western Blot analyses

If not stated otherwise, proteins were extracted by the TCA (Trichloroacetic acid) method. For routine monitoring, samples were loaded into 7.5% Tris-Glycine stain-free pre-casted gels (BioRad). Samples from pull-downs analyses were loaded into 3-8% gradient NuPAGE Tris-Acetate gels (ThermoFisher). Gels were transferred using a semi-dry transfer machine (BioRad) to PVDF membranes and hybridized with the appropriate antibodies in TBST 5% milk buffer. Antibodies for anti-HA(HRP) (3F10, Roche), anti-Smt3 (B.Palancade), anti-Pgk1(HRP) (22C5D8, Abcam) were used at the suggested dilutions and revealed using an ECL reagent (Advansta). When required, HRP-conjugated secondary antibodies from Cell Signaling were used at 1/10000 dilution.

Microscopy and Cell Biology Methods

Live cell imaging was performed with a Spinning Disk Confocal Microscope (CSU-W1, Yokogawa), with an electron multiplying charge device camera (ANDOR Zyla sCMOS) and a ×60/1.35 numerical aperture objective at 30 °C. Cells were centrifuged and plated as a droplet between an SC agarose pad and a glass slice [522]. Images were recorded with 17 z-sections with 0.5 µm spacing for each wavelength at a time. Video recordings were built with images taken 2 minutes apart. Image acquisition was performed using Image J-Fiji [523]. For Yen1 foci observations, cells were grown in SC medium without uracil (SC-URA 2% raffinose), GFP-Yen1 was induced in a short burst with 30 min with Galactose at 2%, followed by addition of Glucose at 2%. DNA damage acute exposures (MMS 0.1% or 10 µg/ml Zeocin) lasted 15 min at room temperature following arrest of GFP-Yen1 expression. After the acute DNA damage, cells were washed once with fresh SC-URA 2% glucose and held for 30 min at 30 °C in this medium, whereas aliquots were removed at the indicated times. Cells showing an accumulation of spots were measured at maximum projection of the GFP channel. Statistical analysis was performed using Fisher's exact test to determine the level of significance between two categories and $\chi 2$ to compare more than two categories and consistency between trials.

For segregation monitoring using strains with the lacO/GFP-LacI array, all cells were recorded for a duration of 3 hrs in their agarose pads. Individual cells were identified with an ongoing chromosome segregation. To determine segregation duration a start point was determined as the frame previous to a 2-fold increase in a single GFP dot intensity immediately before the dot started drifting as two separate dots. The duration of the movement of the two separate dots until they fully separated into daughter cells was registered for each individual cell, cells with dots moving together for the whole duration of the time-lapse were assigned as non-disjunction.

Sumoylation assays and Smt3-bound retention assay

In Sumoylation *ex vivo* assays, the wild-type or mutant Yen1-HA was produced form a pYES2 vector and immuno-precipitated from cell lysates as described [531]. Eluates were subjected to SUMO conjugation as described [503].

For Smt3-retention assays, 6x-His-Smt3 was purified from BL21 *E.coli* cells using a Ni NTA affinity column (Qiagen) following manufacturer indications, eluted with 250mM Imidazole and dialyzed using a G2 Slide-a-Lyzer cassette (Thermo Fisher) with a 10KDa cut-off. Purified Smt3 was subjected to a self-conjugation reaction by adding Aos1-Uba2 and Ubc9 as described [503] and the reaction was subjected to a second purification in a Cobalt HisPur Superflow agarose matrix (Thermo Fisher). Equal amounts of Yen1 or its mutant were added to the non eluted matrix containing poly-Smt3 bound in E buffer (20mM NaH2PO4, 300mM NaCl, 5mM Imidazole, pH 7.4) and binding was allowed for 60 minutes. Columns were then centrifuged to remove the excess buffer and proteins, washed 5 times in washing buffer (E buffer 12.5mM Imidazole) and eluted in denaturing conditions with laemmli buffer 2X at 95ºC. The eluates were loaded into regular SDS PAGE gels and immunoblotted. GST-Smt3 retention assays were performed as described [524] with purified GST-Smt3 obtained by expression of pGEX-4T1-Smt3 into BL21 *E.coli* cells.

Cycloheximide chase experiments

Cycloheximide chase experimetns were basically done as reported [531]. Cultures grown in SC complete modified media (0.1% proline 0.017% YNB w/o ammonium sulfate) were diluted to OD600=0.2 and synchronized with alpha factor (3 µM) for 2hrs. At G1 release, cells were treated with cycloheximide (250 µg/ml) in fresh media and released from G1 arrest and samples were taken at indicated time points and analyzed by TCA extraction and Western Blotting.

Denaturing Histidine pull-downs

For 6xHIS-Smt3 pull-downs, strains containing the expression vectors or the control plasmid were grown in SC-LEU modified medium (0.1% proline, 0.017% YNB without ammonium sulfate). Cells were allowed to grow to OD600=0.3 when CuSO4 was added at 100 µM final concentration in a volume of 100ml. After 1hr, MMS was added to 0.3% and cells were collected 3hrs later. Cells where lysed under denaturing conditions and SUMO-conjugated proteins where isolated basically as described [531].

Synthetic DNA substrates and Yen1 resolvase activity assays

The synthetic HJ-X0 was prepared as described [535] by annealing the Cy5-X0-1, X0-2, X0-3 and X0-4 oligonucleotides (Sigma-Aldrich) in a buffer containing 50 mM Tris-HCl (pH 7.5), 10 mM $MgCl_2$, 100 mM $NaCl_2$. The annealing product was analyzed in a native PAGE to verify the presence of a HJ structure. To test Yen1 activity an enzymatic reaction was performed in 10 µl cleavage buffer (50 mM Tris-HCl (pH 7.5), 1 mM $MgCl_2$, 1 mM DTT) containing 25 nM of Cy5-labled HJ X0 substrate, and equal amounts of immune-precipitated Yen1 or its SIM-defective mutant. After incubation at 30°C for 1 h, the reaction was stopped by adding 2.5 µl of stop buffer (100 mM Tris-HCl (7.5), 50 mM EDTA, 2.5% SDS, 10 mg/ml proteinase K) and further incubated for 30 min at 37°C. Cleavage products were migrated in 10% neutral PAGE, scanned using a Typhoon Scanner and the images were analyzed with ImageQuant (GE Healthcare).

DSB-induced recombination assays

The diploid recombination assays were performed as described previously (for a detailed protocol see [470]). The reporter diploid strains that contain 2 *ade2* hetero-alleles were cleaved by induction of I-

SceI in its *ade2*-I allele and allowed to repair with its ade2-n allele under non-selective conditions to give rise to either ADE2 or *ade2*-n repair products in three types of colonies (red, white and sectored). Outcomes were scored by assigning to each colony the recombination events that correspond to the repair of the two sister-chromatids, and were normalized to the galactose vs glucose plating efficiency.

The distribution of CO and NCO in the ectopic recombination assay based in chromosomes V and II [469] were addressed by southern blot hybridization of ApaLI-PvuII digested genomic DNA from cell populations growing in YP-Lactate after galactose induction of HO. Membranes were hybridized with a *URA3* labeled probe and results were normalized relative to the galactose vs glucose plating efficiency of the strains as described [163].

Acknowledgements
We thank LS Symington, K Dubrana and S Marcand for generous gifts of yeast strains and plasmids. We thank B. Palancade for supplying reagents for the sumoylation assays. We thank the members of the UMR9019 of the CNRS for fruitful discussions and suggestions. This study was supported by grants to GM from Gustave Roussy Foundation (funded in part from donations from Natixis) and from Fondation ARC pour la Recherche sur le Cancer (PJA 20181208087). GM is a full-time INSERM researcher at the CNRS. IT is a full-time CNRS researcher. HD has benefited from a doctoral fellowship from the French Education Ministry.

4.2.5 Supplementary figures

A

	Acid/Polar	Aliphatic	Acid/Polar
Yen1 SIM1	D D D S	L I F V	D E I T
Elg1 SIM2	D D D D	L I V I	S D K S
Elg1 SIM3	H E D D	I S I I	S T S R
Slx5 SIM1	P N E T	V I L I	D S D K
Slx5 SIM2	N N D D	I T I I	R E V G
Slx5 SIM4	S D D G	L T I V	E E R T
Rad18 SIM1	A D D D	L Q I V	A T S E

B

	Acid/Polar	Aliphatic	Acid/Polar	
S. cerevisiae	D D D S	L I F V	D E I T	635-646
T. delbrueckii	G D S S	L I F L	S E S K	589-600
Z. rouxii	E D D S	L V I L	D E I T	553-565
L. quebecensis	N S S S	L I L V	S E R D	599-700
N. dairenensis	E G D S	L V I L	E E N I	629-641
K.saulgeensis	T D D S	L I I L	E E I S	621-632

C

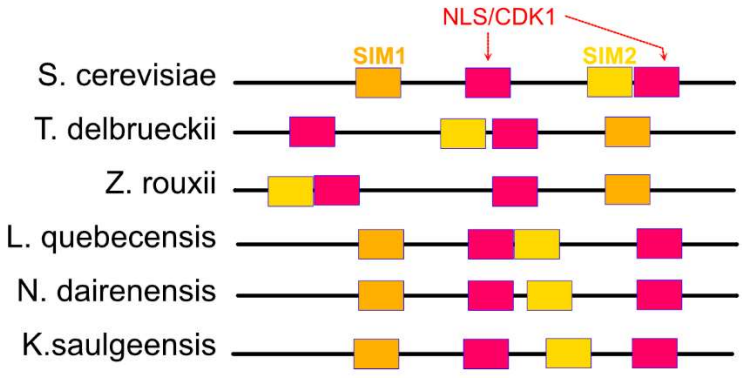

Figure 55 – Supplementary figure 1. *(A) Alignment of Yen1's SIM1 (Aa 635-646) to already characterized SIMs in Slx5, Elg1 and Rad18 presenting an aliphatic core flanked by acidic (D/E), phosphorylatable (S/T) or polar residues (R/K). (B) Alignment of putative SIM motifs found in different yeast species' Yen1 sequences and matching the architecture of Yen1's SIM1 in S.cerevisiae (C) Disposition of SIM1 in S.cerevisiae and other yeast species relative to the SIM2 and the conserved domains of the bi-partite NLS (containing a regulatory CDK1 site).*

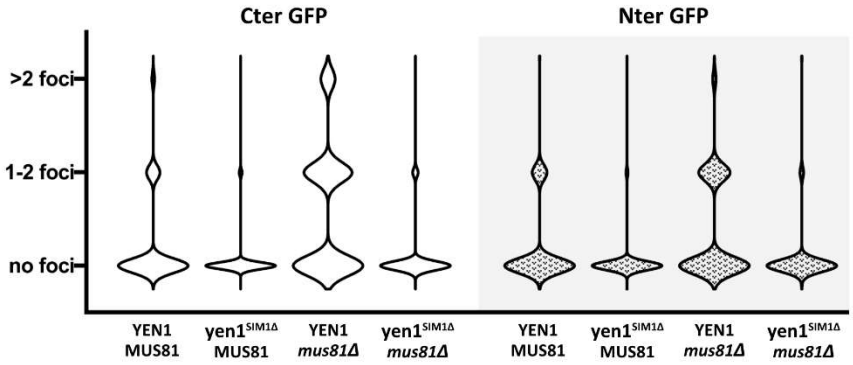

Figure 56 – Supplementary figure 2. *Comparison of foci counting between Cter and Nter GFP fusions of Yen1. Strains all bear chromosomally tagged Yen1-HA wild type and SIM mutants in the indicated genetic backgrounds and carrying its corresponding Yen1-GFP expressing plasmid. Left: Results lifted from figure 51 B, the plasmid containing Yen1 and mutants codes a C-terminal GFP fusion. Right: Corresponding backgrounds and plasmids but with an N-terminal GFP fusion to Yen1 and mutants. These data correspond to preliminary results before a definitive switch to Cter GFP. Though the foci distribution turns out to be very similar. Violin Plots display the distribution of G2/M cells showing no foci, 1-2 foci or more than 2 foci for each strain Only between 100 and 400 unique G2/M cells were counted over 2-3 independent trials depending on strains.*

4.2.6 Supplementary tables

Supplementary Table 1. Yeast strains

Strain	Genotype*	Source or reference
Strains for general purpose		
GM84	*MAT***a** *ADE2 yen1Δ::klURA3* ura3Δ::HphMX	[531]
GM93-5D	*MATα ADE2 yen1Δ::klURA3 mus81Δ::KanMX*	[531]
GM98-4B	*MAT***a** *ADE2 YEN1-HA ura3Δ::HphMX*	[531]
GM98-7B	*MATα ADE2 YEN1-HA mus81Δ::KanMX ura3Δ::HphMX*	[531]
GM481-2A	*MAT***a** *ADE2 YEN1-HA mus81Δ::KanMX ura3Δ::HphMX*	[531]
GM395-5C	*MAT***a** *ADE2 yen1::HIS3 ura3-1*	[531]
GM395-14C	*MAT***a** *ADE2 yen1::HIS3 mus81Δ::KanMX ura3-1*	[531]
GM481-3D	*MAT***a** *ADE2 YEN1-HA slx8Δ::KanMX ura3Δ::HphMX*	This study
GM481-9B	*MAT***a** *ADE2 YEN1-HA mus81Δ::KanMX slx8Δ::KanMX ura3Δ::HphMX*	This study
GM411-2A	*MAT***a** *ADE2 yen1-SIM1Δ-HA ura3Δ::HphMX*	This study
	*MAT***a** *ADE2 yen1-SIM2Δ-HA ura3Δ::HphMX*	This study
GM875-5B	*MAT***a** *ADE2 yen1-SIM1-2ΔΔ-HA ura3Δ::HphMX*	This study
GM411-6D	*MAT***a** *ADE2 yen1-SIM1Δ-HA mus81Δ::KanMX ura3Δ::HphMX*	This study
	*MAT***a** *ADE2 yen1-SIM2-HA mus81Δ::KanMX ura3Δ::HphMX*	This study
	*MAT***a** *ADE2 yen1-SIM1-2ΔΔ-HA mus81Δ::KanMX ura3Δ::HphMX*	This study
Strains for cell biology		
GM304-11C	*MATa* ADE2 Yen1-HA his3-11:pCUP1-GFP12-LacI12:HIS3 trp1-1:256LacO:TRP1 ura3Δ::HphMX	[531]
GM304-6A	*MAT*α ADE2 Yen1-HA mus81::KanMX his3-11:pCUP1-GFP12-LacI12:HIS3 trp1-1:256LacO:TRP1 ura3Δ::HphMX	[531]
747-6D	*MAT*? ADE2 Yen1-SIMΔΔ-HA mus81::KanMX his3-11:pCUP1-GFP12-LacI12:HIS3 trp1-1:256LacO:TRP1 ura3Δ::HphMX	This work
726-13D	*MAT*a ADE2 YEN1-HA HTA1-mCherry::HphMX	This work
726-15C	*MAT*a ADE2 YEN1-HA mus81Δ::KanMX HTA1-mCherry::HphMX	This work
GM427-3D	*MAT?* ADE2 yen1-SIM1Δ-HA mus81Δ::KanMX HTA1-mCherry::HphMX	This work
687-3A	*MATa* ADE2 yen1-SIM2Δ-HA HTA1-mCherry::HphMX	This work
687-6B	*MATa* ADE2 yen1-SIM2Δ-HA mus81Δ::KanMX HTA1-mCherry::HphMX	This work

720-12C	*MATa* ADE2 yen1-SIMΔΔ-HA HTA1-mCherry::HphMX	This work
720-2D	*MATα* ADE2 yen1-SIMΔΔ-HA mus81Δ::KanMX HTA1-mCherry::HphMX	This work
846	yen1-SIMΔΔ-HA mus81Δ::KanMX SIK1-mCherry::HphMX	This work
Strains for crossover monitoring		
LSY2205-24D	*MATα ade2-I lys2::GAL-ISCEI his3::HphMX4 yen1::HIS3*	[177]
LSY2202-42A	*MAT**a** ade2-n his3::NatMX4 met22::klURA3 yen1::HIS3*	[177]
LSY2205-77B	*MAT**a** ade2-I lys2::GAL-ISCEI his3::HphMX4 mus81::KanMX6 yen1::HIS3*	[177]
LSY2202-19D	*MATα ade2-n his3::NatMX4 met22::klURA3 mus81::KanMX6 yen1::HIS3*	[177]
GM379-4C	MATa YEN1-HA ade2-I lys2Δ::pGal-ISceI his3Δ::HphMX	[531]
GM379-13C	*MATα YEN1-HA mus81Δ::KanMX ade2-I lys2::GAL-ISCEI his3::HphMX4*	[531]
GM387-22B	*MATα YEN1-HA ade2-n his3::NatMX4 met22::klURA3*	[531]
GM387-5A	*MAT**a** YEN1-HA mus81Δ::KanMX ade2-n his3::NatMX4 met22::klURA3*	[531]
802-12D	*MATα yen1-SIMΔΔ-HA ade2-I lys2::GAL-ISCEI his3::HphMX4*	This work
801-4A	*MAT**a** yen1-SIMΔΔ-HA ade2-n his3::NatMX4 met22::klURA3*	This work
802-6B	*MATa yen1-SIMΔΔ-HA mus81Δ::KanMX ade2-I lys2::GAL-ISCEI his3::HphMX4*	This work
801-46D	*MATα yen1-SIMΔΔ-HA mus81Δ::KanMX ade2-n his3::NatMX4 met22::klURA3*	This work
	MATa-inc *ADE2 YEN1*-HA *mus81Δ::KanMX ura3::HOcs (V) lys2::ura3-Hocs inc (5.6Kb) (II) ade3::pGAL-HO*	This work
880-6D	*MATa-inc ADE2 yen1-SIMΔΔ-HA mus81Δ::KanMX ura3::HOcs (V) lys2::ura3-HOcs inc (5.6Kb) (II) ade3::pGAL-HO*	This work
Strains for Two-Hybrid		
PJ69-4a	*MAT**a*** trp1-901leu2-3.12 ura3-52 his3-200 gal4Δ gal80Δ LYS2::GAL1-HIS3 GAL2-ADE2 met2::GAL7-lacz	Stan Fields Lab [528]
Pj69-4alpha	*MATα* trp1-901leu2-3.12 ura3-52 his3-200 gal4Δ gal80Δ LYS2::GAL1-HIS3 GAL2-ADE2 met2::GAL7-lacz	Stan Fields Lab [528]

*If not stated otherwise strains background is the W303 genotype (*his3-11, 15 leu2-3, 112 trp1-1 ade2-1 can1-100*), only mating type and differences from the standard genotype are listed. Specific strains in other backgrounds are defined.

Supplementary Table 2. Plasmids

Plasmid	Description
pYES2	*pYES2 (URA3) empty vector, GAL inducible*
pYES2-Yen1-HA	*pYES2 (URA3) derivative, GAL inducible*
pYES2-yen1-SIM1Δ-HA	*pYES2 (URA3) derivative, GAL inducible*
pYES2-yen1-SIM2Δ-HA	*pYES2 (URA3) derivative, GAL inducible*
pYES2-yen1-SIM1-2ΔΔ-HA	*pYES2-TOPO (URA3) derivative, GAL inducible*
pYES2-Yen1-GFP	*pYES2-TOPO (URA3) derivative, GAL inducible*
pYES2- yen1-SIM1Δ-GFP	*pYES2-TOPO (URA3) derivative, GAL inducible*
pYES2- yen1-SIM2Δ-GFP	*pYES2-TOPO (URA3) derivative, GAL inducible*
pYES2- yen1-SIM1-2ΔΔ-GFP	*pYES2-TOPO (URA3) derivative, GAL inducible*
pYES2-GFP-Yen1	*pYES2-TOPO (URA3) derivative, GAL inducible*
pYES2-GFP-yen1-SIM1Δ	*pYES2-TOPO (URA3) derivative, GAL inducible*
pYES2-GFP-yen1-SIM2Δ	*pYES2-TOPO (URA3) derivative, GAL inducible*
pYES2-GFP-yen1-SIM1-2ΔΔ	*pYES2-TOPO (URA3) derivative, GAL inducible*
pRS315	*empty vector (LEU2)*
p1346	*Cu inducible (LEU2) encoding 6xHIS-Smt3 (from B. Palancade)*
pOAD	*AD fusion empty vector (TRP1) (from Stan Fields)*
pOAD-Smt3	*AD fusion with Smt3 (TRP1), derived from pOAD (from Stan Fields)*
pDBD-Yen1	*DBD fusion with Yen1 (LEU2), derived from pOBD2 (from Stan Fields)*
pDBD-Δ'Yen1(354-759)	*DBD fusion with a truncated Yen1 (LEU2), derived from pOBD2 (from Stan Fields)*
pDBD-Yen1-SIM1Δ	*DBD fusion with Yen1-SIM1Δ (LEU2), derived from pOBD2 (from Stan Fields)*
pDBD-Yen1-SIM2Δ	*DBD fusion with Yen1-SIM2Δ (LEU2), derived from pOBD2 (from Stan Fields)*
pDBD-Yen1-SIM1-2ΔΔ	*DBD fusion with Yen1-SIM1-2ΔΔ (LEU2), derived from pOBD2 (from Stan Fields)*
pGEX-4T2	*Vector expressing GST*
pGEX-4T2-Smt3	*Vector expressing a GST fusion with Smt3 in bacteria (AmpR), derived from pGEX-4T2*
pET21b-6His-Smt3	*Vector expressing a 6xHis fusion with Smt3 in bacteria (AmpR), derived from pET21b*
pET21b-6His-Smt3-K11-15-19R	*Vector expressing a 6His fusion with Smt-KR mutant in bacteria (AmpR), derived from pET21b*

5 Research perspectives: Identification of the SUMO-modified protein partners of Yen1

As previously mentioned, an expected function mediated by SIMs may reside in the context-sensitive binding and assembly of proteins at repair foci. An open discussion remains on the actual role of these group-modification networks, with authors suggesting that the local increase of sumoylation promotes the recruitment of factors, regardless of the specificity of interaction between them, while others still advocate for specific protein-to-protein interaction fostered by the SUMO-SIM interactions. Our work finds its place in this discussion, and we would like to provide more evidence on whether SIMs of Yen1 mediate a group of specific interaction to a limited set of partners or a unique interactor, or conversely, if they only bring Yen1 to subnuclear localization with an increased rate of sumoylation regardless of the proteins involved.

The work we have put forth provides compelling evidence for the critical role of sumoylation in the subcellular localization of Yen1 and its proper function during resolution of DNA intermediates of HR. However, it is also clear that we fell short of identifying a suitable, sumoylated, protein partner for such interactions.

The current manuscript presented in the previous section does not reflect the efforts we have made to try to characterize such interactors, and the perspectives envisioned for the continuing research to bring these experiments to a satisfactory conclusion. I will try to summarize in this section some preliminary data we obtained by exploring protein partners suitable to interact with Yen1 via their sumoylated residues and how we plan to adapt our research to answer this question.

5.1 Identification of the SUMO-modified protein partners of Yen1

5.1.1 Smc2-Smc4

Interactions mediated by a SUMO-interacting motif are by definition weak and transient. Especially when compared to interactions mediated by other domains able to recruit factors to specific DNA loci, or to foster formation of stable multi-protein complexes. Be it for complexes acting as heterodimers or higher order structural complexes. For this reason, co-immunoprecipitation and other techniques commonly used to determine protein partners, often fail to identify partners in a sumo-mediated interaction. Moreover, sumoylation is a labile modification, interaction is often achieved by the recognition of the sumo-moiety regardless of the substrate, increasing the possibility of false negative results by the loss of sumoylation after cell lysis. Other sumoylated product present in a lysate may also bring about random *in vitro* contacts, thusly augmenting the rate of false positives by artificially bringing in contact a protein to any.

To overcome said issues, we devised a candidate approach by defining proteins that are sumoylated in Anaphase, during the nuclear localized window of activity of Yen1. A situation that would match the observed phenotype for the SIM ablation of Yen1: a deficient sub-nuclear localization in an overall proficient nuclear localization of the protein.

A first hypothesis emerged around an complex of the SMC family: the condensin pentameric complex composed by the two large subunits, Smc2 and Smc4, and three small subunits including Brn1, Ycg1 and Ycs4 in yeast. All condensin subunits are known to be sumoylated and we hypothesized that

residual JMs may interfere with extruded loops of DNA formed by the activity of Condensin. Stalled loop extrusion would then be sensed by Condensins and coupled to sumoylation in a cascade of events leading to the recruitment of Yen1 among others. This interaction would possibly happen by binding Yen1's SIMs through the SUMO modification of either Smc2, Smc4 or the small sub-units of Condensin.

A first endeavor of co-IP between Smc2 and Yen1 gave promising results. Numerous attempts followed, in order to reproduce it with adequate controls. In the end, in part because of a propensity of Yen1 to bind non-specifically to the matrix, we had to increase the stringency of washes and switch to the IP of Yen1 instead of that of Smc2. In these more stringent conditions, trace amounts of Smc2 were recovered when pulling down Yen1. Although sometimes we could detect faint traces of Smc2 in our controls as well (Figure 57 A2). It was expected that the interaction would be transient, but the results were somewhat underwhelming, especially given the many attempts needed to acquire such a mixed result. The aforementioned shortfalls of a co-IP approach loomed, and we then decided to attempt a more phenotypic approach to determine if malfunction of Condensins was related to localization issues of Yen1.

The Condensin complex is essential. We have no access to Condensin subunit mutants showing a decreased sumoylation neither. We thus decided to use a conditional allele with an auxin-induced degron tag on Smc2, kindly provided by Stephane Marcand [537, 538]. We set up experiments to deplete Smc2 and observe Yen1-GFP in time-lapse microscopy. Depletion of condensin subunit Smc2 is expected to destabilize the whole complex, and trigger chromosome de-condensation in Anaphase. This translates to a characteristic asymmetric distribution of DNA and a related shape for nuclear mass distribution in Anaphase and Telophase cells (Information provided by Stephane Marcand). Our preliminary experiments with a depleted Smc2 allowed us to recapitulate the visualization of cells with de-condensed chromosomes. However, instead of the expected loss of Yen1 foci formation, we observed the presence of a mid-zone foci in almost all of the dividing cells with the de-condensation phenotype. Whereas, in the absence of auxin-induced depletion of Smc2 we observed little to no Yen1 foci (figure 57 B). The severity of the depletion of Condensin in terms of chromosome de-condensation may not reflect the nuanced situation that would occur with the presence of DNA intermediates, but we could not address the situation further at that point.

Alternatively, we hypothesized that the small subunits of condensin that actually slide around the DNA and make direct contact to it, would eventually still be associated during Smc2 depletion. Indeed, Ycs4 and Ycg1 are sumoylated by Siz1/Siz2 much like Yen1, and different form the Mms2-dependent sumoylation of the Smc subunits of the complex [539]. In asynchronous cells, even in conditions of induced DNA damage, co-localization of the two tagged proteins was observed but with no convincing accumulation of Ycs4 concomitant with Yen1 foci (figure 57 C). These additional experiments on the small Condensin subunits will continue in a situation of Smc2 depletion, in parallel with an effort to obtain sumo-less variants on these proteins that will enable a more accurate analysis of their SUMO-associated functions.

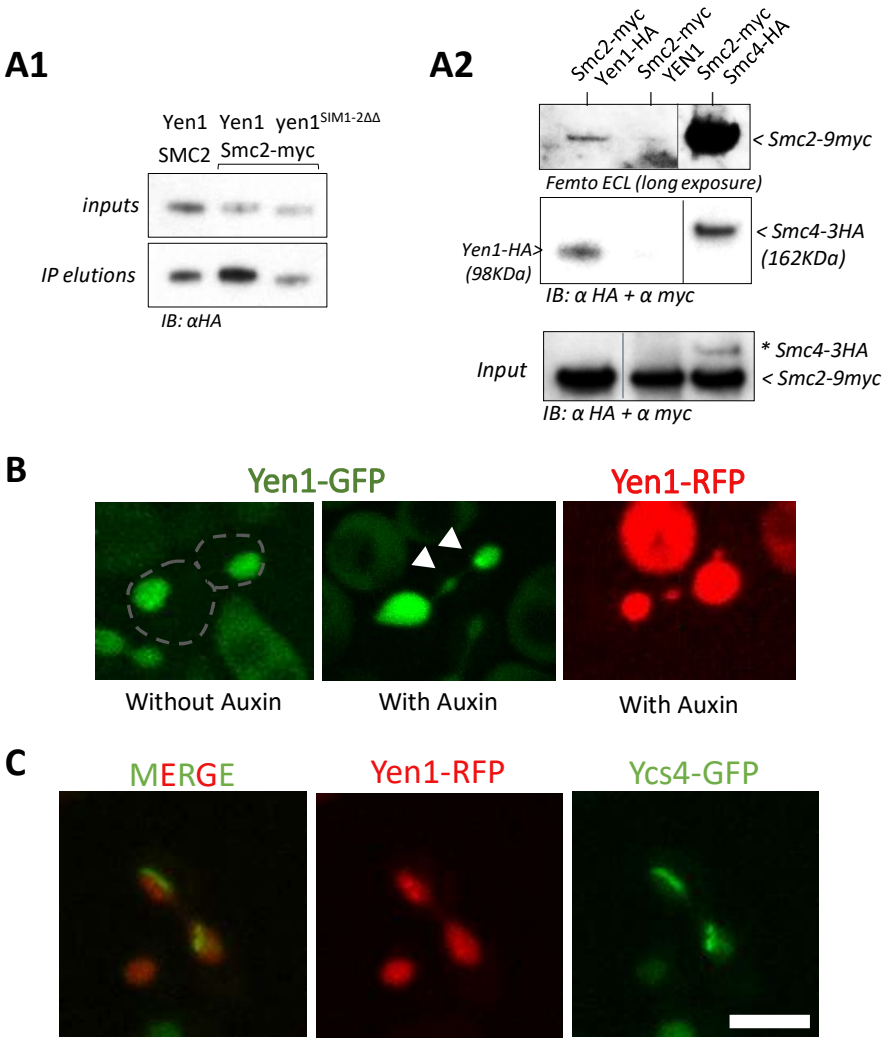

Figure 57. *An investigation of the putative interaction between the condensins and Yen1. (A1) Co-immunoprecipitation assays were performed by pulling down cell extracts with a myc-trap magnetic matrix. Inputs were taken from whole cell extracts. Immunoprecipitates were thoroughly washed and blotted for HA with high sensitivity ECL. (A2) Whole cell extracts were confronted to an HA-tagged sepharose matrix at 4°C. After thorough washing they were blotted for myc with high sensitivity ECL (top). Anti-HA blots (middle and bottom) allowed detection of the immunoprecipitates themselves along with Input levels verification (bottom). (B) Strains are chromosomally tagged with the Auxin inducible Smc2 degron system along with an endogenous Gal promoter and GFP or RFP Yen1 fusion. Cells were synchronized using alpha factor and Yen1 expression induced with a short pulse of galactose. During culture, auxin was added for the middle and right panels. After release cells were plated an followed with time-lapse spinning-disk microscopy with 3 minutes intervals. (C) Cells chromosomally tagged with a Gal promoter fused to Yen1-RFP and a Ycs4 GFP fusion were cultured in asynchronous populations. They were plated following a short burst of galactose induction and a release in glucose. Pictures were taken choosing cells at random only looking at the white light field. White bar: 5 µm.*

5.1.2 Components of the chromosome passenger complex

Chromosome passenger complex (CPC) proteins Sli15 and Ipl1 [540] had been considered as well as putative interactors of Yen1 through sumoylation. The CPC has multiple roles in the control of spindle assembly and the segregation of the chromosomes [541], and re-localizes to the chromosome arms and the spindle mid-zone during Anaphase, in a distribution that may help Yen1 to localize in the vicinity of chromosome areas being held up during chromosome segregation, stuck at the mitotic spindle mid-zone as lagging chromatin. Looking at asynchronous cells under MMS damage (data not shown) and making use of the Smc2 degron system (figure 58 A, B) we did not observe a clear co-

localization of Yen1-mCherry and Ipl1-GFP or Sli15-GFP. Though they sometimes overlapped, other times they only seemed to be close to each other as is evidenced in figure 58. Though not invalidating the hypothesis, these results did not encourage further foray into microscopy analysis of these chromosome passenger complex enzymes. Indeed, we realize that the resident time of a SUMO-mediated co-localization may not be stable enough to be observed by microscopy.

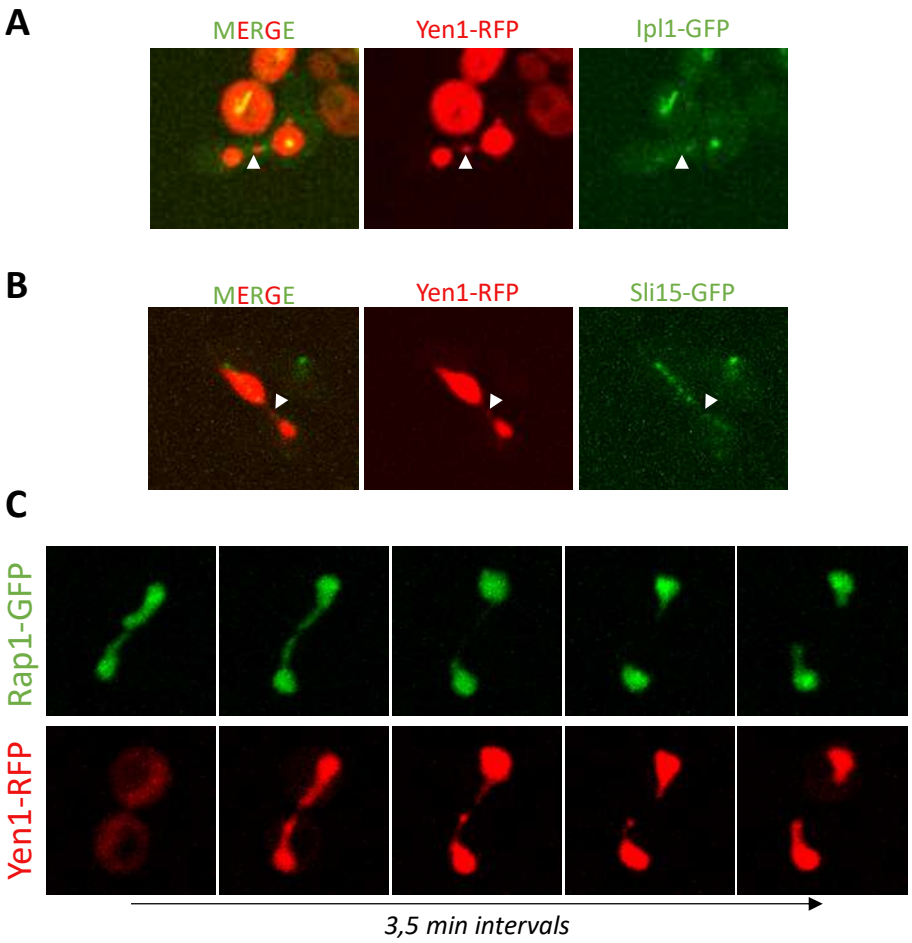

Figure 58. *Co-localization assays for Yen1 and Ipl1, Sli15 or Rap1. Chromosomally tagged cells with a Gal promoter Yen1-RFP fusion and the auxin inducible Smc2 degron system along with a GFP-fusion of the candidate protein (Ipl1, Sli15 or Rap1) were cultivated and synchronized using alpha factor. Auxin was added to the media following Yen1 induction. (A) Pictures of G2 cells in a situation of de-condensation of chromosomes for cells containing Ipl1-GFP. (B) Similar pictures were taken with Sli15-GFP containing cells. (C) Time-lapse of G2/M phase for the Rap1-GFP containing strain.*

5.1.3 The Rap1 protein at telomeres and rDNA sites

Investigations continued with the Rap1 protein, found both in the telomeres and in promoter sites, especially at the rDNA loci. Rap1 may help certain proteins in interfacing with DNA. Also, it is associated with a promotion of meiotic recombination at the HIS4 loci. Furthermore, its binding to DNA introduces a slight distortion which could contribute to Yen1 accessing its substrates. Finally, Rap1 is known to be sumoylated and is targeted by Uls1 which removes sumo-Rap1 from telomeres [388, 539, 542-548]. The actual function of Rap1 sumoylation is unknown, but similar to what we speculated for condensins, we thought that in the event of persistent junctions, Rap1 could stall branch-migration and then be a site of pausing of these DNA intermediates. Sumoylation at these sites would then enable Yen1 to be recruited. We addressed this possibility by looking at both proteins by microscopy in either

asynchronous cells (data not shown) or synchronized Smc2 depleted cells (figure 58 C). In conditions of condensin depletion, we obtained by serendipity a very synchronous situation where almost all cells show Yen1 foci, and in these conditions Rap1 showed co-localization in a majority of cases. However, there were still Yen1 foci specifically unpopulated by Rap1. As explained above these foci were not strictly related to the presence of SIMs in Yen1. The result though is somehow interesting, as it suggests that decondensation of chromosomes induces accumulation of Yen1 at this medial area of the mitotic plane, probably by accumulation of either rDNA or telomeric regions, and Yen1 is recruited to these sites.

5.1.4 Biotin proximity tagging to enforce detection of transient interactions

With our attempts to detect interactions via co-IP and co-localization falling short, we turned our attention to an approach designed to capture even very transient interactions: BioID. In this system, proteins are tagged with the biotinylation enzyme BirA at its C-terminus and using free biotin from the media, BirA will biotinylate any protein in close proximity and thus introduce a durable mark in these interactors that can be used to purify them by using streptavidin affinity columns [549]. The technique is a powerful tool to capture interactions regardless of their strength, but has a couple of caveats. The most important one is the fact that all naturally biotinylated proteins are captured as background. Proteins of interest have to be singled out by comparing to control conditions. Similarly, proximity may not be due to real interactions, in the event of ubiquitous and abundant proteins, this assay may capture proteins that just hit the tagged protein randomly.

Despite these possible limitations we thought that, since Yen1 is a scarce and very controlled protein that only localizes to the nucleus in a strict time-window from Anaphase to G1, the possibility of capturing random collisions was low. Moreover, comparing to control conditions we would enable to sort out only the relevant interactions.

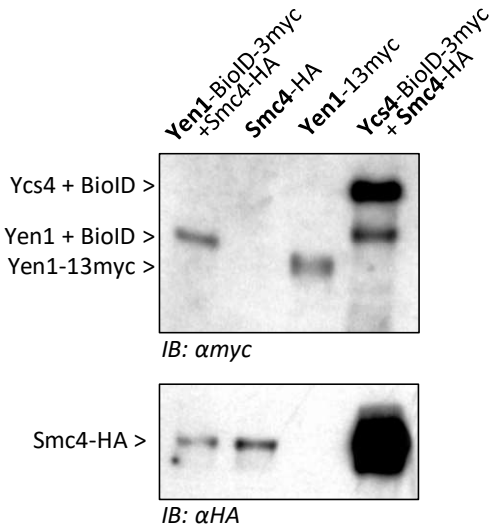

Figure 59. *An attempt at BioID. Whole cell extracts are immunoprecipitated on a streptavidin matrix, pulling down all the biotinylated proteins. Cells are chromosomally tagged with the BirA enzyme allowing biotinylation of nearby proteins (noted BioID) with a 3 myc tag. In this experiment, Yen1 is fused with the BioID machinery. In the rightmost well, Ycs4 is tagged with it. Allowing for a positive control with Smc4 bearing a HA tag. The strain with "Yen1-13myc" has only a myc tag on Yen1 so as to represent a negative control with no BioID biotinylation. The BioID enzyme fusion creates a shift in molecular weight as evidenced by the Yen1-BioID and Yen1-13myc weight difference.*

A first set of experiments was performed to explore the landscape of Yen1-BirA constructs, by pulling biotinylated proteins and comparing the enriched fraction to that obtained using a control strain with a –myc tagged Yen1 lacking BirA. We monitored both by WB and by mass-spectrometry the recovered fractions (Figure 59). As expected, Yen1 was readily recovered by streptavidin columns due to its auto-biotinylation. Either as a testament to the limits of the system or highlighting Yen1's ability to homodimerize. Indeed, BirA auto-biotynilates the tagged proteins in cis in these type of approaches. However, browsing the list of proteins specifically enriched by Yen1 in tandem MS yielded no relevant results, most of the enriched hits were those of Yen1 and even known interactors (Cdc28, Cdc14) were not found significantly elevated. We analyzed in parallel by WB these type of eluates in experimental settings using –HA tags to identify a candidate interactor (i.e. Smc4), we used these approach as well to further validate the technique, by creating interaction couples that we know will be positively enriched (i.e. Ycs4-BirA with Smc4-HA, or Msh6-BirA with Mph1-HA). In our results so far, we have been able to further validate the technique to detect enriched stable partners of our control pairs, but no relevant results have still been obtained with Yen1, often due to background noise issues (i.e. Smc4 background binding to the streptavidin matrix, Figure 59). We keep elaborating strains to sort out candidates by BioID, in an effort that will certainly continue beyond this thesis work, and hopefully, by increasing the stringency on these technique and modifying the protocol to recover proteins in situations were sumoylation is enriched, we may complete this characterization with the identification of Yen1 bona-fide interactors.

5.2 Potential perspectives

Even though it is tantalizing to find the partners enabling Yen1 accumulation in foci and nucleolytic activity, other findings must not be set aside. The direct effects of Yen1 sumoylation for its localization and function still require some further characterization. Indeed, our results show an intimate relation between mutation of Yen1's SIMs and loss of direct covalent sumoylation (Figure 51). Nonetheless, this remains a proxy approach and cannot completely explain whether sumoylation was required in the first place for localization or came as a result of interaction via SIM to sumoylated partners.

Efforts to create Yen1 SUMO-deficient mutants have been unfruitful so far. A set of mutants with multiple substitution of Lysines have been tested, and we have been able to prove that in the absence of Lysines, sumoylation is lost (allR mutant of Yen1). Some bulk, substitutions of two thirds of the lysines yields the same result. Beyond those bulk substitutions, we made little advance in pinpointing individual lysines, either by brute force, testing different combinations of mutants, or by detection of modified lysines by tandem MS. Bulk substitution of large swaths of the protein produce Yen1 versions that are to all evidence non-functional, as we can see them aggregate in inclusion bodies when observed by microscopy. Additionally, they generate abundant degradation bands when observed by WB. The efforts will certainly continue, and we aim to identify at least partially reduced sumoylation deficient mutants of Yen1 to confirm whether they share all the phenotypes described for the SIM mutants, or whether they display other characteristics.

Moreover, the quest for interactors remains relevant. Attempts to determine a network of interactors for Yen1 have been of little help so far [550] and such a breakthrough could make us advance to relevant roles of other proteins in the regulation of crossover levels and completion of chromosome segregation. Efforts in optimizing BioID approaches will certainly require to iterate the scanning of some sumoylated candidates with highly sensitive WB approaches using –HA tags (our more sensitive antibody to date). We are also considering the possibility that BirA tagging may be altering proper Yen1 folding and functions, limiting its interactions. To examine this possibility we started building diploid strains expressing both a wild-type copy of Yen1 and a –BirA tagged copy, to enable heterodimers of Yen1 and increase the possibility of finding interactions with a more physiological Yen1 "dimer".

Extended Summary in French

L'ADN subit des agressions internes ou extérieures quotidiennes qui mettent en danger son intégrité. Bien que la plasticité de l'ADN permette aux êtres vivants de s'adapter à leur environnement, il est primordial de conserver l'intégrité du génome. Les sources et genres de dommages à l'ADN sont variés et nombreux, pour combattre cela, le vivant a sélectionné tout un arsenal de mécanismes de réparation de l'ADN. Parfois spécifiques à un genre de lésions, d'autres fois ayant un spectre d'action plus large. Parmi ces lésions, les cassures doubles brins sont celles qui ont le potentiel le plus délétère. Bien qu'elles ne soient pas les plus communes, du fait de la potentielle perte d'un bras de chromosome entier, elles représentent un défi que la cellule se doit de gérer. Les voies de réparation des cassures double brins sont multiples et complexes, parfois même interconnectées.

La recombinaison homologue est une voie de réparation des cassures double brins qui peut dans certains cas restaurer totalement le chromosome lésé. Dans cette voie, une référence est utilisée pour combler le matériel manquant. De fait, il est préférable d'utiliser les chromatides sœurs. L'utilisation d'un support homologue mais non identique peut mener à des modifications indésirables. Ainsi, cette voie de réparation à lieu principalement à partir de la phase S du cycle cellulaire, lorsque les chromatides sœurs apparaissent à la suite de la réplication. Durant de la recombinaison homologue, la molécule d'ADN double brin de référence et celle brisée sont jointes par complémentarité de bases. Un certain nombre de protéines participent à cette liaison pour permettre la synthèse de réparation. A la suite de quoi, les deux molécules double brins sont physiquement liées et doivent nécessairement être séparées avant la division cellulaire. Sans quoi, les chromatides ne pourraient être séparées correctement ce qui peut mener à des cassures mécaniques ou même la catastrophe mitotique. Ces intermédiaires joints peuvent être dissout par des hélicases. Dans ce cas, la liaison est dénouée en une situation de *non-crossover*, ce qui signifie que la molécule de référence n'est pas modifiée par le processus de réparation. L'intégrité génomique est alors complétement respectée. Sinon, les molécules jointes peuvent être découpées par des nucléases. Dans ce cas, les coupures et ligatures peuvent donner soit un *non-crossover*, soit un *crossover*. C'est-à-dire qu'une partie du matériel génétique est échangé entre les deux chromatides.

Dans la levure *Saccharomyces cerevisiae*, Yen1 est une nucléase. En son absence, combinée à la perte d'autres nucléases, des intermédiaires de recombinaison s'accumulent. Ceux-ci ralentissent la division cellulaire, ou mènent à des cassures. Cela met en exergue l'importance de Yen1 pour la cellule. Cependant, la possibilité de *crossovers* signifie que l'activité de Yen1 est restreinte. En effet, cette dernière est contrôlée par des vagues de phosphorylation dépendantes des phases du cycle cellulaire. Lorsqu'elle est phosphorylée, Yen1 est inactive. Ce n'est qu'au début de l'Anaphase que Yen1 sera dé-phosphorylée pour enfin exercer son action sur les molécules jointes encore présentes. De surcroit, la phosphorylation de Yen1 dans une portion spécifique de sa séquence engendre un changement de sa localisation. Ainsi, autrement qu'en phase G2/M, Yen1 est exportée au cytosol en majorité, comme pour l'empêcher de reconnaitre des intermédiaires de réplication qui pourraient ressembler à des intermédiaires de recombinaison. La déphosphorylation de Yen1 lui permet donc d'être importée au noyau et de cliver les molécules jointes. Enfin, dans la dernière décennie, il a été découvert que Yen1 et bien d'autres protéines de la réparation de l'ADN sont sumoylées. Nait alors la question d'un contrôle d'autant plus strict de Yen1 par le biais de la sumoylation, et peut-être d'autres modifications encore. Dans ce manuscrit, il est décrit la mise en évidence *in vivo* de nouvelles modifications de Yen1. Notamment : Yen1 est ubiquitiné et sumoylé, ainsi que capable d'interagir de façon non-covalente avec des substrat sumoylés.

En tenant compte des informations bibliographiques qui décrivent Yen1 comme un substrat sumoylé, un effort de recherche s'est développé pour mettre cela en évidence *in vitro* et *in vivo*. Un système de *pull-down* de protéines sumoylées a été mis en place. Cela a permis de repérer Yen1 et donc attester de sa modification *in vivo*. Cela permis également de mettre en évidence que les enzymes Siz1 et Siz2 sont nécessaires pour la sumoylation de Yen1. Ce système fut adapté à l'ubiquitine pour montrer que Yen1 est aussi ubiquitiné. *In vitro*, une réaction d'ubiquitination a été reproduites avec succès. De même pour la sumoylation. Il fut ensuite montré que Yen1 interagit avec le complexe Slx5-Slx8, une ubiquitine ligase qui a pour substrat des protéines sumoylées. Il fut montré *in vitro* que Slx5-Slx8 pouvait bien ubiquitiner Yen1. L'effet de cette modification peut se ressentir en l'absence de Slx5-Slx8, où la fraction sumoylée de Yen1 persiste. Ensuite, des expériences vinrent à montrer l'effet de cette modification. La lysine 714 fut identifiée comme la cible préférentielle pour l'ubiquitination de Yen1. En mutant cette lysine, les effets de l'ubiquitination ont pu être appréciés. En l'absence d'ubiquitination, Yen1 est hyperactive. Ce qui se traduit par une augmentation de son accumulation ponctuelle dans le noyau, la récupération de défauts en l'absence d'autres nucléases, ainsi qu'une augmentation du nombre de *crossovers*.

De nombreuses protéines de la réparation de l'ADN sont sumoylées et ubiquitinées. En plus de cela, dans la dernière décennie, il est de plus en plus proposé qu'elles interagissent entre elles par le biais de ces modifications. Des séquences spécifiques (SIMs) permettraient aux protéines d'interagir de façon non-covalente avec SUMO, ou une protéine sumoylée. Il est possible de prédire *in silico* la présence de SIM dans une protéine, même si le consensus peut se révéler vague. Dans le cas de Yen1, deux SIMs prédites ont été retenues et validées expérimentalement. En effet, il a été montré par double-hybride que Yen1 peut interagir avec SUMO. Ceci fut validé par une méthode alternative d'interaction sur chaines *in vitro*. La mutation des SIMs de Yen1 entraine une perte de cette interaction avec SUMO, ce qui pousse à penser qu'elles sont les séquences le permettant. Il convient alors de prendre note de l'importance de cette interaction dans le cadre du contrôle et de l'activité de Yen1. La mutation de ces SIMs entraine une baisse d'activité de Yen1 traduite par une plus grande sensibilité aux dommages des cellules mutées, ainsi qu'une difficulté à séparer les chromatides en fin de mitose, et enfin une diminution des *crossover*. Cependant, *in vitro*, les protéines mutées clivent l'ADN tout autant. Ce qui signifie que cette disparité phénotypique provient du contrôle de Yen1 et non de sa capacité catalytique. En effet, la localisation de Yen1 mutée est modifiée. L'accumulation ponctuelle au noyau est perdue en grande partie, même en situations de dommages à l'ADN. Enfin, il est noté que les niveaux de sumoylation de Yen1 mutée sont bien plus bas que pour la protéine sauvage. Il y a donc un lien indéniable entre ces nouvelles modifications. La sumoylation et l'interaction via SIM sont intimement liées et certainement impactantes pour le contrôle de l'activité de Yen1.

References

1. Hoeijmakers, J.H., *DNA damage, aging, and cancer.* N Engl J Med, 2009. **361**(15): p. 1475-85.

2. Mouw, K.W., et al., *DNA Damage and Repair Biomarkers of Immunotherapy Response.* Cancer Discov, 2017. **7**(7): p. 675-693.

3. Tubbs, A. and A. Nussenzweig, *Endogenous DNA Damage as a Source of Genomic Instability in Cancer.* Cell, 2017. **168**(4): p. 644-656.

4. Sancar, A., et al., *Molecular mechanisms of mammalian DNA repair and the DNA damage checkpoints.* Annu Rev Biochem, 2004. **73**: p. 39-85.

5. Yi, C. and C. He, *DNA repair by reversal of DNA damage.* Cold Spring Harb Perspect Biol, 2013. **5**(1): p. a012575.

6. Abbotts, R. and D.M. Wilson, 3rd, *Coordination of DNA single strand break repair.* Free Radic Biol Med, 2017. **107**: p. 228-244.

7. Chatterjee, N. and G.C. Walker, *Mechanisms of DNA damage, repair, and mutagenesis.* Environ Mol Mutagen, 2017. **58**(5): p. 235-263.

8. De Bont, R. and N. van Larebeke, *Endogenous DNA damage in humans: a review of quantitative data.* Mutagenesis, 2004. **19**(3): p. 169-85.

9. Pfeiffer, P., W. Goedecke, and G. Obe, *Mechanisms of DNA double-strand break repair and their potential to induce chromosomal aberrations.* Mutagenesis, 2000. **15**(4): p. 289-302.

10. Sinha, R.P. and D.P. Hader, *UV-induced DNA damage and repair: a review.* Photochem Photobiol Sci, 2002. **1**(4): p. 225-36.

11. Rastogi, R.P., et al., *Molecular mechanisms of ultraviolet radiation-induced DNA damage and repair.* J Nucleic Acids, 2010. **2010**: p. 592980.

12. Rochette, P.J., et al., *UVA-induced cyclobutane pyrimidine dimers form predominantly at thymine- thymine dipyrimidines and correlate with the mutation spectrum in rodent cells.* Nucleic Acids Res, 2003. **31**(11): p. 2786-94.

13. Kondoh, M., et al., *Light-induced conformational change and product release in DNA repair by (6-4) photolyase.* Journal of the American Chemical Society, 2011. **133**(7): p. 2183-2191.

14. Yokoyama, H. and R. Mizutani, *Structural biology of DNA (6-4) photoproducts formed by ultraviolet radiation and interactions with their binding proteins.* International journal of molecular sciences, 2014. **15**(11): p. 20321-20338.

15. Strumberg, D., et al., *Conversion of Topoisomerase I Cleavage Complexes on the Leading Strand of Ribosomal DNA into 5'-Phosphorylated DNA Double-Strand Breaks by Replication Runoff.* Molecular and Cellular Biology, 2000. **20**(11): p. 3977.

16. Hanawalt, P.C., *The U.V. sensitivity of bacteria: its relation to the DNA replication cycle.* Photochem Photobiol, 1966. **5**(1): p. 1-12.

17. Ceccaldi, R., B. Rondinelli, and A.D. D'Andrea, *Repair Pathway Choices and Consequences at the Double-Strand Break.* Trends Cell Biol, 2016. **26**(1): p. 52-64.

18. Bennett, C.B., et al., *Lethality induced by a single site-specific double-strand break in a dispensable yeast plasmid.* Proc Natl Acad Sci U S A, 1993. **90**(12): p. 5613-7.

19. Mehta, A. and J.E. Haber, *Sources of DNA double-strand breaks and models of recombinational DNA repair.* Cold Spring Harb Perspect Biol, 2014. **6**(9): p. a016428.

20. Gobbini, E., et al., *Functions and regulation of the MRX complex at DNA double-strand breaks.* Microb Cell, 2016. **3**(8): p. 329-337.

21. Ganai, R.A. and E. Johansson, *DNA Replication-A Matter of Fidelity.* Mol Cell, 2016. **62**(5): p. 745-55.

22. Bębenek, A. and I. Ziuzia-Graczyk, *Fidelity of DNA replication-a matter of proofreading.* Curr Genet, 2018. **64**(5): p. 985-996.

23. Clauson, C., O.D. Schärer, and L. Niedernhofer, *Advances in understanding the complex mechanisms of DNA interstrand cross-link repair.* Cold Spring Harb Perspect Biol, 2013. **5**(10): p. a012732.

24. Sander, M., et al., *Proceedings of a workshop on DNA adducts: biological significance and applications to risk assessment Washington, DC, April 13-14, 2004*, in *Toxicol Appl Pharmacol*. 2005: United States. p. 1-20.

25. Cadet, J. and J.R. Wagner, *Oxidatively generated base damage to cellular DNA by hydroxyl radical and one-electron oxidants: similarities and differences.* Arch Biochem Biophys, 2014. **557**: p. 47-54.

26. Izumi, T., et al., *Requirement for human AP endonuclease 1 for repair of 3'-blocking damage at DNA single-strand breaks induced by reactive oxygen species.* Carcinogenesis, 2000. **21**(7): p. 1329-34.

27. Loeb, L.A. and R.J. Monnat, Jr., *DNA polymerases and human disease.* Nat Rev Genet, 2008. **9**(8): p. 594-604.

28. Symington, L.S., R. Rothstein, and M. Lisby, *Mechanisms and regulation of mitotic recombination in Saccharomyces cerevisiae.* Genetics, 2014. **198**(3): p. 795-835.

29. Wang, H., et al., *CtIP maintains stability at common fragile sites and inverted repeats by end resection-independent endonuclease activity.* Mol Cell, 2014. **54**(6): p. 1012-21.

30. Stork, C.T., et al., *Co-transcriptional R-loops are the main cause of estrogen-induced DNA damage.* Elife, 2016. **5**.

31. Helleday, T., et al., *DNA double-strand break repair: from mechanistic understanding to cancer treatment.* DNA Repair (Amst), 2007. **6**(7): p. 923-35.

32. Ray Chaudhuri, A., et al., *Topoisomerase I poisoning results in PARP-mediated replication fork reversal.* Nat Struct Mol Biol, 2012. **19**(4): p. 417-23.

33. Caldecott, K.W., *DNA single-strand break repair.* Exp Cell Res, 2014. **329**(1): p. 2-8.

34. Lindahl, T., *Instability and decay of the primary structure of DNA.* Nature, 1993. **362**(6422): p. 709-15.

35. Azzam, E.I., J.P. Jay-Gerin, and D. Pain, *Ionizing radiation-induced metabolic oxidative stress and prolonged cell injury.* Cancer Lett, 2012. **327**(1-2): p. 48-60.

36. Maier, P., et al., *Cellular Pathways in Response to Ionizing Radiation and Their Targetability for Tumor Radiosensitization.* Int J Mol Sci, 2016. **17**(1).

37. D'Orazio, J., et al., *UV radiation and the skin.* Int J Mol Sci, 2013. **14**(6): p. 12222-48.

38. TEVINI, M., J. BRAUN, and G. FIESER, *THE PROTECTIVE FUNCTION OF THE EPIDERMAL LAYER OF RYE SEEDLINGS AGAINST ULTRAVIOLET-B RADIATION.* Photochemistry and Photobiology, 1991. **53**(3): p. 329-333.

39. Perera, F., et al., *DNA damage from polycyclic aromatic hydrocarbons measured by benzo[a]pyrene-DNA adducts in mothers and newborns from Northern Manhattan, the World Trade Center Area, Poland, and China.* Cancer Epidemiol Biomarkers Prev, 2005. **14**(3): p. 709-14.

40. Cook, J.L., *Tobacco smoke: chemical carcinogenesis and genetic lesions.* Ochsner J, 1999. **1**(3): p. 130-5.

41. Pires, I.M., et al., *Effects of acute versus chronic hypoxia on DNA damage responses and genomic instability.* Cancer Res, 2010. **70**(3): p. 925-35.

42. Scanlon, S.E. and P.M. Glazer, *Multifaceted control of DNA repair pathways by the hypoxic tumor microenvironment.* DNA Repair (Amst), 2015. **32**: p. 180-189.

43. Kantidze, O.L., et al., *Heat Stress-Induced DNA Damage.* Acta Naturae, 2016. **8**(2): p. 75-8.

44. Wang, B., G. Wang, and S. Zhu, *DNA Damage Inducible Protein 1 is Involved in Cold Adaption of Harvested Cucumber Fruit.* Front Plant Sci, 2019. **10**: p. 1723.

45. Bedard, L.L. and T.E. Massey, *Aflatoxin B1-induced DNA damage and its repair.* Cancer Lett, 2006. **241**(2): p. 174-83.

46. Darwish, M.A., et al., *Resveratrol influences platinum pharmacokinetics: A novel mechanism in protection against cisplatin-induced nephrotoxicity.* Toxicol Lett, 2018. **290**: p. 73-82.

47. Castellini, C., et al., *Bisphenol A and Male Fertility: Myths and Realities.* Front Endocrinol (Lausanne), 2020. **11**: p. 353.

48. Kawanishi, S., et al., *Crosstalk between DNA Damage and Inflammation in the Multiple Steps of Carcinogenesis.* Int J Mol Sci, 2017. **18**(8).

49. Witkin, E.M., *The radiation sensitivity of Escherichia coli B: a hypothesis relating filament formation and prophage induction.* Proc Natl Acad Sci U S A, 1967. **57**(5): p. 1275-9.

50. George, J., M. Castellazzi, and G. Buttin, *Prophage induction and cell division in E. coli. III. Mutations sfiA and sfiB restore division in tif and lon strains and permit the expression of mutator properties of tif.* Mol Gen Genet, 1975. **140**(4): p. 309-332.

51. Aylon, Y. and M. Kupiec, *DSB repair: the yeast paradigm.* DNA Repair (Amst), 2004. **3**(8-9): p. 797-815.

52. Brachmann, C.B., et al., *Designer deletion strains derived from Saccharomyces cerevisiae S288C: a useful set of strains and plasmids for PCR-mediated gene disruption and other applications.* Yeast, 1998. **14**(2): p. 115-32.

53. Jasin, M. and R. Rothstein, *Repair of strand breaks by homologous recombination.* Cold Spring Harb Perspect Biol, 2013. **5**(11): p. a012740.

54. Sancar, A., *Structure and function of DNA photolyase.* Biochemistry, 1994. **33**(1): p. 2-9.

55. Kaina, B., et al., *MGMT: key node in the battle against genotoxicity, carcinogenicity and apoptosis induced by alkylating agents.* DNA Repair (Amst), 2007. **6**(8): p. 1079-99.

56. Yang, C.G., et al., *Crystal structures of DNA/RNA repair enzymes AlkB and ABH2 bound to dsDNA.* Nature, 2008. **452**(7190): p. 961-5.

57. Yi, C., C.G. Yang, and C. He, *A non-heme iron-mediated chemical demethylation in DNA and RNA.* Acc Chem Res, 2009. **42**(4): p. 519-29.

58. Shell, S.M. and W.J. Chazin, *XPF-ERCC1: on the bubble.* Structure, 2012. **20**(4): p. 566-8.

59. Huang, J.C., et al., *Human nucleotide excision nuclease removes thymine dimers from DNA by incising the 22nd phosphodiester bond 5' and the 6th phosphodiester bond 3' to the photodimer.* Proc Natl Acad Sci U S A, 1992. **89**(8): p. 3664-8.

60. Friedberg, E.C., *DNA damage and repair.* Nature, 2003. **421**(6921): p. 436-40.

61. Sertic, S., et al., *NER and DDR: Classical music with new instruments.* Cell Cycle, 2012. **11**(4): p. 668-674.

62. Friedberg, E.C., *How nucleotide excision repair protects against cancer.* Nat Rev Cancer, 2001. **1**(1): p. 22-33.

63. Bohr, V.A., et al., *DNA repair in an active gene: removal of pyrimidine dimers from the DHFR gene of CHO cells is much more efficient than in the genome overall.* Cell, 1985. **40**(2): p. 359-69.

64. Madhani, H.D., V.A. Bohr, and P.C. Hanawalt, *Differential DNA repair in transcriptionally active and inactive proto- oncogenes: c-abl and c-mos.* Cell, 1986. **45**(3): p. 417-23.

65. Mellon, I., et al., *Preferential DNA repair of an active gene in human cells.* Proc Natl Acad Sci U S A, 1986. **83**(23): p. 8878-82.

66. Mellon, I., G. Spivak, and P.C. Hanawalt, *Selective removal of transcription-blocking DNA damage from the transcribed strand of the mammalian DHFR gene.* Cell, 1987. **51**(2): p. 241-9.

67. Fousteri, M., et al., *Cockayne syndrome A and B proteins differentially regulate recruitment of chromatin remodeling and repair factors to stalled RNA polymerase II in vivo.* Mol Cell, 2006. **23**(4): p. 471-82.

68. Simandi, Z., *The Role of DNA Polymerase β in Neural Genome Stability.* J Neurosci, 2017. **37**(46): p. 11069-11071.

69. He, Q., et al., *Exonuclease of human DNA polymerase gamma disengages its strand displacement function.* Mitochondrion, 2013. **13**(6): p. 592-601.

70. Kunkel, T.A., *Evolving views of DNA replication (in)fidelity.* Cold Spring Harb Symp Quant Biol, 2009. **74**: p. 91-101.

71. Marinus, M.G., *DNA Mismatch Repair.* EcoSal Plus, 2012. **5**(1).

72. Groothuizen, F.S. and T.K. Sixma, *The conserved molecular machinery in DNA mismatch repair enzyme structures.* DNA Repair (Amst), 2016. **38**: p. 14-23.

73. Kunkel, T.A. and D.A. Erie, *Eukaryotic Mismatch Repair in Relation to DNA Replication.* Annu Rev Genet, 2015. **49**: p. 291-313.

74. Kadyrov, F.A., et al., *A possible mechanism for exonuclease 1-independent eukaryotic mismatch repair.* Proc Natl Acad Sci U S A, 2009. **106**(21): p. 8495-500.

75. Lahue, R.S., K.G. Au, and P. Modrich, *DNA mismatch correction in a defined system.* Science, 1989. **245**(4914): p. 160-4.

76. Hu, C., et al., *Synergism of Dam, MutH, and MutS in methylation-directed mismatch repair in Escherichia coli.* Mutat Res, 2017. **795**: p. 31-33.

77. Manhart, C.M. and E. Alani, *Roles for mismatch repair family proteins in promoting meiotic crossing over.* DNA Repair (Amst), 2016. **38**: p. 84-93.

78. Modrich, P. and R. Lahue, *Mismatch repair in replication fidelity, genetic recombination, and cancer biology.* Annu Rev Biochem, 1996. **65**: p. 101-33.

79. Evans, E. and E. Alani, *Roles for mismatch repair factors in regulating genetic recombination.* Mol Cell Biol, 2000. **20**(21): p. 7839-44.

80. Gao, Y., et al., *Mechanisms of Post-Replication DNA Repair.* Genes (Basel), 2017. **8**(2).

81. Bi, X., *Mechanism of DNA damage tolerance.* World J Biol Chem, 2015. **6**(3): p. 48-56.

82. Silverstein, T.D., et al., *Structural basis for the suppression of skin cancers by DNA polymerase eta.* Nature, 2010. **465**(7301): p. 1039-43.

83. Biertümpfel, C., et al., *Structure and mechanism of human DNA polymerase eta.* Nature, 2010. **465**(7301): p. 1044-8.

84. Johnson, R.E., S. Prakash, and L. Prakash, *Efficient bypass of a thymine-thymine dimer by yeast DNA polymerase, Poleta.* Science, 1999. **283**(5404): p. 1001-4.

85. Branzei, D. and B. Szakal, *DNA damage tolerance by recombination: Molecular pathways and DNA structures.* DNA Repair (Amst), 2016. **44**: p. 68-75.

86. Dianov, G., A. Price, and T. Lindahl, *Generation of single-nucleotide repair patches following excision of uracil residues from DNA.* Mol Cell Biol, 1992. **12**(4): p. 1605-12.

87. Fortini, P. and E. Dogliotti, *Base damage and single-strand break repair: mechanisms and functional significance of short- and long-patch repair subpathways.* DNA Repair (Amst), 2007. **6**(4): p. 398-409.

88. McKinnon, P.J. and K.W. Caldecott, *DNA strand break repair and human genetic disease.* Annu Rev Genomics Hum Genet, 2007. **8**: p. 37-55.

89. Sparks, J.L., et al., *RNase H2-initiated ribonucleotide excision repair.* Mol Cell, 2012. **47**(6): p. 980-6.

90. Frank-Vaillant, M. and S. Marcand, *Transient stability of DNA ends allows nonhomologous end joining to precede homologous recombination.* Mol Cell, 2002. **10**(5): p. 1189-99.

91. Symington, L.S., *Mechanism and regulation of DNA end resection in eukaryotes.* Crit Rev Biochem Mol Biol, 2016. **51**(3): p. 195-212.

92. Symington, L.S. and J. Gautier, *Double-strand break end resection and repair pathway choice.* Annu Rev Genet, 2011. **45**: p. 247-71.

93. Kass, E.M. and M. Jasin, *Collaboration and competition between DNA double-strand break repair pathways.* FEBS Lett, 2010. **584**(17): p. 3703-8.

94. Ingram, S.P., et al., *Mechanistic modelling supports entwined rather than exclusively competitive DNA double-strand break repair pathway.* Scientific Reports, 2019. **9**(1): p. 6359.

95. Emerson, C.H. and A.A. Bertuch, *Consider the workhorse: Nonhomologous end-joining in budding yeast.* Biochemistry and cell biology = Biochimie et biologie cellulaire, 2016. **94**(5): p. 396-406.

96. Bétermier, M., P. Bertrand, and B.S. Lopez, *Is non-homologous end-joining really an inherently error-prone process?* PLoS genetics, 2014. **10**(1): p. e1004086-e1004086.

97. Bahmed, K., K.C. Nitiss, and J.L. Nitiss, *Yeast Tdp1 regulates the fidelity of nonhomologous end joining.* Proceedings of the National Academy of Sciences of the United States of America, 2010. **107**(9): p. 4057-4062.

98. Marcand, S., et al., *Multiple pathways inhibit NHEJ at telomeres.* Genes & development, 2008. **22**(9): p. 1153-1158.

99. Ma, Y., et al., *Hairpin opening and overhang processing by an Artemis/DNA-dependent protein kinase complex in nonhomologous end joining and V(D)J recombination.* Cell, 2002. **108**(6): p. 781-94.

100. Daley, J.M., et al., *Nonhomologous end joining in yeast.* Annu Rev Genet, 2005. **39**: p. 431-51.

101. Mani, R.S., et al., *Dual modes of interaction between XRCC4 and polynucleotide kinase/phosphatase: implications for nonhomologous end joining.* The Journal of biological chemistry, 2010. **285**(48): p. 37619-37629.

102. Herrmann, G., T. Lindahl, and P. Schär, *Saccharomyces cerevisiae LIF1: a function involved in DNA double-strand break repair related to mammalian XRCC4.* Embo j, 1998. **17**(14): p. 4188-98.

103. Mazon, G., E.P. Mimitou, and L.S. Symington, *SnapShot: Homologous recombination in DNA double-strand break repair.* Cell, 2010. **142**(4): p. 646, 646.e1.

104. Li, J., et al., *Pathways and assays for DNA double-strand break repair by homologous recombination.* Acta Biochim Biophys Sin (Shanghai), 2019. **51**(9): p. 879-889.

105. Liu, T. and J. Huang, *DNA End Resection: Facts and Mechanisms.* Genomics Proteomics Bioinformatics, 2016. **14**(3): p. 126-130.

106. Lisby, M., et al., *Choreography of the DNA damage response: spatiotemporal relationships among checkpoint and repair proteins.* Cell, 2004. **118**(6): p. 699-713.

107. Symington, L.S., *End resection at double-strand breaks: mechanism and regulation.* Cold Spring Harb Perspect Biol, 2014. **6**(8).

108. Hirano, T., *At the heart of the chromosome: SMC proteins in action.* Nature Reviews Molecular Cell Biology, 2006. **7**(5): p. 311-322.

109. Mimitou, E.P. and L.S. Symington, *DNA end resection: many nucleases make light work.* DNA Repair (Amst), 2009. **8**(9): p. 983-95.

110. Moynahan, M.E. and M. Jasin, *Mitotic homologous recombination maintains genomic stability and suppresses tumorigenesis.* Nat Rev Mol Cell Biol, 2010. **11**(3): p. 196-207.

111. Cannavo, E., et al., *Regulatory control of DNA end resection by Sae2 phosphorylation.* Nature communications, 2018. **9**(1): p. 4016-4016.

112. Densham, R.M. and J.R. Morris, *Moving Mountains-The BRCA1 Promotion of DNA Resection.* Front Mol Biosci, 2019. **6**: p. 79.

113. Tomimatsu, N., et al., *Phosphorylation of EXO1 by CDKs 1 and 2 regulates DNA end resection and repair pathway choice.* Nature Communications, 2014. **5**(1): p. 3561.

114. Costelloe, T., et al., *The yeast Fun30 and human SMARCAD1 chromatin remodellers promote DNA end resection.* Nature, 2012. **489**(7417): p. 581-584.

115. San-Segundo, P.A. and A. Clemente-Blanco, *Resolvases, Dissolvases, and Helicases in Homologous Recombination: Clearing the Road for Chromosome Segregation.* Genes (Basel), 2020. **11**(1).

116. Cannavo, E., P. Cejka, and S.C. Kowalczykowski, *Relationship of DNA degradation by Saccharomyces cerevisiae Exonuclease 1 and its stimulation by RPA and Mre11-Rad50-Xrs2 to DNA end resection.* Proceedings of the National Academy of Sciences, 2013. **110**(18): p. E1661.

117. Chen, H., M. Lisby, and L.S. Symington, *RPA coordinates DNA end resection and prevents formation of DNA hairpins.* Molecular cell, 2013. **50**(4): p. 589-600.

118. San Filippo, J., P. Sung, and H. Klein, *Mechanism of eukaryotic homologous recombination.* Annu Rev Biochem, 2008. **77**: p. 229-57.

119. Holloman, W.K. and C.M. Radding, *Recombination promoted by superhelical DNA and the recA gene of Escherichia coli.* Proceedings of the National Academy of Sciences of the United States of America, 1976. **73**(11): p. 3910-3914.

120. McEntee, K., G.M. Weinstock, and I.R. Lehman, *Initiation of general recombination catalyzed in vitro by the recA protein of Escherichia coli.* Proceedings of the National Academy of Sciences of the United States of America, 1979. **76**(6): p. 2615-2619.

121. Shibata, T., et al., *Purified Escherichia coli recA protein catalyzes homologous pairing of superhelical DNA and single-stranded fragments.* Proceedings of the National Academy of Sciences of the United States of America, 1979. **76**(4): p. 1638-1642.

122. Symington, L.S., *Role of RAD52 epistasis group genes in homologous recombination and double-strand break repair.* Microbiology and molecular biology reviews : MMBR, 2002. **66**(4): p. 630-670.

123. Conway, A.B., et al., *Crystal structure of a Rad51 filament.* Nature Structural & Molecular Biology, 2004. **11**(8): p. 791-796.

124. Stasiak, A., E. Di Capua, and T. Koller, *Elongation of duplex DNA by recA protein.* J Mol Biol, 1981. **151**(3): p. 557-64.

125. Xu, J., et al., *Cryo-EM structures of human RAD51 recombinase filaments during catalysis of DNA-strand exchange.* Nature structural & molecular biology, 2017. **24**(1): p. 40-46.

126. Danilowicz, C., et al., *RecA homology search is promoted by mechanical stress along the scanned duplex DNA.* Nucleic acids research, 2012. **40**(4): p. 1717-1727.

127. Liu, J., et al., *Presynaptic filament dynamics in homologous recombination and DNA repair.* Crit Rev Biochem Mol Biol, 2011. **46**(3): p. 240-70.

128. Subramanyam, S., et al., *Observation and Analysis of RAD51 Nucleation Dynamics at Single-Monomer Resolution.* Methods Enzymol, 2018. **600**: p. 201-232.

129. Liu, J., et al., *Human BRCA2 protein promotes RAD51 filament formation on RPA-covered single-stranded DNA.* Nat Struct Mol Biol, 2010. **17**(10): p. 1260-2.

130. Pfander, B., et al., *SUMO-modified PCNA recruits Srs2 to prevent recombination during S phase.* Nature, 2005. **436**(7049): p. 428-33.

131. Krejci, L., et al., *DNA helicase Srs2 disrupts the Rad51 presynaptic filament.* Nature, 2003. **423**(6937): p. 305-9.

132. Veaute, X., et al., *The Srs2 helicase prevents recombination by disrupting Rad51 nucleoprotein filaments.* Nature, 2003. **423**(6937): p. 309-12.

133. Liu, J. and W.-D. Heyer, *Who's who in human recombination: BRCA2 and RAD52.* Proceedings of the National Academy of Sciences, 2011. **108**(2): p. 441.

134. Brouwer, I., et al., *Human RAD52 Captures and Holds DNA Strands, Increases DNA Flexibility, and Prevents Melting of Duplex DNA: Implications for DNA Recombination.* Cell Rep, 2017. **18**(12): p. 2845-2853.

135. Spirek, M., et al., *Human RAD51 rapidly forms intrinsically dynamic nucleoprotein filaments modulated by nucleotide binding state.* Nucleic Acids Res, 2018. **46**(8): p. 3967-3980.

136. Feng, Z., et al., *Rad52 inactivation is synthetically lethal with BRCA2 deficiency.* Proceedings of the National Academy of Sciences, 2011. **108**(2): p. 686.

137. Marini, V. and L. Krejci, *Srs2: the "Odd-Job Man" in DNA repair.* DNA Repair (Amst), 2010. **9**(3): p. 268-75.

138. Godin, S., et al., *The Shu complex interacts with Rad51 through the Rad51 paralogues Rad55-Rad57 to mediate error-free recombination.* Nucleic Acids Res, 2013. **41**(8): p. 4525-34.

139. Julin, D.A., P.W. Riddles, and I.R. Lehman, *On the mechanism of pairing of single- and double-stranded DNA molecules by the recA and single-stranded DNA-binding proteins of Escherichia coli.* J Biol Chem, 1986. **261**(3): p. 1025-30.

140. Danilowicz, C., et al., *The differential extension in dsDNA bound to Rad51 filaments may play important roles in homology recognition and strand exchange.* Nucleic Acids Research, 2014. **42**(1): p. 526-533.

141. Gupta, R.C., et al., *Rapid exchange of A:T base pairs is essential for recognition of DNA homology by human Rad51 recombination protein.* Mol Cell, 1999. **4**(5): p. 705-14.

142. Zhao, W., et al., *The BRCA Tumor Suppressor Network in Chromosome Damage Repair by Homologous Recombination.* Annu Rev Biochem, 2019. **88**: p. 221-245.

143. Tavares, E.M., et al., *In vitro role of Rad54 in Rad51-ssDNA filament-dependent homology search and synaptic complexes formation.* Nat Commun, 2019. **10**(1): p. 4058.

144. Lu, D., et al., *Slow extension of the invading DNA strand in a D-loop formed by RecA-mediated homologous recombination may enhance recognition of DNA homology.* J Biol Chem, 2019. **294**(21): p. 8606-8616.

145. Sanchez, H., et al., *Combined optical and topographic imaging reveals different arrangements of human RAD54 with presynaptic and postsynaptic RAD51-DNA filaments.* Proceedings of the National Academy of Sciences of the United States of America, 2013. **110**(28): p. 11385-11390.

146. Van Komen, S., et al., *Superhelicity-driven homologous DNA pairing by yeast recombination factors Rad51 and Rad54.* Mol Cell, 2000. **6**(3): p. 563-72.

147. Wright, W.D. and W.D. Heyer, *Rad54 functions as a heteroduplex DNA pump modulated by its DNA substrates and Rad51 during D loop formation.* Mol Cell, 2014. **53**(3): p. 420-32.

148. Goyal, N., et al., *RAD54 N-terminal domain is a DNA sensor that couples ATP hydrolysis with branch migration of Holliday junctions.* Nature Communications, 2018. **9**(1): p. 34.

149. Mazina, O.M., et al., *Interactions of human rad54 protein with branched DNA molecules.* J Biol Chem, 2007. **282**(29): p. 21068-80.

150. Li, X. and W.D. Heyer, *RAD54 controls access to the invading 3'-OH end after RAD51-mediated DNA strand invasion in homologous recombination in Saccharomyces cerevisiae.* Nucleic Acids Res, 2009. **37**(2): p. 638-46.

151. Northall, S.J., et al., *Remodeling and Control of Homologous Recombination by DNA Helicases and Translocases that Target Recombinases and Synapsis.* Genes (Basel), 2016. **7**(8).

152. Sebesta, M., et al., *Role of PCNA and TLS polymerases in D-loop extension during homologous recombination in humans.* DNA repair, 2013. **12**(9): p. 691-698.

153. Spies, M. and R. Fishel, *Mismatch repair during homologous and homeologous recombination.* Cold Spring Harbor perspectives in biology, 2015. **7**(3): p. a022657-a022657.

154. Tham, K.-C., et al., *Mismatch repair inhibits homeologous recombination via coordinated directional unwinding of trapped DNA structures.* Molecular cell, 2013. **51**(3): p. 326-337.

155. Datta, A., et al., *Mitotic crossovers between diverged sequences are regulated by mismatch repair proteins in Saccaromyces cerevisiae.* Mol Cell Biol, 1996. **16**(3): p. 1085-93.

156. Datta, A., et al., *Dual roles for DNA sequence identity and the mismatch repair system in the regulation of mitotic crossing-over in yeast.* Proc Natl Acad Sci U S A, 1997. **94**(18): p. 9757-62.

157. Heyer, W.D., K.T. Ehmsen, and J. Liu, *Regulation of homologous recombination in eukaryotes.* Annu Rev Genet, 2010. **44**: p. 113-39.

158. Nimonkar, A.V. and S.C. Kowalczykowski, *Second-end DNA capture in double-strand break repair: how to catch a DNA by its tail*, in *Cell Cycle*. 2009: United States. p. 1816-7.

159. Daley, J.M., et al., *Regulation of DNA pairing in homologous recombination.* Cold Spring Harb Perspect Biol, 2014. **6**(11): p. a017954.

160. Osman, F., et al., *Generating crossovers by resolution of nicked Holliday junctions: a role for Mus81-Eme1 in meiosis.* Mol Cell, 2003. **12**(3): p. 761-74.

161. Liu, J., et al., *Srs2 promotes synthesis-dependent strand annealing by disrupting DNA polymerase δ-extending D-loops.* Elife, 2017. **6**.

162. Dupaigne, P., et al., *The Srs2 helicase activity is stimulated by Rad51 filaments on dsDNA: implications for crossover incidence during mitotic recombination.* Mol Cell, 2008. **29**(2): p. 243-54.

163. Mazon, G. and L.S. Symington, *Mph1 and Mus81-Mms4 prevent aberrant processing of mitotic recombination intermediates.* Mol Cell, 2013. **52**(1): p. 63-74.

164. Prakash, R., et al., *Yeast Mph1 helicase dissociates Rad51-made D-loops: implications for crossover control in mitotic recombination.* Genes Dev, 2009. **23**(1): p. 67-79.

165. Huselid, E. and S.F. Bunting, *The Regulation of Homologous Recombination by Helicases.* Genes (Basel), 2020. **11**(5).

166. Panico, E.R., et al., *Genetic evidence for a role of Saccharomyces cerevisiae Mph1 in recombinational DNA repair under replicative stress.* Yeast, 2010. **27**(1): p. 11-27.

167. Fasching, Clare L., et al., *Top3-Rmi1 Dissolve Rad51-Mediated D Loops by a Topoisomerase-Based Mechanism.* Molecular Cell, 2015. **57**(4): p. 595-606.

168. Piazza, A., et al., *Dynamic Processing of Displacement Loops during Recombinational DNA Repair.* Mol Cell, 2019. **73**(6): p. 1255-1266.e4.

169. Bizard, A.H. and I.D. Hickson, *The dissolution of double Holliday junctions.* Cold Spring Harb Perspect Biol, 2014. **6**(7): p. a016477.

170. Swuec, P. and A. Costa, *Molecular mechanism of double Holliday junction dissolution.* Cell Biosci, 2014. **4**: p. 36.

171. Schwartz, E.K. and W.D. Heyer, *Processing of joint molecule intermediates by structure-selective endonucleases during homologous recombination in eukaryotes.* Chromosoma, 2011. **120**(2): p. 109-27.

172. Schwartz, E.K., et al., *Mus81-Mms4 functions as a single heterodimer to cleave nicked intermediates in recombinational DNA repair.* Molecular and cellular biology, 2012. **32**(15): p. 3065-3080.

173. Mazón, G., et al., *The Rad1-Rad10 nuclease promotes chromosome translocations between dispersed repeats.* Nat Struct Mol Biol, 2012. **19**(9): p. 964-71.

174. Boddy, M.N., et al., *Mus81-Eme1 are essential components of a Holliday junction resolvase.* Cell, 2001. **107**(4): p. 537-48.

175. Gaillard, P.H.L., et al., *The endogenous Mus81-Eme1 complex resolves Holliday junctions by a nick and counternick mechanism.* Mol Cell, 2003. **12**(3): p. 747-59.

176. Ip, S.C., et al., *Identification of Holliday junction resolvases from humans and yeast.* Nature, 2008. **456**(7220): p. 357-61.

177. Ho, C.K., et al., *Mus81 and Yen1 promote reciprocal exchange during mitotic recombination to maintain genome integrity in budding yeast.* Mol Cell, 2010. **40**(6): p. 988-1000.

178. Blanco, M.G., et al., *Functional overlap between the structure-specific nucleases Yen1 and Mus81-Mms4 for DNA-damage repair in S. cerevisiae.* DNA Repair (Amst), 2010. **9**(4): p. 394-402.

179. Tay, Y.D. and L. Wu, *Overlapping roles for Yen1 and Mus81 in cellular Holliday junction processing.* J Biol Chem, 2010. **285**(15): p. 11427-32.

180. Coulon, S., et al., *Slx1-Slx4 Are Subunits of a Structure-specific Endonuclease That Maintains Ribosomal DNA in Fission Yeast.* Molecular Biology of the Cell, 2003. **15**(1): p. 71-80.

181. Kaliraman, V. and S.J. Brill, *Role of SGS1 and SLX4 in maintaining rDNA structure in Saccharomyces cerevisiae.* Current genetics, 2002. **41**(6): p. 389-400.

182. Muñoz-Galván, S., et al., *Distinct roles of Mus81, Yen1, Slx1-Slx4, and Rad1 nucleases in the repair of replication-born double-strand breaks by sister chromatid exchange.* Molecular and cellular biology, 2012. **32**(9): p. 1592-1603.

183. Fekairi, S., et al., *Human SLX4 is a Holliday junction resolvase subunit that binds multiple DNA repair/recombination endonucleases.* Cell, 2009. **138**(1): p. 78-89.

184. Wyatt, H.D., et al., *Coordinated actions of SLX1-SLX4 and MUS81-EME1 for Holliday junction resolution in human cells.* Mol Cell, 2013. **52**(2): p. 234-47.

185. Talhaoui, I., M. Bernal, and G. Mazon, *The nucleolytic resolution of recombination intermediates in yeast mitotic cells.* FEMS Yeast Res, 2016. **16**(6).

186. García-Luis, J. and F. Machín, *Mus81-Mms4 and Yen1 resolve a novel anaphase bridge formed by noncanonical Holliday junctions.* Nat Commun, 2014. **5**: p. 5652.

187. Mathiasen, D.P. and M. Lisby, *Cell cycle regulation of homologous recombination in Saccharomyces cerevisiae.* FEMS Microbiology Reviews, 2014. **38**(2): p. 172-184.

188. Szakal, B. and D. Branzei, *Premature Cdk1/Cdc5/Mus81 pathway activation induces aberrant replication and deleterious crossover.* EMBO J, 2013. **32**(8): p. 1155-67.

189. Gallo-Fernández, M., et al., *Cell cycle-dependent regulation of the nuclease activity of Mus81-Eme1/Mms4.* Nucleic Acids Res, 2012. **40**(17): p. 8325-35.

190. Matos, J., et al., *Regulatory control of the resolution of DNA recombination intermediates during meiosis and mitosis.* Cell, 2011. **147**(1): p. 158-72.

191. Eissler, C.L., et al., *The Cdk/cDc14 module controls activation of the Yen1 holliday junction resolvase to promote genome stability.* Mol Cell, 2014. **54**(1): p. 80-93.

192. Smith, C.E., B. Llorente, and L.S. Symington, *Template switching during break-induced replication.* Nature, 2007. **447**(7140): p. 102-105.

193. Davis, A.P. and L.S. Symington, *RAD51-dependent break-induced replication in yeast.* Mol Cell Biol, 2004. **24**(6): p. 2344-51.

194. Lydeard, J.R., et al., *Break-induced replication and telomerase-independent telomere maintenance require Pol32.* Nature, 2007. **448**(7155): p. 820-3.

195. Malkova, A., et al., *RAD51-dependent break-induced replication differs in kinetics and checkpoint responses from RAD51-mediated gene conversion.* Molecular and cellular biology, 2005. **25**(3): p. 933-944.

196. Donnianni, R.A. and L.S. Symington, *Break-induced replication occurs by conservative DNA synthesis.* Proceedings of the National Academy of Sciences, 2013. **110**(33): p. 13475.

197. Malkova, A. and G. Ira, *Break-induced replication: functions and molecular mechanism.* Current opinion in genetics & development, 2013. **23**(3): p. 271-279.

198. Sallmyr, A. and A.E. Tomkinson, *Repair of DNA double-strand breaks by mammalian alternative end-joining pathways.* J Biol Chem, 2018. **293**(27): p. 10536-10546.

199. Sugawara, N., G. Ira, and J.E. Haber, *DNA length dependence of the single-strand annealing pathway and the role of Saccharomyces cerevisiae RAD59 in double-strand break repair.* Mol Cell Biol, 2000. **20**(14): p. 5300-9.

200. Ramakrishnan, S., et al., *Single-strand annealing between inverted DNA repeats: Pathway choice, participating proteins, and genome destabilizing consequences.* PLoS Genet, 2018. **14**(8): p. e1007543.

201. Schmid, C.W., *Alu: structure, origin, evolution, significance and function of one-tenth of human DNA.* Prog Nucleic Acid Res Mol Biol, 1996. **53**: p. 283-319.

202. Bhargava, R., D.O. Onyango, and J.M. Stark, *Regulation of Single-Strand Annealing and its Role in Genome Maintenance.* Trends Genet, 2016. **32**(9): p. 566-575.

203. Sfeir, A. and L.S. Symington, *Microhomology-Mediated End Joining: A Back-up Survival Mechanism or Dedicated Pathway?* Trends in biochemical sciences, 2015. **40**(11): p. 701-714.

204. Sinha, S., et al., *Risky business: Microhomology-mediated end joining.* Mutation research, 2016. **788**: p. 17-24.

205. Villarreal, D.D., et al., *Microhomology directs diverse DNA break repair pathways and chromosomal translocations.* PLoS genetics, 2012. **8**(11): p. e1003026-e1003026.

206. Deng, S.K., et al., *RPA antagonizes microhomology-mediated repair of DNA double-strand breaks.* Nat Struct Mol Biol, 2014. **21**(4): p. 405-12.

207. Putnam, C.D., V. Pennaneach, and R.D. Kolodner, *Saccharomyces cerevisiae as a model system to define the chromosomal instability phenotype.* Mol Cell Biol, 2005. **25**(16): p. 7226-38.

208. Hashimoto, S., H. Anai, and K. Hanada, *Mechanisms of interstrand DNA crosslink repair and human disorders.* Genes Environ, 2016. **38**: p. 9.

209. Bakker, S.T., J.P. de Winter, and H. te Riele, *Learning from a paradox: recent insights into Fanconi anaemia through studying mouse models.* Dis Model Mech, 2013. **6**(1): p. 40-7.

210. Daee, D.L. and K. Myung, *Fanconi-like crosslink repair in yeast.* Genome Integrity, 2012. **3**(1): p. 7.

211. Gourzones, C., C. Bret, and J. Moreaux, *Treatment May Be Harmful: Mechanisms/Prediction/Prevention of Drug-Induced DNA Damage and Repair in Multiple Myeloma.* Front Genet, 2019. **10**: p. 861.

212. Deans, A.J. and S.C. West, *DNA interstrand crosslink repair and cancer.* Nat Rev Cancer, 2011. **11**(7): p. 467-80.

213. Legerski, R.J., *Repair of DNA interstrand cross-links during S phase of the mammalian cell cycle.* Environmental and molecular mutagenesis, 2010. **51**(6): p. 540-551.

214. Gobbini, E., et al., *Interplays between ATM/Tel1 and ATR/Mec1 in sensing and signaling DNA double-strand breaks.* DNA Repair (Amst), 2013. **12**(10): p. 791-9.

215. Lanz, M.C., D. Dibitetto, and M.B. Smolka, *DNA damage kinase signaling: checkpoint and repair at 30 years.* The EMBO Journal, 2019. **38**(18): p. e101801.

216. Nakada, D., K. Matsumoto, and K. Sugimoto, *ATM-related Tel1 associates with double-strand breaks through an Xrs2-dependent mechanism.* Genes & development, 2003. **17**(16): p. 1957-1962.

217. Falck, J., J. Coates, and S.P. Jackson, *Conserved modes of recruitment of ATM, ATR and DNA-PKcs to sites of DNA damage.* Nature, 2005. **434**(7033): p. 605-611.

218. Lee, J.-H. and T.T. Paull, *ATM Activation by DNA Double-Strand Breaks Through the Mre11-Rad50-Nbs1 Complex.* Science, 2005. **308**(5721): p. 551.

219. You, Z., et al., *ATM Activation and Its Recruitment to Damaged DNA Require Binding to the C Terminus of Nbs1.* Molecular and Cellular Biology, 2005. **25**(13): p. 5363.

220. Paciotti, V., et al., *The checkpoint protein Ddc2, functionally related to S. pombe Rad26, interacts with Mec1 and is regulated by Mec1-dependent phosphorylation in budding yeast.* Genes & development, 2000. **14**(16): p. 2046-2059.

221. Zou, L. and S.J. Elledge, *Sensing DNA Damage Through ATRIP Recognition of RPA-ssDNA Complexes.* Science, 2003. **300**(5625): p. 1542.

222. Mantiero, D., et al., *Dual role for Saccharomyces cerevisiae Tel1 in the checkpoint response to double-strand breaks.* EMBO reports, 2007. **8**(4): p. 380-387.

223. Shiotani, B. and L. Zou, *Single-stranded DNA orchestrates an ATM-to-ATR switch at DNA breaks.* Molecular cell, 2009. **33**(5): p. 547-558.

224. Ciccia, A. and S.J. Elledge, *The DNA damage response: making it safe to play with knives.* Molecular cell, 2010. **40**(2): p. 179-204.

225. Dai, Y. and S. Grant, *New insights into checkpoint kinase 1 in the DNA damage response signaling network.* Clinical cancer research : an official journal of the American Association for Cancer Research, 2010. **16**(2): p. 376-383.

226. Zannini, L., D. Delia, and G. Buscemi, *CHK2 kinase in the DNA damage response and beyond.* Journal of molecular cell biology, 2014. **6**(6): p. 442-457.

227. Kruse, J.P. and W. Gu, *Modes of p53 regulation.* Cell, 2009. **137**(4): p. 609-22.

228. Torres-Rosell, J., et al., *The Smc5–Smc6 complex and SUMO modification of Rad52 regulates recombinational repair at the ribosomal gene locus.* Nature Cell Biology, 2007. **9**(8): p. 923-931.

229. Gotta, M., et al., *The clustering of telomeres and colocalization with Rap1, Sir3, and Sir4 proteins in wild-type Saccharomyces cerevisiae.* J Cell Biol, 1996. **134**(6): p. 1349-63.

230. Marcand, S., *How do telomeres and NHEJ coexist?* Mol Cell Oncol, 2014. **1**(3): p. e963438.

231. Badie, S., et al., *BRCA2 acts as a RAD51 loader to facilitate telomere replication and capping.* Nature structural & molecular biology, 2010. **17**(12): p. 1461-1469.

232. Claussin, C. and M. Chang, *The many facets of homologous recombination at telomeres.* Microb Cell, 2015. **2**(9): p. 308-321.

233. Varon, R., et al., *Nibrin, a novel DNA double-strand break repair protein, is mutated in Nijmegen breakage syndrome.* Cell, 1998. **93**(3): p. 467-76.

234. Yang, R., et al., *Genome-wide analysis associates familial colorectal cancer with increases in copy number variations and a rare structural variation at 12p12.3.* Carcinogenesis, 2014. **35**(2): p. 315-23.

235. Kaneko, H. and N. Kondo, *Clinical features of Bloom syndrome and function of the causative gene, BLM helicase.* Expert Rev Mol Diagn, 2004. **4**(3): p. 393-401.

236. Rapakko, K., et al., *Germline alterations in the 53BP1 gene in breast and ovarian cancer families.* Cancer Lett, 2007. **245**(1-2): p. 337-40.

237. Bartkova, J., et al., *DNA damage response mediators MDC1 and 53BP1: constitutive activation and aberrant loss in breast and lung cancer, but not in testicular germ cell tumours.* Oncogene, 2007. **26**(53): p. 7414-22.

238. Petrucelli, N., M.B. Daly, and G.L. Feldman, *Hereditary breast and ovarian cancer due to mutations in BRCA1 and BRCA2.* Genet Med, 2010. **12**(5): p. 245-59.

239. Gatti, R.A., et al., *The pathogenesis of ataxia-telangiectasia. Learning from a Rosetta Stone.* Clin Rev Allergy Immunol, 2001. **20**(1): p. 87-108.

240. O'Driscoll, M., et al., *A splicing mutation affecting expression of ataxia-telangiectasia and Rad3-related protein (ATR) results in Seckel syndrome.* Nat Genet, 2003. **33**(4): p. 497-501.

241. Karppinen, S.M., et al., *Identification of a common polymorphism in the TopBP1 gene associated with hereditary susceptibility to breast and ovarian cancer.* Eur J Cancer, 2006. **42**(15): p. 2647-52.

242. Nissar, S., et al., *RAD51 G135C gene polymorphism and risk of colorectal cancer in Kashmir.* Eur J Cancer Prev, 2014. **23**(4): p. 264-8.

243. Sun, H., et al., *RAD51 G135C polymorphism is associated with breast cancer susceptibility: a meta-analysis involving 22,399 subjects.* Breast Cancer Res Treat, 2011. **125**(1): p. 157-61.

244. Silva, S.N., et al., *Breast cancer risk and common single nucleotide polymorphisms in homologous recombination DNA repair pathway genes XRCC2, XRCC3, NBS1 and RAD51.* Cancer Epidemiol, 2010. **34**(1): p. 85-92.

245. Vuorela, M., et al., *Further evidence for the contribution of the RAD51C gene in hereditary breast and ovarian cancer susceptibility.* Breast Cancer Res Treat, 2011. **130**(3): p. 1003-10.

246. Meetei, A.R., et al., *A human ortholog of archaeal DNA repair protein Hef is defective in Fanconi anemia complementation group M.* Nat Genet, 2005. **37**(9): p. 958-63.

247. Ballew, B.J., et al., *Germline mutations of regulator of telomere elongation helicase 1, RTEL1, in Dyskeratosis congenita.* Hum Genet, 2013. **132**(4): p. 473-80.

248. Crossan, G.P., et al., *Disruption of mouse Slx4, a regulator of structure-specific nucleases, phenocopies Fanconi anemia.* Nat Genet, 2011. **43**(2): p. 147-52.

249. Kim, Y., et al., *Mutations of the SLX4 gene in Fanconi anemia.* Nat Genet, 2011. **43**(2): p. 142-6.

250. Stoepker, C., et al., *SLX4, a coordinator of structure-specific endonucleases, is mutated in a new Fanconi anemia subtype.* Nat Genet, 2011. **43**(2): p. 138-41.

251. Gregg, S.Q., A.R. Robinson, and L.J. Niedernhofer, *Physiological consequences of defects in ERCC1-XPF DNA repair endonuclease.* DNA Repair (Amst), 2011. **10**(7): p. 781-91.

252. Olivier, M., M. Hollstein, and P. Hainaut, *TP53 mutations in human cancers: origins, consequences, and clinical use.* Cold Spring Harb Perspect Biol, 2010. **2**(1): p. a001008.

253. Chen, H., S. Zhang, and Z. Wu, *Fanconi anemia pathway defects in inherited and sporadic cancers.* Translational pediatrics, 2014. **3**(4): p. 300-304.

254. Akkari, Y.M., et al., *DNA replication is required To elicit cellular responses to psoralen-induced DNA interstrand cross-links.* Mol Cell Biol, 2000. **20**(21): p. 8283-9.

255. de Renty, C. and N.A. Ellis, *Bloom's syndrome: Why not premature aging?: A comparison of the BLM and WRN helicases.* Ageing research reviews, 2017. **33**: p. 36-51.

256. Cunniff, C., J.A. Bassetti, and N.A. Ellis, *Bloom's Syndrome: Clinical Spectrum, Molecular Pathogenesis, and Cancer Predisposition.* Mol Syndromol, 2017. **8**(1): p. 4-23.

257. Berry, J.L., et al., *The RB1 Story: Characterization and Cloning of the First Tumor Suppressor Gene.* Genes, 2019. **10**(11).

258. Cavenee, W.K., et al., *Expression of recessive alleles by chromosomal mechanisms in retinoblastoma.* Nature, 1983. **305**(5937): p. 779-84.

259. Dryja, T.P., et al., *Homozygosity of chromosome 13 in retinoblastoma.* N Engl J Med, 1984. **310**(9): p. 550-3.

260. Bhattacharya, S. and A. Asaithamby, *Repurposing DNA repair factors to eradicate tumor cells upon radiotherapy.* Translational cancer research, 2017. **6**(Suppl 5): p. S822-S839.

261. Hosoya, N. and K. Miyagawa, *Targeting DNA damage response in cancer therapy.* Cancer science, 2014. **105**(4): p. 370-388.

262. Kaelin, W.G., *The Concept of Synthetic Lethality in the Context of Anticancer Therapy.* Nature Reviews Cancer, 2005. **5**(9): p. 689-698.

263. Helleday, T., *The underlying mechanism for the PARP and BRCA synthetic lethality: clearing up the misunderstandings.* Mol Oncol, 2011. **5**(4): p. 387-93.

264. Fong, P.C., et al., *Inhibition of poly(ADP-ribose) polymerase in tumors from BRCA mutation carriers.* N Engl J Med, 2009. **361**(2): p. 123-34.

265. Rottenberg, S., et al., *High sensitivity of BRCA1-deficient mammary tumors to the PARP inhibitor AZD2281 alone and in combination with platinum drugs.* Proc Natl Acad Sci U S A, 2008. **105**(44): p. 17079-84.

266. Farmer, H., et al., *Targeting the DNA repair defect in BRCA mutant cells as a therapeutic strategy.* Nature, 2005. **434**(7035): p. 917-21.

267. Liu, X., et al., *Somatic loss of BRCA1 and p53 in mice induces mammary tumors with features of human BRCA1-mutated basal-like breast cancer.* Proc Natl Acad Sci U S A, 2007. **104**(29): p. 12111-6.

268. Evers, B., T. Helleday, and J. Jonkers, *Targeting homologous recombination repair defects in cancer.* Trends Pharmacol Sci, 2010. **31**(8): p. 372-80.

269. Bryant, H.E., et al., *Specific killing of BRCA2-deficient tumours with inhibitors of poly(ADP-ribose) polymerase.* Nature, 2005. **434**(7035): p. 913-7.

270. Giovannini, S., et al., *Synthetic lethality between BRCA1 deficiency and poly(ADP-ribose) polymerase inhibition is modulated by processing of endogenous oxidative DNA damage.* Nucleic Acids Research, 2019. **47**(17): p. 9132-9143.

271. Kerscher, O., R. Felberbaum, and M. Hochstrasser, *Modification of proteins by ubiquitin and ubiquitin-like proteins.* Annu Rev Cell Dev Biol, 2006. **22**: p. 159-80.

272. Finley, D., *Recognition and processing of ubiquitin-protein conjugates by the proteasome.* Annu Rev Biochem, 2009. **78**: p. 477-513.

273. Oh, E., D. Akopian, and M. Rape, *Principles of Ubiquitin-Dependent Signaling.* Annu Rev Cell Dev Biol, 2018. **34**: p. 137-162.

274. Pickart, C.M. and M.J. Eddins, *Ubiquitin: structures, functions, mechanisms.* Biochim Biophys Acta, 2004. **1695**(1-3): p. 55-72.

275. Dougherty, S.E., et al., *Expanding Role of Ubiquitin in Translational Control.* International journal of molecular sciences, 2020. **21**(3): p. 1151.

276. Alonso, A., et al., *Emerging roles of sumoylation in the regulation of actin, microtubules, intermediate filaments, and septins.* Cytoskeleton (Hoboken, N.J.), 2015. **72**(7): p. 305-339.

277. Su, S., Y. Zhang, and P. Liu, *Roles of Ubiquitination and SUMOylation in DNA Damage Response.* Curr Issues Mol Biol, 2020. **35**: p. 59-84.

278. Finley, D., et al., *The ubiquitin-proteasome system of Saccharomyces cerevisiae.* Genetics, 2012. **192**(2): p. 319-60.

279. Swatek, K.N. and D. Komander, *Ubiquitin modifications.* Cell Res, 2016. **26**(4): p. 399-422.

280. Geiss-Friedlander, R. and F. Melchior, *Concepts in sumoylation: a decade on.* Nat Rev Mol Cell Biol, 2007. **8**(12): p. 947-56.

281. Shimizu, Y., Y. Okuda-Shimizu, and L.M. Hendershot, *Ubiquitylation of an ERAD substrate occurs on multiple types of amino acids.* Mol Cell, 2010. **40**(6): p. 917-26.

282. Streich, F.C., Jr. and C.D. Lima, *Structural and functional insights to ubiquitin-like protein conjugation.* Annual review of biophysics, 2014. **43**: p. 357-379.

283. Davey, N.E. and D.O. Morgan, *Building a Regulatory Network with Short Linear Sequence Motifs: Lessons from the Degrons of the Anaphase-Promoting Complex.* Mol Cell, 2016. **64**(1): p. 12-23.

284. Dove, K.K. and R.E. Klevit, *RING-Between-RING E3 Ligases: Emerging Themes amid the Variations.* J Mol Biol, 2017. **429**(22): p. 3363-3375.

285. Kliza, K. and K. Husnjak, *Resolving the Complexity of Ubiquitin Networks.* Frontiers in Molecular Biosciences, 2020. **7**: p. 21.

286. Komander, D. and M. Rape, *The ubiquitin code.* Annu Rev Biochem, 2012. **81**: p. 203-29.

287. Peng, J., et al., *A proteomics approach to understanding protein ubiquitination.* Nat Biotechnol, 2003. **21**(8): p. 921-6.

288. Hoege, C., et al., *RAD6-dependent DNA repair is linked to modification of PCNA by ubiquitin and SUMO.* Nature, 2002. **419**(6903): p. 135-41.

289. Kwon, Y.T. and A. Ciechanover, *The Ubiquitin Code in the Ubiquitin-Proteasome System and Autophagy.* Trends Biochem Sci, 2017. **42**(11): p. 873-886.

290. Koyano, F., et al., *Ubiquitin is phosphorylated by PINK1 to activate parkin.* Nature, 2014. **510**(7503): p. 162-6.

291. Ohtake, F., et al., *Ubiquitin acetylation inhibits polyubiquitin chain elongation.* EMBO Rep, 2015. **16**(2): p. 192-201.

292. Hutchins, A.P., et al., *The repertoires of ubiquitinating and deubiquitinating enzymes in eukaryotic genomes.* Mol Biol Evol, 2013. **30**(5): p. 1172-87.

293. Grou, C.P., et al., *The de novo synthesis of ubiquitin: identification of deubiquitinases acting on ubiquitin precursors.* Scientific Reports, 2015. **5**(1): p. 12836.

294. Bayer, P., et al., *Structure determination of the small ubiquitin-related modifier SUMO-1.* J Mol Biol, 1998. **280**(2): p. 275-86.

295. Takahashi, Y., A. Toh-e, and Y. Kikuchi, *A novel factor required for the SUMO1/Smt3 conjugation of yeast septins.* Gene, 2001. **275**(2): p. 223-31.

296. Johnson, E.S., *Protein modification by SUMO.* Annu Rev Biochem, 2004. **73**: p. 355-82.

297. Sampson, D.A., M. Wang, and M.J. Matunis, *The small ubiquitin-like modifier-1 (SUMO-1) consensus sequence mediates Ubc9 binding and is essential for SUMO-1 modification.* J Biol Chem, 2001. **276**(24): p. 21664-9.

298. Rodriguez, M.S., C. Dargemont, and R.T. Hay, *SUMO-1 conjugation in vivo requires both a consensus modification motif and nuclear targeting.* J Biol Chem, 2001. **276**(16): p. 12654-9.

299. Chang, C.C., et al., *SUMOgo: Prediction of sumoylation sites on lysines by motif screening models and the effects of various post-translational modifications.* Sci Rep, 2018. **8**(1): p. 15512.

300. Gareau, J.R. and C.D. Lima, *The SUMO pathway: emerging mechanisms that shape specificity, conjugation and recognition.* Nat Rev Mol Cell Biol, 2010. **11**(12): p. 861-71.

301. Bernier-Villamor, V., et al., *Structural basis for E2-mediated SUMO conjugation revealed by a complex between ubiquitin-conjugating enzyme Ubc9 and RanGAP1.* Cell, 2002. **108**(3): p. 345-56.

302. Lamoliatte, F., et al., *Large-scale analysis of lysine SUMOylation by SUMO remnant immunoaffinity profiling.* Nat Commun, 2014. **5**: p. 5409.

303. Takahashi, Y., et al., *Cytoplasmic sumoylation by PIAS-type Siz1-SUMO ligase.* Cell Cycle, 2008. **7**(12): p. 1738-44.

304. Johnson, E.S. and A.A. Gupta, *An E3-like factor that promotes SUMO conjugation to the yeast septins.* Cell, 2001. **106**(6): p. 735-44.

305. Hickey, C.M., N.R. Wilson, and M. Hochstrasser, *Function and regulation of SUMO proteases.* Nat Rev Mol Cell Biol, 2012. **13**(12): p. 755-66.

306. Palvimo, J.J., *PIAS proteins as regulators of small ubiquitin-related modifier (SUMO) modifications and transcription.* Biochem Soc Trans, 2007. **35**(Pt 6): p. 1405-8.

307. Cheng, C.H., et al., *SUMO modifications control assembly of synaptonemal complex and polycomplex in meiosis of Saccharomyces cerevisiae.* Genes Dev, 2006. **20**(15): p. 2067-81.

308. Aravind, L. and E.V. Koonin, *SAP - a putative DNA-binding motif involved in chromosomal organization.* Trends Biochem Sci, 2000. **25**(3): p. 112-4.

309. Yunus, A.A. and C.D. Lima, *Structure of the Siz/PIAS SUMO E3 ligase Siz1 and determinants required for SUMO modification of PCNA.* Mol Cell, 2009. **35**(5): p. 669-82.

310. Suzuki, R., et al., *Solution structures and DNA binding properties of the N-terminal SAP domains of SUMO E3 ligases from Saccharomyces cerevisiae and Oryza sativa.* Proteins, 2009. **75**(2): p. 336-47.

311. Potts, P.R. and H. Yu, *The SMC5/6 complex maintains telomere length in ALT cancer cells through SUMOylation of telomere-binding proteins.* Nat Struct Mol Biol, 2007. **14**(7): p. 581-90.

312. Branzei, D., et al., *Ubc9- and mms21-mediated sumoylation counteracts recombinogenic events at damaged replication forks.* Cell, 2006. **127**(3): p. 509-22.

313. Zhao, X. and G. Blobel, *A SUMO ligase is part of a nuclear multiprotein complex that affects DNA repair and chromosomal organization.* Proc Natl Acad Sci U S A, 2005. **102**(13): p. 4777-82.

314. de Carvalho, C.E. and M.P. Colaiácovo, *SUMO-mediated regulation of synaptonemal complex formation during meiosis.* Genes Dev, 2006. **20**(15): p. 1986-92.

315. Abrieu, A. and D. Liakopoulos, *How Does SUMO Participate in Spindle Organization?* Cells, 2019. **8**(8).

316. Jeram, S.M., et al., *An improved SUMmOn-based methodology for the identification of ubiquitin and ubiquitin-like protein conjugation sites identifies novel ubiquitin-like protein chain linkages.* Proteomics, 2010. **10**(2): p. 254-65.

317. Srikumar, T., et al., *Global analysis of SUMO chain function reveals multiple roles in chromatin regulation.* J Cell Biol, 2013. **201**(1): p. 145-63.

318. Keiten-Schmitz, J., K. Schunck, and S. Müller, *SUMO Chains Rule on Chromatin Occupancy.* Frontiers in cell and developmental biology, 2020. **7**: p. 343-343.

319. Psakhye, I., F. Castellucci, and D. Branzei, *SUMO-Chain-Regulated Proteasomal Degradation Timing Exemplified in DNA Replication Initiation.* Molecular cell, 2019. **76**(4): p. 632-645.e6.

320. Jansen, N.S. and A.C.O. Vertegaal, *A Chain of Events: Regulating Target Proteins by SUMO Polymers.* Trends Biochem Sci, 2020.

321. Perry, J.J., J.A. Tainer, and M.N. Boddy, *A SIM-ultaneous role for SUMO and ubiquitin.* Trends Biochem Sci, 2008. **33**(5): p. 201-8.

322. Psakhye, I. and S. Jentsch, *Protein group modification and synergy in the SUMO pathway as exemplified in DNA repair.* Cell, 2012. **151**(4): p. 807-820.

323. Desterro, J.M., M.S. Rodriguez, and R.T. Hay, *SUMO-1 modification of IkappaBalpha inhibits NF-kappaB activation.* Mol Cell, 1998. **2**(2): p. 233-9.

324. Lamoliatte, F., et al., *Targeted identification of SUMOylation sites in human proteins using affinity enrichment and paralog-specific reporter ions.* Mol Cell Proteomics, 2013. **12**(9): p. 2536-50.

325. Horigome, C., et al., *PolySUMOylation by Siz2 and Mms21 triggers relocation of DNA breaks to nuclear pores through the Slx5/Slx8 STUbL.* Genes Dev, 2016. **30**(8): p. 931-45.

326. Praefcke, G.J., K. Hofmann, and R.J. Dohmen, *SUMO playing tag with ubiquitin.* Trends Biochem Sci, 2012. **37**(1): p. 23-31.

327. Uzunova, K., et al., *Ubiquitin-dependent proteolytic control of SUMO conjugates.* J Biol Chem, 2007. **282**(47): p. 34167-75.

328. Zhang, Z. and A.R. Buchman, *Identification of a member of a DNA-dependent ATPase family that causes interference with silencing.* Mol Cell Biol, 1997. **17**(9): p. 5461-72.

329. Ii, T., et al., *The yeast Slx5-Slx8 DNA integrity complex displays ubiquitin ligase activity.* Cell Cycle, 2007. **6**(22): p. 2800-9.

330. Prudden, J., et al., *SUMO-targeted ubiquitin ligases in genome stability.* EMBO J, 2007. **26**(18): p. 4089-101.

331. Nagai, S., et al., *Functional targeting of DNA damage to a nuclear pore-associated SUMO-dependent ubiquitin ligase.* Science, 2008. **322**(5901): p. 597-602.

332. Sriramachandran, A.M. and R.J. Dohmen, *SUMO-targeted ubiquitin ligases.* Biochim Biophys Acta, 2014. **1843**(1): p. 75-85.

333. Tan, W., Z. Wang, and G. Prelich, *Physical and Genetic Interactions Between Uls1 and the Slx5-Slx8 SUMO-Targeted Ubiquitin Ligase.* G3 (Bethesda, Md.), 2013. **3**(4): p. 771-780.

334. Nie, M., et al., *SUMO-targeted ubiquitin ligase activity can either suppress or promote genome instability, depending on the nature of the DNA lesion.* PLOS Genetics, 2017. **13**(5): p. e1006776.

335. Kumar, R. and K. Sabapathy, *RNF4-A Paradigm for SUMOylation-Mediated Ubiquitination.* Proteomics, 2019. **19**(21-22): p. e1900185.

336. Hannich, J.T., et al., *Defining the SUMO-modified proteome by multiple approaches in Saccharomyces cerevisiae.* J Biol Chem, 2005. **280**(6): p. 4102-10.

337. Parker, J.L. and H.D. Ulrich, *A SUMO-interacting motif activates budding yeast ubiquitin ligase Rad18 towards SUMO-modified PCNA.* Nucleic Acids Res, 2012. **40**(22): p. 11380-8.

338. Grabbe, C. and I. Dikic, *Functional roles of ubiquitin-like domain (ULD) and ubiquitin-binding domain (UBD) containing proteins.* Chem Rev, 2009. **109**(4): p. 1481-94.

339. Hurley, J.H., S. Lee, and G. Prag, *Ubiquitin-binding domains.* Biochem J, 2006. **399**(3): p. 361-72.

340. Vadlamudi, R.K., et al., *p62, a phosphotyrosine-independent ligand of the SH2 domain of p56lck, belongs to a new class of ubiquitin-binding proteins.* J Biol Chem, 1996. **271**(34): p. 20235-7.

341. Bertolaet, B.L., et al., *UBA domains mediate protein-protein interactions between two DNA damage-inducible proteins.* J Mol Biol, 2001. **313**(5): p. 955-63.

342. Bertolaet, B.L., et al., *UBA domains of DNA damage-inducible proteins interact with ubiquitin.* Nat Struct Biol, 2001. **8**(5): p. 417-22.

343. Chen, L., et al., *Ubiquitin-associated (UBA) domains in Rad23 bind ubiquitin and promote inhibition of multi-ubiquitin chain assembly.* EMBO reports, 2001. **2**(10): p. 933-938.

344. Dieckmann, T., et al., *Structure of a human DNA repair protein UBA domain that interacts with HIV-1 Vpr.* Nat Struct Biol, 1998. **5**(12): p. 1042-7.

345. Withers-Ward, E.S., et al., *Biochemical and structural analysis of the interaction between the UBA(2) domain of the DNA repair protein HHR23A and HIV-1 Vpr.* Biochemistry, 2000. **39**(46): p. 14103-12.

346. Hofmann, K. and L. Falquet, *A ubiquitin-interacting motif conserved in components of the proteasomal and lysosomal protein degradation systems.* Trends Biochem Sci, 2001. **26**(6): p. 347-50.

347. Polo, S., et al., *A single motif responsible for ubiquitin recognition and monoubiquitination in endocytic proteins.* Nature, 2002. **416**(6879): p. 451-5.

348. Shih, S.C., et al., *Epsins and Vps27p/Hrs contain ubiquitin-binding domains that function in receptor endocytosis.* Nat Cell Biol, 2002. **4**(5): p. 389-93.

349. Bilodeau, P.S., et al., *The Vps27p Hse1p complex binds ubiquitin and mediates endosomal protein sorting.* Nat Cell Biol, 2002. **4**(7): p. 534-9.

350. Raiborg, C., et al., *Hrs sorts ubiquitinated proteins into clathrin-coated microdomains of early endosomes.* Nat Cell Biol, 2002. **4**(5): p. 394-8.

351. Klapisz, E., et al., *A ubiquitin-interacting motif (UIM) is essential for Eps15 and Eps15R ubiquitination.* J Biol Chem, 2002. **277**(34): p. 30746-53.

352. Shih, S.C., et al., *A ubiquitin-binding motif required for intramolecular monoubiquitylation, the CUE domain.* The EMBO journal, 2003. **22**(6): p. 1273-1281.

353. Lee, S., et al., *Structural basis for ubiquitin recognition and autoubiquitination by Rabex-5.* Nature structural & molecular biology, 2006. **13**(3): p. 264-271.

354. Randles, L. and K.J. Walters, *Ubiquitin and its binding domains.* Frontiers in bioscience (Landmark edition), 2012. **17**: p. 2140-2157.

355. Bienko, M., et al., *Ubiquitin-binding domains in Y-family polymerases regulate translesion synthesis.* Science, 2005. **310**(5755): p. 1821-4.

356. Wickliffe, K.E., et al., *The mechanism of linkage-specific ubiquitin chain elongation by a single-subunit E2.* Cell, 2011. **144**(5): p. 769-781.

357. Beauclair, G., et al., *JASSA: a comprehensive tool for prediction of SUMOylation sites and SIMs.* Bioinformatics, 2015. **31**(21): p. 3483-91.

358. Fisher, R.D., et al., *Structure and ubiquitin binding of the ubiquitin-interacting motif.* J Biol Chem, 2003. **278**(31): p. 28976-84.

359. Minty, A., et al., *Covalent modification of p73alpha by SUMO-1. Two-hybrid screening with p73 identifies novel SUMO-1-interacting proteins and a SUMO-1 interaction motif.* J Biol Chem, 2000. **275**(46): p. 36316-23.

360. Song, J., et al., *Identification of a SUMO-binding motif that recognizes SUMO-modified proteins.* Proc Natl Acad Sci U S A, 2004. **101**(40): p. 14373-8.

361. Song, J., et al., *Small ubiquitin-like modifier (SUMO) recognition of a SUMO binding motif: a reversal of the bound orientation.* J Biol Chem, 2005. **280**(48): p. 40122-9.

362. Heerwagen, J.H., et al., *Environmental design, work, and well being: managing occupational stress through changes in the workplace environment.* Aaohn j, 1995. **43**(9): p. 458-68.

363. Ouyang, J., et al., *Direct binding of CoREST1 to SUMO-2/3 contributes to gene-specific repression by the LSD1/CoREST1/HDAC complex.* Mol Cell, 2009. **34**(2): p. 145-54.

364. Escobar-Cabrera, E., et al., *Characterizing the N- and C-terminal Small ubiquitin-like modifier (SUMO)-interacting motifs of the scaffold protein DAXX.* J Biol Chem, 2011. **286**(22): p. 19816-29.

365. Bermudez-Lopez, M., et al., *Sgs1's roles in DNA end resection, HJ dissolution, and crossover suppression require a two-step SUMO regulation dependent on Smc5/6.* Genes Dev, 2016. **30**(11): p. 1339-56.

366. Dhingra, N. and X. Zhao, *Intricate SUMO-based control of the homologous recombination machinery.* Genes Dev, 2019. **33**(19-20): p. 1346-1354.

367. Torrecilla, I., J. Oehler, and K. Ramadan, *The role of ubiquitin-dependent segregase p97 (VCP or Cdc48) in chromatin dynamics after DNA double strand breaks.* Philos Trans R Soc Lond B Biol Sci, 2017. **372**(1731).

368. Bergink, S., et al., *Role of Cdc48/p97 as a SUMO-targeted segregase curbing Rad51-Rad52 interaction.* Nat Cell Biol, 2013. **15**(5): p. 526-32.

369. Kohler, J.B., et al., *Concerted action of the ubiquitin-fusion degradation protein 1 (Ufd1) and Sumo-targeted ubiquitin ligases (STUbLs) in the DNA-damage response.* PLoS One, 2013. **8**(11): p. e80442.

370. Mullen, J.R. and S.J. Brill, *Activation of the Slx5-Slx8 ubiquitin ligase by poly-small ubiquitin-like modifier conjugates.* J Biol Chem, 2008. **283**(29): p. 19912-21.

371. Zhao, Y., et al., *Crosstalk between ubiquitin and other post-translational modifications on chromatin during double-strand break repair.* Trends in cell biology, 2014. **24**(7): p. 426-434.

372. Filtz, T.M., W.K. Vogel, and M. Leid, *Regulation of transcription factor activity by interconnected post-translational modifications.* Trends in pharmacological sciences, 2014. **35**(2): p. 76-85.

373. Wojcik, F., et al., *Functional crosstalk between histone H2B ubiquitylation and H2A modifications and variants.* Nature Communications, 2018. **9**(1): p. 1394.

374. Sagar, G.D.V., et al., *Ubiquitination-induced conformational change within the deiodinase dimer is a switch regulating enzyme activity.* Molecular and cellular biology, 2007. **27**(13): p. 4774-4783.

375. Butt, T.R., et al., *SUMO fusion technology for difficult-to-express proteins.* Protein Expr Purif, 2005. **43**(1): p. 1-9.

376. Butt, T.R., et al., *Ubiquitin fusion augments the yield of cloned gene products in Escherichia coli.* Proc Natl Acad Sci U S A, 1989. **86**(8): p. 2540-4.

377. Malakhov, M.P., et al., *SUMO fusions and SUMO-specific protease for efficient expression and purification of proteins.* J Struct Funct Genomics, 2004. **5**(1-2): p. 75-86.

378. Kuo, D., M. Nie, and A.J. Courey, *SUMO as a solubility tag and in vivo cleavage of SUMO fusion proteins with Ulp1.* Methods Mol Biol, 2014. **1177**: p. 71-80.

379. Geng, F., S. Wenzel, and W.P. Tansey, *Ubiquitin and proteasomes in transcription.* Annu Rev Biochem, 2012. **81**: p. 177-201.

380. Ohi, M.D., et al., *Structural insights into the U-box, a domain associated with multi-ubiquitination.* Nat Struct Biol, 2003. **10**(4): p. 250-5.

381. Nasmyth, K., J.M. Peters, and F. Uhlmann, *Splitting the chromosome: cutting the ties that bind sister chromatids.* Science, 2000. **288**(5470): p. 1379-85.

382. Jin, L., et al., *Mechanism of ubiquitin-chain formation by the human anaphase-promoting complex.* Cell, 2008. **133**(4): p. 653-65.

383. Johnson, E.S. and G. Blobel, *Cell cycle-regulated attachment of the ubiquitin-related protein SUMO to the yeast septins.* J Cell Biol, 1999. **147**(5): p. 981-94.

384. Ribet, D., et al., *SUMOylation of human septins is critical for septin filament bundling and cytokinesis.* J Cell Biol, 2017. **216**(12): p. 4041-4052.

385. Gillies, J., et al., *SUMO Pathway Modulation of Regulatory Protein Binding at the Ribosomal DNA Locus in Saccharomyces cerevisiae.* Genetics, 2016. **202**(4): p. 1377.

386. Colomina, N., C. Guasch, and J. Torres-Rosell, *Analysis of SUMOylation in the RENT Complex by Fusion to a SUMO-Specific Protease Domain*, in *The Mitotic Exit Network: Methods and Protocols*, F. Monje-Casas and E. Queralt, Editors. 2017, Springer New York: New York, NY. p. 97-117.

387. D'Amours, D. and A. Amon, *At the interface between signaling and executing anaphase—Cdc14 and the FEAR network.* Genes & Development, 2004. **18**(21): p. 2581-2595.

388. Lescasse, R., et al., *End-joining inhibition at telomeres requires the translocase and polySUMO-dependent ubiquitin ligase Uls1.* Embo j, 2013. **32**(6): p. 805-15.

389. Westerbeck, J.W., et al., *A SUMO-targeted ubiquitin ligase is involved in the degradation of the nuclear pool of the SUMO E3 ligase Siz1.* Molecular Biology of the Cell, 2013. **25**(1): p. 1-16.

390. Ohkuni, K., et al., *SUMO-Targeted Ubiquitin Ligase (STUbL) Slx5 regulates proteolysis of centromeric histone H3 variant Cse4 and prevents its mislocalization to euchromatin.* Mol Biol Cell, 2016. **27**(9): p. 1500-10.

391. Schweiggert, J., et al., *Regulation of a Spindle Positioning Factor at Kinetochores by SUMO-Targeted Ubiquitin Ligases.* Dev Cell, 2016. **36**(4): p. 415-27.

392. Höpfler, M., et al., *Slx5/Slx8-dependent ubiquitin hotspots on chromatin contribute to stress tolerance.* The EMBO journal, 2019. **38**(11).

393. Jackson, S.P. and D. Durocher, *Regulation of DNA damage responses by ubiquitin and SUMO.* Mol Cell, 2013. **49**(5): p. 795-807.

394. Sun, Y., et al., *A conserved SUMO-Ubiquitin pathway directed by RNF4/SLX5-SLX8 and PIAS4/SIZ1 drives proteasomal degradation of topoisomerase DNA-protein crosslinks.* bioRxiv, 2019: p. 707661.

395. Ulrich, H.D., *Ubiquitin and SUMO in DNA repair at a glance.* J Cell Sci, 2012. **125**(Pt 2): p. 249-54.

396. Cremona, C.A., et al., *Extensive DNA damage-induced sumoylation contributes to replication and repair and acts in addition to the mec1 checkpoint.* Mol Cell, 2012. **45**(3): p. 422-32.

397. Ripley, B.M., M.S. Gildenberg, and M.T. Washington, *Control of DNA Damage Bypass by Ubiquitylation of PCNA.* Genes (Basel), 2020. **11**(2).

398. Parker, J.L. and H.D. Ulrich, *Mechanistic analysis of PCNA poly-ubiquitylation by the ubiquitin protein ligases Rad18 and Rad5.* EMBO J, 2009. **28**(23): p. 3657-66.

399. Hang, L.E., et al., *Regulation of Ku-DNA association by Yku70 C-terminal tail and SUMO modification.* J Biol Chem, 2014. **289**(15): p. 10308-17.

400. Psakhye, I. and S. Jentsch, *Protein group modification and synergy in the SUMO pathway as exemplified in DNA repair.* Cell, 2012. **151**(4): p. 807-20.

401. Altmannova, V., et al., *Rad52 SUMOylation affects the efficiency of the DNA repair.* Nucleic Acids Res, 2010. **38**(14): p. 4708-21.

402. Esta, A., et al., *Rad52 Sumoylation Prevents the Toxicity of Unproductive Rad51 Filaments Independently of the Anti-Recombinase Srs2.* PLOS Genetics, 2013. **9**(10): p. e1003833.

403. Sacher, M., et al., *Control of Rad52 recombination activity by double-strand break-induced SUMO modification.* Nat Cell Biol, 2006. **8**(11): p. 1284-90.

404. Dou, H., et al., *Regulation of DNA repair through deSUMOylation and SUMOylation of replication protein A complex.* Mol Cell, 2010. **39**(3): p. 333-45.

405. Dou, H., et al., *SUMOylation and de-SUMOylation in response to DNA damage.* FEBS Lett, 2011. **585**(18): p. 2891-6.

406. Elia, A.E., et al., *RFWD3-Dependent Ubiquitination of RPA Regulates Repair at Stalled Replication Forks.* Mol Cell, 2015. **60**(2): p. 280-93.

407. Bermudez-Lopez, M., et al., *The Smc5/6 complex is required for dissolution of DNA-mediated sister chromatid linkages.* Nucleic Acids Res, 2010. **38**(19): p. 6502-12.

408. Bonner, J.N., et al., *Smc5/6 Mediated Sumoylation of the Sgs1-Top3-Rmi1 Complex Promotes Removal of Recombination Intermediates.* Cell Rep, 2016. **16**(2): p. 368-378.

409. Torres-Rosell, J., et al., *The Smc5-Smc6 complex and SUMO modification of Rad52 regulates recombinational repair at the ribosomal gene locus.* Nat Cell Biol, 2007. **9**(8): p. 923-31.

410. Saponaro, M., et al., *Cdk1 targets Srs2 to complete synthesis-dependent strand annealing and to promote recombinational repair.* PLoS Genet, 2010. **6**(2): p. e1000858.

411. Bohgaki, M., et al., *RNF168 ubiquitylates 53BP1 and controls its response to DNA double-strand breaks.* Proc Natl Acad Sci U S A, 2013. **110**(52): p. 20982-7.

412. Elia, A.E., et al., *Quantitative Proteomic Atlas of Ubiquitination and Acetylation in the DNA Damage Response.* Mol Cell, 2015. **59**(5): p. 867-81.

413. Bologna, S., et al., *Sumoylation regulates EXO1 stability and processing of DNA damage.* Cell Cycle, 2015. **14**(15): p. 2439-50.

414. Popovic, D., D. Vucic, and I. Dikic, *Ubiquitination in disease pathogenesis and treatment.* Nat Med, 2014. **20**(11): p. 1242-53.

415. Walden, H. and M.M. Muqit, *Ubiquitin and Parkinson's disease through the looking glass of genetics.* Biochem J, 2017. **474**(9): p. 1439-1451.

416. Krumova, P., et al., *Sumoylation inhibits alpha-synuclein aggregation and toxicity.* J Cell Biol, 2011. **194**(1): p. 49-60.

417. O'Rourke, J.G., et al., *SUMO-2 and PIAS1 modulate insoluble mutant huntingtin protein accumulation.* Cell Rep, 2013. **4**(2): p. 362-75.

418. Kho, C., et al., *SUMO1-dependent modulation of SERCA2a in heart failure.* Nature, 2011. **477**(7366): p. 601-5.

419. Maeda, D., et al., *Ubc9 is required for damage-tolerance and damage-induced interchromosomal homologous recombination in S. cerevisiae.* DNA Repair (Amst), 2004. **3**(3): p. 335-41.

420. Wang, Q., et al., *SUMO-specific protease 1 promotes prostate cancer progression and metastasis.* Oncogene, 2013. **32**(19): p. 2493-8.

421. Mizuuchi, K., et al., *T4 endonuclease VII cleaves holliday structures.* Cell, 1982. **29**(2): p. 357-65.

422. Symington, L.S. and R. Kolodner, *Partial purification of an enzyme from Saccharomyces cerevisiae that cleaves Holliday junctions.* Proc Natl Acad Sci U S A, 1985. **82**(21): p. 7247-51.

423. West, S.C. and A. Korner, *Cleavage of cruciform DNA structures by an activity from Saccharomyces cerevisiae.* Proc Natl Acad Sci U S A, 1985. **82**(19): p. 6445-9.

424. Parsons, C.A. and S.C. West, *Resolution of model Holliday junctions by yeast endonuclease is dependent upon homologous DNA sequences.* Cell, 1988. **52**(4): p. 621-9.

425. Elborough, K.M. and S.C. West, *Resolution of synthetic Holliday junctions in DNA by an endonuclease activity from calf thymus.* EMBO J, 1990. **9**(9): p. 2931-6.

426. Connolly, B., et al., *Resolution of Holliday junctions in vitro requires the Escherichia coli ruvC gene product.* Proc Natl Acad Sci U S A, 1991. **88**(14): p. 6063-7.

427. Iwasaki, H., et al., *Escherichia coli RuvC protein is an endonuclease that resolves the Holliday structure.* EMBO J, 1991. **10**(13): p. 4381-9.

428. Davies, A.A. and S.C. West, *Formation of RuvABC-Holliday junction complexes in vitro.* Curr Biol, 1998. **8**(12): p. 725-7.

429. van Gool, A.J., et al., *Functional interactions between the holliday junction resolvase and the branch migration motor of Escherichia coli.* EMBO J, 1998. **17**(6): p. 1838-45.

430. Hyde, H., et al., *Resolution of recombination intermediates by a mammalian activity functionally analogous to Escherichia coli RuvC resolvase.* J Biol Chem, 1994. **269**(7): p. 5202-9.

431. Chen, X.B., et al., *Human Mus81-associated endonuclease cleaves Holliday junctions in vitro.* Mol Cell, 2001. **8**(5): p. 1117-27.

432. Ciccia, A., A. Constantinou, and S.C. West, *Identification and characterization of the human mus81-eme1 endonuclease.* J Biol Chem, 2003. **278**(27): p. 25172-8.

433. Constantinou, A., et al., *Holliday junction resolution in human cells: two junction endonucleases with distinct substrate specificities.* Embo j, 2002. **21**(20): p. 5577-85.

434. Bastin-Shanower, S.A., et al., *The mechanism of Mus81-Mms4 cleavage site selection distinguishes it from the homologous endonuclease Rad1-Rad10.* Mol Cell Biol, 2003. **23**(10): p. 3487-96.

435. Boddy, M.N., et al., *Mus81-Eme1 are essential components of a Holliday junction resolvase.* Cell, 2001. **107**(4): p. 537-48.

436. Boddy, M.N., et al., *Damage tolerance protein Mus81 associates with the FHA1 domain of checkpoint kinase Cds1.* Mol Cell Biol, 2000. **20**(23): p. 8758-66.

437. de los Santos, T., et al., *The Mus81/Mms4 endonuclease acts independently of double-Holliday junction resolution to promote a distinct subset of crossovers during meiosis in budding yeast.* Genetics, 2003. **164**(1): p. 81-94.

438. McPherson, J.P., et al., *Involvement of mammalian Mus81 in genome integrity and tumor suppression.* Science, 2004. **304**(5678): p. 1822-6.

439. Dendouga, N., et al., *Disruption of murine Mus81 increases genomic instability and DNA damage sensitivity but does not promote tumorigenesis.* Mol Cell Biol, 2005. **25**(17): p. 7569-79.

440. Hanada, K., et al., *The structure-specific endonuclease Mus81 contributes to replication restart by generating double-strand DNA breaks.* Nat Struct Mol Biol, 2007. **14**(11): p. 1096-104.

441. Trowbridge, K., et al., *Synthetic lethality of Drosophila in the absence of the MUS81 endonuclease and the DmBlm helicase is associated with elevated apoptosis.* Genetics, 2007. **176**(4): p. 1993-2001.

442. Lieber, M.R., *The FEN-1 family of structure-specific nucleases in eukaryotic DNA replication, recombination and repair.* Bioessays, 1997. **19**(3): p. 233-40.

443. Yang, W., *Nucleases: diversity of structure, function and mechanism.* Q Rev Biophys, 2011. **44**(1): p. 1-93.

444. Furukawa, T., et al., *OsSEND-1: a new RAD2 nuclease family member in higher plants.* Plant Mol Biol, 2003. **51**(1): p. 59-70.

445. Nishino, T., Y. Ishino, and K. Morikawa, *Structure-specific DNA nucleases: structural basis for 3D-scissors.* Curr Opin Struct Biol, 2006. **16**(1): p. 60-7.

446. Tsutakawa, S.E., J. Lafrance-Vanasse, and J.A. Tainer, *The cutting edges in DNA repair, licensing, and fidelity: DNA and RNA repair nucleases sculpt DNA to measure twice, cut once.* DNA Repair (Amst), 2014. **19**: p. 95-107.

447. Furukawa, T. and H. Shimada, *The RAD2 Family of Nucleases in Higher Plants.* Japan Agricultural Research Quarterly: JARQ, 2009. **43**: p. 87-93.

448. Tomlinson, C.G., et al., *Substrate recognition and catalysis by flap endonucleases and related enzymes.* Biochem Soc Trans, 2010. **38**(2): p. 433-7.

449. Grasby, J.A., et al., *Unpairing and gating: sequence-independent substrate recognition by FEN superfamily nucleases.* Trends Biochem Sci, 2012. **37**(2): p. 74-84.

450. Lee, S.H., et al., *Human Holliday junction resolvase GEN1 uses a chromodomain for efficient DNA recognition and cleavage.* Elife, 2015. **4**.

451. Tsutakawa, S.E., et al., *Human flap endonuclease structures, DNA double-base flipping, and a unified understanding of the FEN1 superfamily.* Cell, 2011. **145**(2): p. 198-211.

452. Blus, B.J., K. Wiggins, and S. Khorasanizadeh, *Epigenetic virtues of chromodomains.* Crit Rev Biochem Mol Biol, 2011. **46**(6): p. 507-26.

453. Eissenberg, J.C., *Structural biology of the chromodomain: form and function.* Gene, 2012. **496**(2): p. 69-78.

454. Yap, K.L. and M.M. Zhou, *Structure and mechanisms of lysine methylation recognition by the chromodomain in gene transcription.* Biochemistry, 2011. **50**(12): p. 1966-80.

455. Smothers, J.F. and S. Henikoff, *The HP1 chromo shadow domain binds a consensus peptide pentamer.* Curr Biol, 2000. **10**(1): p. 27-30.

456. Canzio, D., et al., *Chromodomain-mediated oligomerization of HP1 suggests a nucleosome-bridging mechanism for heterochromatin assembly.* Mol Cell, 2011. **41**(1): p. 67-81.

457. Cowieson, N.P., et al., *Dimerisation of a chromo shadow domain and distinctions from the chromodomain as revealed by structural analysis.* Curr Biol, 2000. **10**(9): p. 517-25.

458. Li, J., et al., *Structural basis for specific binding of human MPP8 chromodomain to histone H3 methylated at lysine 9.* PLoS One, 2011. **6**(10): p. e25104.

459. Eissler, C.L., et al., *The Cdk/cDc14 module controls activation of the Yen1 holliday junction resolvase to promote genome stability*, in *Mol Cell*. 2014. p. 80-93.

460. Blanco, M.G., J. Matos, and S.C. West, *Dual control of Yen1 nuclease activity and cellular localization by Cdk and Cdc14 prevents genome instability.* Mol Cell, 2014. **54**(1): p. 94-106.

461. Chan, Y.W. and S.C. West, *Spatial control of the GEN1 Holliday junction resolvase ensures genome stability.* Nat Commun, 2014. **5**: p. 4844.

462. Rass, U., et al., *Mechanism of Holliday junction resolution by the human GEN1 protein.* Genes Dev, 2010. **24**(14): p. 1559-69.

463. Rass, U. and S.C. West, *Synthetic junctions as tools to identify and characterize Holliday junction resolvases.* Methods Enzymol, 2006. **408**: p. 485-501.

464. Bellendir, S.P., et al., *Substrate preference of Gen endonucleases highlights the importance of branched structures as DNA damage repair intermediates.* Nucleic Acids Res, 2017. **45**(9): p. 5333-5348.

465. Bellendir, S.P. and J. Sekelsky, *An elegans Solution for Crossover Formation.* PLoS Genet, 2013. **9**(7): p. e1003658.

466. Bailly, A.P., et al., *The Caenorhabditis elegans homolog of Gen1/Yen1 resolvases links DNA damage signaling to DNA double-strand break repair.* PLoS Genet, 2010. **6**(7): p. e1001025.

467. Bauknecht, M. and D. Kobbe, *AtGEN1 and AtSEND1, two paralogs in Arabidopsis, possess holliday junction resolvase activity.* Plant Physiol, 2014. **166**(1): p. 202-16.

468. Wyatt, H.D.M. and S.C. West, *Holliday junction resolvases.* Cold Spring Harbor perspectives in biology, 2014. **6**(9): p. a023192-a023192.

469. Agmon, N., et al., *The role of Holliday junction resolvases in the repair of spontaneous and induced DNA damage.* Nucleic Acids Res, 2011. **39**(16): p. 7009-19.

470. Mazon, G., et al., *The Rad1-Rad10 nuclease promotes chromosome translocations between dispersed repeats.* Nat Struct Mol Biol, 2012. **19**(9): p. 964-71.

471. Garcia-Luis, J. and F. Machin, *Mus81-Mms4 and Yen1 resolve a novel anaphase bridge formed by noncanonical Holliday junctions.* Nat Commun, 2014. **5**: p. 5652.

472. Ölmezer, G., et al., *Replication intermediates that escape Dna2 activity are processed by Holliday junction resolvase Yen1.* Nat Commun, 2016. **7**: p. 13157.

473. Grigaitis, R., et al., *Phosphorylation of the RecQ Helicase Sgs1/BLM Controls Its DNA Unwinding Activity during Meiosis and Mitosis.* Dev Cell, 2020. **53**(6): p. 706-723 e5.

474. Wild, P., et al., *Network Rewiring of Homologous Recombination Enzymes during Mitotic Proliferation and Meiosis.* Mol Cell, 2019. **75**(4): p. 859-874 e4.

475. Dehé, P.-M. and P.-H.L. Gaillard, *Control of structure-specific endonucleases to maintain genome stability.* Nature Reviews Molecular Cell Biology, 2017. **18**(5): p. 315-330.

476. Ubersax, J.A., et al., *Targets of the cyclin-dependent kinase Cdk1.* Nature, 2003. **425**(6960): p. 859-64.

477. Loog, M. and D.O. Morgan, *Cyclin specificity in the phosphorylation of cyclin-dependent kinase substrates.* Nature, 2005. **434**(7029): p. 104-8.

478. Rock, J.M. and A. Amon, *The FEAR network.* Current biology : CB, 2009. **19**(23): p. R1063-R1068.

479. Queralt, E. and F. Uhlmann, *Cdk-counteracting phosphatases unlock mitotic exit.* Curr Opin Cell Biol, 2008. **20**(6): p. 661-8.

480. Stegmeier, F., R. Visintin, and A. Amon, *Separase, polo kinase, the kinetochore protein Slk19, and Spo12 function in a network that controls Cdc14 localization during early anaphase.* Cell, 2002. **108**(2): p. 207-20.

481. Visintin, R., et al., *The phosphatase Cdc14 triggers mitotic exit by reversal of Cdk-dependent phosphorylation.* Mol Cell, 1998. **2**(6): p. 709-18.

482. Stegmeier, F. and A. Amon, *Closing mitosis: the functions of the Cdc14 phosphatase and its regulation.* Annu Rev Genet, 2004. **38**: p. 203-32.

483. Kosugi, S., et al., *Systematic identification of cell cycle-dependent yeast nucleocytoplasmic shuttling proteins by prediction of composite motifs.* Proc Natl Acad Sci U S A, 2009. **106**(25): p. 10171-6.

484. De Muyt, A., et al., *BLM helicase ortholog Sgs1 is a central regulator of meiotic recombination intermediate metabolism.* Mol Cell, 2012. **46**(1): p. 43-53.

485. Arter, M., et al., *Regulated Crossing-Over Requires Inactivation of Yen1/GEN1 Resolvase during Meiotic Prophase I.* Dev Cell, 2018. **45**(6): p. 785-800.e6.

486. Argueso, J.L., et al., *Competing Crossover Pathways Act During Meiosis in Saccharomyces cerevisiae.* Genetics, 2004. **168**(4): p. 1805.

487. Lorenz, A., S.C. West, and M.C. Whitby, *The human Holliday junction resolvase GEN1 rescues the meiotic phenotype of a Schizosaccharomyces pombe mus81 mutant.* Nucleic Acids Res, 2010. **38**(6): p. 1866-73.

488. Gao, M., et al., *A novel role of human holliday junction resolvase GEN1 in the maintenance of centrosome integrity.* PLoS One, 2012. **7**(11): p. e49687.

489. Hendriks, I.A., et al., *Site-specific mapping of the human SUMO proteome reveals co-modification with phosphorylation.* Nature Structural & Molecular Biology, 2017. **24**(3): p. 325-336.

490. Szostak, J.W., et al., *The double-strand-break repair model for recombination.* Cell, 1983. **33**(1): p. 25-35.

491. Bzymek, M., et al., *Double Holliday junctions are intermediates of DNA break repair.* Nature, 2010. **464**(7290): p. 937-41.

492. Ira, G., et al., *Srs2 and Sgs1-Top3 suppress crossovers during double-strand break repair in yeast.* Cell, 2003. **115**(4): p. 401-11.

493. Mitchel, K., et al., *Molecular structures of crossover and noncrossover intermediates during gap repair in yeast: implications for recombination.* Mol Cell, 2010. **38**(2): p. 211-22.

494. Gallo-Fernandez, M., et al., *Cell cycle-dependent regulation of the nuclease activity of Mus81-Eme1/Mms4.* Nucleic Acids Res, 2012. **40**(17): p. 8325-35.

495. Flotho, A. and F. Melchior, *Sumoylation: a regulatory protein modification in health and disease.* Annu Rev Biochem, 2013. **82**: p. 357-85.

496. Takahashi, Y., et al., *Yeast Ull1/Siz1 is a novel SUMO1/Smt3 ligase for septin components and functions as an adaptor between conjugating enzyme and substrates.* J Biol Chem, 2001. **276**(52): p. 48973-7.

497. Nie, M. and M.N. Boddy, *Cooperativity of the SUMO and Ubiquitin Pathways in Genome Stability.* Biomolecules, 2016. **6**(1): p. 14.

498. Sarangi, P. and X. Zhao, *SUMO-mediated regulation of DNA damage repair and responses.* Trends Biochem Sci, 2015. **40**(4): p. 233-42.

499. Xie, Y., et al., *The yeast Hex3.Slx8 heterodimer is a ubiquitin ligase stimulated by substrate sumoylation.* J Biol Chem, 2007. **282**(47): p. 34176-84.

500. Uzunova, K., et al., *Ubiquitin-dependent proteolytic control of SUMO conjugates.* J Biol Chem, 2007. **282**(47): p. 34167-75.

501. Wang, Z., G.M. Jones, and G. Prelich, *Genetic analysis connects SLX5 and SLX8 to the SUMO pathway in Saccharomyces cerevisiae.* Genetics, 2006. **172**(3): p. 1499-509.

502. Mullen, J.R., et al., *Requirement for three novel protein complexes in the absence of the Sgs1 DNA helicase in Saccharomyces cerevisiae.* Genetics, 2001. **157**(1): p. 103-18.

503. Bretes, H., et al., *Sumoylation of the THO complex regulates the biogenesis of a subset of mRNPs.* Nucleic Acids Res, 2014. **42**(8): p. 5043-58.

504. Parker, J.L., et al., *SUMO modification of PCNA is controlled by DNA.* EMBO J, 2008. **27**(18): p. 2422-31.

505. Olmezer, G., et al., *Replication intermediates that escape Dna2 activity are processed by Holliday junction resolvase Yen1.* Nat Commun, 2016. **7**: p. 13157.

506. Sung, M.K. and W.K. Huh, *Bimolecular fluorescence complementation analysis system for in vivo detection of protein-protein interaction in Saccharomyces cerevisiae.* Yeast, 2007. **24**(9): p. 767-75.

507. Hickey, C.M., Y. Xie, and M. Hochstrasser, *DNA Binding by the MATalpha2 Transcription Factor Controls its Access to Alternative Ubiquitin-modification Pathways.* Mol Biol Cell, 2018.

508. Burgess, R.C., et al., *The Slx5-Slx8 complex affects sumoylation of DNA repair proteins and negatively regulates recombination.* Mol Cell Biol, 2007. **27**(17): p. 6153-62.

509. Thu, Y.M., et al., *Slx5/Slx8 Promotes Replication Stress Tolerance by Facilitating Mitotic Progression.* Cell Rep, 2016. **15**(6): p. 1254-65.

510. Matos, J. and S.C. West, *Holliday junction resolution: regulation in space and time.* DNA Repair (Amst), 2014. **19**: p. 176-81.

511. Munoz-Galvan, S., et al., *Distinct roles of Mus81, Yen1, Slx1-Slx4, and Rad1 nucleases in the repair of replication-born double-strand breaks by sister chromatid exchange.* Mol Cell Biol, 2012. **32**(9): p. 1592-603.

512. Matos, J., M.G. Blanco, and S.C. West, *Cell-cycle kinases coordinate the resolution of recombination intermediates with chromosome segregation.* Cell Rep, 2013. **4**(1): p. 76-86.

513. Rubenstein, E.M. and M. Hochstrasser, *Redundancy and variation in the ubiquitin-mediated proteolytic targeting of a transcription factor.* Cell Cycle, 2010. **9**(21): p. 4282-5.

514. Xie, Y., et al., *SUMO-independent in vivo activity of a SUMO-targeted ubiquitin ligase toward a short-lived transcription factor.* Genes Dev, 2010. **24**(9): p. 893-903.

515. Cook, C.E., M. Hochstrasser, and O. Kerscher, *The SUMO-targeted ubiquitin ligase subunit Slx5 resides in nuclear foci and at sites of DNA breaks.* Cell Cycle, 2009. **8**(7): p. 1080-9.

516. Jentsch, S. and I. Psakhye, *Control of nuclear activities by substrate-selective and protein-group SUMOylation.* Annu Rev Genet, 2013. **47**: p. 167-86.

517. Bohm, S., et al., *Disruption of SUMO-targeted ubiquitin ligases Slx5-Slx8/RNF4 alters RecQ-like helicase Sgs1/BLM localization in yeast and human cells.* DNA Repair (Amst), 2015. **26**: p. 1-14.

518. Sarbajna, S., D. Davies, and S.C. West, *Roles of SLX1-SLX4, MUS81-EME1, and GEN1 in avoiding genome instability and mitotic catastrophe.* Genes Dev, 2014. **28**(10): p. 1124-36.

519. Spinella, J.F., et al., *Whole-exome sequencing of a rare case of familial childhood acute lymphoblastic leukemia reveals putative predisposing mutations in Fanconi anemia genes.* BMC Cancer, 2015. **15**: p. 539.

520. Kuligina, E., et al., *Value of bilateral breast cancer for identification of rare recessive at-risk alleles: evidence for the role of homozygous GEN1 c.2515_2519delAAGTT mutation.* Fam Cancer, 2013. **12**(1): p. 129-32.

521. Medves, S., et al., *A high rate of telomeric sister chromatid exchange occurs in chronic lymphocytic leukaemia B-cells.* Br J Haematol, 2016. **174**(1): p. 57-70.

522. Tran, P.T., A. Paoletti, and F. Chang, *Imaging green fluorescent protein fusions in living fission yeast cells.* Methods, 2004. **33**(3): p. 220-5.

523. Schindelin, J., et al., *Fiji: an open-source platform for biological-image analysis.* Nat Methods, 2012. **9**(7): p. 676-82.

524. Ulrich, H.D. and A.A. Davies, *In vivo detection and characterization of sumoylation targets in Saccharomyces cerevisiae.* Methods Mol Biol, 2009. **497**: p. 81-103.

525. Rouviere, J.O., et al., *A SUMO-dependent feedback loop senses and controls the biogenesis of nuclear pore subunits.* Nat Commun, 2018. **9**(1): p. 1665.

526. Kotwaliwale, C.V., et al., *A pathway containing the Ipl1/aurora protein kinase and the spindle midzone protein Ase1 regulates yeast spindle assembly.* Dev Cell, 2007. **13**(3): p. 433-45.

527. Batte, A., et al., *Recombination at subtelomeres is regulated by physical distance, double-strand break resection and chromatin status.* EMBO J, 2017. **36**(17): p. 2609-2625.

528. James, P., J. Halladay, and E.A. Craig, *Genomic libraries and a host strain designed for highly efficient two-hybrid selection in yeast.* Genetics, 1996. **144**(4): p. 1425-36.

529. Albert, B., et al., *Systematic characterization of the conformation and dynamics of budding yeast chromosome XII.* J Cell Biol, 2013. **202**(2): p. 201-10.

530. Gritenaite, D., et al., *A cell cycle-regulated Slx4-Dpb11 complex promotes the resolution of DNA repair intermediates linked to stalled replication.* Genes Dev, 2014. **28**(14): p. 1604-19.

531. Talhaoui, I., et al., *Slx5-Slx8 ubiquitin ligase targets active pools of the Yen1 nuclease to limit crossover formation.* Nat Commun, 2018. **9**(1): p. 5016.

532. Kerscher, O., *SUMO junction-what's your function? New insights through SUMO-interacting motifs.* EMBO Rep, 2007. **8**(6): p. 550-5.

533. Parnas, O., et al., *Elg1, an alternative subunit of the RFC clamp loader, preferentially interacts with SUMOylated PCNA.* EMBO J, 2010. **29**(15): p. 2611-22.

534. Steiner, S., J. Kohli, and K. Ludin, *Functional interactions among members of the meiotic initiation complex in fission yeast.* Curr Genet, 2010. **56**(3): p. 237-49.

535. Benson, F.E. and S.C. West, *Substrate specificity of the Escherichia coli RuvC protein. Resolution of three- and four-stranded recombination intermediates.* J Biol Chem, 1994. **269**(7): p. 5195-201.

536. Bauer, S.L., J. Chen, and S.U. Åström, *Helicase/SUMO-targeted ubiquitin ligase Uls1 interacts with the Holliday junction resolvase Yen1.* PLoS One, 2019. **14**(3): p. e0214102.

537. Guérin, T.M., et al., *Condensin-Mediated Chromosome Folding and Internal Telomeres Drive Dicentric Severing by Cytokinesis.* Mol Cell, 2019. **75**(1): p. 131-144.e3.

538. Morawska, M. and H.D. Ulrich, *An expanded tool kit for the auxin-inducible degron system in budding yeast.* Yeast, 2013. **30**(9): p. 341-351.

539. Albuquerque, C.P., et al., *Distinct SUMO ligases cooperate with Esc2 and Slx5 to suppress duplication-mediated genome rearrangements.* PLoS genetics, 2013. **9**(8): p. e1003670-e1003670.

540. Makrantoni, V., et al., *Phosphorylation of Sli15 by Ipl1 is important for proper CPC localization and chromosome stability in Saccharomyces cerevisiae.* PloS one, 2014. **9**(2): p. e89399-e89399.

541. Haase, J., et al., *Distinct Roles of the Chromosomal Passenger Complex in the Detection of and Response to Errors in Kinetochore-Microtubule Attachment.* Developmental cell, 2017. **42**(6): p. 640-654.e5.

542. Chymkowitch, P., et al., *Sumoylation of Rap1 mediates the recruitment of TFIID to promote transcription of ribosomal protein genes.* Genome research, 2015. **25**(6): p. 897-906.

543. Lickwar, C.R., et al., *Genome-wide protein-DNA binding dynamics suggest a molecular clutch for transcription factor function.* Nature, 2012. **484**(7393): p. 251-255.

544. White, M.A., et al., *DNA-binding protein RAP1 stimulates meiotic recombination at the HIS4 locus in yeast.* Proc Natl Acad Sci U S A, 1991. **88**(21): p. 9755-9.

545. White, M.A., et al., *A promoter deletion reduces the rate of mitotic, but not meiotic, recombination at the HIS4 locus in yeast.* Curr Genet, 1992. **21**(2): p. 109-16.

546. White, M.A., M. Dominska, and T.D. Petes, *Transcription factors are required for the meiotic recombination hotspot at the HIS4 locus in Saccharomyces cerevisiae.* Proc Natl Acad Sci U S A, 1993. **90**(14): p. 6621-5.

547. Gilson, E. and S.M. Gasser, *Repressor Activator Protein 1 and Its Ligands: Organising Chromatin Domains*, in *Nucleic Acids and Molecular Biology*, F. Eckstein and D.M.J. Lilley, Editors. 1995, Springer Berlin Heidelberg: Berlin, Heidelberg. p. 308-327.

548. Müller, T., et al., *Imaging the asymmetrical DNA bend induced by repressor activator protein 1 with scanning tunneling microscopy.* J Struct Biol, 1994. **113**(1): p. 1-12.

549. Roux, K.J., D.I. Kim, and B. Burke, *BioID: A Screen for Protein-Protein Interactions.* Current Protocols in Protein Science, 2013. **74**(1): p. 19.23.1-19.23.14.

550. Bittmann, J., et al., *An advanced cell cycle tag toolbox reveals principles underlying temporal control of structure-selective nucleases.* Elife, 2020. **9**.

nature COMMUNICATIONS

ARTICLE

DOI: 10.1038/s41467-018-07364-x OPEN

Slx5-Slx8 ubiquitin ligase targets active pools of the Yen1 nuclease to limit crossover formation

Ibtissam Talhaoui[1], Manuel Bernal[1], Janet R. Mullen[2], Hugo Dorison[1], Benoit Palancade[3], Steven J. Brill[2] & Gerard Mazón[1]

The repair of double-stranded DNA breaks (DSBs) by homologous recombination involves the formation of branched intermediates that can lead to crossovers following nucleolytic resolution. The nucleases Mus81-Mms4 and Yen1 are tightly controlled during the cell cycle to limit the extent of crossover formation and preserve genome integrity. Here we show that Yen1 is further regulated by sumoylation and ubiquitination. In vivo, Yen1 becomes sumoylated under conditions of DNA damage by the redundant activities of Siz1 and Siz2 SUMO ligases. Yen1 is also a substrate of the Slx5-Slx8 ubiquitin ligase. Loss of Slx5-Slx8 stabilizes the sumoylated fraction, attenuates Yen1 degradation at the G1/S transition, and results in persistent localization of Yen1 in nuclear foci. Slx5-Slx8-dependent ubiquitination of Yen1 occurs mainly at K714 and mutation of this lysine increases crossover formation during DSB repair and suppresses chromosome segregation defects in a *mus81Δ* background.

[1] CNRS UMR 8200, Université Paris-Sud - Université Paris-Saclay, Gustave Roussy, 114 rue Édouard Vaillant, 94800 Villejuif, France. [2] Department of Molecular Biology and Biochemistry, Rutgers University, Piscataway, NJ 08854, USA. [3] Institut Jacques Monod, CNRS UMR 7592, Université Paris Diderot, Sorbonne Paris Cité, 15 rue Hélène Brion, 75013 Paris, France. These authors contributed equally: Ibtissam Talhaoui, Manuel Bernal. Correspondence and requests for materials should be addressed to G.M. (email: gerard.mazon@gustaveroussy.fr)

omologous recombination (HR) is a key repair pathway for the maintenance of genome integrity. HR is involved in the repair of double-strand breaks (DSB) generated by endogenous or exogenous sources of DNA damage and it plays an important role in the repair of damage associated with DNA replication[1]. A variety of DNA joint molecules (JM) form during the different steps of the HR pathway and these are sequentially matured into novel intermediates or dismantled by different specialized proteins to prevent their persistence into mitosis. Failure to resolve joint-molecule intermediates results in chromosome segregation defects[1–4]. In yeast, the helicase Sgs1, together with Rmi1 and Top3, mediates the dissolution of double Holliday Junctions (dHJ) to ensure a non-crossover outcome[2,3], and similar NCO outcomes are generated by helicases, such as Mph1 or Srs2[4–6]. In contrast to the dissolution pathways, nucleolytic processing of recombination intermediates can result in reciprocal crossovers (CO), with the risk of loss of heterozygosity (LOH), or chromosome translocations, both of which are genome-destabilizing events[1,7].

Nucleolytic processing of HR intermediates is strictly controlled and appears to be used as a last option to cope with orphan HJs and other intermediates that cannot be dissolved by the Sgs1-mediated pathway[4,8]. Whereas Mus81-Mms4 is hyper activated in late G2/M phase by Cdc5- and Cdc28/CDK1-dependent phosphorylation of Mms4[9–11], Cdc28 phosphorylates Yen1 to prevent its activity and nuclear localization until anaphase[12,13]. In anaphase, the Cdc14 phosphatase gradually dephosphorylates Yen1, and this late activation of Yen1 ensures that persistent recombination intermediates are resolved before mitotic exit[12,13]. Although CO levels are minimized by the late activation of nucleases, their windows of activity are likely to overlap with those of DNA helicases that dissociate intermediates to form NCOs. It is thus possible that another layer of control is required subsequent to chromatin binding to prevent the use of nucleases when other factors are available. The tight regulation of these nucleases also highlights the risk of their uncontrolled activity in other cell-cycle phases, and suggests that their turnover might be enforced to remove active pools from the nucleus when they are no longer needed.

Regulation by coupling of the small ubiquitin-like modifier (SUMO)[14] has emerged as a potent means to fine tune the amount and activity of specific pools of proteins, especially during DNA-mediated transactions[15]. In *Saccharomyces cerevisiae*, the enzymes involved in SUMO conjugation are the E1 Aos1-Uba2 activating enzyme dimer, the E2 conjugating enzyme Ubc9, and a limited set of E3 ligases (including Siz1, Siz2, and Mms21) that provide substrate selectivity[16–18]. Although protein sumoylation regulates multiple cellular activities, it has been shown to be especially important during the DNA damage response[19–21]. Important players of the HR pathway are found among the sumoylated DNA repair targets, including Rad52, PCNA, RPA, and Sgs1[20,22–26]. Some lines of evidence link sumoylation to specific pathways that locally target repair factors to degradation by the action of SUMO-targeted ubiquitin ligases (STUbLs)[27,28] to prevent the toxic effects of their persistent activation. Two STUbLs are thought to operate in *S.cerevisiae*, the Slx5–Slx8 complex[29,30] and the Uls1 protein[31,32]. Mutations in *SLX5* and *SLX8* result in slow growth or lethality in combination with components of the SUMO metabolic pathway[33] highlighting its role in regulating sumoylated proteins. The *SLX5* and *SLX8* genes were originally identified by their requirement for the viability of *sgs1*Δ cells[34], and this lethality is partially explained by the accumulation of sumoylated substrates in the *sgs1*Δ background.

In this work, we explored the hypothesis that there is crosstalk between Slx5–Slx8 and Yen1. We demonstrate that Yen1 is a sumoylation target and that Slx5–Slx8 participates in its regulation by ubiquitination of its lysine 714. Slx5–Slx8 prevents persistent accumulation of a fraction of Yen1 associated with sites of activity in late G2/M and helps maintain the balance between pro- and anti-crossover pathways during HR.

Results

Yen1 is sumoylated after DNA damage via Siz1/Siz2. STUbLs have been shown to recognize sumoylated substrates[27], including certain nuclear proteins that participate in the DNA damage response[28]. Because Yen1 was identified in a screen for sumoylated proteins following DNA damage[25], we analyzed how Yen1 is sumoylated in vivo and whether it interacts with Slx5–Slx8.

To detect the Yen1 post-translational modification of Yen1 by SUMO and ubiquitin (Ub), we tagged the endogenous gene with a single C–terminal HA epitope. The *YEN1-HA* allele was judged to be functional as it showed no effect on the methyl-methane sulfonate (MMS) sensitivity of a *mus81*Δ strain (Supplementary Figure 1a). Further, Yen1-HA immunoblots revealed phosphorylated and unphosphorylated forms with the expected cell-cycle regulation[12] (Fig. 1a).

Using a 6xHIS-Smt3-expressing plasmid[35], we performed a Histidine pull-down experiment to detect Yen1 among the sumoylated proteins. Sumoylated Yen1 was detected as a faint signal in the eluates of unperturbed cells (Fig. 1b, extended exposure) and the recovery of sumoylated Yen1 was not greatly increased by inhibiting proteasomal degradation by treatment with MG132 (Fig. 1b). However, after MMS treatment, we recovered a clear ladder of sumoylated Yen1 forms whose abundance increased in the presence of MG132 (Fig. 1b).

The Yen1-SUMO conjugates migrated as a doublet of two discrete bands near 120 KDa (Fig. 1b), these forms shifted when using a different tagged version of Smt3 further confirming their sumoylated nature (Supplementary Figure 1). We also observed higher MW bands may be due to multiple sumoylations or chains of SUMO or Ub. The major bands detected from pull-downs resemble those detected following in vitro sumoylation assays where immunoprecipitated Yen1-HA was incubated with purified Smt3-3KR, E1 (Aos1-Uba2), and E2 (Ubc9) enzymes (Fig. 1c, Supplementary Figure 1c). Sumoylation under mild MMS treatment was also detected with Yen1-HA immunoprecipitation after lysis in denaturing conditions of cells with induced expression of Yen1-HA but endogenous levels of Smt3 (Fig. 1d). We did not detect significant Yen1 sumoylation in pull-downs from *siz1Δ siz2Δ* double-mutant strains confirming the requirement of these E3 ligases in vivo. Interestingly, one of the two major Yen1 sumoylation bands disappeared in the *siz1*Δ single-mutant pull-down, suggesting some sites have a strong preference for Siz1 as E3 ligase (Fig. 1e).

To complement our in vivo observations, we tested whether highly purified Yen1 produced in *E. coli* was a substrate for sumoylation in vitro. A sumoylation reaction consisting of Smt3, Aos1-Uba2 (E1), Ubc9 (E2), and Siz2 (E3), triggered the formation of Yen1 products that migrated as a ladder of bands with a more intense band at 120 KDa similar to the major forms observed in vivo (Fig. 1f). Increased concentrations of Siz2 stimulated Yen1 sumoylation, which occurred at a lower yield in the absence of E3 (Fig. 1f, g). Similar to what has already been reported for other proteins[36,37], we observed increased Yen1 sumoylation in vitro in the presence of its DNA substrate (Fig. 1g). We conclude that the Yen1 forms detected following in vitro sumoylation are largely reminiscent of those detected in vivo (Fig. 1b). The fact that Yen1 sumoylation is stimulated by MMS treatment suggest that it is a response to substrates that accumulate during DNA damage.

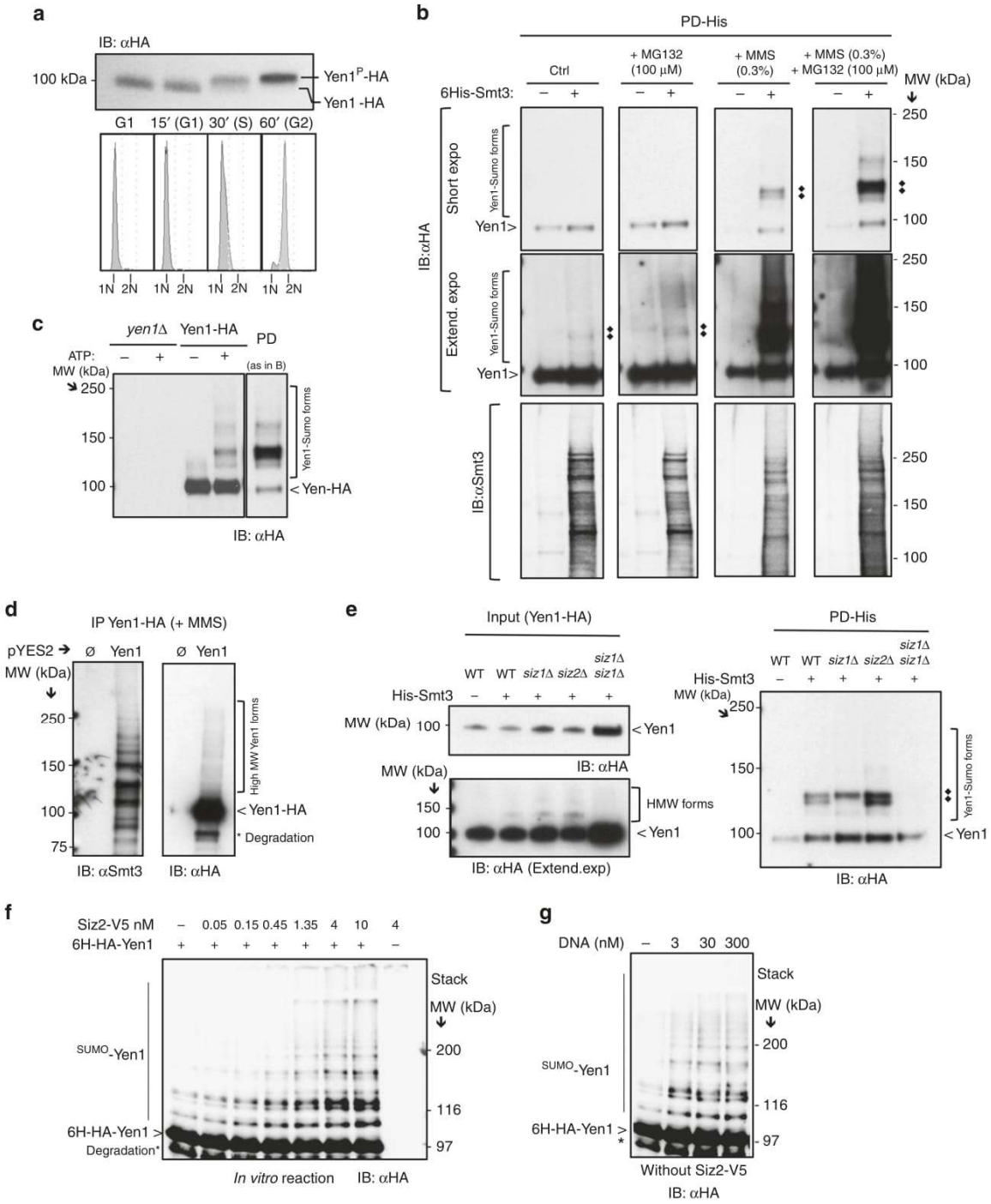

To test whether substrate recognition is important for sumoylation of Yen1 in vivo, we introduced amino acid substitutions in the four central CDK1 sites to generate phospho-deleted or phospho-mimic alleles. Previous work has shown that phospho-mimic mutations in the central CDK1 sites of Yen1 impair substrate cleavage and reduce its association with DNA[12,13]. However, analysis of Smt3 pull-downs following MMS treatment showed no significant difference in sumoylation compared to the wild-type Yen1 (Supplementary Figure 1d). To directly test the possibility that the Yen1 sumoylation is stimulated by its substrates, we analysed Smt3 pull-downs from a *dna2Δ pif1* strain. It has been shown that Yen1 is important in eliminating replication-dependent recombination intermediates in this strain[38]. Compared to wild-type, more abundant sumoylation was observed in *dna2Δ pif1* cells (Supplementary Figure 1d). This supports the idea that sumoylation of Yen1 occurs in a context where Yen1 activity is required.

Fig. 1 Yen1 is sumoylated in vivo and in vitro. **a** A wild-type chromosomally tagged *YEN1-HA* strain was synchronized with alpha factor and released into fresh medium to observe phosphorylation of Yen1 by immunoblot (upper) and progression through the cell cycle by FACS (lower). **b** Wild-type strains expressing Yen1-HA, with (+) or without (−) pCUP-6xHIS-Smt3, were subjected to MMS challenge followed by denaturing Ni-NTA pull-down and immunoblot analysis. Yen1 was detected by anti-HA (top and middle) and a prominent sumoylated doublet is indicated (black rhombus). Membranes were also probed with anti-Smt3 (bottom). Note that un-sumoylated Yen1 binds to Ni due to a histine-rich region. **c** Yen1-HA was overexpressed in wild-type asynchronous cells, immunoprecipitated with anti-HA, eluted by HA peptide competition and mixed with Aos1-Uba2, Ubc9, and Smt3-3KR in the presence or absence of ATP. After immunoblotting with anti-HA sumoylated forms were detected in the presence of ATP that migrate at similar sizes to those detected in the PD experiments shown in **b** (far right duplicate for comparison). A control reaction was made with HA-immunoprecipitation of a *yen1*Δ strain eluted with the same amount of HA peptide. **d** *yen1*Δ cells expressing Yen1-HA from a Gal-inducible plasmid or harboring a control plasmid were subjected to MMS treatment (0.03%), and extracts were immunoprecipitated using anti-HA prior to immunoblotting with anti-Smt3 (left) or anti-HA (right). **e** Indicated strains (WT, *siz1Δ*, *siz2Δ*, or *siz1Δ siz2Δ*) with (+) or without (−) pCUP-6xHIS-Smt3 were subjected to pull-down analysis of Smt3 as in **b** in conditions of MMS damage and eluates were analysed by immunoblot. The input used for PD was immunoblotted to allow normalization and comparison between strains (bottom). **f** Purified recombinant 6His-HA-Yen1 protein was incubated under sumoylation conditions with the indicated concentrations of Siz2 followed by immunoblotting with anti-HA. Asterisk indicates breakdown products of Yen1 carried from purification. **g** Sumoylation reactions were performed as in **f** but with increasing amounts of synthetic Holliday junction DNA, 458 nM Yen1 and in the absence of Siz2. All experiments were independently replicated at least three times and images are representative of the reproducible results obtained

Yen1 is a substrate of the Slx5–Slx8 ubiquitin ligase. Having established that Yen1 is sumoylated, we next investigated whether the Slx5–Slx8 STUbL recognized and further processed the modified protein. To determine whether Yen1 and Slx5 physically interact or are in proximity in the nucleus, we used the bimolecular fluorescence complementation (BiFC) approach[39]. Cells expressing the complementary VN-Yen1 and VC-Slx5 epitope-tagged proteins displayed fluorescent signal in discrete foci (Fig. 2a), similar to what has been described for another Slx5–Slx8-substrate interaction[40]. The BiFC interaction was nuclear as determined by introducing a Nup49-mCherry marker (Fig. 2a). The Yen1–Slx5 interaction was confirmed using a pull-down approach. Cells containing the *YEN1-HA* allele were transformed with a pYES2 plasmid expressing GST-Slx5 under a galactose inducible promoter or an empty vector as control. After induction of GST-Slx5, cell extracts were applied to a glutathione column and Yen1 was specifically detected in the eluates (Fig. 2b). Finally, the association of Slx5 with Yen1 was further confirmed by a two-hybrid assay where DBD-Yen1 bound AD-Slx5 (Fig. 2c). These data indicate that Yen1 and Slx5 are in close proximity and may physically interact in yeast.

The fact that Yen1 is sumoylated and interacts with the STUbL component Slx5 prompted us to investigate whether it was ubiquitinated by Slx5–Slx8. We first asked whether Slx5–Slx8 could directly recognize Yen1 as substrate by reconstituting the ubiquitination reaction in vitro. Combined with the E1 (Uba1) and E2 (Ubc5), Slx5–Slx8 ubiquitinated Yen1 producing a major band around 110 KDa and a less intense ladder of higher MW bands (Fig. 3a). No ubiquitination was detected when using a RING mutant of Slx5 in the reaction (*slx5–6*), and no cross-reacting products were detected by the anti-HA antibody when Yen1 was not added to the reaction, further confirming the specificity of detection of the Yen1 ubiquitinated forms (Fig. 3a). Ubiquitination was stimulated by the presence of DNA (Fig. 3b), suggesting that DNA enhances ubiquitination but is not essential for the reaction. Although Slx5–Slx8 is able to ubiquitinate Yen1 in vitro in the absence of prior sumoylation we cannot exclude the possibility that sumoylation is required for ubiquitination in vivo.

To determine whether the in vivo ubiquitinated Yen1 was dependent on Slx5/Slx8, we employed a pull-down approach. Using a 6xHIS-Ub expression plasmid we detected mono-ubiquitinated Yen1 in the pull-down eluates and a faint ladder of poly-ubiquitination (Fig. 3c). Yen1 ubiquitination was not largely increased under MMS treatment of cells and was not importantly altered after *slx8*Δ deletion (Fig. 3c). From the results obtained it is difficult to estimate the contribution of Slx5/8 to the Yen1 ubiquitination in vivo that also possibly involves another general turnover pathway that mask the modification of a small fraction of Yen1 by Slx5/8 as already observed for other substrates[41].

We then explored the possibility that Slx5–Slx8-mediated degradation of Yen1 would target the sumoylated version of this protein. To this aim, we asked whether inactivation of Slx5–Slx8 affected the stability of sumoylated Yen1 detected after MMS treatment. Wild-type and cells harboring deletions of either *SLX8* or *SLX5* expressing 6xHIS-Smt3 were collected after exposure to MMS 0.3%. After Smt3 pull-down, an increase in the sumoylated Yen1 fraction (≈5-fold) was detected in the *slx8*Δ and *slx5*Δ strains (Fig. 3d). Treatment with the proteasome inhibitor MG132 reduced the differences in the recovery of the sumoylated fractions between the wild type and the *slx5*/*slx8* mutants suggesting that this increase might be due to the combined effects of more DNA damage in the absence of Slx5/Slx8[42] and decreased removal in these strains of sumoylated proteins[43], including Yen1.

***slx8*Δ cells present persistent Yen1 foci**. We next addressed the possible impact of Slx5–Slx8 impairment on the dynamics and function of Yen1. The cell-cycle regulation or degree of Yen1 phosphorylation was not grossly altered by deletion of *SLX8* (Fig. 4a). An *slx8*Δ single deletion showed no increase in MMS sensitivity when combined with *yen1*Δ, although *yen1*Δ displayed the known synergistic defect when combined to *mus81*Δ (Fig. 4b). A subtle increase in sensitivity for the *slx8*Δ *yen1*Δ mutant was detected with the radiomimetic drug Zeocin, but this was not as pronounced as the synergistic effects of *slx8Δ mus81Δ*.

To identify potential defects in the nuclear transport and distribution of Yen1 in the absence of Slx5–Slx8 we GFP-tagged Yen1 at its N-terminus, where we previously obtained positive BiFC data (Fig. 2). After mildly inducing GFP-Yen1 from a plasmid in a strain carrying Hta1-mCherry and a fully functional *YEN1-HA* endogenous allele cells were judged to be healthy and we observed the expected cellular distribution of wild-type Yen1 with its nuclear exclusion occurring at S-phase (Supplementary Figure 2).

Compared to wild type, *slx8*Δ cells were three times more likely to display Yen1 foci (Fig. 4c, Supplementary Figure 2). To characterize the phenotype, cells were classified as containing no focus, 1–2 foci per cell, more than 2 foci and rare events with abnormal features (Fig. 4d, Supplementary Figure 2). The *slx8*Δ cells showed foci of all classes in G2/M, and there was a dramatic increase in cells with 1–2 foci in G1 phase.

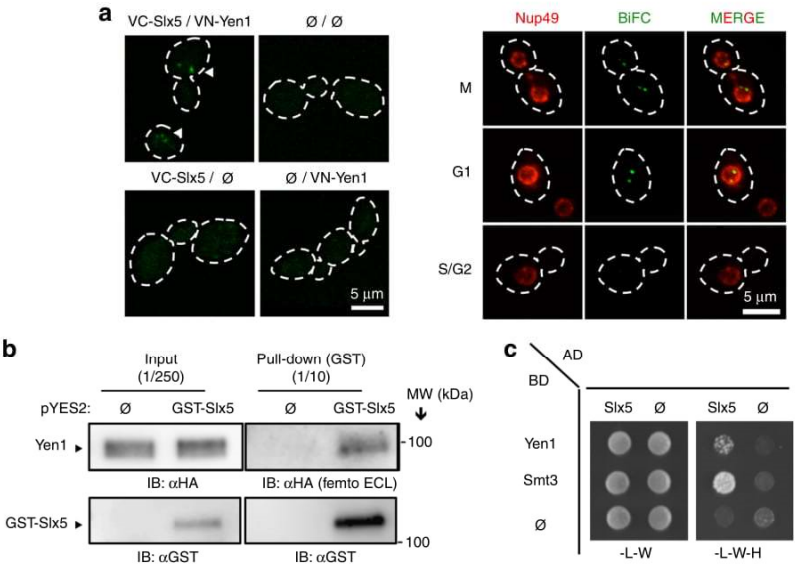

Fig. 2 Yen1 interacts with Slx5–Slx8 in the nucleus. **a** Diploid strains carrying one allele of galactose inducible VC-Slx5 and VN-Yen1 with wild-type copies of *YEN1* and *SLX5* in the homologous chromosomes were observed by live microscopy. BiFC (white arrows) signal denotes an interaction between the two BiFC (Venus) epitopes. Control diploids lacking one or both of the epitope-tagged proteins (ϕ) were used to substract background signal. A plasmid carrying Nup49-mCherry was transformed on the diploid strain harboring VC-Slx5/VN-Yen1 to visualize the nuclear perimeter. BiFC interactions were only detected in the nuclear compartment. **b** Cells carrying either an empty vector or a pYES2 plasmid expressing GST-Slx5 under galactose control were grown in selective media and induced with galactose for 3 h. Lysates were then applied to a glutathione-sepharose column. After washing, the bound proteins were eluted and immunoblotted with α-HA (upper) or α-GST (lower). **c** Two-hybrid assays were performed with strains carrying the indicated activating domain (AD) or DNA binding domain (BD) fusions. Strains were grown in selective media lacking leucine (L) and tryptophan (W) prior to spotting on media lacking histidine (H) to detect a positive interaction. Experiments were independently replicated three times and images are representative of the reproducible results obtained

Yen1 foci may reflect accumulation of non-degraded or chromatin-associated protein, resulting from faulty nuclease activity or impaired turnover. We compared foci formation in wild type and *slx8*Δ cells to those formed in cells carrying the nuclease dead $Yen1^{E193A,E195A}$ ($Yen1^{ND}$). As expected, $Yen1^{ND}$ also showed higher foci accumulation compared to wild type suggesting that GFP-Yen1 reflects, at least partially, dynamics of an active protein. However, $Yen1^{ND}$ did not accumulate foci in G1 as observed in *slx8*Δ cells (Fig. 4d). We used video microscopy to determine the duration of the foci before they were dispersed. The *slx8*Δ Yen1 foci were about three times more stable (30.4 min) than those detected in wild-type cells (12.3 min) and 50% more stable than $Yen1^{ND}$ (20.9 min) (Fig. 4e). This supports the idea that foci accumulation due to faulty nuclease activity is different from that detected in a strain devoid of Slx5/8. The average intensity of these foci, compared to the nuclear average intensity, was not increased between the different strains.

A closer analysis by video microscopy time-lapses allowed us to observe the disappearance of nuclear signal in cells morphologically in G1 by following the intensity of GFP in both the nuclear and cytoplasmic compartments (Fig. 4f, Supplementary Figure 3). Although most of the signal present in the nucleus was transferred and diluted into the cytoplasm we observed a decline in overall signal during cytoplasmic re-localization (Fig. 4f, Supplementary Figure 3). This suggests that a wave of degradation occurs in a small window of time after nuclear exclusion (at the G1 to S transition). Compared to cells with no focus at the G1-S transition, cells with a focus showed increased nuclear signal for a larger time suggesting its rate of re-localization and degradation is altered (Supplementary Figure 3).

The Slx5–Slx8 Ub ligase is known to target substrates that are subject to stage-specific degradation as well as constitutive turnover[27]. Thus, a possible explanation for the accumulation of Yen1 in foci that persist until G1 in the *slx8*Δ mutant, is that Slx5–Slx8 targets only a fraction of Yen1. To test this hypothesis we further determined whether Yen1 is degraded at the G1-S transition as suggested by the microscopy time-lapse experiments by performing a cycloheximide chase experiment on cells synchronized in G1 (Fig. 4g, h, i). Under these conditions, we detected the disappearance of Yen1 following release from G1 (Fig. 4g). The degradation of Yen1 was at least partially dependent on the presence of a functional proteasome as MG132 largely prevented the degradation. In the absence of Slx8, 20–30% of Yen1 (relative to its G1 level) persisted 150 min after addition of cycloheximide, a time at which the protein was completely degraded in wild-type cells. These data show that whereas Slx5–Slx8 plays a role in Yen1 turnover, it is not the only pathway targeting Yen1 for degradation.

Yen1 localizes to the nucleolus in the absence of DNA damage. It has been previously reported that *slx8*Δ induces a larger amount of DNA damage by interfering with the control of multiple targets associated with DNA repair[42]. Slx5–Slx8 co-localizes to sites of stalled replication or to Rad52 foci[42], suggesting that its deletion will impair the normal function of replication and recombination and generate multiple sites of damage. Contrary to this view, we detected only 1–2 Yen1 foci in the majority of *slx8*Δ cells; this result suggests that Yen1 clusters specifically in a nuclear region that may experience more spontaneous damage.

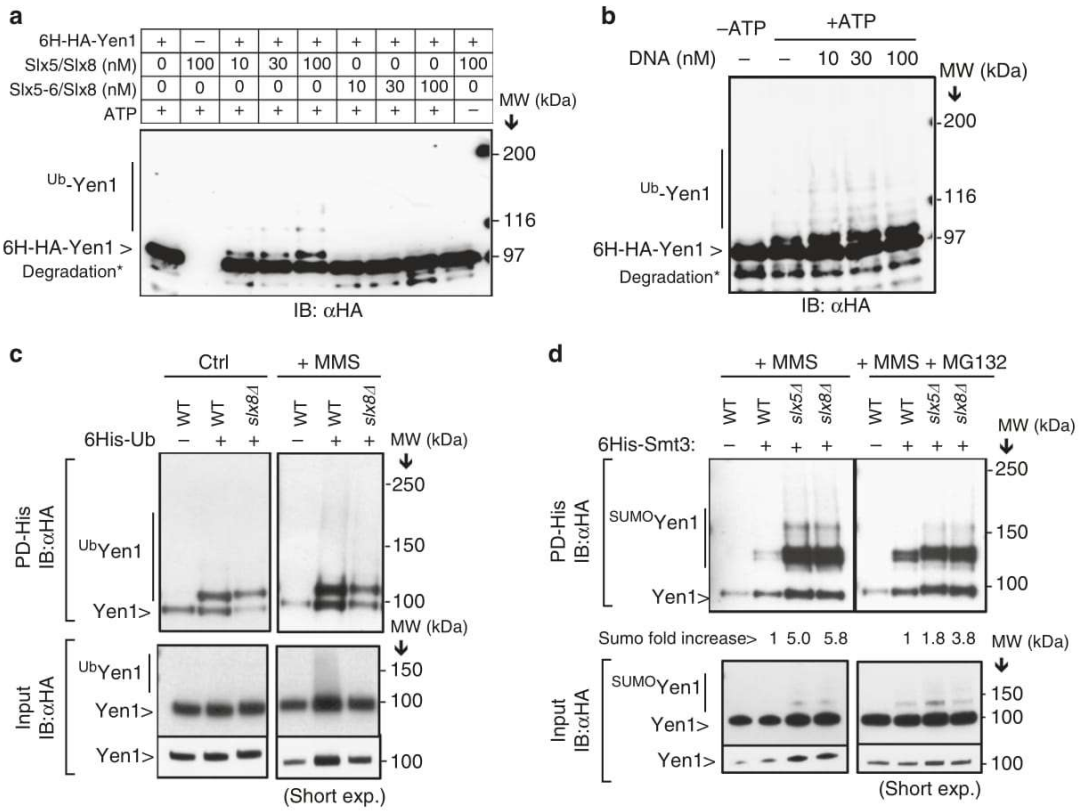

Fig. 3 Yen1 is a direct substrate of the Slx5–Slx8 ubiquitin ligase. **a** H6-HA-Yen1 (916 nM) was ubiquitinated in vitro in the presence of the indicated concentrations of either Slx5/Slx8 or the RING mutant Slx5–6/Slx8 and 0.2 μM DNA. Control lanes with H6-HA-Yen1 in the absence of E3 and Slx5/8 in the absence of Yen1 are shown. Breakdown products of Yen1 are marked with an asterisk. **b** The ubiquitination reaction was performed as above but with 50 nM Slx5–Slx8 and increasing amounts of DNA. **c** Strains expressing 6xHis-Ub were subjected to different growth conditions and lysed to pull-down ubiquitinated proteins under denaturing conditions, input Yen1-HA levels were controlled to allow comparisons. **d** Smt3 denaturing pull-downs were performed in wild type, *slx5*Δ, or *slx8*Δ cells (all in a *pdr5*Δ background) after growth in the presence of MMS. The fold increase in the sumoylated fraction indicated at the bottom of the gel is an average of three trials. Inputs were controlled in each trial to allow comparison of the eluted sumoylated proteins

We speculated that Yen1 accumulates in the absence of exogenous DNA damage in the nucleolus, where rDNA loci often generate DNA structures that are substrates for Yen1 activity[8]. Indeed, most of the Yen1 foci detected in *slx8*Δ cells, where foci appeared in a large fraction of cells, co-localized with the Sik1 and Nop1 nucleolar markers (Fig. 5a, Supplementary Figure 4). In wild-type cells, the foci also accumulated in the nucleolus and also localized adjacent to the rDNA array on chromosome XII (Fig. 5b), indicating that Yen1 normally resides there. Slx5–Slx8 localizes to nucleolar sites[42], and accordingly, we often detected interaction by BiFC of Slx5 and Yen1 adjacent to nucleolar stained regions (Supplementary Figure 4b). Interestingly, we also detected Yen1 foci associated with lagging chromatin between the nuclear masses in a number of *slx8*Δ cells (Supplementary Figure 4c). This suggests that Yen1 is associated with chromatin regions that are having difficulty segregating, where the nuclease may act to resolve joint-molecule intermediates.

After Zeocin or MMS treatment, wild type and *slx8*Δ cells accumulated foci in larger numbers than untreated cells. But in *slx8*Δ cells, many of these foci failed to diffuse significantly after 3.5 h (Fig. 5c, d). Furthermore, when *slx8*Δ cells carrying a Sik1 nucleolar marker were treated with Zeocin or MMS we found that some foci induced after the drug challenge de-localized from the nucleolus (Fig. 5e, f, Supplementary Figure 4), demonstrating that foci are dynamic and can be formed at other undetermined nuclear sites.

Lysine^{714} is the main Slx5/8 target in Yen1. In order to identify the lysine residues in Yen1 that are targeted by Slx5–Slx8, we performed a mass-spectrometry of immunoprecipitated Yen1-3xFLAG following exposure of cells to MMS. We recovered a peptide harboring a modification consistent with the presence of ubiquitin on the lysine 714. Although the score was below the level of significance, we generated an endogenous replacement with the allele *yen1-K714R*-HA.

Our previous experiments with ubiquitin pull-downs showed that Yen1 was not exclusively ubiquitinated by Slx5–Slx8 in vivo (Fig. 3c). Therefore, we tested the lysine mutant by in vitro ubiquitination using Slx5–Slx8 and recombinant Yen1-K714R. As shown in Fig. 6a, the K714R mutation prevented Yen1 ubiquitination in vitro, supporting the identification of K714 as a target for the ubiquitin ligase. As expected, pull-down analyses with the strains harboring Yen1^{K714R} did not eliminate the recovery of ubiquitinated Yen1. This is likely due to the presence of overlapping pathways of ubiquitin-mediated turnover of Yen1. However we can nonetheless see a decrease in overall ubiquitination in the K714R mutant (Fig. 6b).

Foci distribution and sumoylation in *yen1-K714R cells*. To determine the effect of the K714R mutation, we initially assessed its cell-cycle regulated localization and activity. Yen1 is phosphorylated by Cdc28 (Cdk1) in S-phase and is de-phosphorylated

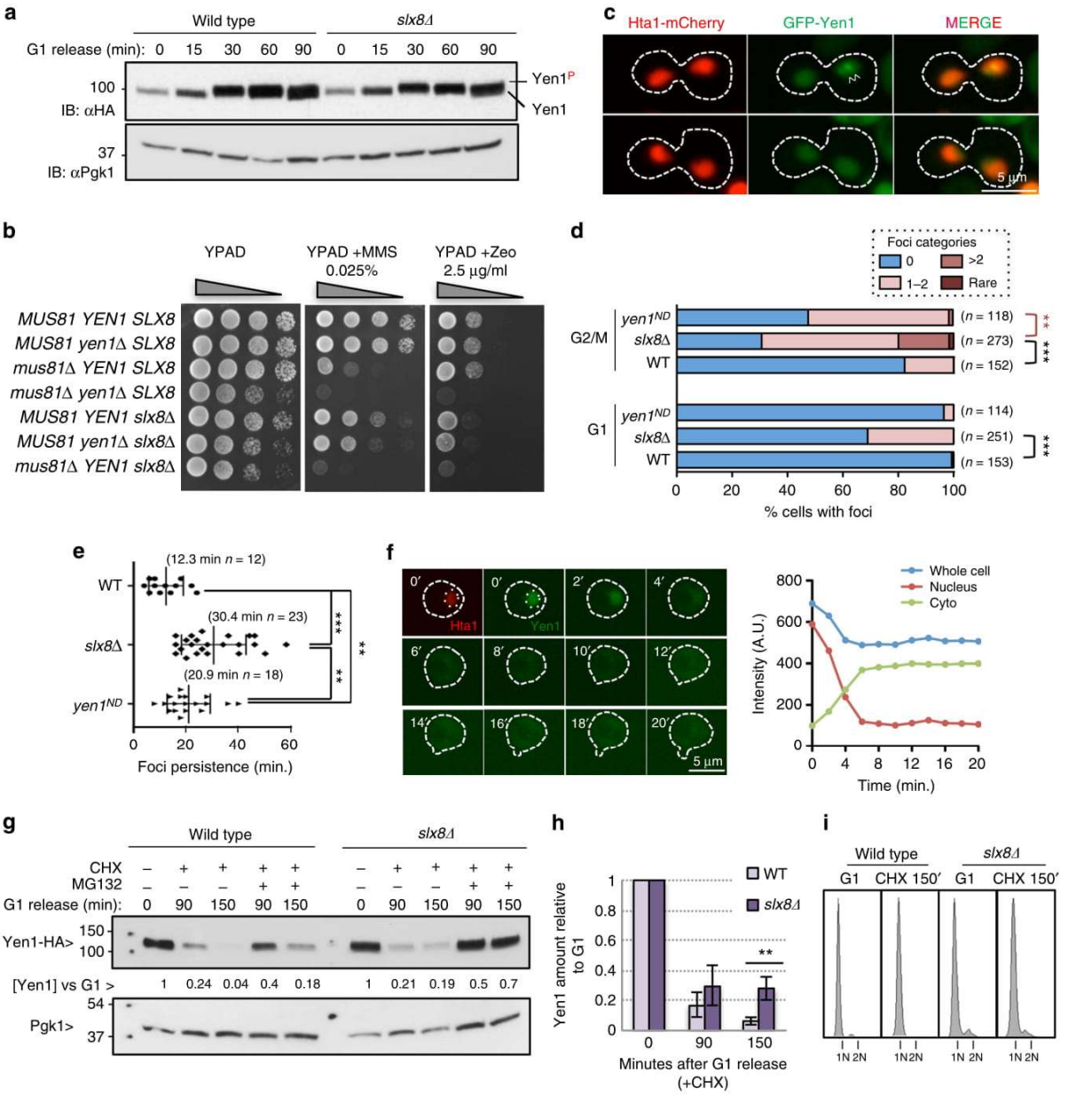

Fig. 4 Deletion of *SLX8* alters the nuclear distribution and turnover of a fraction of Yen1. **a** Wild type and *slx8*Δ cells were synchronized in G1 and released to observe the phosphorylation of Yen1 as a function of cell-cycle progression. **b** Serial dilutions of the indicated strains were spotted onto YPAD media containing different genotoxins. **c** Cells with an endogenous *HTA1*-mCherry carrying plasmids expressing wild-type GFP-Yen1 were observed microscopically after a short induction of the fusion protein. Shown are cells presenting normal nuclear localization (lower) or presenting foci (white arrows, upper). **d** G1 and G2/M cells of the indicated genetic backgrounds were microscopically examined as in **c** and classified according to the number of foci they displayed. The graphs show the percentage of cells in each category. The total number of cells individually scored from three video recordings are indicated as (*n*). Categories were subjected to the Fischer's exact test, asterisks denote significant levels at $P < 0.001$(***) or $P < 0.005$(**). **e** The duration of foci in the indicated genetic backgrounds was measured by video-microscopy analysis. The mean ± s.d. of the duration time and *n* are indicated, error bars denote s.d. Asterisks refer to significance at the $P < 0.05$ (**) and $P < 0.001$ (***) levels in unpaired two-tailed Student's *t*-test. **f** Cells expressing GFP-Yen1 and Hta1-mCherry were observed by video-microscopy in 2′ time-lapse frames. GFP total intensity of the whole cell, the nucleus and the cytoplasm was determined for 5 z-planes and used to calculate the total GFP intensity in each compartment. The graph displays the time course of GFP intensity in a single cell **g** The indicated *pdr5*Δ strains, that are permeable to MG132, were synchronized in G1 and subjected to cycloheximide (CHX) treatment during their release from G1 arrest. Where indicated, cells were pre-treated with MG132 for 30 min before, and during release in the presence of CHX. PGK1 was used to normalize the amount of Yen1. **h** Quantitation of the fraction of Yen1, compared to G1, remaining at the indicated times after release into CHX. The mean ± s.d. of triplicate assays is shown; statistically significant difference in unpaired two-tailed Student's *t*-test is indicated (**$P < 0.05$)**. i** FACS analysis of cells at the beginning and at the end of the CHX treatment

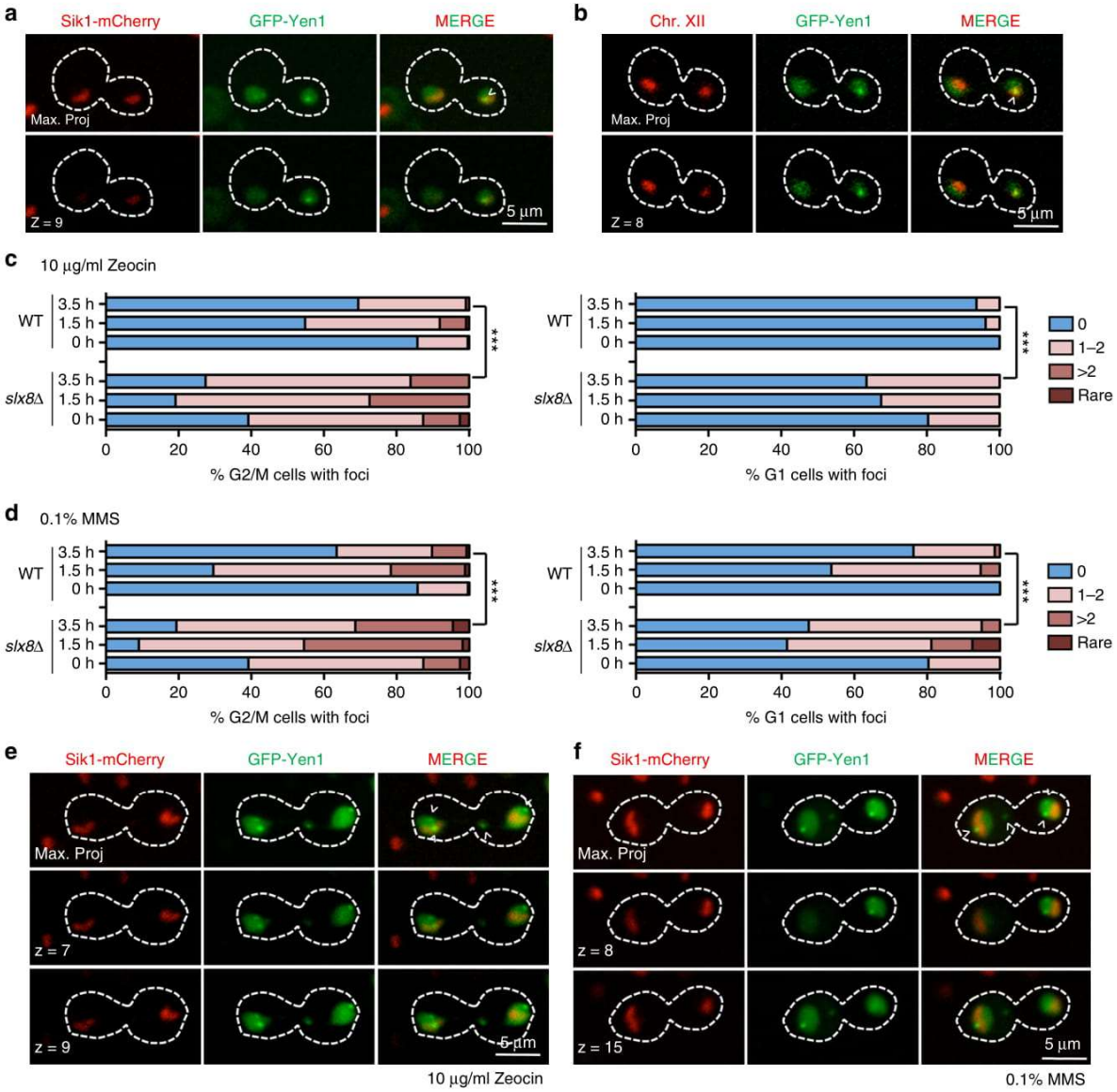

Fig. 5 Yen1 foci are dynamic and localize preferentially to nucleolar sites in the absence of DNA damage. **a** *slx8*Δ cells carrying a *SIK1*-mCherry endogenous marker and an inducible GFP-Yen1 expressing plasmid were observed after short induction of the fusion protein. The white arrow denotes co-localizing signal of GFP-Yen1 with Sik1-mCherry. **b** Wild-type cells carrying a TetO-TetR array tag on chromosome XII and an inducible GFP-Yen1 expressing plasmid were observed after short induction of the fusion protein. **c** Cells were subjected to acute challenge with Zeocin (0.01 mg/ml) and observed during their recovery as in Fig. 4. Cells displaying the designated categories of GFP-Yen1 foci were scored at the indicated time points. The total number of cells analysed (*n*) from two independent recordings were as follows: WT 0 h ($n_{G1} = 81$, $n_{G2/M} = 267$), WT 1.5 h ($n_{G1} = 78$, $n_{G2/M} = 124$), WT 3.5 h ($n_{G1} = 110$, $n_{G2/M} = 118$), *slx8*Δ 0 h ($n_{G1} = 107$, $n_{G2/M} = 79$), *slx8*Δ 1.5 h ($n_{G1} = 40$, $n_{G2/M} = 73$), *slx8*Δ 3.5 h ($n_{G1} = 52$, $n_{G2/M} = 62$). **d** Cells were subjected to an acute challenge with 0.1% MMS and for foci were observed as in **c**. The total number of cells analysed (*n*) from two independent recordings were as follows: WT 0 h ($n_{G1} = 81$, $n_{G2/M} = 267$), WT 1.5 h ($n_{G1} = 95$, $n_{G2/M} = 98$), WT 3.5 h ($n_{G1} = 139$, $n_{G2/M} = 137$), *slx8*Δ 0 h ($n_{G1} = 107$, $n_{G2/M} = 79$), *slx8*Δ 1.5 h ($n_{G1} = 53$, $n_{G2/M} = 55$), *slx8*Δ 3.5 h ($n_{G1} = 40$, $n_{G2/M} = 67$). **e** *slx8*Δ cells carrying *SIK1*-mCherry were observed after Zeocin challenge to determine GFP-Yen1 co-localization. White arrows indicate GFP-Yen1 foci. **f** *slx8*Δ cells were observed as in **e**, but were subjected to MMS treatment. White arrows indicate GFP-Yen1 foci. Images are representative of the reproducible results obtained after three independent trials. Statistical significance at $P < 0.0001$ in Fischer's exact test at 3.5 h recovery points is indicated by asterisks in **c** and **d**

by Cdc14 at anaphase[44]. No major difference could be detected when analyzing the mutant *yen1-K714R* as compared to wild type (Fig. 6c, Supplementary Figure 5). Nuclear shuttling of Yen1^{K714R} was identical to wild-type Yen1, with S-phase exclusion occurring in both strains (Fig. 6d). Interestingly, we detected a modest increase in Yen1^{K714R} foci in undamaged conditions, further increased in a *mus81*Δ background (Fig. 6d), suggesting the persistence of Yen1^{K714R} foci is specifically observed if there are increased substrates. This increase in foci in the *yen1-K714R mus81*Δ double mutant did not result in increased DNA damage

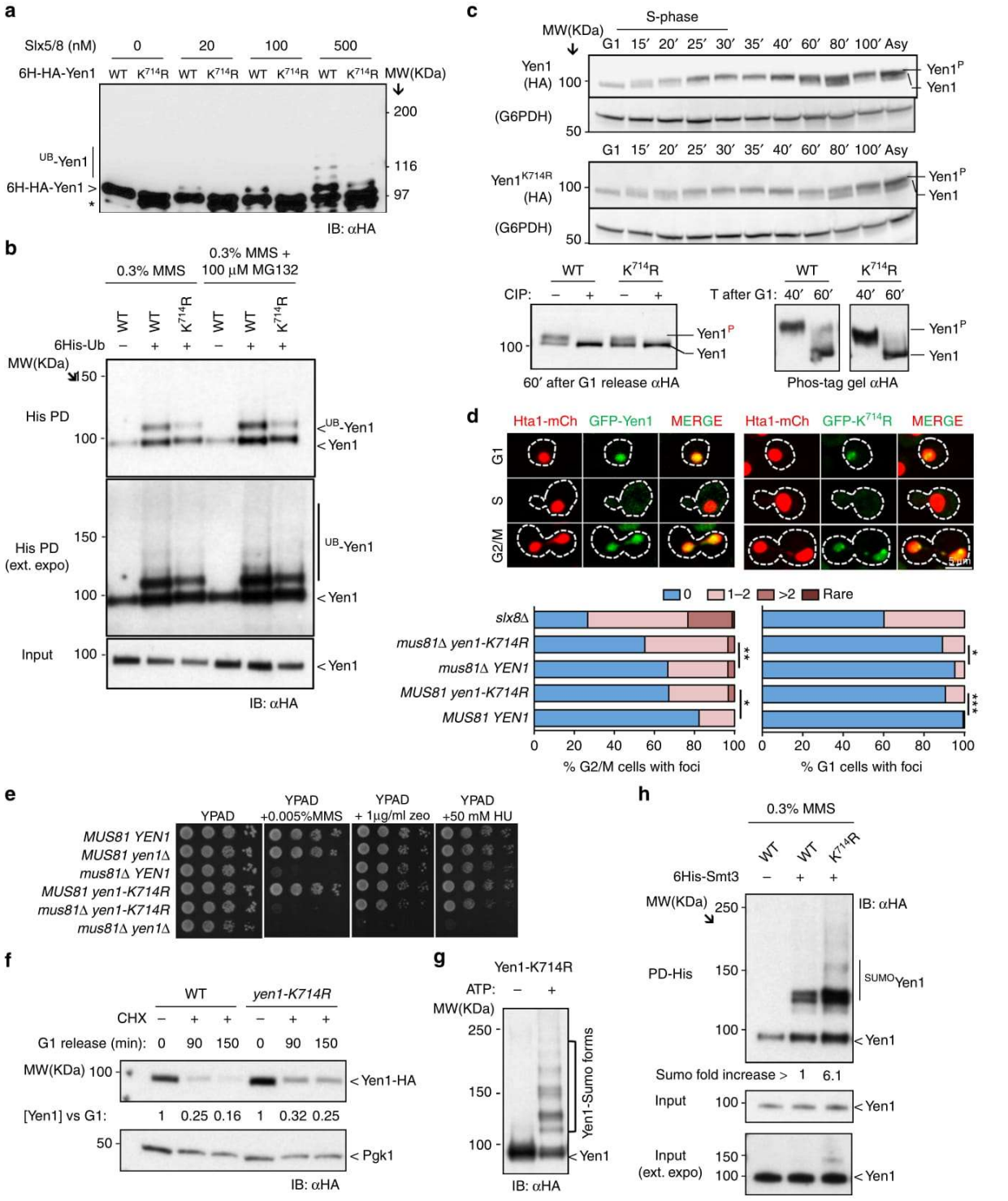

sensitivity (Fig. 6e, Supplementary Figure 5), however, suggesting that locally accumulated Yen1^{K714R} retained the ability to complement the loss-of-Mus81 nuclease. A cycloheximide chase experiment with the *yen1-K714R* strain resulted in the detection of a more persistent Yen1 fraction 150 min after G1 release (Fig. 6f) that is in agreement with the observation of increased Yen1 foci. Yen1-K714R was still sumoylated both in in vitro assays with immunoprecipitated Yen1-HA or in pull-down experiments (Fig. 6g, h). The modified forms recovered from pull-downs were more abundant in the mutant strain compared to the wild type suggesting that the lysine substitution triggers stabilization of the Yen1 sumoylated fraction similarly to the effects observed in the experiments with *slx8*Δ and *slx5*Δ cells (Fig. 3).

Fig. 6 K714 is ubiquitinated by Slx5–Slx8. **a** Recombinant 6xHIS-HA-Yen1 and the mutant 6xHIS-HA-Yen1-K714R (916 nM) were subjected to in vitro ubiquitination as in Fig. 3a. **b** 6xHis-Ubiquitin pull-downs were performed on cells expressing 6His-Ub and carrying endogenous Yen1-HA or its variant Yen1-K714R-HA following treatment with the indicated genotoxics. **c** Strains carrying endogenous Yen1-HA or its K714R variant were synchronized with alpha factor in G1 and proteins extracted at indicated time points after G1 release and immunoblotted with anti-HA. At time points where Yen1 is modified by CDK1, extracts were subjected to phosphatase treatment (CIP+) and also subjected to phos-tag gel separation. **d** Strains carrying *HTA1*-mCherry and the indicated GFP-Yen1 expression plasmids were examined microscopically as in Fig. 4c to assess the presence of the proteins. Foci were quantified as a function of cell-cycle phase, which was determined by cell morphology. The total number of analysed cells (*n*) and independent video recordings (VR) were as follows: WT ($n_{G1} = 105$, $n_{G2/M} = 153$, VR = 3), *yen1*-K714R ($n_{G1} = 106$, $n_{G2/M} = 64$, VR = 3), *mus81*Δ ($n_{G1} = 294$, $n_{G2/M} = 337$, VR = 3), *mus81*Δ *yen1*-K714R ($n_{G1} = 203$, $n_{G2/M} = 306$, VR = 3), *slx8*Δ ($n_{G1} = 166$, $n_{G2/M} = 172$, VR = 3). Statistical differences were estimated by the Fischer's exact test and significance is indicated by asterisks $P < 0.05$(*), $P < 0.005$(**), $P < 0.001$(***). **e** Sensitivity to the indicated genotoxics was determined by spotting serial dilutions of different strains on the indicated media. **f** Cycloheximide chase experiment showing persistence of Yen1 after a G1 release in the presence of CHX. **g** Immunoprecipitated Yen1-K714R-HA was eluted and the protein was sumoylated with Aos1-Uba2, Ubc9, and Smt3-3KR in the presence or absence of ATP. Samples were de-phosphorylated with CIP before loading. **h** 6xHIS-Smt3 pull-downs were performed on cells expressing 6HIS-Smt3 and carrying *YEN1-HA* or its variant *yen1-K714R-HA* under conditions of MMS treatment as indicated. The average fold enrichment is indicated at the bottom of the blot

Increased crossover formation in *yen1-K714R* cells. To test possible gain-of-function effects of Yen1^{K714R} we measured mitotic CO levels. A gain-of-function of Yen1 would likely increase the rate of CO resolution during DSB repair without affecting sensitivity to DNA damaging agents. To test this hypothesis, we used the diploid strain able to screen CO/BIR levels after an I-SceI-induced DSB[45]. Introduction of -1xHA tagged Yen1 in these strains did not affect the CO levels previously reported[46] and were within experimental variation. As expected for this assay, the *mus81*Δ strain showed a slightly reduced CO level that was further reduced in the *mus81Δ yen1Δ* strain, along with a parallel increase in BIR (Fig. 7a). Surprisingly, when introduced alone, Yen1^{K714R} increased the overall CO levels above those of wild type. Further, when *yen1-K714R* was combined with *mus81*Δ, instead of a decrease in CO levels as expected for a loss-of-function *YEN1* allele, we observed a nearly twofold increase in COs compared to *mus81*Δ alone (Fig. 7a). These CO levels are above those expected for wild type and consistent with a gain-of-function phenotype.

yen1-K714R* suppresses segregation defects of *mus81Δ. One effect of the failure to repair recombination intermediates is the accumulation of joint-molecules in mitosis that lead to mis-segregation of chromosomes and ultimately an increase or decrease in chromosome number. The *mus81Δ yen1Δ* strain display such segregation defects even in the absence of DSBs induced by exogenous sources[45]. In order to test the *yen1-K714R* mutant for a gain-of-function phenotype, we devised an improved assay for chromosome segregation fidelity. Genetic systems that monitor mis-segregation have the limitation of looking at viable endpoints and cannot recover unviable ones. We therefore chose to look at real-time chromosome segregation by using a fluorescent array tag on chromosome IV (Fig. 7b, Supplementary Figure 6). Using this approach we confirmed that *mus81Δ yen1Δ* cells are severely impaired in chromosome segregation (Fig. 7c). Segregation defects were observed in 35% of *mus81*Δ single mutants, and more than 60% of *mus81Δ yen1Δ* cells (Fig. 7c). Under the same conditions, *yen1*-K714R partially suppressed the *mus81*Δ defects (Fig. 7c). The ability of Yen1^{K714R} to suppress *mus81*Δ defects is further evidence of a gain-of-function phenotype consistent with the idea that more spontaneous joint-molecule intermediates are resolved in cells expressing Yen1^{K714R} than in wild-type cells. Because elevated Yen1 expression has been shown to suppress *mus81Δ* phenotypes[47], we compared the effect of Yen1 over-expression to the phenotypes of the *yen1-K714R* mutant. Expression of plasmid borne wild-type Yen1-HA, suppressed *mus81Δ* segregation defects to levels similar to those observed in a *mus81Δ yen1-K714R* strain (Fig. 7d). Thus, even though Yen1-HA protein levels were extremely high following induction (see Supplementary Figure 7b), suppression was no better than that achieved by endogenous levels of Yen1^{K714R}. Interestingly, long-term high-level expression of Yen1 appeared to be deleterious to *mus81Δ* cells. Chronic but mild over-expression of Yen1-HA (0.1% galactose induction) resulted in *mus81*Δ cells that were more sensitive to MMS than their un-induced counterparts even though Yen1-HA expression was only slightly higher than endogenous levels (Supplementary Figure 7).

Discussion

Nucleolytic processing of recombination intermediates by Yen1 has been proposed to be an option of last resort that is needed to prevent chromosomal segregation defects and genome rearrangements in mitosis[48]. Accordingly, Yen1 has a tightly controlled operational window that is limited to the anaphase—telophase period of mitosis. Here, it removes the last intermediates that physically connect the chromosomes[44,49]. Although the window of Yen1 activity is known to rely on cell-cycle driven phosphorylation and de-phosphorylation[12,13], we establish here for the first time a new layer of control involving Slx5–Slx8 dependent ubiquitination of Yen1 (see model in Supplementary Figure 8). Slx5/8 targets a minor fraction of Yen1 that is detected as a more persistent pool associated with nucleolar or active sites on the chromatin (Figs. 4 and 5). We have identified K714 as the major target of Slx5–Slx8 (Fig. 6). The fact that significant levels of ubiquitinated Yen1 were recovered from *slx8*Δ cells, is in full agreement with reports that other Slx5/8 targets are redundantly targeted by alternative ubiquitination pathways to ensure rapid destruction in different contexts or sub-nuclear compartments[41,50,51].

Our analysis of the transition between G1 and S phases clearly indicates that there is a wave of Yen1 destruction before S-phase entry, when most of the previously nuclear protein is targeted for proteasomal degradation (Fig. 4). Our data suggest this is a general turnover pathway that is not controlled by Slx5/8. This pathway degrades most of the Yen1 pool, similar to what has been described for other Slx5/8 targets[51]. One plausible explanation for why Slx5/8 targets such a minor fraction of Yen1 is that it can be quickly degraded, or evicted from the nucleus before S-phase starts. In agreement with such a hypothesis, we see a fraction of Yen1 that remains un-degraded in cycloheximide chase experiments performed in cells that are synchronized in G1. The amount of Yen1 that remains un-degraded is about 20% of the total found at the beginning of the experiment, although this may reflect an increased amount of Yen1 associated with chromatin or active sites in cells devoid of Slx5/8[42,52]. Under wild-type conditions, we might expect the fraction of Yen1 being targeted by Slx5/8 to be more transient. Our data are also compatible with a

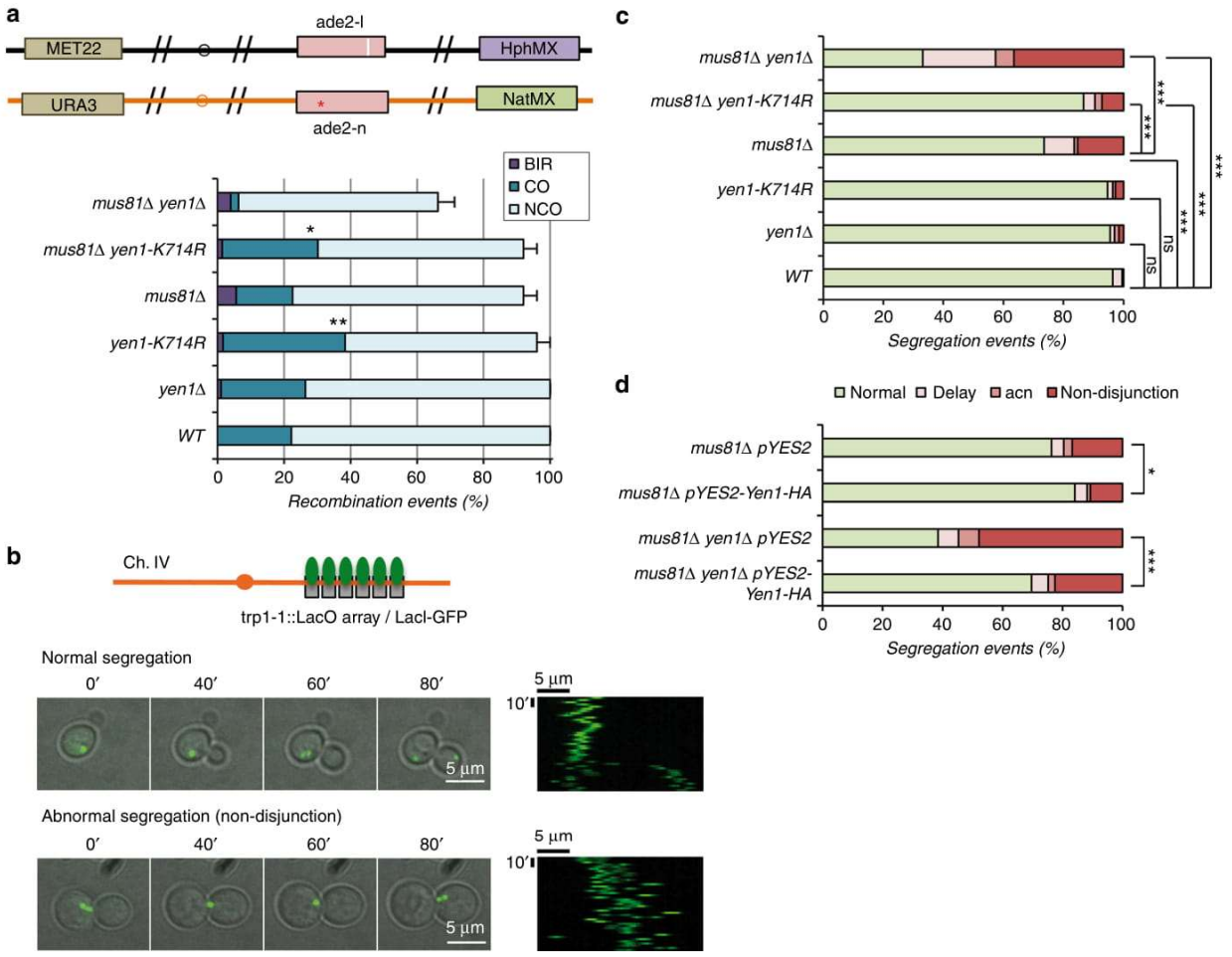

Fig. 7 Yen1-K714R increases COs and suppresses spontaneous chromosome segregation defects in *mus81*Δ cells. **a** Diagram explaining the Chr. XV DSB-induced crossover reporters. Recombination outcomes were scored in white/red sectored colonies of the indicated strains and normalized to its plating efficiency (PE). The number of independent experiment trials (T) and the total number of recombination events scored (*n*) were as follows: WT ($T = 6$, $n = 158$), *yen1*Δ ($T = 9$, $n = 538$), *mus81*Δ ($T = 5$, $n = 168$), *mus81*Δ *yen1*Δ ($T = 9$, $n = 160$), *yen1*-K714R ($T = 5$, $n = 230$), and *mus81*Δ *yen1*-K714R ($T = 5$, $n = 230$). **b** A strain harboring a lacO/GFP-LacI array tag on chromosome IV was followed by video-microscopy to discriminate chromosome segregation in timely manner from aberrant segregation. Images display a typical normal and aberrant segregation and its respective kymograph. **c** GFP foci of the indicated strains were observed by video-microscopy and chromosomal segregation was scored as to whether it displayed a proper phenotype (normal) or one of three types of defective phenotypes (non-disjunction, delay, and aberrant chromosome number (acn)). The total number of cells analysed (*n*) and independent video-recordings (VR) were as follows: WT ($n = 606$, VR = 3), *yen1*Δ ($n = 133$, VR = 3), *yen1*-K714R ($n = 131$, VR = 3), *mus81*Δ ($n = 259$, VR = 5), *yen1-K714R mus81*Δ ($n = 448$, VR = 3) and *yen1Δ mus81Δ* ($n = 289$, VR = 3). **d** Segregation events scored as in **c** were determined for *mus81*Δ and *mus81Δ yen1Δ* strains containing a pYES2 plasmid expressing Yen1-HA under Galactose-inducible control or an empty pYES2 and subjected to acute over-expression of Yen1-HA or the equivalent mock induction prior to the recording of the video-microscopy. The total number of cells analysed from three VRs were as follows: *mus81*Δ (+pYES2) $n = 245$, *mus81*Δ (+pYES2-Yen1) $n = 391$, *mus81Δ yen1Δ* (+pYES2) $n = 117$, *mus81*Δ *yen1*Δ (+pYES2-Yen1) $n = 218$. Statistically significant differences in **a** between CO and other outcomes and in **c** and **d** between normal and abnormal categories were determined by the Fischer's exact test, asterisks refer to significance at the $P < 0.001$(***), $P < 0.005$(**) or $P < 0.05$(*)

SUMO-independent role of Slx5/8 in targeting Yen1 (Fig. 3). SUMO independence has previously been observed in certain Slx5/8 substrates. These substrates are thought to be targeted by Slx5/8 binding to sumoylated partner proteins[40] or to substrate structural features that mimic SUMO[51].

Sumoylation has been proposed as a mechanism to rapidly form protein complexes under stress conditions[20], or to recruit factors that need to associate at precise cellular localizations in a timely constrained manner[53]. We speculate that Yen1 is sumoylated in stressful situations, and that Slx5/8 ubiquitination ensures any remaining Yen1 that is strongly associated with DNA at the end of G1 will be effectively degraded before replication starts. In such a hypothesis, sumoylation would not be a pre-requisite for Slx5/8 targeting, but sumoylated Yen1 would be targeted due to its preferential association with DNA or chromatin regions that preclude it from being exported or degraded at S-phase similar to what has been described for proteins associated with the kinetochore[40]. Although, we consider it unlikely, our data does not exclude the possibility that Slx5/8 ubiquitination does not directly trigger Yen1 degradation, but only influences its local association with other partners or its DNA substrates. For example, the extended nuclear persistence of a limited Yen1

fraction could also result from its association with nuclear sites that are inhibitory to a general mechanism of degradation that has yet to be described and is responsible for eliminating the majority of the Yen1 protein before S-phase.

The fact that Yen1 is regulated by multiple mechanisms, including phosphorylation, nuclear exclusion, and protein turnover, suggests that Yen1 inhibition is especially important for preventing DNA damage during DNA replication when structures generated at the replication forks may be a substrate for Yen1 cleavage. In agreement with this hypothesis, hyperactive forms of Yen1 that are constitutively nuclear ($Yen1^{ON}$) sensitize cells to high doses of MMS[12]. This has been interpreted as an increased sensitivity to conditions where forks stall more frequently. Similarly, we can detect a suppressive effect linked to over-expression of Yen1, but chronic mis-regulation of Yen1 levels sensitizes cells and causes deleterious side effects (Fig. 7, Supplementary Figure 7), whereas we did not detect an increased sensitivity to MMS in *yen1*-K714R cells. It is important to keep in mind that redundant controls are probably able to restrict Yen1 activity if overall levels are not largely altered, but these controls may not be sufficient to cope with a chronic over-expression of the nuclease. With moderate excess of Yen1, the protein may still become dissociated from chromatin and exported prior to S-phase and it can still be phosphorylated by CDK1 to inhibit its activity thus explaining limited impacts in MMS sensitivity. Nonetheless, we see a striking increase in CO formation with the *yen1*-K714R allele following a DSB, suggesting that the Slx5/8 control plays an important role in maintaining the preference for the use of NCO pathways (Sgs1- or Mph1-dependent pathways) whenever these factors are available. It is known that Slx5/8 is needed to allow re-localization of DSBs to nuclear pores[54] and could thus regulate the ability of repair factors to gain access to the intermediates of DSB repair[54,55]. We suggest that Slx5/8 may be responsible for clearing Yen1 from DNA intermediates where Sgs1- is already recruited, or for limiting Yen1's ability to associate to these intermediates. The fact that the K714R mutation allows increased recovery of sumoylated Yen1 (Fig. 6) raises the interesting possibility that sumoylation favors Yen1 activity over other proteins capable of dismantling joint-molecule intermediates. Slx5–Slx8 may regulate access of different proteins by removing sumoylated Yen1 from DNA intermediates if its recruited in the presence of NCO determinants like Sgs1. Mapping of the multiple sites of Yen1 sumoylation will be required to determine whether sumoylation is strictly required for Yen1 functions in vivo, and whether different sites or levels of sumoylation influence its binding to known partners, or proteins yet to be described. Should any potential "sumo-less" mutants, bearing multiple lysine replacements, be neutral with respect to Yen1's protein folding, it would be possible to draw conclusions on the effect of sumoylation on Yen1's localization and nuclease activitiy. Similarly, a more extended study on the biochemical activities of in vitro fully-sumoylated Yen1 will help test whether sumoylation alters Yen1's specificity for its different substrates.

Yen1 has a specific role in dealing with replication intermediates that are usually handled by Dna2[38] and it plays a role in suppressing the accumulation of JM intermediates that originate in the rDNA locus[8]. These JM contain either orphan HJs or D-loop -derived intermediates that do not mature into dHJs, and thus are not dissolved by the BLM ortholog Sgs1 and its associated proteins[4,8]. Slx5/8 could thus ensure that Yen1 is only used as the last option even in situations when recruitment has been enforced by a sumoylation cascade[20]. If the human GEN1 ortholog is regulated similarly, we expect that mutations equivalent to the K714R identified here may recapitulate the hyper-crossover phenotypes we observed without a major effect on cell viability. Such mutations might be found to have a cancer predisposition phenotype due to its increased genome instability. Defects in GEN1 turnover would be expected to give rise to a phenotype similar to that of impaired BLM helicase, or a defect in factors enforcing NCO pathways. The redundancy in the pathways of nucleolytic resolution during HR in humans[56] makes it difficult to determine a precise role of GEN1 mutations in cancer predisposition, with scarce evidence to date[57–59]. However, should the active pools of GEN1 be similarly regulated in human cells, it may be possible to identify mutations that destabilize the balance between CO and NCO outcomes.

Methods

Yeast strains and growth conditions. *S. cerevisiae* strains and plasmids used in this study are listed in Supplementary Tables 1 and 2. The *YEN1*-HA allele was generated by inserting a FactorXa cleavage site and a single-HA epitope at its C-terminus using PCR amplification with a dedicated oligonucleotide. Mutants in the different designated loci where either obtained by crossing or by gene replacement with the indicated selective cassettes. Cells were typically grown in YP (1% yeast extract; 2% peptone) or SC media with 2% glucose or alternatively with 2% raffinose or 2% galactose in strains under inducible conditions. A modified medium (SC with 0.17% YNB without ammonium sulfate, 0.1% proline and 0.003% SDS) was used for the cycloheximide and MG132 assays and for the Smt3/Ubi pull-down assays. Methyl methane sulfonate (MMS, Sigma), Zeocin (Zeo, Invitrogen) and hydroxyurea (HU, Sigma) were added to YPD medium at the designated doses for DNA damage sensitivity assays.

Western blot analyses. Proteins were extracted by the TCA (Trichloroacetic acid) method if not stated otherwise. Samples were loaded into 7.5% or 4–15% gradient Tris-Glycine BioRad stain-free pre-casted gels for routine analysis. Samples from pull-downs analyses were loaded into 3–8% gradient NuPAGE Tris-Acetate gels (Invitrogen). Gels were transferred to PVDF membranes using a semi-dry transfer machine (BioRad) and hybridized on TBST 5% milk with the appropriate antibodies. Antibodies were used at the suggested dilution: anti-HA-HRP (3F10, Roche) 1:1000 (1:500 for pull-down analysis), anti-Ubiquitin (P4D1, Biolegends) 1:1000, anti-Smt3 (provided by B.Palancade) 1:2000, anti-G6PDH (A9521, Sigma) 1:20,000, anti-Pgk1-HRP (22C5D8, Abcam) 1:10,000, anti-GST-HRP (GERPN1236, Sigma) 1:5000. When required, HRP-conjugated secondary antibodies from Cell Signaling (anti-Mouse-HRP, anti-Rabbit-HRP) were used at 1:10,000 dilution. Western blots were revealed with WesternBright ECL solution (Advansta) or WesternBright Sirius HRP subsrate if required (Advansta). Blots were cropped in order to arrange figures without any lane substitution and conserving the area with immunoblotting signal (examples of uncropped images are available in Supplementary Figure 9).

Microscopy and cell biology. Live cell imaging was performed with a Spinning Disk Confocal Microscope (CSU-W1, Yokogawa), with an electron multiplying charge device camera (ANDOR Zyla sCMOS) and a ×60/1.35 numerical aperture objective at 30 °C. Cells were mounted on agarose pads as described[60] and imaging recorded 15 z-sections with 0.5 µm spacing. Image acquisition was performed using Fiji (ImageJ)[61]. Cells were grown in synthetic complete medium without uracil (SC-URA 2% raffinose), GFP-Yen1 was induced in a short burst with 30 min with Galactose at 2%, followed by addition of Glucose at 2%. DNA damage acute exposures (MMS 0.1% or 10 µg/ml Zeocin) lasted 15 min at room temperature following arrest of GFP-Yen1 expression. After the acute DNA damage, cells were washed once with fresh SC-URA 2% glucose and held for 30 min at 30 °C in this medium, whereas aliquots were removed at the indicated times. Cells showing an accumulation of spots were measured at maximum projection of the GFP channel. Statistical analysis was performed using Fisher's exact test to determine the level of significance between two categories and χ^2 to compare more than two categories and consistency between trials.

Cycloheximide chase experiments. Cultures grown in SC complete modified media (0.1% proline 0.017% YNB w/o ammonium sulfate) were diluted to OD 600 = 0.2 and synchronized with alpha factor (3 µM) for 2 h. At G1 release, cells were treated with cycloheximide (250 µg/ml) in fresh media and when indicated cells were pre-treated with MG132 (100 µg/ml) 30 min before G1 release. At every given time point 1 ml of culture was removed and frozen in presence of 25 mM sodium azide. Proteins were extracted by the TCA method and analyzed by 7.5% SDS-PAGE and western blot.

Pull-downs and immunoprecipitation. For 6xHIS-Smt3 and 6xHIS-Ubi4 pull-downs, strains containing the expression vectors or the control plasmid were grown in SC-LEU modified medium (0.1% proline, 0.17% YNB without ammonium sulfate). Cells were allowed to grow to OD 600 = 0.3 when $CuSO_4$ was added at 100 µM final concentration in a volume of 100 ml. After 1 h MMS was added to 0.3% and cells were collected 3 h later. For cultures inhibited for proteasome

degradation MG132 was added to 100 µM 2 h before collecting the cells. Cells where lysed under denaturing conditions and SUMO or ubiquitin-conjugated proteins where isolated basically as described[35,62–64] with the modifications detailed in Supplementary methods section. In GST-pull-downs cells were lysed in IP buffer (40 mM Tris-HCl (pH 7.5), 10% Glycerol 0.1% NP40 150 mM NaCl) and cleared lysates bound to Glutathione Sepharose (GE Healthcare). After washes, proteins were eluted directly in Laemmli buffer. For the detection of sumoylated Yen1-HA forms by immunoprecipitation cells were lysed in TCA buffer by bead-beating at 4 °C. After centrifugation, precipitated proteins were washed once in cold acetone and then, pellets were resuspended in denaturing-IP buffer (0.5 M Tris-base, 6.5% SDS, 100 mM DTT, and 12% glycerol) and heated during 20 min at 65°C before centrifugation at 16,000g for 10 min. Each 45 µl of soluble protein were diluted in 1.5 ml of RIPA buffer (50 mM Tris (pH 7.5), 150 mM NaCl, 5 mM EDTA, and 1% Triton X-100) containing protease inhibitors (EDTA free, Roche) and applied to anti-HA conjugated Agarose (Pierce), the bound fraction was eluted in Urea-loading buffer (8 M urea, 200 mM Tris-HCl (pH 6.8), 1 mM EDTA, 5% SDS, 0.1% bromophenol blue and 1.5% DTT).

Protein purification and in vitro assays. HIS6-tagged recombinant proteins were produced in *E. coli* BL21-RIL cells as described[65]. Proteins were purified on a 1 ml His-Trap column using an AKTA FPLC (GE Healthcare). The peak fractions were identified by SDS-PAGE, pooled, and dialyzed to buffer A (25 mM Tris-HCl (pH 7.5), 1 mM EDTA, 0.01% NP40, 1 mM DTT, 10% glycerol, and 0.1 mM PMSF) containing 300 mM NaCl and stored at −80 °C. Ub, Uba1, and UbcH5 were obtained from Boston Biochem.

In vitro full reconstituted sumoylation and ubiquitination assays with recombinant 6H-HA-Yen1 were performed in the presence of 20 mM HEPES (pH 7.5), 5 mM $MgCl_2$, 2 mM ATP, 5 µM $ZnSO_4$, and 0.1 mM DTT. Sumoylation reactions were incubated at 30 °C for 40 min and contained 10 nM Aos1/Uba2, 60 nM Ubc9, 0–10 nM Siz2-V5, 1.5 µM His6-Smt3-G98, and 0.7 µM Yen1 in a total volume of 20 µl. Ubiquitination reactions were incubated at 30 °C for 30 min and contained 10 nM Uba1, 60 nM Ubc5, 0–500 nM Slx5–Slx8, and 1.5 µM Ub in a 20 µl reaction. Where present, Holliday junction DNA, comprised of four 49-nt oligonucleotides, was added at 0.2 µM.

In in vitro Sumoylation assays with Yen1-1xHA from yeast, Yen1 was immunoprecipitated from cell lysates in native IP buffer using anti-HA conjugated Agarose (Pierce) and the protein was eluted with HA peptide (Sigma) competition. Eluates were subjected to SUMO conjugation as described[35].

DSB-induced *ade2* recombination assay. The diploid recombination assays were performed basically as described[46]. Briefly, diploid strains containing 2 hetero-alleles of *ade2* are cleaved in its *ade2*-I allele by induction of I-SceI and allowed to repair under non-selective conditions (YPD) to give rise to either ADE2 or *ade2*-n repair products in three types of colonies (red, white, and sectored). Outcomes were scored as in ref. [46] by assigning to each colony the recombination events that correspond to the repair of the two sister-chromatids. A more detailed overview is available at Supplementary methods section.

Data availability

The data that support the findings of this study are available from the corresponding author upon reasonable request.

Received: 6 March 2018 Accepted: 1 October 2018
Published online: 27 November 2018

References

1. Symington, L. S., Rothstein, R. & Lisby, M. Mechanisms and regulation of mitotic recombination in Saccharomyces cerevisiae. *Genetics* **198**, 795–835 (2014).
2. Szostak, J. W., Orr-Weaver, T. L., Rothstein, R. J. & Stahl, F. W. The double-strand-break repair model for recombination. *Cell* **33**, 25–35 (1983).
3. Bzymek, M., Thayer, N. H., Oh, S. D., Kleckner, N. & Hunter, N. Double Holliday junctions are intermediates of DNA break repair. *Nature* **464**, 937–941 (2010).
4. Mazon, G. & Symington, L. S. Mph1 and Mus81-Mms4 prevent aberrant processing of mitotic recombination intermediates. *Mol. Cell* **52**, 63–74 (2013).
5. Prakash, R. et al. Yeast Mph1 helicase dissociates Rad51-made D-loops: implications for crossover control in mitotic recombination. *Genes Dev.* **23**, 67–79 (2009).
6. Ira, G., Malkova, A., Liberi, G., Foiani, M. & Haber, J. E. Srs2 and Sgs1-Top3 suppress crossovers during double-strand break repair in yeast. *Cell* **115**, 401–411 (2003).
7. Mitchel, K., Zhang, H., Welz-Voegele, C. & Jinks-Robertson, S. Molecular structures of crossover and noncrossover intermediates during gap repair in yeast: implications for recombination. *Mol. Cell* **38**, 211–222 (2010).
8. Garcia-Luis, J. & Machin, F. Mus81-Mms4 and Yen1 resolve a novel anaphase bridge formed by noncanonical Holliday junctions. *Nat. Commun.* **5**, 5652 (2014).
9. Matos, J., Blanco, M. G., Maslen, S., Skehel, J. M. & West, S. C. Regulatory control of the resolution of DNA recombination intermediates during meiosis and mitosis. *Cell* **147**, 158–172 (2011).
10. Gallo-Fernandez, M., Saugar, I., Ortiz-Bazan, M. A., Vazquez, M. V. & Tercero, J. A. Cell cycle-dependent regulation of the nuclease activity of Mus81-Eme1/Mms4. *Nucleic Acids Res.* **40**, 8325–8335 (2012).
11. Szakal, B. & Branzei, D. Premature Cdk1/Cdc5/Mus81 pathway activation induces aberrant replication and deleterious crossover. *EMBO J.* **32**, 1155–1167 (2013).
12. Blanco, M. G., Matos, J. & West, S. C. Dual control of Yen1 nuclease activity and cellular localization by Cdk and Cdc14 prevents genome instability. *Mol. Cell* **54**, 94–106 (2014).
13. Eissler, C. L. et al. The Cdk/cDc14 module controls activation of the Yen1 holliday junction resolvase to promote genome stability. *Mol. Cell* **54**, 80–93 (2014).
14. Johnson, E. S. Protein modification by SUMO. *Annu. Rev. Biochem.* **73**, 355–382 (2004).
15. Flotho, A. & Melchior, F. Sumoylation: a regulatory protein modification in health and disease. *Annu. Rev. Biochem.* **82**, 357–385 (2013).
16. Johnson, E. S. & Gupta, A. A. An E3-like factor that promotes SUMO conjugation to the yeast septins. *Cell* **106**, 735–744 (2001).
17. Takahashi, Y., Kahyo, T., Toh, E. A., Yasuda, H. & Kikuchi, Y. Yeast Ull1/Siz1 is a novel SUMO1/Smt3 ligase for septin components and functions as an adaptor between conjugating enzyme and substrates. *J. Biol. Chem.* **276**, 48973–48977 (2001).
18. Zhao, X. & Blobel, G. A SUMO ligase is part of a nuclear multiprotein complex that affects DNA repair and chromosomal organization. *Proc. Natl Acad. Sci. USA* **102**, 4777–4782 (2005).
19. Nie, M. & Boddy, M. N. Cooperativity of the SUMO and ubiquitin pathways in genome stability. *Biomolecules* **6**, 14 (2016).
20. Psakhye, I. & Jentsch, S. Protein group modification and synergy in the SUMO pathway as exemplified in DNA repair. *Cell* **151**, 807–820 (2012).
21. Sarangi, P. & Zhao, X. SUMO-mediated regulation of DNA damage repair and responses. *Trends Biochem. Sci.* **40**, 233–242 (2015).
22. Sacher, M., Pfander, B., Hoege, C. & Jentsch, S. Control of Rad52 recombination activity by double-strand break-induced SUMO modification. *Nat. Cell Biol.* **8**, 1284–1290 (2006).
23. Pfander, B., Moldovan, G. L., Sacher, M., Hoege, C. & Jentsch, S. SUMO-modified PCNA recruits Srs2 to prevent recombination during S phase. *Nature* **436**, 428–433 (2005).
24. Hoege, C., Pfander, B., Moldovan, G. L., Pyrowolakis, G. & Jentsch, S. RAD6-dependent DNA repair is linked to modification of PCNA by ubiquitin and SUMO. *Nature* **419**, 135–141 (2002).
25. Cremona, C. A. et al. Extensive DNA damage-induced sumoylation contributes to replication and repair and acts in addition to the mec1 checkpoint. *Mol. Cell* **45**, 422–432 (2012).
26. Bonner, J. N. et al. Smc5/6 mediated sumoylation of the Sgs1-Top3-Rmi1 complex promotes removal of recombination intermediates. *Cell Rep.* **16**, 368–378 (2016).
27. Sriramachandran, A. M. & Dohmen, R. J. SUMO-targeted ubiquitin ligases. *Biochim. Biophys. Acta* **1843**, 75–85 (2014).
28. Prudden, J. et al. SUMO-targeted ubiquitin ligases in genome stability. *EMBO J.* **26**, 4089–4101 (2007).
29. Ii, T., Fung, J., Mullen, J. R. & Brill, S. J. The yeast Slx5-Slx8 DNA integrity complex displays ubiquitin ligase activity. *Cell Cycle* **6**, 2800–2809 (2007).
30. Xie, Y. et al. The yeast Hex3.Slx8 heterodimer is a ubiquitin ligase stimulated by substrate sumoylation. *J. Biol. Chem.* **282**, 34176–34184 (2007).
31. Uzunova, K. et al. Ubiquitin-dependent proteolytic control of SUMO conjugates. *J. Biol. Chem.* **282**, 34167–34175 (2007).
32. Zhang, Z. & Buchman, A. R. Identification of a member of a DNA-dependent ATPase family that causes interference with silencing. *Mol. Cell Biol.* **17**, 5461–5472 (1997).
33. Wang, Z., Jones, G. M. & Prelich, G. Genetic analysis connects SLX5 and SLX8 to the SUMO pathway in Saccharomyces cerevisiae. *Genetics* **172**, 1499–1509 (2006).
34. Mullen, J. R., Kaliraman, V., Ibrahim, S. S. & Brill, S. J. Requirement for three novel protein complexes in the absence of the Sgs1 DNA helicase in Saccharomyces cerevisiae. *Genetics* **157**, 103–118 (2001).
35. Bretes, H. et al. Sumoylation of the THO complex regulates the biogenesis of a subset of mRNPs. *Nucleic Acids Res.* **42**, 5043–5058 (2014).
36. Parker, J. L. et al. SUMO modification of PCNA is controlled by DNA. *EMBO J.* **27**, 2422–2431 (2008).
37. Altmannova, V. et al. Rad52 SUMOylation affects the efficiency of the DNA repair. *Nucleic Acids Res.* **38**, 4708–4721 (2010).

38. Olmezer, G. et al. Replication intermediates that escape Dna2 activity are processed by Holliday junction resolvase Yen1. *Nat. Commun.* **7**, 13157 (2016).
39. Sung, M. K. & Huh, W. K. Bimolecular fluorescence complementation analysis system for in vivo detection of protein-protein interaction in Saccharomyces cerevisiae. *Yeast* **24**, 767–775 (2007).
40. Schweiggert, J., Stevermann, L., Panigada, D., Kammerer, D. & Liakopoulos, D. Regulation of a spindle positioning factor at kinetochores by SUMO-targeted ubiquitin ligases. *Dev. Cell* **36**, 415–427 (2016).
41. Hickey, C. M., Xie, Y. & Hochstrasser, M. DNA binding by the MATalpha2 transcription factor controls its access to alternative ubiquitin-modification pathways. *Mol. Biol. Cell* **29**, 542–556 (2018).
42. Burgess, R. C., Rahman, S., Lisby, M., Rothstein, R. & Zhao, X. The Slx5-Slx8 complex affects sumoylation of DNA repair proteins and negatively regulates recombination. *Mol. Cell Biol.* **27**, 6153–6162 (2007).
43. Thu, Y. M. et al. Slx5/Slx8 promotes replication stress tolerance by facilitating mitotic progression. *Cell Rep.* **15**, 1254–1265 (2016).
44. Matos, J. & West, S. C. Holliday junction resolution: regulation in space and time. *DNA Repair* **19**, 176–181 (2014).
45. Ho, C. K., Mazon, G., Lam, A. F. & Symington, L. S. Mus81 and Yen1 promote reciprocal exchange during mitotic recombination to maintain genome integrity in budding yeast. *Mol. Cell* **40**, 988–1000 (2010).
46. Mazon, G., Lam, A. F., Ho, C. K., Kupiec, M. & Symington, L. S. The Rad1-Rad10 nuclease promotes chromosome translocations between dispersed repeats. *Nat. Struct. Mol. Biol.* **19**, 964–971 (2012).
47. Munoz-Galvan, S. et al. Distinct roles of Mus81, Yen1, Slx1-Slx4, and Rad1 nucleases in the repair of replication-born double-strand breaks by sister chromatid exchange. *Mol. Cell Biol.* **32**, 1592–1603 (2012).
48. Matos, J., Blanco, M. G. & West, S. C. Cell-cycle kinases coordinate the resolution of recombination intermediates with chromosome segregation. *Cell Rep.* **4**, 76–86 (2013).
49. Talhaoui, I., Bernal, M. & Mazon, G. The nucleolytic resolution of recombination intermediates in yeast mitotic cells. *FEMS Yeast Res.* **16**, pii: fow065 (2016).
50. Rubenstein, E. M. & Hochstrasser, M. Redundancy and variation in the ubiquitin-mediated proteolytic targeting of a transcription factor. *Cell Cycle* **9**, 4282–4285 (2010).
51. Xie, Y., Rubenstein, E. M., Matt, T. & Hochstrasser, M. SUMO-independent in vivo activity of a SUMO-targeted ubiquitin ligase toward a short-lived transcription factor. *Genes Dev.* **24**, 893–903 (2010).
52. Cook, C. E., Hochstrasser, M. & Kerscher, O. The SUMO-targeted ubiquitin ligase subunit Slx5 resides in nuclear foci and at sites of DNA breaks. *Cell Cycle* **8**, 1080–1089 (2009).
53. Jentsch, S. & Psakhye, I. Control of nuclear activities by substrate-selective and protein-group SUMOylation. *Annu. Rev. Genet.* **47**, 167–186 (2013).
54. Horigome, C. et al. PolySUMOylation by Siz2 and Mms21 triggers relocation of DNA breaks to nuclear pores through the Slx5/Slx8 STUbL. *Genes Dev.* **30**, 931–945 (2016).
55. Bohm, S., Mihalevic, M. J., Casal, M. A. & Bernstein, K. A. Disruption of SUMO-targeted ubiquitin ligases Slx5-Slx8/RNF4 alters RecQ-like helicase Sgs1/BLM localization in yeast and human cells. *DNA Repair* **26**, 1–14 (2015).
56. Sarbajna, S., Davies, D. & West, S. C. Roles of SLX1-SLX4, MUS81-EME1, and GEN1 in avoiding genome instability and mitotic catastrophe. *Genes Dev.* **28**, 1124–1136 (2014).
57. Spinella, J. F. et al. Whole-exome sequencing of a rare case of familial childhood acute lymphoblastic leukemia reveals putative predisposing mutations in Fanconi anemia genes. *BMC Cancer* **15**, 539 (2015).
58. Kuligina, E. et al. Value of bilateral breast cancer for identification of rare recessive at-risk alleles: evidence for the role of homozygous GEN1 c.2515_2519delAAGTT mutation. *Fam. Cancer* **12**, 129–132 (2013).
59. Medves, S. et al. A high rate of telomeric sister chromatid exchange occurs in chronic lymphocytic leukaemia B-cells. *Br. J. Haematol.* **174**, 57–70 (2016).
60. Tran, P. T., Paoletti, A. & Chang, F. Imaging green fluorescent protein fusions in living fission yeast cells. *Methods* **33**, 220–225 (2004).
61. Schindelin, J. et al. Fiji: an open-source platform for biological-image analysis. *Nat. Methods* **9**, 676–682 (2012).
62. Johnson, E. S. & Blobel, G. Cell cycle-regulated attachment of the ubiquitin-related protein SUMO to the yeast septins. *J. Cell Biol.* **147**, 981–994 (1999).
63. Ulrich, H. D. & Davies, A. A. In vivo detection and characterization of sumoylation targets in Saccharomyces cerevisiae. *Methods Mol. Biol.* **497**, 81–103 (2009).
64. Rouviere, J. O. et al. A SUMO-dependent feedback loop senses and controls the biogenesis of nuclear pore subunits. *Nat. Commun.* **9**, 1665 (2018).
65. Mullen, J. R. & Brill, S. J. Activation of the Slx5-Slx8 ubiquitin ligase by poly-small ubiquitin-like modifier conjugates. *J. Biol. Chem.* **283**, 19912–19921 (2008).

Acknowledgements

We thank LS Symington, M Hall, S Marcand, K Dubrana, S Leon, S Dokudovskaya, O Gadal, and S Biggins for generous gifts of yeast strains and plasmids. We thank LS Symington for critical reading and comments on the manuscript. We thank J. Rouviere for assistance in the setting of sumoylation assays. This study was supported by a starting grant to G.M. from the joint program of the CNRS and INSERM (ATIP-Avenir), a grant to G.M. from Gustave Roussy Foundation funded from donations from Natixis, grants from Fondation ARC pour la Recherche sur le Cancer and Ligue Nationale Contre le Cancer (LNCC) to B.P. and a grant from the National Institutes of Health to S.J.B. (GM101613). G.M. is a full-time INSERM researcher at the CNRS. M.B. has benefited from a post-doctoral funding from the LNCC.

Author contributions

G.M. obtained funding and designed the experimental plan. G.M., S.J.B., M.B., and I.T. designed experiments. I.T. contributed to Figs. 1, 3, 4 and 6, Supplementary Figures 1, 5 and 8; M.B. contributed to Figs. 4, 5, 6 and 7 and Supplementary Figures 1, 2, 3, 4, 6 and 7; H.D. contributed to Fig. 2 and Supplementary Figure 4; S.J.B. and J.M. contributed to Figs. 1, 3 and 6; G.M. contributed to Figs. 1, 4, 6 and 7, and Supplementary Figures 1, 5 and 8, strain crossing and constructions; B.P. contributed to Fig. 1 and shared reagents and strains. G.M. wrote the paper with major contributions from B.P. and S.J.B.

Additional information

Supplementary Information accompanies this paper at https://doi.org/10.1038/s41467-018-07364-x.

Competing interests: The authors declare no competing interests.

Reprints and permission information is available online at http://npg.nature.com/reprintsandpermissions/

Publisher's note: Springer Nature remains neutral with regard to jurisdictional claims in published maps and institutional affiliations.

Open Access This article is licensed under a Creative Commons Attribution 4.0 International License, which permits use, sharing, adaptation, distribution and reproduction in any medium or format, as long as you give appropriate credit to the original author(s) and the source, provide a link to the Creative Commons license, and indicate if changes were made. The images or other third party material in this article are included in the article's Creative Commons license, unless indicated otherwise in a credit line to the material. If material is not included in the article's Creative Commons license and your intended use is not permitted by statutory regulation or exceeds the permitted use, you will need to obtain permission directly from the copyright holder. To view a copy of this license, visit http://creativecommons.org/licenses/by/4.0/.

© The Author(s) 2018

Titre : Contrôle de la résolvase Yen1 en relation avec SUMO dans la mitose

Mots clés : Recombinaison homologue, réparation de l'ADN, Yen1, SUMO, SIM, STUbL

Résumé : La réparation de cassures d'ADN double brins par recombinaison homologue nécessite la formation d'intermédiaires multibrins qui peuvent être le lieu de formation de crossovers après résolution par des nucléases. La modification de protéines par ubiquitine et SUMO est un mode de contrôle répandu parmi les protéines de la réparation de l'ADN. De plus, certaines protéines de la réparation de cassures double brins interagissent entre elles, lorsqu'elles sont sumoylées, par le biais de motifs d'interaction avec SUMO (SIMs). La nucléase Yen1 subit un contrôle rigoureux lors du cycle cellulaire dans le but de limiter la formation de crossover et ainsi de préserver l'intégrité du génome. Dans ce manuscrit, il sera mis en évidence que Yen1 est régulé de surcroit par l'ubiquitination, la sumoylation et enfin l'interaction non covalente avec le modificateur SUMO via ses SIMs désormais découverts. Yen1 est sumoylé par les SUMO ligases Siz1 et Siz2, d'autant plus en conditions de dommages à l'ADN. En plus de quoi, Yen1 est un substrat de l'ubiquitine ligase Slx5-Slx8. En absence de cette dernière, la fraction sumoylée de Yen1 persiste, ce qui mène à la localisation durable de Yen1 en accumulation ponctuelle dans le noyau. L'ubiquitination de Yen1 par Slx5-Slx8 a surtout lieu à la lysine 714. Une mutation de cette lysine augmente la formation de crossovers, et annule également les défauts de ségrégation des chromosomes qui peuvent avoir lieu en l'absence d'autres nucléases. D'autre part, l'action nucléolytique de Yen1 ne s'effectue correctement que lorsque celui-ci peut interagir de façon non covalente avec des partenaires sumoylés. Des mutations dans les SIMs de Yen1 réduisent sa capacité à découper et résoudre les intermédiaires de la recombinaison, ce qui donne lieu à une augmentation de l'instabilité génomique et de la mauvaise ségrégation des chromosomes.

Title : Sumo-directed control of the resolvase Yen1 in mitotic cells

Keywords : Homologous recombination, DNA repair, Yen1, SUMO, SIM, STUbL

Abstract : The repair of double-stranded DNA breaks (DSBs) by homologous recombination involves the formation of branched intermediates that can lead to crossovers following nucleolytic resolution. Ubiquitin and SUMO modification is commonplace amongst the DNA damage repair proteins. What is more, a number of DSB repair factors interact with each other when sumoylated, making use of SUMO interaction motifs (SIMs). The nuclease Yen1 is tightly controlled during the cell cycle to limit the extent of crossover formation and preserve genome integrity. In this manuscript we describe further regulation of Yen1 by ubiquitination, sumoylation and non-covalent interaction with SUMO through its newly characterized SIMs. Yen1 is sumoylated by Siz1 and Siz2 SUMO ligases, especially in conditions of DNA damage. Furthermore, Yen1 is a substrate of the Slx5-Slx8 ubiquitin ligase. Loss of Slx5-Slx8 stabilizes the sumoylated fraction of Yen1, and results in persistent localization of Yen1 in nuclear foci. Slx5-Slx8-dependent ubiquitination of Yen1 occurs mainly at K714 and mutation of this lysine increases crossover formation during DSB repair and suppresses chromosome segregation defects when other nucleases are unavailable. In addition, proper and timely nucleolytic processing from Yen1 is dependent on interactions mediated by non-covalent binding to sumoylated partners. Mutations in the motifs that allow SUMO-mediated recruitment of Yen1 leads to its mis-localization, decreasing Yen1's ability to resolve DNA joint-molecule intermediates and resulting in increased genome instability and chromosome mis-segregation.